Universidade de Aveiro Departamento de Química
2005

Ana Maria Antunes Dias

Propriedades Termodinâmicas de Misturas Líquidas Substituintes do Sangue

Thermodynamic Properties of Blood Substituting Liquid Mixtures

dissertação apresentada à Universidade de Aveiro para cumprimento dos requisitos necessários à obtenção do grau de Doutor em Engenharia Química, realizada sob a orientação científica da Dra. Isabel Maria Delgado Jana Marrucho Ferreira, Professora Auxiliar do Departamento de Química da Universidade de Aveiro e do Dr. João Manuel da Costa Araújo Pereira Coutinho, Professor Associado do Departamento de Química da Universidade de Aveiro

Apoio financeiro da FCT e do FSE no âmbito do III Quadro Comunitário de Apoio.

Aos meus pais, irmãos, tios, primos e avós pelo amor incondicional

Aos meus amigos por me aceitarem como sou

Aos meus orientadores pela confiança

o júri

presidente

Prof. Dr. Joaquim Manuel Vieira
professor catedrático do Departamento de Cerâmica e Vidro da Universidade de Aveiro

Prof. Dra. Lourdes Fernandez Vega
senior research scientist do Instituto de Ciências de Materiais de Barcelona

Prof. Dr. Eduardo Jorge Morilla Filipe
professor auxiliar do Instituto Superior Técnico da Universidade Técnica de Lisboa

Prof. Dra. Isabel Maria Almeida Fonseca
professora associada da Faculdade de Ciências e Tecnologia da Universidade de Coimbra

Prof. Dr. António José Venâncio Ferrer Correia
professor catedrático do Departamento de Química da Universidade de Aveiro

Prof. Dra. Isabel Maria Delgado Jana Marrucho Ferreira
professora auxiliar do Departamento de Química da Universidade de Aveiro

Prof. Dr. João Manuel da Costa e Araújo Pereira Coutinho
professor associado do Departamento de Química da Universidade de Aveiro

agradecimento

Com todo o carinho aqui fica o meu agradecimento muito especial a todos aqueles que me ajudaram a trilhar este caminho.

Aos meus orientadores, por acreditarem em mim mesmo quando eu não acreditava. Por aturarem os meus choros e bloqueios sempre com uma palavra de apoio, incentivo e sempre com a mesma confiança. Recebi da vossa parte muito mais que conhecimento. Muito obrigada parece-me pouco....

Aos meus colegas/amigos, António, Lara, Nelson, Nuno, Mara, Maria Jorge, Carla, Fátima M., Fátima V., Pedro e Joana que me fizeram sentir completamente integrada e feliz. Nunca me esquecerei dos nossos almoços e pausas para café. Por todas as vezes que aturaram as minhas demoras, as minhas dúvidas, os meus problemas informáticos e não só, muito obrigada! À Ana Caço não me atrevo a agradecer...fica muito mais do que a amizade, fica uma relação de irmãs e até de comadres (madrinha orgulhosa)!

Aos colegas/amigos do 15.1.11, Luís, Sérgio, Susana, Cristiano, Sara, que me apoiaram nos dias maus e fizeram-me rir no dia a dia. Acho que nunca tantas asneiras foram ditas por metro quadrado, mas por mim, foi óptimo! À Sónia agradeço a presença, as alegrias e desabafos partilhados, os lanches...

Ao senhor Morais e ao senhor Ivo agradeço a paciência para interpretar os meus rabiscos, sempre com sugestões válidas, pelos trabalhos extra e “desenrasques” que me ajudaram tantas vezes. Agradeço a ambos o apoio, a ajuda e a amizade.

O tempo que passei no estrangeiro foi também muito gratificante a nível profissional e pessoal.

Em Espanha, agradeço à Dra Lourdes Vega ter-me recebido no seu grupo e ter-me integrado nele. Nunca me senti uma estranha. A relação foi muito além da profissional. Ao Pep devo muitíssimo. Para além da amizade, por todas as explicações e respostas aos muitos mails que tinham como assunto “Olá + trabalho”. Quero também agradecer ao Félix. Quando os mails deixaram de ser suficientemente interactivos passamos a discutir crossover através do messanger! Sempre disponíveis para as minhas dúvidas, com muita paciência para o meu stress...o meu sincero agradecimento.

Quero aqui também agradecer ao Luizildo, à Maria Eugénia, ao Pedro, muito especialmente ao Aurélio (nunca esquecerei o dia do Magnum) e a todos os que tornaram a minha estadia em Espanha tão especial. Ao Carmelo dedico as palavras de Rita Ferro Rodrigues.

Em Pau tive a sorte de trabalhar com pessoas com uma capacidade de trabalho e dedicação incrível nomeadamente o Dr. Jean-Luc, o Dr. Hervé Carrier e o Dr. Jerôme Pauly. Descobri o prazer de beber Jurançon ao fim do dia de trabalho “apenas” porque tinhamos passado mais um dia. Aos meus colegas de laboratório Frederic Plantier, Michel Milhet, Thomas Lafitte e muito especialmente ao Jean-Marc por me terem feito sentir tão bem, muito obrigada!

À Alice e à Priscilla quero agradecer, para além da amizade, o terem-me ajudado a descobrir esse país que me encanta tanto, o Brasil.

Uma palavra de agradecimento também para o Dr. Manuel Piñeiro pela disponibilidade e simpatia com que sempre nos recebeu quando precisámos de usar o densimetro. Também ao Dr. Luís Paulo Rebelo pela cooperação nas medições que fizémos na Universidade Nova.

Sou feliz por todos os amigos que fiz, por todas as pessoas que conheci, por todas as oportunidades que tive de viajar e alargar os meus horizontes. Mas nada disto teria sido possível sem o apoio incondicional da minha família. Obrigada por aturarem o meu mau-humor, pelos lanches no quarto, por todos os cuidados, pela preocupação, pela presença e apoio diários, pelo amor, por existirem....não teria conseguido sem vocês.

A coragem e a perseverança nos momentos difíceis e a alegria e o entusiasmo quando as coisas corriam bem devo-o a todos os que aqui mencionei e a muitos outros mas também, sem dúvida, à presença constante de Deus que, apesar do meu desleixo, fez questão de estar sempre comigo.

Não há maior alegria do que ter a certeza de que se pudesse voltar atrás voltaria a fazer tudo o que fiz.....

palavras-chave

perfluoroalcanos, oxigénio, dióxido de carbono, densidade, pressão de vapor, solubilidade, VLE, LLE, sof-SAFT

resumo

Este trabalho tem como objectivo a medição e modelação de propriedades termodinâmicas de compostos fluorados. Os fluoralcanos são alcanos onde os átomos do hidrogénio foram total ou parcialmente substituídos por átomos de flúor. São caracterizados por forças intramoleculares fortes e forças intermoleculares fracas que lhes conferem propriedades peculiares e tornam atractiva a sua utilização numa grande variedade de áreas incluindo a ambiental, industrial e biomédica. As aplicações mais relevantes destes compostos são efectivamente encontradas no campo da biomedicina. Tendo por base a elevada solubilidade de gases respiratórios nestes compostos, os perfluoroalcanos e as suas emulsões podem ser utilizados para oxigenação de tecidos, como agentes anti-tumurais, para conservação de orgãos, em cirurgia oftalmológica, como suplementos para meios de cultura e administração de fármacos, entre outras.

A escolha do melhor fluoroalcano a usar em cada aplicação assim como a previsão do comportamento de um dado fluoroalcano ou misturas que envolvam fluoroalcanos só é possível se as propriedades termodinâmicas destes compostos forem conhecidas com exactidão. Surpreendentemente, os dados experimentais para estes sistemas são escassos ou mesmo inexistentes na literatura tornando difícil concluir acerca da aplicabilidade dos modelos termodinâmicos correntes na descrição de propriedades de sistemas fluorados.

Este trabalho contribui com novos dados experimentais de densidade, pressão de vapor e solubilidade de gases e alcanos em fluoroalcanos líquidos. Dois novos aparelhos foram construídos e validados para medir pressões de vapor e solubilidade de gases à pressão atmosférica. Fluoroalcanos com diferentes estruturas moleculares foram escolhidos para este estudo de modo a concluir sobre a influência da estrutura, do comprimento da cadeia e da substituição de grupos terminais nas propriedades termodinâmicas destes compostos.

Os dados experimentais medidos foram modelados usando a Teoria Estatística de Fluidos Associantes (SAFT) e no caso particular deste trabalho, a versão soft-SAFT. De acordo com os resultados experimentais medidos, a equação foi implementada pela adição de novos termos para justificar ou descrever correctamente as evidências experimentais observadas. Pela primeira vez um termo polar foi incluído no modelo soft-SAFT para concluir acerca da influência do quadrupolo na solubilidade do dióxido de carbono em perfluoroalcanos líquidos. Da mesma forma, um procedimento recursivo, baseado na teoria de renormalização de grupos, foi incluído no modelo de modo a contabilizar as flutuações de longo alcance que caracterizam a região crítica permitindo a descrição dos diagramas globais de fases de perfluoroalcanos puros.

keywords perfluoroalkanes, oxygen, carbon dioxide, density, vapour pressure, solubility, VLE, LLE, soft-SAFT

abstract

The aim of this work is the measurement and modelling of thermodynamic properties of highly fluorinated compounds. Fluoroalkanes are alkanes where the hydrogen atoms where total or partially substituted by fluorine atoms. As a result of their strong intramolecular and weak intermolecular forces they present peculiar properties that make them able to be used in a variety of areas including environmental, industrial and biomedical. Their most relevant applications are actually found in the biomedical field. Based on the large solubility of respiratory gases in these compounds, perfluorochemicals and their emulsions can be used in tissue oxygenation fluids, anti-tumural agents, perfusates for isolated organs, surgical tools for ophthalmology, cell culture media supplements, drug formulations and delivery, among others.

The choice of the best fluoroalkane to use for each application as well as the prediction of the behaviour of a given fluoroalkane or mixtures involving fluoroalkanes is only possible if accurate thermodynamic data for these compounds is available. Remarkably, experimental data for these systems is scarce or even inexistent in the open literature and so, limited conclusions can be taken about the applicability of current thermodynamic models to correctly describe fluorinated systems.

This work contributes with new experimental data for density, vapour pressure and solubility of gases and alkanes in liquid fluoroalkanes. New apparatus were built and validated to measure vapour pressure data and solubility of gases at atmospheric pressures. Different molecular structures were chosen for the perfluoroalkanes studied in order to conclude about the influence of the structure, chain length and the substitution of terminal groups on the thermodynamic properties of these compounds.

Experimental data measured was modelled using the Statistical Associating Fluid Theory (SAFT), in this particular case, the soft-SAFT version. According to the experimental results measured in this work, the equation was improved by the addition of new terms trying to justify or correctly describe the experimental evidences observed. For the first time a polar term was included in the soft-SAFT model to account for the quadrupole moment on the carbon dioxide and aromatic molecules in order to study its influence on the solubility of the gas in the liquid perfluorochemicals. Also, to correctly describe the global phase diagrams of pure perfluoroalkanes, a crossover procedure based on the renormalization group theory was included to account for the long range fluctuations that characterize the critical region and that the traditional models do not account for.

Contents

Notation

Abbreviations

AAD	Absolute Averaged Deviation
EoS	Equation of State
LCST	Lower Critical Solution Temperature
LJ	Lennard-Jones
LLE	Liquid-Liquid Equilibrium
RDF	Radial Distribution Function
SAFT	Statistical Associating Fluid Theory
UCST	Upper Critical Solution Temperature
VLE	Vapour-Liquid Equilibrium

Roman symbols

A	Helmholtz free energy
B	second virial coefficient
C	concentration
CN	carbon number
G	pair correlation function
G^0	standard Gibbs energy associated with the hypothetical changes that happen in the solute neighborhood when the molecules are transferred from the gas phase to a hypothetical solution where the mole fraction of solute is equal to one
G^*	standard Gibbs energy associated with the changes that occur in the solute neighborhood during dissolution process due to the transference of one solute molecule from the pure perfect gas state to an infinitely dilute state in the solvent, at a given temperature T
H^0	standard enthalpy associated with the hypothetical changes that happen in the solute neighborhood when the molecules are transferred from the gas phase to a hypothetical solution where the mole fraction of solute is equal to one
H*	standard enthalpy associated with the changes that occur in the solute neighborhood during dissolution process due to the transference of one solute molecule from the pure perfect gas state to an infinitely dilute state in the solvent, at a given temperature T
k	volume of association
k_B	Boltzmann constant
L	Ostwald coefficient at temperature and total pressure of the system
Mw	molecular weight
m	chain length
N_A	Avogadro's number
P	pressure
P^{sat}	vapour pressure
Q	quadrupole moment
R	ideal gas constant
S^0	standard entropy associated with the hypothetical changes that happen in the solute neighborhood when the molecules are transferred from the gas phase to a hypothetical solution where the mole fraction of solute is equal to one

S^*	standard entropy associated with the changes that occur in the solute neighborhood during dissolution process due to the transference of one solute molecule from the pure perfect gas state to an infinitely dilute state in the solvent, at a given temperature T
T	temperature
V^L	volume of liquid solution after equilibrium is reached
V^V	volume of gas solubilized in the liquid solution
V^0	molar volume of the pure component
X	fraction of nonbonded molecules
x	mole fraction of the liquid phase
x_p	fraction of segments in a chain that contain the quadrupole
y	mole fraction of the vapour phase
Z	compressibility factor

Greek symbols

α	isobaric thermal expansibility of the solvent
Δ	association strength
ε	association energy
η	size parameter of the generalized Lorentz-Berthelot combination rules
μ	chemical potential
ξ	energy parameter of the generalized Lorentz-Berthelot combination rules
ρ	density
σ	size parameter of the intermolecular potential / diameter
ϕ	volume fraction
Ω	grand thermodynamic potential

Subscript

1, 2	solvent, solute
c	critical

Superscript

calc	calculated
cav	cavity
exp	experimental
int	interaction
sat	saturated
L	liquid phase
V	vapor phase

List of Tables

List of Figures

Part I.

GENERAL INTRODUCTION

"Fluorine leaves nobody indifferent; it flames emotions be that affections or aversions. As a substitute, it is rarely boring, always good for a surprise, but often completely unpredictable" (Schlosser and Michel, 1996).

I.1. Fluorine Properties

Although this work focuses on the study of highly fluorinated compounds and their mixtures, a brief discussion of the properties of elemental fluorine is useful to assist in understanding the unusual properties of these compounds. The Fluorine (*F)* atom is characterized by a high electronegativity, relatively small size, very low polarizability, tightly bound with three non-bonding electron pairs, excellent overlap between *F* 2s and 2p orbitals with corresponding orbitals of other second period elements (Smart, 2001). Fluorine has an electronegativity of 4.0 on the Pauling scale, which is the highest of all the elements. This extreme electronegativity results in fluorine drawing electrons from adjacent atoms, thus creating polar bonds. For example, the electronegativity difference between fluorine and carbon is 1.5 units, which indicates that the electrons are shared unequally between the two atoms and that there is a partial negative charge on the fluorine and a partial positive charge on the carbon.

The incorporation of fluorine atoms into organic materials imparts dramatic changes in physical properties as well as chemical reactivities of the molecules. Actually, depending upon the site and level of fluorination, organofluorine compounds have solvent properties ranging from extreme non-polar perfluoroalkanes to the extraordinarily polar solvent, hexafluoroisopropanol (Smart, 2001). Also, fluorination always increases the steric size of alkyl groups. The effective van der Waals radius for trifluoromethyl compared to other hydrocarbon alkyl groups clearly shows that it is a much larger group than methyl: 1.80 Å for CH_3 and 2.20 for CF_3 (Smart, 2001). It is important to notice that, the steric size (van der Waals radious or volume) is an absolute term, an intrinsic molecular property, but whether or not it causes a steric effect is entirely dependent on the nature of the transition state for a particular process, since it defines the degree of coloumbic interaction between the atom or group in question and other atoms. According to Clark (1999), the steric effects are more significant with perfluoroalkanes with only C-F bonds. For example, perfluoroalkanes and Teflon® have helical chain conformation, instead of the zig-zag chain conformation characteristic of alkanes, to relieve steric impediment and repulsive interactions between adjacent fluorine atoms on alternative carbon atoms, originating a shielding of the carbon backbone by fluorine atoms.

I.2. Perfluoroalkanes

Perfluoroalkanes (PFCs) are synthetic fluorinated hydrocarbons. They are formulated by substituting fluorine to replace hydrogen atoms on common organic compounds (Sargent and Seffl, 1970 and Drakesmith, 1997). Fluorine's extreme electronegativity endows C-F bonds to possess relatively high ionic bond characters, resulting in the strongest bond with carbon as shown in Table I.1. Moreover, addition of fluorine atoms influences adjacent bond energies. For example, CF_3-CF_3 bond is 10 kcal/mole stronger than CH_3-CH_3 bond (Banks, 1970).

Table I.1. Average Bond Dissociation Energies (kcal/mole) (Banks and Tatlow, 1986)

C-F	C-Cl	C-Br	C-I	C-H	C-O	C-C	C-N
116	81	68	51	99	86	83	72

Fluorine's high ionization potential and relatively low polarizability lead to very weak inter-molecular forces (Fielding, 1979) which, together with the strong intra-molecular forces, are the main responsible for the interesting properties presented by perfluoroalkanes when compared with the corresponding hydrocarbons, as for example:

- higher solubility for gases (the highest known among organic liquids)
- exceptional chemical and biological inertness
- excellent spreading characteristics and high fluidity
- lower surface tensions
- lower refractive indices (lower than 1.3)
- higher vapour pressures
- higher densities
- higher viscosities
- higher isothermal compressibilities
- lower internal pressures
- poorer solvency for organics
- non-polar molecules
- nearly ideal liquids

Table I.2 quantifies some of the properties given above.

Table I.2. Physicochemical Properties of Perfluoroalkane Liquids

Property	Range	Units
Gas Solubility (37ºC @ 1 atm)		
Oxygen	33 - 66	mL/100mL PFC
Carbon Dioxide	140 - 210	mL/100mL PFC
Diffusion Coefficient (37ºC @ 1 atm)		
Oxygen	2 - 5.8 x 10^{-5}	cm^2/sec
Carbon Dioxide	1.1 - 1.3 x 10^{-5}	cm^2/sec
Vapor Pressure (37ºC @ 1 atm)	0.2 - 400	mm Hg
Surface Tension (25ºC @ 1 atm)	13.6 - 18	dynes/cm
Spreading Coefficient	-0.2 to +4.5	dynes/cm
Density (25ºC @ 1 atm)	1.58 - 2.02	g/mL
Kinematic Viscosity (25ºC @ 1 atm)	0.8 - 8	cS
Log P	6.1 -9.7	--
Lipid Solubility (37ºC)	0.14 - 1.70	μgm PFC/mglipid/mmHg

Data based on a survey of 18 perfluoroalkane liquids

A related and unusual property of the perfluorinated hydrocarbons is that they become more volatile than the parent hydrocarbon when the chain length exceeds four carbons. Figure I.1 compares the boiling point and other physical properties for alkanes and perfluoroalkanes of a variety of carbon numbers. According to Ellis et al. (2002), the strong electronic repulsion of adjacent fluorine atoms, which results in the rigid backbone of the chain, coupled with the large partial negative charge associated with each fluorine atom, results in the vapor pressure of these molecules being substantially higher than could be predicted based purely upon the mass of the molecules. The authors compared the boiling points of noble gases, perfluoroalkanes and normal alkanes of similar molecular weights and observed that in each case, the perfluoroalkane behaves more like a noble gas than an alkane of corresponding molecular weight. This suggests that there are minimal intermolecular interactions in perfluorocarbons and that their volatility may be related more to their molar mass than the hydrocarbons.

Hildebrand and Rotariu, (1952) stated that perfluoroalkanes were undoubtedly far less flexible than alkanes due to the size of fluorine atoms and hence they could be expected to pack in a somewhat more orderly, parallel array in the liquid state, especially at lower temperatures. More recently, molecular simulation studies were performed in

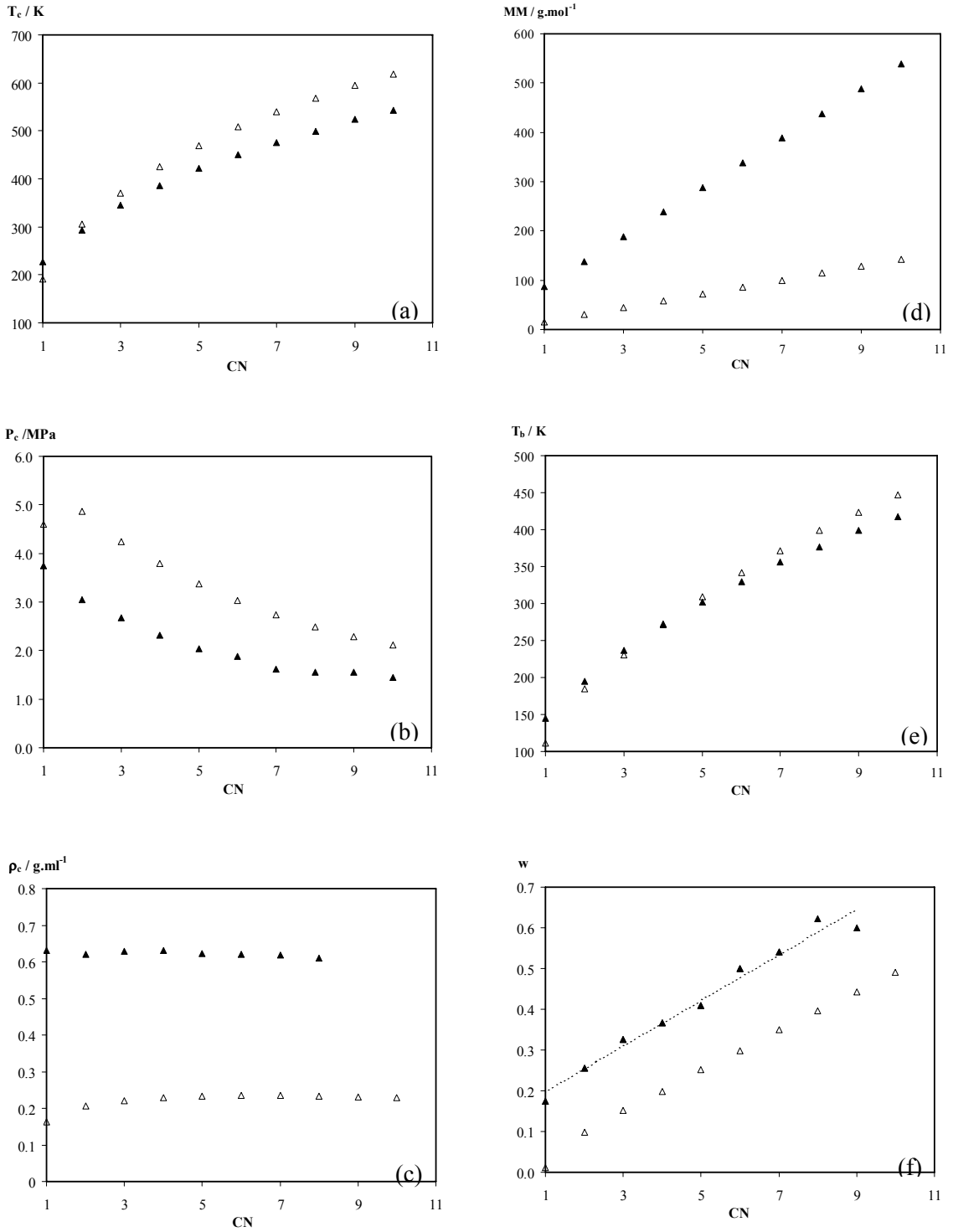

Figure I.1. Comparison between physical properties for the homologous linear series of alkanes and perfluoroalkanes (filled symbols): (a) critical temperature, (b) critical pressure, (c) critical density, (d) molecular weight, (e) boiling temperature and (e) acentric factor. Data from NIST DataBase. Tb and acentric factors for C > 6 calculated from vapour pressure data measured in this work.

order to compare the liquid-phase structure of the pure perfluoroalkanes and the corresponding alkanes (Watkins and Jorgensen, 2001 and Gomes and Padua, 2003). Conformational and structural properties of the liquid phases were obtained applying the molecular dynamics method using flexible, all-atom force fields containing electrostatic charges. The new OPLS-AA (optimised potentials for liquid simulations) model adds explicit sites and partial charges to individual atoms in addition to a finer representation of the conformational energetics. These recently proposed models for long-chain perfluoroalkanes (Watkins and Jorgensen, 2001) provide a more detailed, and probably more accurate, molecular description than previous attempts based on the united-atom framework (Shin et al., 1992 and Cui et al., 1998). The results obtained showed that most of the dihedral angles in the carbon skeleton of n-alkanes adopt values close to 180º with occasional occurrence gauche defects. When compared to the corresponding n-perfluoroalkanes, the population of gauche defects is smaller in the latter case, indicating a more rigid molecular backbone. This suggests that cavities present naturally in the liquid phase may be larger in fluoroalkanes than in alkanes. In addition, it was verified that spontaneous cavities are larger and more easily formed in the fluorocarbon, corresponding to smaller free energies of cavity formation, than in the equivalent hydrocarbon (Gomes and Pádua, 2003). Experimentally, it was also verified that, the excess chemical potential, i.e., work needed to insert the 133Xe radioisotope into a solvent, was much lower for perfluoroalkanes than for alkanes (Kennan and Pollack, 1988 and Pollack et al., 1989).

Perfluoroalkanes behave like typical non-associated, non-polar liquids, with solubility for gases depending essentially on the molecule's shape (Chandler, 1978). A formal two-step dissolution process, consisting first on the opening a cavity in the solvent large enough to fit the gas molecule and then the introduction of the gas in this cavity, is often postulated for the purpose of discussing and predicting solubility data. Based on this model the molecular simulations discussed above justify the higher capacity of these compounds to solubilize gases as oxygen and carbon dioxide but cannot explain why carbon dioxide, being a bigger molecule, is more soluble than oxygen. Moreover, solubilities of gases decrease in the order $CO_2 > O_2 > CO > N_2 > H_2 > He$, following a decrease in molecular volume of the solute (Bonaventura et al., 1998).

The dissolution of O_2 or NO in diverse liquid PFCs has been investigated by NMR using the perturbation induced on the nuclear relaxation of the ^{13}C nuclei of the PFC by the

paramagnetic species (Hamza et al., 1981 and Serratrice et al., 1985). The results were rationalized on the basis of the easiness of formation of cavities within the liquid rather than the existence of any specific interaction again indicating that the cavities opened by these solutes in perfluoroalkanes are significantly larger than in alkanes. Oxygen solubility depends somewhat on molecular structure. For similar molecular weight, the differences in O_2 solubility can reach 20-25%. Linear perfluoroalkanes, including those that have a double bond, an oxygen atom, or a terminal bromine atom, have an advantage over the cyclic and polycyclic perfluoroalkanes (Riess, 1984). Terminal alkyl chain resulted in slightly reduced O_2 solubility (Meinert and Knoblish, 1993).

When perfluoroalkanes are mixed with alkanes, the deviations from ideality are positive and larger than those of nearly all other classes of mixtures containing only non-polar and non-eletrolyte substances. The most striking consequences of the extent of the deviations are, in bulk properties, marked positive azeotopy (double azeotrope can even arise in the perfluorobenzene/benzeme system) and usually liquid-liquid immiscibility (Scott, 1958) and also in surface properties, negative aneotropy or surface azeotropy (McLure et al., 1973). Differences in chain flexibility of the two component molecules and the weak interaction energy interplay are most probably the main responsible for the occurrence of these phenomena (Calado et al., 1978).

I.3. Applications

The first fluorinated compounds were synthesised during the II World War, as part of the Manhattan project, when scientists were looking for a material that was able to resist to chemical attack and long-term thermal stability at high temperatures to serve as coating for volatile elements in radioactive isotope production. The importance of the inclusion of fluorine atoms in organic molecules is well documented from the number of publications/year regarding fluorinated compounds, which increased from ≈ 35 in 1960 to ≈ 910 in 2004. The first articles relating synthesis, purification and measurement of physical properties of highly fluorinated perfluoroalkanes were published in the fifties. Since then, a constant increase in the number of publications occurred till 1990. In the last fifteen years, the number of publications/year increased from ≈ 70 (in 1990) to ≈ 200 (in 2004). The increase in the number of publications verified in the last years is related with

the numerous applications that highly fluorinated compounds are finding in different areas including biomedical, industrial and environmental.

I.3.1. Biomedical Purposes

In 1966, Clark and Gollan showed that mice immersed in oxygenated silicone oil or liquid fluorocarbon could breathe (Clark and Gollan, 1966). Nowadays, the application of perfluoroalkanes for biomedical purposes is mainly being carried out using them as pure liquids for liquid ventilation or in the emulsified form, if they are to be injected. A neat fluorocarbon, $C_8F_{17}Br$ or *perflubron*, is currently investigated in Phase II for treatment of acute respiratory failure by liquid ventilation (Kraft, 2001) and other liquid and gaseous perfluoroalkanes are being used as high-density intraoperative fluids for eye surgery (Miller et al., 1997). In the late 1970s, the first commercial perfluoroalkane emulsion, Fluosol-DA 20% was tested in humans. Presently at least five companies are developing a red blood cell substitute based on perfluorochemicals: Allience (Oxygent), HemoGen (Oxyfluor), Sanguine (PHERO 2), Synthetic Blood International (Oxycyte) and the Russian OJSC SPC Perftoran (Perftoran). Perfluoroalkane in water emulsions constitute safe and cost-effective vehicles for *in vivo* oxygen delivery. The release and uptake of gases by perfluoroalkane emulsions is facilitated once gases are dissolved in liquid perfluoroalkane and are not covalently bound to the perfluoroalkane molecules as in the case of hemoglobin. Furthermore, the perfluorochemical microdroplets that carry oxygen are $1/70^{th}$ of the size of red blood cells. They can, therefore, reach areas of the body virtually inaccessible to red blood cells and they can be easily eliminated from the organism. Phase III clinical trials conducted on such emulsions have shown that they can help in preventing the risk of oxygen deficiency in tissues, and reducing the need for donor blood transfusion during surgery. Cardiovascular, oncological and organ-preservation indications are under investigation. Potential applications of red cell blood substitute include all the situations of surgical anemia, some haemolytic anemias, ischemic disease, angioplasty, extracorporeal organ perfusion, cardioplegia (Cohn, 2000), radiotherapy of tumours (Rowinsky, 1999) and as an ultrasound contrast agent to detect myocardial perfusion abnormalities (Porter et al., 1995).

The specific physicochemical properties of fluoroalkanes mentioned previously have triggered numerous applications of these compounds in the field of oxygen delivery.

Some of these properties influence the amount and diffusivity of gases in PFCs (solubility, diffusion coefficients), others influence how the liquid PFC moves within the lung (vapor pressure, surface tension, spreading coefficient density, kinematic viscosity) and others influence the biodistribution of the PFC (partition coefficient (log P), lipid solubility) (Wolfson et al., 1998). Respiratory gas carrying capacity varies among fluids and is different for O_2 (35–70 ml gas/dL @ 25°C; >3× that of blood) than CO_2 (122–225 ml/dL @25°C; approximately 4×> that for O_2) according to Table I.2. Although several hundreds of such compounds have been screened over the past twenty years, very few were found to meet the appropriate physicochemical and biological criteria for in vivo oxygen delivery. This includes high purity, rapid excretion, aptitude to forming stable emulsions, absence of clinically significant side-effects and large scale, cost-effective industrial feasibility (Riess, 2001).

Fluorinated lipids and fluorinated surfactants can be used to promote the stability of various colloidal systems, including different types of emulsions, vesicles and tubules that also show promising for controlled release drug delivery due to the strong tendency that these molecules have to self-assemble. The potential of non-polar hydrocarbon-in-fluorocarbon emulsions, multiple emulsions and gel emulsions is a new field giving the first steps (Kraft, 2001).

I.3.2. Industrial Purposes

There are a large number of documented applications of perfluoroalkanes in the industry. Among others, perfluoroalkanes are been used

1) As co-solvents in supercritical extraction: improving the solubility of hydrophilic substances in supercritical reaction or extraction media (Raveendran and Wallen, 2002). In many supercritical fluid applications carbon dioxide is widely used as the near-critical solvent. As an example, the formation of water in CO_2 microemulsions offers a new approach to biological processes, organic synthesis, nanoparticle chemistry and dry cleaning (Stone et al., 2003). Although CO_2 has many advantages, its poor solvency with respect to polar compounds can be a problem. Until now, attempts to find suitable hydrocarbon-based surfactants have had a limited success. One strategy that has proven quite successful for overcoming this limitation is to make use of CO_2-philic functional groups to behave as surfactants. It has been verified that the solubility of a compound in

carbon dioxide is increased if it contains a fluorinated alkyl segment, since CO_2 is more soluble in fluorinated compounds than in their hydrocarbon counterparts (Hoefling et al., 1991). Non-polar perfluorocarbon species show increased solubility in supercritical CO_2 and have been used in the design of CO_2-philic surfactants, chelating agents and ligands in order to improve the solubility of polymers, metals and catalysts (Osswald et al., 2001).

2) As medium in two-phase reaction mixture: in a novel separation and purification technique that is attracting current interest in organic synthesis and process development, in the immobilization of expensive metal catalysts called *"Fluorous Phase Organic Synthesis"* (FPOS) (Horvath and Rabai, 1994). The hydrophobicity of fluorinated compounds that makes them immiscible with water and with many common organic solvents, their ability to form a homogenous solution at elevated temperatures with several of these solvents, their inertness, their solubility in supercritical CO_2 and their ability to dissolve gases contributes to the increasing popularity of the "Fluorous Phase" in organic syntheses (Gladysz, 1994; Studer et al., 1997 and Betzemeier and Knochel, 1999). By introducing perfluorinated ligands, a catalyst is solubilized and simultaneously immobilized in the "Fluorous Phase". By increasing the temperature, the biphasic system forms a homogenous solution and the catalytic process can take place. Cooling down the reaction mixture leads to the reformation of two separate phases. Afterwards, easy product isolation and the recovery of the perfluoro-tagged metal catalyst can be achieved by simple phase separation. The isolation and recovery of perfluorinated components can be accomplished not only by a phase separation of immiscible liquid layers but also by solid-liquid extraction using a perfluorinated non-polar stationary phase (Horvath and Rabai, 1994).

3) As refrigerants: short-chain halocarbons that are used as refrigerants, aerosol propellants and foam blowing agents. Initially, the chlorofluorocarbons (CFCs) were used for this purpose, but they were implicated in stratospheric ozone depletion (Molina and Rowland, 1974) and have subsequently been replaced by the hydrofluorocarbons (HFCs) (Wallington et al., 1994). The CFCs were typically fully halogenated methanes while the HFCs are generally partially fluorinated ethanes such as HFC 134a (1,1,1,2-tetrafluoroethane), which is the most commonly used HFC. Other short chain perfluoroalkanes used as evaporative fluorocarbon cooling for the semiconductor pixel and

micro-strip sensors include perfluoro-*n*-propane, perfluoro-*n*-butane, trifluoro-iodo-methane (CF_3I) and custom C_3F_8/C_4F_{10} mixtures (Vacek et al., 2000).

4) In cell culture aeration: one of the first reported works in this field came out in 1988 with the work of Cho and Wang. Inadequate supply of oxygen is one of the major problems in industrial as well as in lab-scale production of biomass, since oxygen is sparingly soluble in aqueous media. An approach to the problem of limited oxygen supply is to modify the medium in such a way that it dissolves more oxygen. This approach consists of the inclusion of oxygen carriers such as haemoglobin, hydrocarbons and perfuorocarbons (Elibol and Mavituna, 1999). PFCs and their emulsions can facilitate respiratory-gas delivery to both procaryotic and eucaryotic cells in culture, including those in bioreactor systems. Such gaseous enhancement often stimulates biomass production and yields of commercially important cellular products. The recoverability, and hence recycle ability, of otherwise expensive PFCs from aqueous culture medium makes their routine use commercially feasible (Lowe, 2002).

I.3.3. For Environmental Purposes

Due to the exceptional solubility of carbon dioxide in perfluoroalkanes these compounds are being studied for industrial and environmental applications as the removal of carbon dioxide from gaseous effluents (Wasanasathian and Peng, 2001).

Biological carbon dioxide fixation has been extensively investigated as part of efforts to solve the global warming problem. Several researchers have reported using algae culture to sequester carbon dioxide in the flue gas discharged from a boiler and a power plant (Negoro et al., 1993; Hamasaki et al., 1994 and Kishimoto et al., 1994). Besides the advantage of the removal of the pollutant gases, most of the times these algae have the ability to produce a commercial valuable product as is the case of hydrogen or □-carotene (Miura et al., 1997). One of the intrinsic problems for scaling up the algae culture system is the accumulation of photosynthetic produced oxygen, which in the case of photosynthetic microalgae works as an inhibitor for cell growth. To overcome this limitation, oxygen must be quickly remove out of the culture systems. An innovative approach for removing high concentration of oxygen is by the introduction of a perfluoroalkanes in the medium Cho and Wang (1988). In this case, carbon dioxide is the nutrient and oxygen is the waste. Therefore, the function of perfluoroalkanes used for algae will be inverse to that for

animals. That is, in this case perfluoroalkanes act as the CO_2-releasing and O_2-carrying vehicles.

I.4. Motivation

Despite the current interest in these fluorinated compounds, there are questions relating their behaviour that are still unanswered, most of the times due to lack of experimental data. For many of the applications discussed above, the importance of density, vapour pressure and gas solubility data is clear. Also, from a fundamental point of view, these data can provide information about bulk liquid structure, the organization of the solvent around a solute and the interactions between them.

One of the first attempts to estimate the thermophysical properties of perfluoroalkanes was reported by Lawson et al. (1978) who used a group-contribution method specially developed for perfluoroalkanes, to calculate properties such as the solubility parameter, the enthalpy of vaporization, vapour pressure and solubility of oxygen at 298 K. The method can provide only a qualitative estimation of these properties and only for one temperature. The use of common group-contribution methods to thermophysical property estimation often cannot be applied because they do not have information for the CF_2 and CF_3 groups or the information they have is not reliable, since it is based on the rare experimental data reported for perfluoroalkanes.

Predictions of gas solubilities in perfluoroalkanes have been made using Hildebrand's solubility parameter δ (Gjaldbaek, 1963 and Hildebrand, 1970). For two fluids to be mutually soluble, they need to have similar δ values. The δ values of perfluoroalkanes are between 12 and 16 $MPa^{1/2}$, as compared to 11.6 $MPa^{1/2}$ for oxygen, 12.3 $MPa^{1/2}$ for carbon dioxide, 14-18 $MPa^{1/2}$ for alkanes, and 47.9 for water. Semiempirical approaches to gas solubilities were derived from the scaled particle theory. These approaches express the free energy of solution as the sum of the free energies for formation of cavities in the solvent and that of the interaction between solute and solvent (Pierotti, 1976). Correlations also exist between O_2 solubilities and the solvent's surface tension (Uhlig, 1937), the solubility parameter (Lee, 1970), solvent's viscosity (Wesseler, 1977) and solvent's compressibility (Serratrice, 1982) since these are all manifestations of the solvent's degree of cohesiveness.

In 1996, a method based on molecular descriptors was proposed to predict a host of unknown physicochemical properties of perfluoroalkanes (Gabriel et al., 1996). The input parameters were categorized as empiric properties, geometric indices, or quantum mechanical descriptors and then, individual algorithms were developed for each independent variable function, namely, oxygen solubility, log P, vapour pressure, viscosity, and density. Those algorithms were expected to assist in the prediction of the physical properties of perfluoroalkane liquids, such that the design of new perfluoroalkanes and selection from currently available perfluoroalkane liquids could be optimised for each application (Gabriel et al., 1996).

Modelling of the thermodynamic properties of pure perfluoroalkanes and their mixtures in an extended range of thermodynamic conditions is a recent research field. Since 1998, essentially molecular simulation and different versions of the SAFT equation of state (EoS) are being used to model perfluoroalkanes and their mixtures. Table I.3 resumes literature data available mentioning the method and the systems used by the different authors. These works helped to elucidate some questions relating perfluoroalkanes and their behaviour but new questions/discussions appeared and there are still many aspects to elucidate.

This work intends to be a contribution in the effort devoted to the characterization of perfluoroalkanes and their mixtures. Recent publications relating perfluoroalkanes systems apply different approaches to describe their properties but the conclusions taken cannot be generalized once experimental data is not available to confirm their accuracy and applicability. The main objective is to complement/validate experimental data available in the literature and also present new experimental data that, besides the practical direct interest, can help to answer/validate the theories and models relating highly fluorinated systems.

The thesis is organized in two parts. The first part deals with the experimental data measured: density, vapour pressure, solubility of gases, namely oxygen at atmospheric pressure and carbon dioxide at high pressure and liquid-liquid equilibrium for alkane + perfluoroalkanes mixtures. The apparatus built to measure vapour pressure and oxygen solubility data are presented as well as the experimental procedure used. Among the studied perfluoroalkanes are the ones that are currently been used for the applications

Table I.3. Literature data relative to the modelling of thermodynamic properties of pure perfluoroalkanes and their mixtures. PFC = Perfluoroalkane; HC = Alkane; MC = Monte Carlo; MD = Molecular Dynamics

System	Modelling	Reference
PFC (C_1-C_4) + HC (C_1-C_8)	SAFT - VR	McCabe et al., 1998
Pure PFCs C_5 - C_{16}	Molecular Simulation: MC	Cui et al., 1998
CO_2 + C_6H_{14} CO_2 + C_6F_{14}	Molecular Simulation: MC	Cui et al., 1999
Xe + PFC (C_1-C_2)	SAFT - VR	McCabe et al., 2001
Xe + C_6H_{14} Xe + C_6F_{14}	Molecular Simulation: MD SAFT – VR	Bonifácio et al., 2002
PFC + HC	Molecular Simulation: MD	Song et al. 2003
CO_2 + C_6H_{14} CO_2 + C_6F_{14}	Molecular Simulation: MD	Gomes and Pádua, 2003
O_2 + C_6H_{14} O_2 + C_6F_{14}	Molecular Simulation: MD	Dias et al. 2003
Pure PFCs (C_4-C_7)	Molecular Simulation: MD	McCabe et al., 2003
CO_2 + HC (C_6-C_8) CO_2 + PFC (C_6-C_7)	SAFT - VR	Colina et al., 2004
O_2, CO_2, H_2O + Substituted PFCs	Molecular Simulation: MD	Deschamps et al., 2004
Pure PFCs (C_6; C_9)	Cubic EoS	Piñeiro et al., 2004
CO_2 + HC (C_6-C_{13}) + PFC (C_6-C_8)	SAFT - VR	Colina and Gubbins, 2005
CO_2 + HC (C_6;C_{10}) + PFC (C_6;C_{10})	Molecular Simulation: MC	Zang and Siepman, 2005
PFC (C_5-C_8) + HC (C_5-C_8)	SAFT - VR	Morgado et al. 2005

mentioned above, as is the case of perfluoro-n-hexane, perfluoro-n-octane, perfluorodecalin and 1Br-perfluoro-n-octane.

The second part addresses the thermodynamic modelling of the properties and solubilities measured. In this work, the soft-SAFT equation of state (EoS) is used to study the behaviour of bulk properties of fluid systems at thermodynamic equilibrium, mainly vapour-liquid equilibria, but also liquid-liquid coexistence and critical behaviour. The main difference between the soft-SAFT EoS and the other SAFT versions is that the reference

term is a Lennard-Jones that accounts simultaneously for the attractive and the repulsive term of the interaction potential. One of the main advantages of using a molecular based EoS as the soft-SAFT is that the parameters are physically meaningful and independent of the thermodynamic conditions. Also, contrarily to simple mean-field approaches it is possible to explicitly consider intramolecular as well as intermolecular interactions. Furthermore, and probably the most important feature, is that SAFT is an approach in which the different microscopic contributions that control the macroscopic properties of the fluid are explicitly considered when building the theory.

In this sense, non-ideal contributions, such as molecular shape, polarity and association, can be introduced in the development of the equation according to the system in study originating a robust and versatile tool for the prediction of thermodynamic properties of complex systems. The systems studied include pure perfluoroalkanes, alkanes, gases as xenon, radon, oxygen and carbon dioxide and mixtures between them. The equation was used to correlate/predict vapour pressure and density data of the pure compounds, vapour-liquid equilibrium of gases and alkanes in perfluoroalkanes and liquid-liquid equilibrium between perfluoroalkanes and alkanes.

For all the properties studied, the results given by the sof-SAFT Eos are always compared with the results given by a cubic EoS, in this case the Peng-Robinson EoS. The solubility of oxygen in perfluoroalkanes was also modelled using the Regular Solution Theory in an entirely predictive manner in order to quantify the importance of the entropic contribution during the dissolution process.

References

Banks, R. E. *Fluorocarbons and Their Derivatives* Macdonald Technical & Scientific: London, (1970) 7-69

Banks, R. E.; Tatlow, J. C., *A Guide to Modern Organofluorine Chemistry,* Journal of Fluorine Chemistry (1986) 33: 227

Betzemeier, B.; Knochel, P., *Perfluorinated Solvents - a Novel Reaction Medium in Organic Chemistry,* Top. Curr. Chem. (1999) 206: 61

Bonaventura, C.; Tesh, S.; Faulkner, K. M.; Kraiter, D.; Crumbliss, A. L., *Conformational Fluctuations in Deoxy Hemoglobin Revealed as a Major Contributor to Anionic Modulation of Function Through Studies of the Oxygenation and Oxidation of Hemoglobins A(0) and Deer Lodge Beta 2(NA2)His -> Arg,* Biochemistry (1998) 37: 496

Bonifácio, R. P.; Filipe, E. J. M.; McCabe, C.; Gomes, M. F. C.; Pádua, A H. A., *Predicting the Solubility of Xenon in n-hexane and n-perfluorohexane: A Simulation and Theoretical Study,* Molecular Physics (2002) 100: 2547

Calado, J. C.; McLure, I. M.; Soares, V., *Surface Tension for Octafluorocyclobutane, n-butane and their Mixtures from 233 K to 254 K, and Vapour Pressure, Excess Gibbs Function and Excess Volume for the Mixture at 233 K,* Fluid Phase Equilibria, (1978) 2: 199

Chandler, D., *Structures of Molecular Liquids*, Annu. Rev. Phys. Chem. (1978) 29: 441

Cho, M. H.; Wang, S. S., *Enhancement of Oxygen-Transfer in Hybridoma Cell-Culture by Using a Perfluorocarbon as an Oxygen Carrier,* Biotechnology Letters (1988) 10: 855

Clark, L. C. Gollan F., *S u rvival of Mammals Breathing Organic Liquids Equilibrated with Oxygen at Atmospheric Pre s s u re,* Science (1966) 152: 1755

Clark, E. S., *The Molecular Conformations of Polytetrafluoroethylene: Forms II and IV,* Polymer (1999) 40: 4659

Cohn SM., *Blood Substitutes in Surgery,* S u rgery (2000) 127: 599

Colina, C. M.; Galindo, A.; Blas, F. J.; Gubbins, K.E. *Phase Behavior of Carbon Dioxide Mixtures with n-alkanes and n-perfluoroalkanes* Fluid Phase Equilibria (2004) 222–223: 77

Colina, C. M.; Gubbins, K. E. *Vapor-Liquid and Vapor-Liquid-Liquid Equilibria of Carbon Dioxide/n-perfluoroalkane/n-alkane Ternary Mixtures* J. Phys. Chem. B (2005) 109: 2899

Cui, S. T.; Siepmann, J. I.; Cochran, H. D.; Cummings, P. T., *Intermolecular Potentials and Vapor-Liquid Phase Equilibria of Perfluorinated Alkanes,* Fluid Phase Equilibria (1998) 146: 51

Cui, S. T.; Cochran, H. D.; Cummings, P. T. *Vapor-Liquid Phase Coexistence of Alkane-Carbon Dioxide and Perfluoroalkane-carbon dioxide Mixtures* J. Phys. Chem. B (1999) 10: 4485

Deschamps, J.; Gomes, M. F. C.; Padua, A. A. H., *Solubility of Oxygen, Carbon Dioxide and Water in Semifluorinated Alkanes and in Perfluorooctylbromide by Molecular Simulation,* Journal of Fluorine Chemistry (2004) 125: 409

Dias, A. M. A.; Bonifácio, R. P.; Marrucho, I. M.; Pádua A. A. H.; Gomes, M. F. C. *Solubility of Oxygen in n-hexane and in n-perfluorohexane. Experimental Determination and Prediction by Molecular Smulation* Phys. Chem. Chem. Phys. (2003) 5: 543

Drakesmith, F. G. *Organofluorine Chemistry - Techniques* in Topics in Current Chemistry (1997) 193: 197

Elibola, M.; Mavituna, F., *A Remedy to Oxygen Limitation Problem in Antibiotic Production: Addition of Perfuorocarbon,* Biochemical Engineering Journal (1999) 3: 1

Ellis, D. A; Cahill, T. M.; Mabury, S. A.; Cousins, I. T.; Mackay, D. *Partitioning of Organofluorine Compounds in the Environment*, The Handbook of Environmental Chemistry Vol. 3, Chapter 2, Organofluorines, ed. by A.H.Neilson, 2002

Fielding, H. C. *Organofluorine Surfactants and Textile Chemicals*, in Organofluorine Chemicals and Their Industrial Applications, Banks, R. E., Editor. (1979) Ellis Horwood for the Society of Chemical Industry: Chichster, Great Britain. p. 214-234;

Gabriel J. L., Miller T. F., Wolfson M. R., Shaffer T. H., *Quantitative Structure-Activity Relationship of Perfluorinated Hetero-hydrocarbons as Potential Respiratory Media: Application to Oxygen Solubility, log P, Viscosity, Vapor Pressure and Density,* ASAIO J. (1996) 42: 968

Gjaldbaek, J. C., *The Solubility of Hydrogen, Oxygen and Ethane in Normal Hydrocarbons*, Acta Chemica Scandinavica (1963) 17: 127

Gladysz, J. A. *Are Teflon Ponytails the Coming Fashion for Catalysts*, Science (1994) 266: 55

Gomes, M. F. C.; Padua, A. A. H. *Interactions of Carbon Dioxide with Liquid Fluorocarbons* Journal of Physical Chemistry B (2003) 107 (50): 14020

Hamasaki, A.; Shioji, N.; Ikuta, Y.; Hukuda, Y.; Makita, T.; Hirayama, K.; Matutaki, H.; Tukamota, T.; Sasaki, S. *Carbon Dioxide Fixation by Microalgae Photosynthesis Using Actual Flue Gas* Appl. Biochem. Biotechnol. (1994) 45/46: 799

Hamza, M. A.; Serratrice, G.; Stébé, M. J.; Delpuech, J. J., *Solute-Solvent Interactions in Perfluorocarbon Solutions of Oxygen – an NMR Study*, J. Am. Chem. Soc**.** (1981) *103*: 3733

Hildebrand, J. H.; Rotariu, G. J., *Molecular Order in n-heptane and n-perfluoro-heptane,* J. Am. Chem. Soc. (1952) 4455
Hildebrand J. H., Prausnitz, J. M., Scott, R. L., *Regular and Related Solutions*, Van Nostrand Reinhold, New York, 1970, Chapter 8

Hoefling, T. A.; Enick, R. M.; Beckman, E. J. *Microelmulsions in Near-critical and Supercritical CO_2*, J. Phys. Chem. (1991) 95: 7127

Horvath, I. T.; Rabai, J. *Facile Catalyst Separation Without Water-Fluorous Biphase Hydroformylation of Olefins*, Science (1994) 266: 72

Kennan, R. P.; Pollack, G. L., *Solubility of Xenon in Perfluoroalkanes: Temperature Dependence and Thermodynamics*, J. Chem. Phys. (1988) 89: 517

Kishimoto, T.; Okakuta, T.; Nagashima, H.; Monowa, T.; Yokoyama, S. Y.; Yamaberi, K. *CO_2 Fixation and Oil Production Using Micro-algae* Journal of Fermentation and Bioengineering (1994) 78: 479

Krafft, M .P., *Fluorocarbons and Fluorinated Amphiphiles in Drug Delivery and Biomedical Research* Advanced Drug Delivery Reviews (2001) 47: 209– 228

Lawson, D. D.; Moacanin, J.; Scherer, K. V.; Terranova, T. F.; Ingham, J. D. *Methods for Estimation of Vapor-pressures and Oxygen Solubilities of Fluorochemicals for Possible Application in Artificial Blood Formulations* J. Fluorine Chem. (1978) 12: 221

Lee, L. H. *Relationships Between Solubility Parameters and Surface Tensions of Liquids*, J. of Paint Technology (1970) 42: 365

Lowe KC, *Perfluorochemical Respiratory Gas Carriers: Benefits to Cell Culture Systems* Journal of Fluorine Chem. (2002) 118 (1-2): 19

McCabe C.; Galindo A.; Gil-Villegas A.; Jackson G. *Predicting the High-Pressure Phase Equilibria of Binary Mixtures of Perfluoro-n-alkanes plus n-alkanes using the SAFT-VR Approach* J. of Phys. Chem. B (1998) 102 (41): 8060

McCabe, C.; Dias, L. M. B.; Jackson, G.; Filipe, E. J. M. *On the liquid mixtures of xenon, alkanes and perfluorinated compounds* Phys. Chem. Chem. Phys. (2001) 3: 2852

McCabe, C.; Bedrov, D.; Borodin, O.; Smith, G. D.; Cummings, P. T. *Transport Properties of Perfluoroalkanes using Molecular Dynamics Simulation: Comparison of United- and Explicit-atom Models* Ind. Eng. Chem. Res. (2003) 42: 6956

McLure, I. A.; Edmonds B., *Extremes in Surface-tension of Fluorocarbon + Hydrocarbon Mixtures*, Nature (1973) 241: 71

Meinert, H.; Knoblich, A., *The Use of Semifluorinated Alkanes in Blood-substitutes*, Biomater., Artif. Cells, Immobilization Biotechnol. (1993) 21: 583

Miller, J. H., Jr.; Googe, J. M., Jr.; Hoskins, J. C., *Combined Macular Hole and Cataract Surgery*, Am. J. Ophthalmol. (1997) 123: 705

Miura, Y.; Akano, T.; Fukatsu, K.; Miyasaka, H.; Mizogushi, T.; Yagi, K.; Maeda, T.; Ikuta, Y.; Matsumoto, H. *Stably Sustained Hydrogen Production by Biophotolysis in Natural Day/Night Cycle* Energy Conversion and Management (1997) 38 suppl: 533

Molina, M. J., Rowland, R. S. *Stratospheric Sink for Chlorofluoromethanes: Chlorine Atom Catalyzed Destruction of Ozone* Nature (1974) 249: 810

Morgado, P.; McCabe, C.; Filipe, E. J. M. *Modelling the Phase Behaviour and Excess Properties of Alkane + Perfluoroalkane Binary Mixtures With the SAFT–VR Approach* Fluid Phase Equilibria (2005) 228–229: 389

Negoro, M. A.; Hamasaki, Y.; Kuta, I.; Makita, T.; Hirayama, K.; Suzuki, S. *Carbon Dioxide Fixation by Microalgae Photosynthesis Using Actual Flue Gas Discharged from a Boiler* Appl. Biochem. Biotechnol (1993) 39/40: 643

Osswald, T.; Schneider, S.; Wang, S.; Bannwarth, W. *Stille Couplings in Supercritical CO_2 Catalyzed with Perfluoro-tagged and un-tagged Pd Complexes* Tetrahedron Letters (2001) 42: 2965

Pierotti, R. A., *Scaled Particle Theory of Aqueous and non-aqueous Solutions*, Chem. Rev. (1976) 76: 717

Piñeiro, M. M.; Bessières, D.; Gacio, J. M.; Saint-Guirons, H.; Legido, J. L. *Determination of High-pressure Liquid Density for n-perfluorohexane and n-perfluorononane* Fluid Phase Equilibria (2004) 220: 125

Pollack, G. L.; Kennan, R. P.; Himm, J. F.; Carr, P. W., *Diffusion of Xenon in Liquid Alkanes – Temperature Dependence Measurements with a New Method-Stokes-Einstein and Hhard-sphere Theories*, J. Chem. Phys. (1989) 90: 6569

Porter, T. R.; Xie, F.; Kricsfeld, A.; Kilzer, K., *Noninvasive Identification of Acute Myocardial-ischemia and Reperfusion with Contrast Ultrasound using Intravenous Perfluoropropane Exposed Sonicated Dextrose Albumin*, J. Am. Coll. Cardiol. (1995) 26: 33

Raveendran, P.; Wallen, S. L., *Cooperative C-H Center Dot Center Dot Center Dot O Hydrogen Bonding in CO_2-Lewis Base Complexes: Implications for Solvation in Supercritical CO_2*, J. Am. Chem. Soc. (2002) 124: 12590

Riess, J. G. *Reassessment of Criteria for the Selection of Perfluorochemicals for Second-Generation Blood Substitutes: Analysis of Structure/Property Relationships*. Artif Organs. (1984) 8: 44

Riess, J. G. *Oxygen Carriers ("Blood Substitutes"): Raison d'Etre, Chemistry, and Some Physiology* Chem. Rev. (2001) 101: 2797

Rowinsky EK. *Novel Radiation Sensitizers Targeting Tissue Hypoxia*, Oncology (Huntingt) (1999) 13: 61

Sargent, J. W.; Seffl, R. J., *Properties of Perfluorinated Liquid,* Fed Proc. (1970) 29: 1699
Schlosser, M.; Michel, D., *About the Physical Size of Fluorine Substituents,* Tetrahedron (1996) 52: 99

Scott, R.L., *The Anomalous Behaviour of Fluorocarbon Solutions,* J. Phys. Chem. (1958) 62: 136

Shin, S.; Collazo, N.; Rice, S. A., *A Molecular-dynamics Study of the Packing Structures in Monolayes of Partially Fluorinated Amphiphiles*, J. Chem.Phys. (1992) 96: 1352

Serratrice, G.; Delpuech, J.J.; Diguet, R., *Isothermal Compressibility of Fluorocarbons-Relationship with the Solubility of Gases*, Nouv. J. Chim. (1982) 6: 489

Serratrice, G.; Stébé, M. J.; Delpuech, J. J., *The Structure of Liquid Fluorocarbons – Oxygen and Nitric-oxide as Paramagnetic Probes*, J. Chim. Phys. (1985) 82: 579

Smart, B. E., *Fluorine Substituent Effects (on bioactivity*), J. Fluorine Chemistry (2001) 109: 3

Song, W.; Rossky, P. J.; Maroncelli, M. *Modeling Alkane-perfluoroalkane Interactions Using All-atom Potentials: Failure of the Usual Combining Rules* J. Chem. Chem. Phys. (2003) 119: 1945

Stone, M. T.; Rocha, S. R. P.; Rossky, P. J.; Johnston, K. P. J., *Molecular Differences Between Hydrocarbon and Fluorocarbon Surfactants at the CO_2/Water Interface,* J. Phys. Chem. B (2003) 107: 10185

Studer, A; Hadida, S; Ferritto, R.; Kim, S. Y.; Jeger, P; Wipf, P; Curran, D. P., *Fluorous Synthesis: a Fluorous-phase Strategy for Improving Separation Efficiency in Organic Synthesis,* Science (1997) 275: 823

Uhlig, H. H., *The Solubilities of Gases and Surface Tension,* J. Phys. Chem. (1937) 41: 1215

Vacek, V.; Hallewell, G.; Ilie, S.; Lindsay, S. *Perfluorocarbons and Their Use in Cooling Systems for Semiconductor Particle Detectors* Fluid Phase Equilibria (2000) 174: 191

Wallington, T. J.; Schneider, W. F.; Worsnop, D. R.; Nielsen, O. J.; Sehested, J. Debruyn, W. J.; Shorter, J. A., *The Environmental Impacts of CFC Replacements – HFCs and HCFCs,* Environ Sci. Technol (1994) 28: 320

Wasanasathian, A., Peng, C-A, *Enhancement of Microalgal Growth by Using Perfluorocarbon as Oxygen Carrier*, Artificial Cells, Blood Substitutes, & Immobilization Biotechnolog (2001) 29: 47

Watkins, E. K.; Jorgensen, W. L., *Perfluoroalkanes: Conformational Analysis and Liquid-State Properties from ab Initio and Monte Carlo Calculations,* J. Phys. Chem. A (2001) 105: 4118

Wesseler, E. P.; Iltis, R.; Clark, L., *Solubility of Oxygen in Highly Fluorinated Liquids*, J. Fluorine Chem. (1977) 9:137
Wolfson, M. R.; Greenspan, J. S.; Shaffer, T. H. *Liquid-Assisted Ventilation: an Alternative Respiratory Modality* Pediatric Pulmonology (1998) 26: 42

Zhang, L.; Siepmann, J. I. *Pressure Dependence of the Vapor-Liquid-Liquid Phase Behaviour in Ternary Mixtures Consisting of n-alkanes, n-perfluoroalkanes, and Carbon Dioxide* J. Phys. Chem. B (2005) 109: 2911

II. Part

EXPERIMENTAL METHODS, RESULTS AND DISCUSSION

II. 1. Introduction

The increasing number of applications of fluorinated compounds in medicine, environment, and industry requires a precise knowledge of the thermophysical properties of these substances. In spite of their many applications, literature data relating these compounds is in some cases old and many times discrepant; in other cases only one set of results can be found and, for some compounds with current application, experimental data is completely inexistent. It is therefore of both practical and theoretical interest to measure the thermophysical properties of these compounds to create a wide and reliable experimental database in order to understand their different behaviour and to be able to accurately predict it.

In this work, densities, vapour pressures, solubility of gases, oxygen at low pressure and carbon dioxide at high pressure, and liquid – liquid equilibria data for alkane + perfluoralkane mixtures were measured. Density and vapour pressure data is needed not only to select the best perfluoroalkane for a given application but also for solubility data calculation as will be explained later.

Density data was measured with a commercial vibrating tube Antón Paar DSA-48 densimeter between 288.15 and 313.15 K at atmospheric pressure based on the mechanical oscillator principle using a thermostatized cell with a U shape.

An apparatus based on the static method was built to measure vapour pressure data between 288 K and 333 K. Pressure on this apparatus was measured with a high precision temperature compensated, quartz pressure transducer (ParoScientific Inc. model 2100A-101).

The solubility of oxygen and carbon dioxide were measured at different thermodynamic conditions chosen according to the main application of each system. An accurate apparatus based on the saturation method was built to measure the solubility of oxygen in pure perfluoroalkanes at atmospheric pressure and temperatures ranging from 288 to 313K. The solubility is determined by measuring the quantity of gas dissolved in an accurately known volume of solvent at constant pressure and temperature. The apparatus has a simple design and can be easily adapted to measure the solubility of systems with different solubilities. Linear and cyclic fully saturated fluorochemicals (from C_6 to C_9 and perfluorodecalin) and also substituted fluorochemicals (1Br-Perfluorooctane, 1H-Perfluorooctane, 1H, 8H-Perfluorooctane) were studied in order to conclude about the

influence of the structure, chain length and the substitution of terminal groups on the solubility of oxygen.

The solubility of carbon dioxide was studied for different perfluoroalkanes including linear (perfluoro-n-octane), cyclic (perfluorodecalin and perfluoromethylcyclohexane) and aromatic compounds (perfluorobenzene and perfluorotoluene), at pressures up to 120 bar and temperatures ranging from 293 to 353 K. Measurements were performed using a high-pressure cell with a sapphire window that allows observation of the point at which the phase boundary is crossed. The different molecular architectures were chosen aiming at checking the influence of the structures on their miscibility with carbon dioxide.

The liquid-liquid equilibria (LLE) of binary mixtures of perfluoro-n-octane plus alkanes, n-C_nH_{2n+2} (n = 6 - 9), were measured, using the synthetic method, by turbidimetry at atmospheric pressure, and using a light scattering technique for measurements at pressures up to 1500 bar.

The main objective is to collect and compare data for different saturated and non-saturated fluorinated compounds that are being studied/used for different applications. Experimental data are correlated using appropriate equations for the temperature ranges studied. Whenever possible, experimental data measured is compared with literature data available; comparison is done among the different methods and purities of samples used. For some of the fluorinated compounds studied, new experimental and correlated data is presented.

II.1.1. Materials

The origin and purities, checked by gas chromatography, of the compounds used in this work are summarized in Table II.1. Both solvents and gases were used without further purification.

Most of the fluorocarbon samples used by earlier authors for measurements of thermodynamic properties of perfluoroalkanes were prepared by the fluorination of the corresponding hydrocarbons with cobalt trifluoride. The resulting crude fluorocarbons were then submitted to a sequence of purification procedures to obtain the purest sample possible. Among those procedures where the reflux with an alkaline solution of potassium permanganate to remove unsaturated compounds, silica gel adsorption, fractional

distillation with more then 80 stages and fractional crystallization. Even so, Good et al. (1959) reported that after treatment with a neutral permanganate solution to remove olefinic impurities by oxidation followed by distillation in an efficient fractionating column and by silica gel percolation of selected fractions of distilled material, the purity of the best sample of perfluoromethylcyclohexane was only in the order of 98%.

Table II.1. Purities and Origin of the Compounds Studied in This Work

Compound	Formula	Origin	Purity (%)
Oxygen	O_2	Air Liquid	99.999
Carbon Dioxide	CO_2	Messer France	99.90
Perfluoro-n-hexane	C_6F_{14}	Aldrich	99.11
Perfluoro-n-heptane	C_7F_{16}	Aldrich	85
Perfluoro-n-octane	C_8F_{18}	Aldrich	98.36
Perfluoro-n-nonane	C_9F_{20}	Apollo Scientific	99.18
1Br-Perfluoro-n-octane	1Br-C_8F_{17}	ABCR	99.90
1H-Perfluoro-n-octane	1H-C_8F_{17}	Interchim	97.05
1H,8H-Perfluoro-n-octane	1H,8H-C_8F_{16}	Apollo Scientific	99.10
Perfluorodecalin	$C_{10}F_{18}$	ABCR	99.88
Perfluorobenzene	C_6F_6	Fluorochem	99.99
Perfluorotoluene	C_7F_8	Apollo Scientific	99.80
Perfluoromethylcyclohexane	C_7F_{14}	Apollo Scientific	99.98
n-Hexane	C_6H_{14}	Aldrich	99.01
n-Heptane	C_7H_{16}	Aldrich	99.34
n-Octane	C_8H_{18}	Aldrich	99.33
n-Nonane	C_9H_{20}	Aldrich	99.00

Crowder et al. (1967) stated that fluorocarbons are substances difficult to purify by fractional distillation because impurities in the form of fluorocarbon derivatives containing other elements, such as hydrogen, oxygen, and nitrogen, may form constant-boiling mixtures with the fluorocarbon or may boil at very nearly the same temperature. Also, structural isomers boil very close to one another, within a few degrees or tenths of degree. In their work, the authors used samples with purities approaching 100% only achieved using gas chromatography to purify the samples.

Nowadays, purities higher than 99% can be easily obtained for most of the perfluorocarbons. The main producers claim that the impurities present in the samples are essentially isomers of the main component.

I.2. Density

I.2.1. Bibliographic revision

Density data can be measured both directly or indirectly using different methods. Between the most common methods for atmospheric pressure measurements are the volumetric and the hydrostatic weighting measurements (Pádua,1994).

Volumetric methods are those that require the knowledge of the volume of the sample container. Its main disadvantage is that they are relative methods, which means that calibrations have to be performed along the experimental conditions to be studied, using calibrating fluids with densities similar to those to be measured. Volumetric measurements are usually performed using picnometers (Bauer et al., 1972), or densimeters with a vibrating tube with a U or V shape (Albert et al., 1984). Both techniques have a precision of 0.0005% but the accuracy obtained using the picnometer is higher (0.02%) than using the U vibrating tube (0.1%). However, the vibrating tube method is easy to operate and requires less amount of sample to be used.

Hydrostatic weighting methods are the direct application of the Arquimedes principle, measuring the density of the fluid through the impulsion recorded by a solid body immersed in that fluid. There are essentially three hydrostatic weighting methods: the fluctuation technique, the magnetic levitation and the direct method. The fluctuation technique equilibrates a solid body immersed into the fluid in study for fixed conditions of temperature and pressure (Girard G., 1987), while the magnetic levitation or indirect method determines the impulsion applied to a solid body by measuring the force needed to levitate it, being this force related to the density of the fluid under study (Greer et al., 1974). The direct method measures the apparent weight of a float immersed into the fluid using an analytic balance. (Hales et al., 1983). The main advantage of this last method is that the volume problem is discarded being the measurements absolutes with no need of calibrations. The direct method, besides being simpler to apply, gives the best precision and accuracy (0.005% and 0.02% respectively against 0.01% and 0.1% obtained for the

fluctuation and magnetic float methods) just compared with the results obtained when picnometers are used.

Table II.2 compiles references where density data for fluorinated compounds heavier than C_6 could be found, reporting the methods and measuring conditions in each case. Comparison with data measured in this work will be presented in the following section.

Table II.2. Compilation of the References Reporting Experimental Density Data for Fluorinated Compounds

Method	Sample purity (%)	T (K) range	P (bar) range	Reference
		C_6F_{14}		
Pycnometer	96.5	273 - 323	1	Stiles et al (1952)
Pycnometer	99.98	288 - 318	1	Dunlap et al (1958)
Vibrating tube	99	283 - 315	1 - 400	Piñeiro et al (2004)
		C_8F_{18}		
Pycnometer	Purified*	293 - 323	1	Haszeldine at al. (1951)
Picnometer	Purified*	298 - 343	1	Kreglewski (1962)
		C_9F_{20}		
Pycnometer	Purified*	273 - 333	1	Haszeldine et al. (1951)
Vibrating tube	99	283 - 343	1 - 400	Piñeiro et al (2004)
		C_6F_6		
Pycnometer	99.995	398 - 517	1	Douslin et al. (1969)
Magnetic float	99.98	293 - 423	1	Hales (1970)
Magnetic float	99.97	293 - 490	1	Hales et al. (1974)
		C_7F_8		
Magnetic float	99.87	293 - 490	1	Hales et al. (1974)
		C_7F_{14}		
Not reported	Purified*	298	1	Glew et al. (1956)

* The authors purified the samples used but do not state the final purity.

I.2.2. Apparatus

Density was measured with a commercial vibrating tube Antón Paar DSA-48 densimeter between 288.15 and 313.15 K at atmospheric pressure based on the mechanical oscillator principle. The precision of the measurements is $\pm$ 5x10^{-5} g.cm^{-3}. This method was chosen since, as mentioned above, it uses a small

amount of sample, which is an advantage when dealing with fluorinated compounds with high purity that are very expensive.

The cell used to measure the density has a U shape and is inserted in a glass jacket filled with a high thermal conductivity gas and covered with copper in order to guarantee a proper heat transfer between the thermostat and the measuring sample. The temperature is measured with a NTC sensor with a precision of $\pm 10^{-2}$ K.

The measuring principle is based on the calculation of the frequency of resonance of a mechanic oscillator with a given mass *m* and volume V_0, which is excited to be in resonance. The value of the natural oscillation period changes when the sample to be measured is introduced in the oscillator. The oscillation period can be expressed as:

$$\tau = 2\pi\left(\frac{m+\rho V_0}{K}\right)^{1/2} \tag{II.1}$$

where *K* is the elastic constant of the oscillator. Equation II.1 can be expressed explicitly in density as:

$$\rho = \frac{K\tau^2}{4\pi^2 V_0} - \frac{m}{V_0} \quad \equiv \quad C_1\tau^2 - C_2 \tag{II.2}$$

where C_1 and C_2 are characteristic constants of the apparatus which depend on temperature and that are determined using reference fluids with known density

$$C_1 = \frac{\rho_1 - \rho_2}{\tau_1^{\,2} - \tau_2^{\,2}} \tag{II.3}$$

$$C_2 = \frac{\tau_2^{\,2}\rho_1 - \tau_1^{\,2}\rho_2}{\tau_1^{\,2} - \tau_2^{\,2}} \tag{II.4}$$

Densities ρ_1 and ρ_2 and the oscillation periods τ_1 and τ_2 correspond to the reference fluids at the same conditions of pressure and temperature. Water mili-Q and n-heptane (Fluka 99.5%) were used as references. The uncertainty of the measurements is $\pm 5\text{x}10^{-5}$ g.cm^{-3} with an accuracy of $\pm 1\text{x}10^{-5}$ g.cm^{-3}.

I.2.3. Experimental results and Discussion

Density data measured in this work is presented in Table II.3. For the temperature range studied, experimental data was found to be correctly described by a linear equation of the type:

$$\rho_{calc} = A - BT \qquad \text{(II.5)}$$

where T is the temperature. Coefficients for Equation II.5 are reported in Table II.4.

Table II.3. Experimental and Calculated Liquid Densities of the Studied Compounds

T K	ρ_{exp} g.cm^{-3}	ρ_{calc} g.cm^{-3}	$\Delta\rho^a$ g.cm^{-3}
		C_6F_{14}	
288.15	1.7056	1.7056	0.00072
293.15	1.6910	1.6910	0.00043
298.15	1.6761	1.6761	-0.00006
303.15	1.6611	1.6611	-0.00074
313.15	1.6302	1.6302	-0.00285
		C_8F_{18}	
288.15	1.7902	1.7903	-0.00017
293.15	1.7775	1.7774	0.00005
298.15	1.7648	1.7646	0.00018
303.15	1.7519	1.7517	0.00018
313.15	1.7258	1.7259	-0.00015
		C_9F_{20}	
288.15	1.8122	1.8122	-0.00016
293.15	1.8001	1.8001	0.00001
298.15	1.7879	1.7879	0.00011
303.15	1.7757	1.7757	0.00012
313.15	1.7509	1.7509	-0.00015
		1Br-C_8F_{17}	
288.15	1.9386	1.9386	-0.00006
293.15	1.9267	1.9266	0.00007
298.15	1.9148	1.9147	0.00013
303.15	1.9028	1.9027	0.00014
308.15	1.8908	1.8907	0.00008
313.15	1.8786	1.8787	-0.00007

[a] $\Delta\rho = \rho_{exp} - \rho_{calc}$

Table II.3. (continued)

T K	ρ_{exp} g.cm^{-3}	ρ_{calc} g.cm^{-3}	$\Delta\rho^{a}$ g.cm^{-3}
	1H-C_8F_{17}		
288.15	1.7736	1.7738	-0.00016
293.15	1.7618	1.7618	-0.00002
298.15	1.7499	1.7498	0.00007
303.15	1.7379	1.7378	0.00008
308.15	1.7258	1.7258	0.00000
313.15	1.7136	1.7138	-0.00018
	1H,8H-C_8F_{16}		
288.15	1.7753	1.7754	-0.00009
293.15	1.7644	1.7644	0.00004
298.15	1.7534	1.7533	0.00010
303.15	1.7424	1.7423	0.00010
308.15	1.7313	1.7313	0.00004
313.15	1.7202	1.7203	-0.00009
	$C_{10}F_{18}$		
288.15	1.9528	1.9529	-0.00008
293.15	1.9417	1.9417	0.00002
298.15	1.9305	1.9304	0.00007
303.15	1.9192	1.9191	0.00007
313.15	1.8966	1.8966	-0.00007
	C_6F_6		
288.15	1.6289	1.6289	-0.00009
293.15	1.6175	1.6175	-0.00001
298.15	1.6062	1.6061	0.00005
303.15	1.5948	1.5947	0.00005
308.15	1.5833	1.5833	0.00001
313.15	1.5718	1.5719	-0.00010
	C_7F_8		
288.15	1.6828	1.6829	-0.00015
293.15	1.6722	1.6723	-0.00004
298.15	1.6616	1.6616	0.00002
303.15	1.6509	1.6509	0.00003
308.15	1.6402	1.6402	-0.00003
313.15	1.6294	1.6295	-0.00016

[a] $\Delta\rho = \rho_{exp} - \rho_{calc}$

Table II.4. Constants for Density Correlation Using Equation II.5

Compound	A	B x10^3	δ^a x10^3
C_6F_{14}	2.5754	3.0172	0.30
C_8F_{18}	2.5323	2.5750	0.15
C_9F_{20}	2.5182	2.4497	0.12
1Br-C_8F_{17}	2.6295	2.3976	0.11
1H-C_8F_{17}	2.4654	2.4002	0.10
1H,8H-C_8F_{16}	2.4106	2.2045	0.08
$C_{10}F_{18}$	2.6015	2.2509	0.07
C_6F_6	2.2867	2.2827	0.06
C_7F_8	2.2984	2.1359	0.09

[a] $\delta = \left[\sum \left(\rho_{\exp} - \rho_{calc}\right)^2 / n\right]^{0.5}$, n being the number of experimental points

The literature density values for perfluoro-n-hexane, perfluoro-n-heptane, perfluoro-n-octane, perfluoro-n-nonane, perfluorobenzene and perfluorotoluene are compared in Figures II.1 to II.4 with the data measured in this work. For simplicity, comparisons for perfluorobenzene and perfluorotoluene are shown in the same figure since only one set of literature data was found for each compound.

Experimental data obtained for perfluoro-n-hexane agree, within 7x10^{-4}g/cm^3, with data measured by Piñeiro et al. (2004), whose measurements were performed with the same method used in this work but with a degassed sample. Also, the data obtained are systematically higher than data measured by Kennan et al. (1988) and Dunlap et al. (1958) for both an air saturated and a degassed sample and lower than those measured by Stiles et al. (1952). Both authors used picnometers to perform the measurements. Kennan et al. (1988) and Stiles et al. (1952) do not refer the degree of air saturation of their samples.

Kreglewski (1962) and Haszeldine et al. (1951) measured the density of perfluoro-n-octane using picnometers. The authors do not state the purity of their compounds. The values measured in this work agree well with those of Kreglewki (1962) but differ to within 0.7 % from the data reported by Haszeldine et al. (1951).

For perfluoro-n-nonane, density data was compared with the only data found in the literature measured by Piñeiro et al., 2004, and the agreement obtained is similar to the case of perfluoro-n-hexane. The author used the same method and purity of this work.

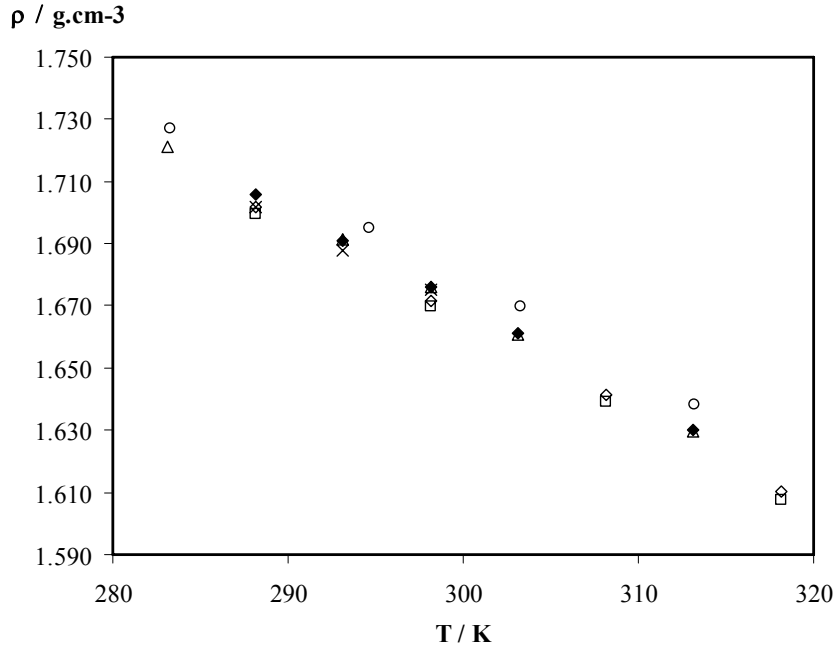

Figure II.1. Comparison between experimental density data for perfluoro-n-hexane measured in this work (♦) and literature data measured by (○) Stiles et al. (1952); (Δ) Piñeiro et al. (2004); (□) Dunlap et al. (1958) air saturated sample; (◊) Dunlap et al. (1958) degassed sample and (x) Kennan et al. (1988).

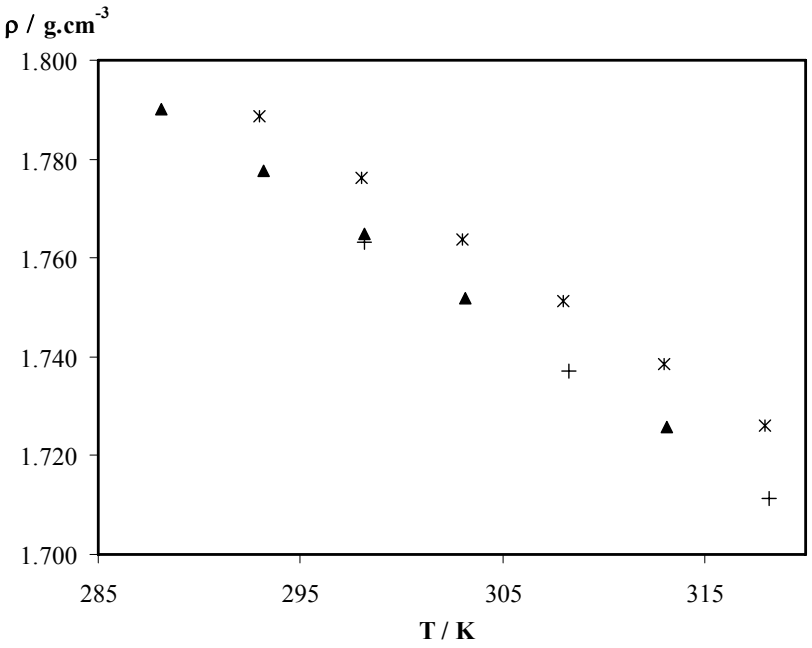

Figure II.2. Comparison between experimental density data for perfluoro-n-octane measured in this work (▲) and literature data measured by (*) Haszeldine et al. (1951) and (+) Kreglewski (1962).

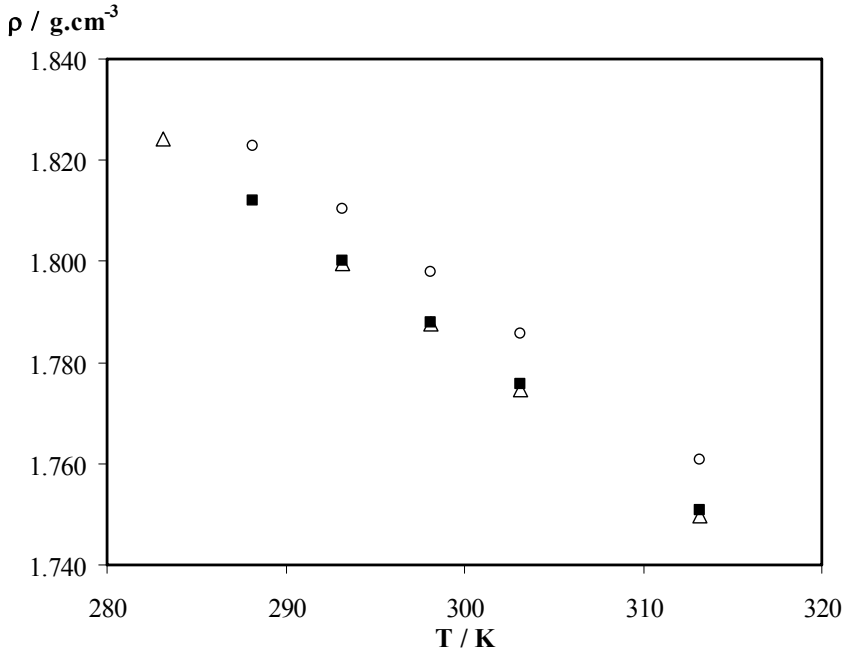

Figure II.3. Comparison between experimental density data for perfluoro-n-nonane measured in this work (■) and literature data measured by (*) Haszeldine et al. (1951) and (Δ) Piñeiro et al. (2004).

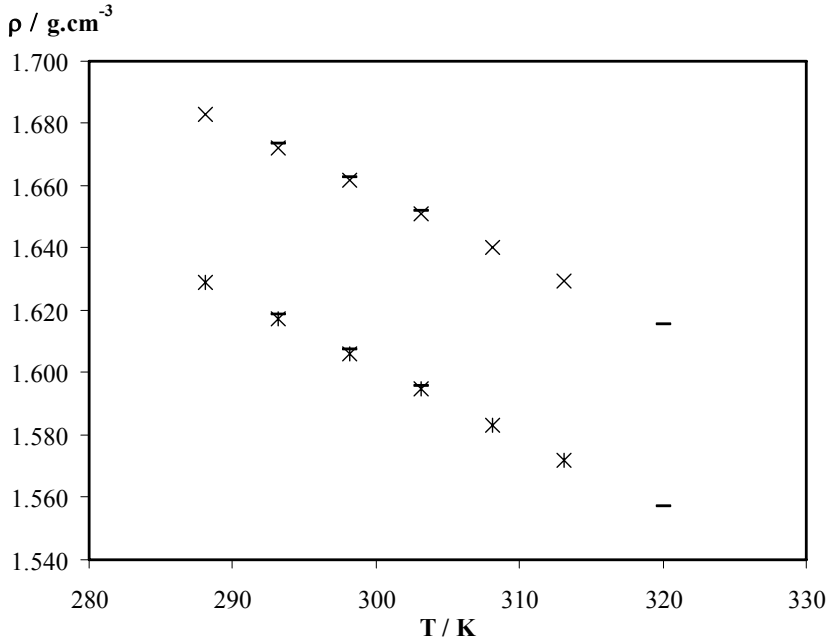

Figure II.4. Comparison between experimental density data for perfluorobenzene (*) and perfluorotoluene (x) measured in this work and literature data measured by (–) Hales et al. (1974).

Hales et al. (1974) measured the density of degassed samples of perfluorobenzene and perfluorotoluene by weighing with and without activation of a solenoid, which maintains a magnetically controlled float in the centre of the sample, according to a procedure described elsewhere (Hales et al, 1970). The densities measured for those compounds in the present work are in both cases systematically lower, by 1.2×10^{-3} g/cm^3, than those measured by these authors.

The effect of dissolved air on the density of perfluoro-n-hexane and perfluorobenzene was studied by Dunlap et al. (1958) and Hales et al. (1974), respectively. In the case of perfluoro-n-hexane, densities of the degassed sample were about 2.0×10^{-3} g/cm^3 higher than those of the air saturated sample. In the case of perfluorobenzene, differences between degassed and air saturated samples were about 7.5×10^{-4} g/cm^3. Those differences are related with the solvent's capacity to dissolve components of the air which is higher in the case of perfluoro-n-hexane (Dias et al., 2004; Evans et al., 1971). This observation cannot entirely justify the differences between density data measured in this work and literature data. In fact, differences observed for perfluorobenzene and perfluorotoluene, around 1.2×10^{-3} g/cm^3, are higher than would be expected just from considering the effect of dissolved air in the sample. For perfluoro-n-hexane, data measured by Dunlap et al. (1958), for an air saturated sample, are lower than those obtained in this work. Also, the comparison between the data measured in this work and reported by Piñeiro et al. (2004), seems to indicate that the methods used in both works are not very sensitive to differences between densities of degassed and air saturated samples. The different methods used to measure the densities are probably the main reason for the differences observed.

I.2.4. Derived properties

At the thermodynamic conditions used to measure density data in this work it is possible to calculate the isobaric thermal expansion coefficient α_P along the saturation curve at 298.15 K, using Equation II.6. Values obtained for the fluorinated compounds studied in this work are reported in Table II.5.

$$\alpha_P = -\frac{1}{\rho}\left(\frac{\partial \rho}{\partial T}\right)_P \qquad \text{(II.6)}$$

Table II.5. Derived Coefficients of Thermal Expansion at 298.15 K, α_P, of the Studied Compounds.

Compound	$\alpha_P \times 10^3$ (K^{-1})
C_6F_{14}	1.87 ± 0.05
C_8F_{18}	1.47 ± 0.04
C_9F_{20}	1.38 ± 0.04
1Br-C_8F_{17}	1.26 ± 0.03
1H-C_8F_{17}	1.38 ± 0.03
1H,8H-C_8F_{16}	1.27 ± 0.02
$C_{10}F_{18}$	1.12 ± 0.03
C_6F_6	1.43 ± 0.02
C_7F_8	1.29 ± 0.02

I. 3. Vapour pressure

I.3.1. Bibliographic revision

There are essentially five different methods that can be used to measure vapour pressure data. The choice between them is mainly due to the different thermodynamic ranges of application of each as well as with the accuracy required for the measurements. A brief overview of the main features of each of those methods follows.

Dynamic method – also called ebulliometric method, measures the boiling temperature, which pertains to a specific pressure. The recommended range of application is from 10^3 Pa up to 10^5 Pa, between 20ºC and 100ºC with an estimated repeatability up to 25% between 10^3 and $2x10^3$ Pa and 1-5% between $2x10^3$ and 10^5 Pa. This method has also been recommended for boiling point determination and is useful for that purpose up to 350ºC.

Static method - measures, at thermodynamic equilibrium, the vapour pressure established in a closed system at a specified temperature. This method is suitable for one-component and multicomponent solids and liquids. The recommended range of application is from 10 Pa up to 10^5 Pa, between 0ºC and 100ºC, with an estimated repeatability of 5-10%.

Isoteniscope - this standardized method is also a static method but is usually not suitable for multicomponent systems. The recommended range of application is from 100 Pa up to10^5 Pa, between 0ºC and 100ºC, with an estimated repeatability of 5-10%.

Vapour pressure balance - the quantity of substance leaving a cell per unit time through an apparatus of known size is determined under vacuum conditions in such a way that return of the substance into the cell is negligible (by measuring the pulse generated on a sensitive balance by a vapour jet or by measuring the weight loss). The recommended range of application is from 10^{-3} Pa up to 1 Pa, between 0ºC and 100ºC, with an estimated repeatability of 5-20%.

Gas saturation method - a stream of inert carrier gas is passed over the substance in such a way that it becomes saturated with its vapour and the vapour is then collected in a suitable trap. Measurement of the amount of material transported by a known amount of carrier gas is used to calculate the vapour pressure at a given temperature. The recommended range of application is up to 1 Pa, with an estimated repeatability of 10-30%.

Table II.6 compiles references where vapour pressure data for fluorinated compounds, higher then C_6 could be found, reporting the methods and measuring conditions for each case. Comparison with data measured in this work will be performed in the following section.

Table II.6. Compilation of the References Reporting Experimental Vapour Pressure Data for Fluorinated Compounds

Method	Sample purity (%)	T range (K)	Reference
	C_6F_{14}		
Dynamic	96.5	284 - 343	Stiles et al. (1952)
Static	99.98	303 - 331	Dunlap et al. (1958)
Up to 1atm - Isoteniscope > 1 atm - Dynamic	≈ 100	256 - 448	Crowder et al. (1967)
Static	Purified*	524 - 452	Ermakov et al. (1967)
P, V, T Measurements	98	433 - 449	Mousa (1978)
	C_8F_{18}		
Dynamic	Purified*	310 - 380	Kreglewski (1962)
Static	Purified*	368 - 502	Ermakov et al. (1967)
	C_9F_{20}		
Static	Purified*	387 - 524	Ermakov et al. (1967)
	C_6F_6		
Dynamic	99.9	293 - 358	Patrick and Prosser (1964)
Dynamic	99.97	310 - 362	Counsell et al. (1965)
Dynamic	99.99	216 - 387	Douslin and Osborn (1965)
Dynamic	> 99.95	370 - 515	Evans and Tiley (1966)
Static	99.995	398 - 516	Douslin et al. (1969)
Dynamic	99.995	290 - 378	Ambrose (1981)
Dynamic	99.95	318 - 377	Ambrose et al. (1990)
	C_7F_8		
Dynamic	99.89	290 - 400	Ambrose et al. (1981)
	C_7F_{14}		
Not reported	Purified*	272 - 314	Glew et al. (1956)
Dynamic	98	311 - 384	Good et al. (1959)

* The authors purified the samples used but do not state the final purity.

I.3.2. Apparatus and Procedure

In this work, an apparatus based on the static method was built to measure the vapour pressures of the compounds under study. A scheme of the set-up is depicted in Figure II.5. It consists mainly of a glass sample cell (A), a thermostatic bath (B), a temperature measurement system, pressure measuring system (C) and a temperature controlled glass vacuum line interconnecting the sample cell to the degassing system and to the pressure sensor.

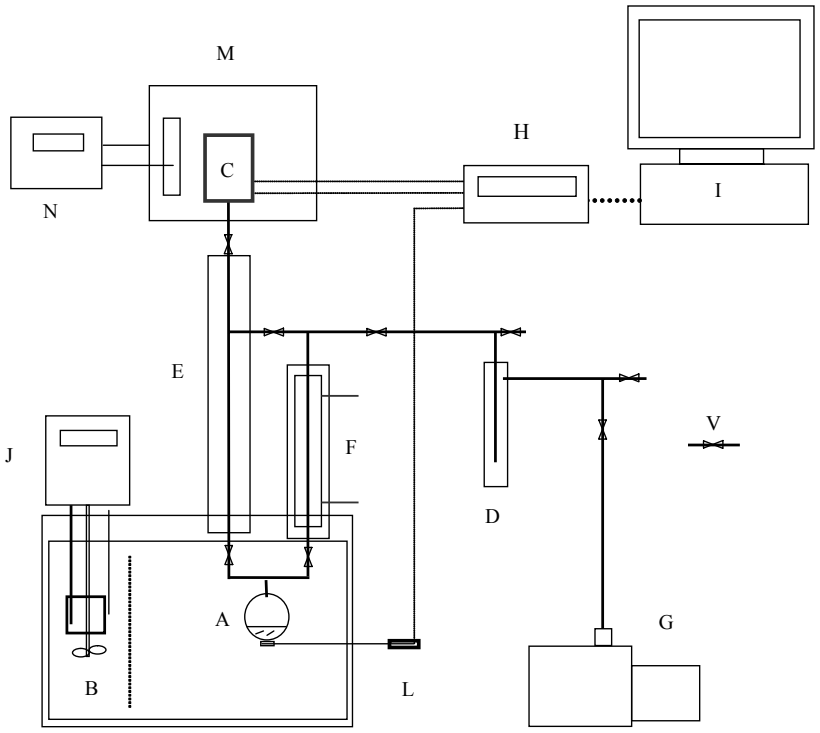

Figure II.5. Scheme of the vapor pressure apparatus: A, Cell; B, water bath; C, pressure transducer; D, liquid nitrogen trap; E, hot water jacket protected tube; F, condenser; G, vacuum pump; H, datalogger; I, computer; J, temperature controller; L, cell temperature sensor (Pt100); M, hot-block box for the pressure sensor; N, PID temperature controller; V, high vacuum Teflon valves.

For the studied temperature range, water was used as thermostatic bath fluid. The temperature in the bath was controlled with a digitally controlled immersion thermostat, Digiterm 100 (J). For temperatures below 298 K a refrigerated immersion cooling coil was used. The stability and uniformity of the temperature in the working area of the thermostatic bath was better than ± 0.01 K.

The temperature of the glass sample cell was measured with a calibrated Pt100 temperature sensor, class 1/10 (L), using a 6 ½ dataloger system (H) (Agilent model 34401A) for continuously data acquisition with an uncertainty of ± 0.05 K. Beforehand, in accordance to the International Temperature Scale of 1990, IST-90, this sensor was calibrated against a SPRT (25 ohm; Tinsley, 5187A) temperature probe using an ASL bridge model F26.

In pressure measurements, a high precision temperature compensated, quartz pressure tranducer (C) (ParoScientific Inc. model 2100A-101) was used. The accuracy of the pressure transducer is ± 0.01% in the working range (0 to 1.38) MPa. Two output frequency signs (corresponding to the sensor temperature and the quartz pressure sensor) were registered in the 6½ dataloger system (Agilent model 34401A) and the corresponding pressure was calculated using the calibration function that includes temperature compensation.

In the glass vacuum line, all glass connections were assembled with greaseless spherical joints, teflon O-rings and high vacuum teflon valves. The vacuum line is connected to the rotatory vacuum pump (G) (BOC Edwards, model RV5) through a glass cold trap (D) filled with liquid nitrogen.

The apparatus was designed to permit degassing of the solvent using the condenser (F). The solvent is refluxed to the sample cell (A) while non-condensable gases are pumped out. Previous experience with the degassing of fluorinated compounds for solubility measurements showed that they could be better and faster degassed through successive melting/freezing cycles while vacuum pumping non-condensable gases and that was the procedure used in this work. The sample cell with a volume of 10 cm^3, containing the degassed solvent is then immersed in the thermostatic water bath. When the equilibrium temperature is reached, the apparatus is isolated from the vacuum source and the sample cell valve is opened to connect the sample container to the closed line and the quartz pressure sensor. After pressure stabilization, the pressure and time experimental data are recorded and the correct pressure value is obtained by extrapolation to the initial time of a pressure versus time relation. To avoid condensation, the apparatus from the sample cell to the pressure transducer is maintained at a higher temperature than the sample cell. This heating system, includes a hot water jacket protected tube (E) and a hot-block box (M) for the pressure transducer.

I.3.3. Experimental Results and Discussion

To evaluate the accuracy and estimate the precision of the experimental apparatus, the vapor pressure of perfluorobenzene was measured. Perfluorobenzene was chosen as the reference fluid because the vapor pressures of the compounds studied in this work are of the same order of magnitude of perfluorobenzene in the temperature range studied. Also, perfluorobenzene is a compound included in the IUPAC recommendations of reference materials for pressure-volume-temperature relations (IUPAC, 1987), since agreement between normal boiling temperatures of perfluorobenzene measured by Counsell et al. (1965), Douslin et al. (1965) and Ambrose (1981) are within a range of 0.005 K. All the measurements were carried using comparative ebulliometric apparatus. More recently, Ambrose et al. (1990) re-measured the vapor pressure of perfluorobenzene using the same technique with an absolute deviation from the previous results lower then 0.015 kPa. Findlay et al. (1969) also measured the vapor pressure of perfluorobenzene but using a static method.

A comparison between the experimental data measured in this work and literature data is presented in Table II.7. Literature data used were calculated with the equations reported by the authors as being the best fit to their experimental data. Absolute deviations between experimental and literature data are shown in Figure II.6. Data from Ambrose et al. (1990) are not included in the figure since they coincide with the ones from Ambrose (1981). From these results, an accuracy better than 0.1 kPa can be stated for the measurements performed in this work.

The vapor pressures for the studied compounds are reported in Table II.8 along with values calculated with the Antoine equation,

$$ln\left(P/\mathrm{kPa}\right) = A - \frac{B}{\left(T/\mathrm{K}\right) + C} \tag{II.7}$$

where P is the vapor pressure, T is the temperature and A, B and C are adjustable constants. The Antoine constants adjusted to the experimental data are reported in Table II.9.

Table II.7. Comparison Between Experimental and Literature Vapor Pressures of Perfluorobenzene. Pressure in kPa.

T K	P_{exp} kPa	P_{lit} (Counsell et al.,1965)	P_{lit} (Douslin et al.,1965)	P_{lit} (Ambrose, 1981)	P_{lit} (Ambrose et al., 1990)	P_{lit} (Findaly et al.,1969)
288.23	6.90		6.79			6.84
293.51	9.00		8.94	8.94		8.99
297.98	11.16		11.17	11.18		11.22
302.96	14.20		14.18	14.19		14.23
307.96	17.93		17.85	17.87		17.88
312.96	22.25	22.28	22.27	22.29		22.27
317.96	27.56	27.56	27.55	27.58	27.58	27.49
322.96	33.85	33.82	33.81	33.84	33.84	
327.95	41.16	41.18	41.17	41.20	41.20	
333.01	49.95	49.91	49.89	49.93	49.93	

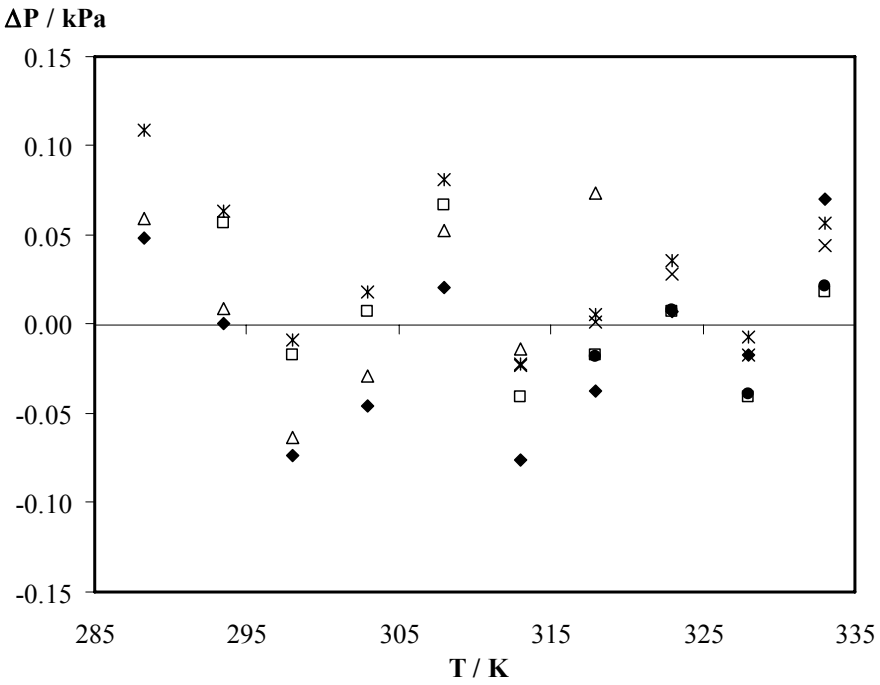

Figure II.6. Comparison between correlated experimental and literature vapor-pressure data of perfluoroperfluorobenzene: (♦) this work; (□), Ambrose (1981); (Δ), Findlay et al. (1969); (x) Counsell et al. (1965) and (*) Douslin et al. (1965). $\Delta P = P_{exptl} - P_{calcd}$.

Table II.8. Experimental and Calculated Vapour Pressures of the Studied Compounds

T K	P_{exp} kPa	P_{calc} kPa	ΔP[a] kPa
	C_6F_{14}		
288.31	18.78	18.76	0.02
293.22	23.58	23.59	-0.01
298.09	29.28	29.31	-0.03
302.98	36.19	36.16	0.03
307.97	44.38	44.41	-0.03
313.17	54.56	54.54	0.02
318.15	65.86	65.86	0.00
323.13	78.91	78.99	-0.08
328.11	94.08	94.09	-0.01
333.10	111.39	111.37	0.02
	C_8F_{18}		
288.13	2.21	2.17	0.04
293.03	2.85	2.85	0.00
298.14	3.74	3.77	-0.03
303.34	4.89	4.94	-0.06
308.19	6.32	6.32	0.01
313.09	8.02	8.02	0.00
318.17	10.19	10.20	-0.01
323.14	12.86	12.80	0.06
328.15	15.96	15.97	-0.02
333.21	19.89	19.83	0.06
	C_9F_{20}		
288.18	0.68	0.69	-0.01
293.18	0.94	0.95	-0.01
298.11	1.29	1.28	0.01
303.10	1.71	1.71	0.00
308.19	2.32	2.29	0.03
313.17	3.06	3.02	0.05
318.22	3.99	3.96	0.03
323.15	5.14	5.14	0.00
328.15	6.59	6.64	-0.04
333.15	8.42	8.52	-0.10

[a] $\Delta P = P_{exp} - P_{calc}$

Table II.8. (continued)

T K	P_{exp} kPa	P_{calc} kPa	ΔP^a kPa
1Br – C_8F_{17}			
288.22	0.38	0.38	0.00
293.20	0.54	0.53	0.01
298.08	0.69	0.72	-0.03
303.26	0.98	0.98	0.00
308.22	1.30	1.31	-0.01
313.18	1.67	1.72	-0.05
318.09	2.24	2.24	0.00
322.92	2.89	2.88	0.01
327.88	3.69	3.69	0.00
332.78	4.70	4.68	0.02
1H – C_8F_{17}			
288.35	1.18	1.18	0.00
293.26	1.60	1.60	0.01
298.26	2.18	2.15	0.04
303.19	2.84	2.84	0.00
308.15	3.72	3.74	-0.02
313.13	4.87	4.87	0.00
318.06	6.22	6.28	-0.06
323.01	8.07	8.03	0.04
328.00	10.25	10.25	0.00
332.89	12.83	12.83	0.00
1H, 8H – C_8F_{16}			
289.31	0.55	0.58	-0.03
293.26	0.75	0.75	0.00
298.2	0.99	1.02	-0.03
303.18	1.43	1.38	0.05
308.17	1.92	1.84	0.08
313.18	2.49	2.43	0.06
318.14	3.12	3.17	-0.05
323.15	4.07	4.10	-0.03
328.15	5.26	5.24	0.02
333.14	6.64	6.65	-0.01

Table II.8. (continued)

T K	P_{exp} kPa	P_{calc} kPa	ΔP[a] kPa
	$C_{10}F_{18}$		
288.25	0.57	0.52	0.05
293.25	0.73	0.71	0.02
298.21	0.91	0.94	-0.03
303.29	1.25	1.25	0.00
308.23	1.59	1.62	-0.04
313.22	2.05	2.10	-0.05
318.21	2.66	2.70	-0.04
323.18	3.45	3.44	0.01
328.17	4.41	4.35	0.06
333.20	5.47	5.47	0.00
	C_7F_8		
288.23	2.18	2.22	-0.04
293.20	2.95	2.95	0.00
298.28	3.87	3.91	-0.04
303.18	5.09	5.07	0.02
308.15	6.54	6.54	0.00
313.15	8.43	8.37	0.06
318.15	10.69	10.62	0.07
323.15	13.38	13.36	0.02
328.45	16.86	16.89	-0.03
333.93	21.31	21.33	-0.02

[a] $\Delta P = P_{exp} - P_{calc}$

Vapor pressure data were found in the literature for perfluoro-n-hexane, perfluoro-n-octane and perfluorotoluene and comparison with data measured in this work is done in Figures II.7 to II.9. No vapor pressure data for the other studied compounds was found in the literature.

Table II.9. Constants for the Antoine Equation

	Antoine constants			
Compound	**A**	**B**	**C**	**δ[a]**
C_6F_{14}	13.719	2442.990	-61.853	0.033
C_8F_{18}	16.294	4205.105	-17.205	0.037
C_9F_{20}	21.373	7498.037	56.755	0.042
$C_{10}F_{18}$	15.938	4525.811	-15.354	0.037
1Br-C_8F_{17}	15.330	4001.198	-42.571	0.021
1H-C_8F_{17}	16.905	4487.951	-20.213	0.026
1H,8H-C_8F_{17}	13.659	2999.816	-78.177	0.040
C_6F_6	14.271	2885.821	-54.500	0.048
C_7F_8	15.239	3549.981	-42.445	0.035

[a] $\delta = \left[\sum \left(p_{\exp} - p_{calc}\right)^2 / n\right]^{0.5}$, n being the number of experimental points

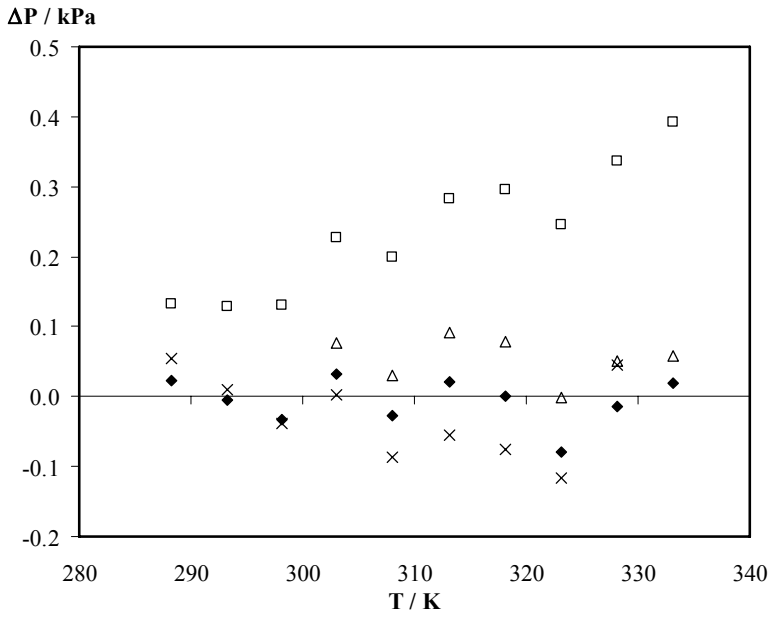

Figure II.7. Comparison between correlated experimental vapor pressure data of perfluoro-n-hexane measured in this work (♦) and correlated literature data measured by Stiles et al. (1952) (□); Dunlap et al. (1958) (Δ) and Crowder et al. (1967) (×). $\Delta P = P_{exp} - P_{calc}$.

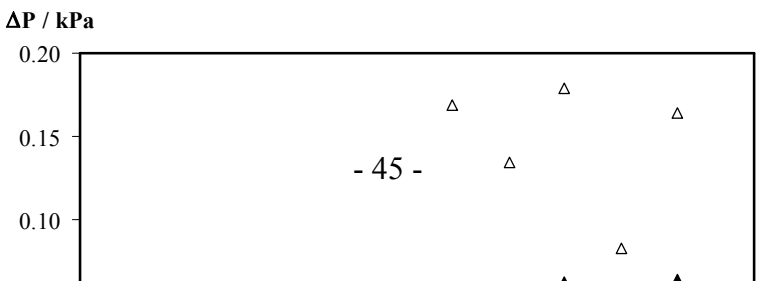

Figure II.8. Comparison between correlated experimental vapor pressure data of perfluoro-n-octane measured in this work (▲) and correlated literature data measured by Kreglewski et al. (1962) (Δ). $\Delta P = P_{exp} - P_{calc}$.

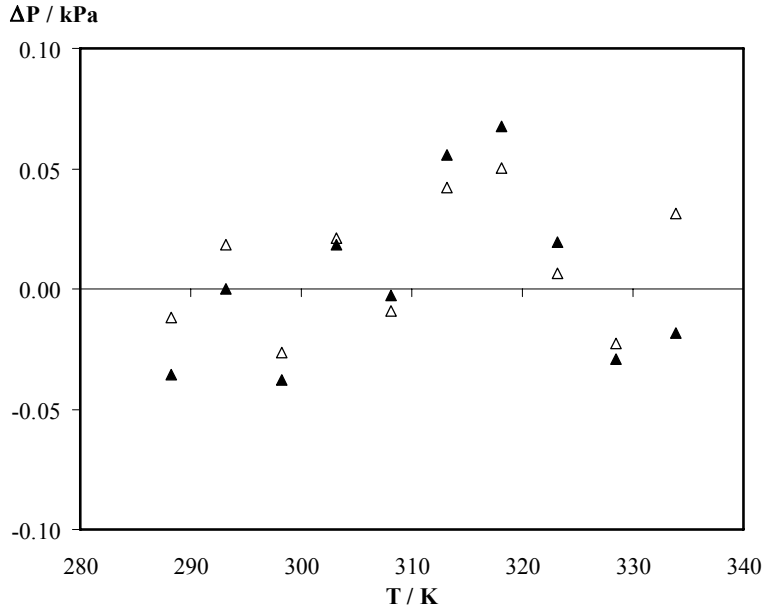

Figure II.9. Comparison between correlated experimental and literature vapor pressure data of perfluorotoluene measured in this work (▲), and correlated literature data measured by Ambrose et al. (1981) (Δ). $\Delta P = P_{exp} - P_{calc}$.

Experimental data obtained for perfluoro-n-hexane are in good agreement with data measured both by Dunlap et al. (1958) and Crowder et al. (1967). The authors used the static and ebulliometric methods to perform the measurements respectively and both of them used mercury manometers to read the pressure. Larger deviations are found when comparisons with data measured by Stiles et al. (1952) are done.

In the case of perfluoro-n-octane, vapor pressure data measured in this work is systematically lower than data measured by Kreglewski (1962) by 2% The author used comparative ebulliometry to perform the measurements.

Vapor pressure data measured for perfluorotoluene agree, to within the accuracy stated for the method, with data measured by Ambrose et al. (1981) whose measurements were performed using comparative ebulliometry.

I.3.4. Derived properties

The enthalpy of vaporization and the Hildebrand or solubility parameter of a given compound can be easily accessed from vapour pressure data. The enthalpies of vaporization are calculated by means of the Clausius-Clapeyron equation

$$\Delta H^{vap} = T\Delta S^{vap} = RT^2\left(\frac{d\ln P}{dT}\right)\left(1+\frac{(B_2 - V^L)P}{RT}\right) \qquad \text{(II.8)}$$

where B_2 is the second virial coefficient and V^L the saturated liquid volume assuming that:

- The change in volume that accompanies evaporation or sublimation is equal to the volume of the vapor produced, which is a good assumption at moderate or low pressures.

- The enthalpy of vaporization (or sublimation) is constant over the temperature range of interest. This is never really true, but changes in these ΔH's are very small at low and moderate pressures. Only approaching the critical point, this assumption will fail completely.

At the conditions measured in this work it was also assumed that:

- The vapor is an ideal gas, which is a good assumption at moderate pressures for most substances.

- The external pressure doesn't affect the vapor pressure. There is a slight dependence on external pressure. Equation II.8 was then simplified to the usual relation

$$\Delta H^{vap} = T\Delta S^{vap} = RT^2\left(\frac{d\ln P}{dT}\right) \quad \text{(II.9)}$$

ΔH_1^{vap} was calculated at a mean temperature equal to 310.50 K and then corrected to a reference temperature, in this case equal to 298.15 K, using the correlation mentioned by Chickos (1992).

Having the enthalpy of vaporization at a required temperature, and if this is well below the boiling point of the liquid, the Hildebrand or solubility parameter may be evaluated assuming that the vapor is ideal

$$\delta = \sqrt{\frac{\Delta H^{vap} - RT}{V^L}} \quad \text{(II.10)}$$

where V^L is the molar volume of the pure compound at the same temperature at which ΔH^{vap} was calculated (Barton, 1991).

The boiling temperature, and the enthalpies of vaporization and solubility parameter at 298 K are given in Table II.10. Comparison with literature data is carried whenever possible.

Table II.10. Derived Boiling Temperatures, T_b, Standard Molar Enthalpies of Vaporization at 298.15 K, ΔH^{vap}, and Solubility Parameter at 298.15 K, δ

	Tb (K)	**ΔH^{vap} (kJ.mol^{-1})**	**δ (J.cm^{-3})$^{1/2}$**	**Reference**
C_6F_{14}	330.29 ± 0.02	32.47 ± 0.11	12.2	This work
	330.38			Stiles et al., 1952
	330.30			Dunlap et al., 1958
	330.31			Crowder at al., 1967
		32.4	12.1	Barton, 1991
C_8F_{18}	377.36 ± 0.03	39.88 ± 0.15	12.3	This work
	377.15			Hildebrand et al., 1950
	380.15			Benning et al., 1949
	378.96			Kreglewski, 1962
	376.45			Haszeldine et al., 1951
C_9F_{20}	390.76 ± 0.02	45.27 ± 0.23	12.5	This work
	398.45			Haszeldine et al., 1951
$C_{10}F_{18}$	415.17 ± 0.03	41.54 ± 0.52	12.8	This work
	415.05			Haszeldine et al., 1951
1Br-C_8F_{17}	416.11 ± 0.02	45.63 ± 0.36	12.9	This work
1H-C_8F_{17}	385.48 ± 0.02	43.35 ± 0.19	13.0	This work
1H,8H-C_8F_{16}	399.43 ± 0.03	45.80 ± 016	13.7	This work
C_6F_6	353.47 ± 0.02	36.08 ± 0.07	17.0	This work
	353.41			Hales et al., 1974
C_7F_8	376.70 ± 0.03	40.52 ± 0.18	16.4	This work
	377.73			Hales et al., 1974

I.4. Solubility at atmospheric pressure

I.4.1. Bibliographic revision

Several methods have been used to date to measure the solubility of gases in liquids. Detailed reviews of experimental techniques and methods of treatment of data, applications, main advantages and disadvantages have been published in the literature (Battino and Clever, 1966; Hildebrand et al., 1970; Clever and Battino, 1975 and Clever and Battino, 2003).

A major classification between the different methods splits them into chemical methods, which depend on the chemical properties of the gas, and physical methods, that do not depend on the gas properties (Battino et al., 1966). Physical methods have been by far the most used to measure solubility data mainly due to their versatility since chemical methods are specific for a given gas. They consist in the quantification of the amount of gas that solubilizes in a solvent by measuring properties as temperature, pressure, volume and composition of the system.

Physical methods can be further divided into saturation methods, when the degassed solvent is saturated with a volume of gas that can be determined at a given pressure and temperature and extraction methods, where the dissolved gas is removed from a previously saturated solution in conditions at which its volume can be calculated at a given pressure and temperature. It is essentially the opposite of the saturation method. Here again the saturation methods are by far the most common. The first apparatus based on the saturation method was developed by Bunsen in 1858. Later, in 1894 Ostwald built a similar apparatus in which the main difference is in the determination of the volume of gas. The Ostwald apparatus was the base for the many different set ups developed since then such as the apparatus used by Lannung (1930) and Morrison and Billet (1948). There have been many designs of volumetric apparatus always looking for higher precisions and simplicity. Designs of apparatus for measuring absorption of gas by volumetric methods, but capable of greater precision are reviewed by Battino and Clever (1966) and Clever and Battino (1975). Many workers have advocated saturating the gas with solvent's vapour before it contacts the solvent in the equilibrium cell. This has sometimes been called the *wet* method of measuring solubilities of gases. Other workers have used the *dry* method in which pure gas is the one contacting with the solvent (Fogg and Gerrad, 1991). This method requires an exact knowledge of the vapour pressure of the solvent to quantitatively

access the amount of dissolved gas. Between the most important contributions to an accurately measuring procedure for the solubility of gases are the apparatuses developed by Cook and Hanson (1957) with an estimated precision of 0.05-0.1%, by Ben-Naim and Baer (1963) with an estimated precision of 0.2% and by Benson and Krause (1976) with an estimated precision of 0.02%. The most significant advance in experimental technique for determining Henry coefficients of gases in liquids is undoubtedly the apparatus developed by Benson and Krause (1976), the precision (and accuracy) of which surpasses any previous design. Based on the apparatus of Ben-Naim and Baer (1963), with the introduction of small modifications, were developed the apparatus of Carnicer et al. (1979) with a precision of 0.7%, Wilhelm and Battino (1971a) with a precision of 1% and Vosmansky and Dohnal (1987) with a precision of 0.5%. Although different apparatus based on the saturation method have been built and still are nowadays (Serra and Palavra, 2003 and Miguel et al., 2000), the essential differences between them focus on pre-saturation of the gas in solvent's vapours (wet or dry method), on the promotion of a good gas-liquid contact (agitation of the gas-liquid mixture, drainage of a liquid film into the gas bulk, bubbling, etc) on method used to determine the volume of solvent and gas dissolved (calibrated cells and burettes/manometers/pressure sensors) and on the method used to measure pressure (mercury manometers, vacuum detectors, pressure sensors) and temperature (water/air baths and thermometers with sensibilities ranging from 0.005 to 0.1ºC).

Other methods that can be used for solubility data measurements include gas chromatographic methods, with a precision between 1 and 2%, mass spectroscopy methods with an estimated precision of 1% and radioactivity methods, which are restricted to those gases where appropriate radioactive isotopes are available (Clever and Battino, 2003).

Literature data relating the solubility of oxygen in fluorinated compounds is old and scarce. When the interest in the study of these compounds started in the seventies, some solubility measurements were performed but most of the times at only one temperature (mainly at 298.15 K but also at 310.15 K). Keeping in mind the main application of these compounds as oxygen carriers in artificial blood substitutes, although solubility data have certainly been recently measured, none of these data are available in the open literature. Table II.11 compiles references where oxygen solubility data for some of the fluorinated compounds studied in this work can be found, reporting the methods and measuring

conditions in each case. Comparison with data measured in this work will be presented in the following section.

Table II.11. Compilation of References Reporting Experimental Oxygen Solubility Data in Fluorinated Compounds

Solvent	Method	T range (K)	Reference
C_7F_{16}	Saturation	298	Gjaldbaek (1952)
C_8F_{18}	Gas Chromatography	298	Wesseler et al. (1977)
	Saturation	290 - 313	Gomes et al. (2004)
C_9F_{20}	Not reported	298	Wesseler et al. (1977)
$C_{10}F_{18}$	Gas Chromatography	298	Wesseler et al. (1977)
	Saturation	289 - 313	Gomes et al. (2004)
1Br-C_8F_{17}	Gas Chromatography	298	Wesseler et al. (1977)
	Not reported	298	Riess (2001)
	Electrode	310	Skurts and Reese (1978)
	Saturation	290 - 317	Gomes et al. (2004)

I.4.2. Apparatus and procedure

The solubility apparatus and procedure employed in this work are similar to that described by Ben-Naim and Baer (1963) where the solubility is determined by measuring the quantity of gas dissolved in an accurately known volume of solvent at constant pressure and temperature. In this case the wet method is used which means that the gas was pre-saturated with the solvent before contacting the solvent in the equilibrium cell. The apparatus depicted in Figure II.10 has a simple design and can be easily adapted to measure the solubility of systems with different solubilities. It consists of a mercury manometer, M, with a mercury reservoir, R, a dissolution cell, Ve, and a gas line with a pre-saturator, PS, where the gas is saturated with the solvent. The apparatus, built in glass, has valves from J. Young, which permit a vacuum of ± 0.001mbar, are resistant to chemical damage, do not use grease and resist to temperatures between –20 and 200ºC. Among the most important factors for an accurate measurement using this type of apparatus are the degassing process, the saturation of the gas, the contact between gas and

solvent and the control of the temperature of the entire system in order to avoid condensation of the vapor.

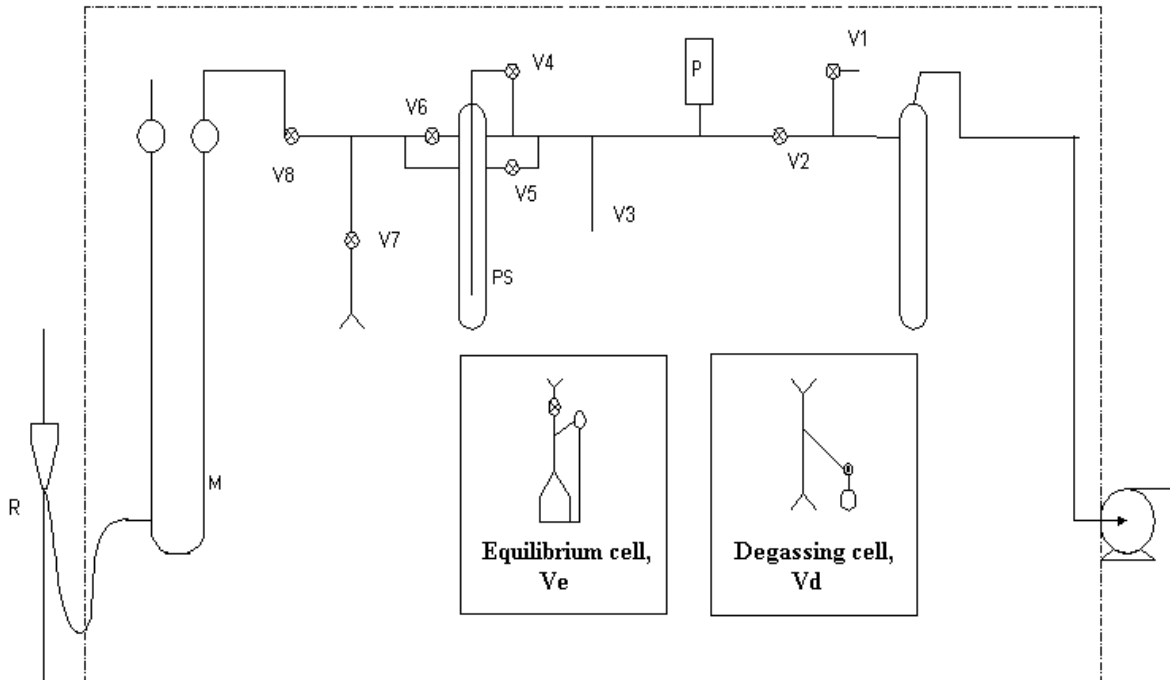

Figure II.10. Experimental apparatus: Vi - Valves; PS - Pre-saturator; P - Vacuum gauge; M - Mercury Manometer; R - Mercury Reservoir

The solvent is degassed thought successive melting/freezing cycles. The degassing cell, Vd, filled with pure solvent is connected to the solubility apparatus. Opening valve V_1 the entire line is connected to a vacuum source, a RV3 high vacuum pump from Edwards, capable of reaching a vacuum of 0.08 mbar. The solvent is then degassed by successive melting/freezing cycles while vacuum pumping non-condensable gases. The degassing is considered complete when no pressure variation in two consecutive cycles is detected with the pressure gauge, P. Besides being an expeditious method, the quantity of solvent lost with this degassing method is minimum when compared with other degassing procedures. By turning upside down the degassing cell, the equilibrium cell is filled with the degassed solvent under its own vapor pressure. The pre-saturator is also filled with an amount of solvent enough to guarantee a correct saturation of the gas and the same degassing principle is used for its degasification.

After evacuating the system, the solute gas is introduced in the line through valve V_3. Closing valves V_2 and V_5, the gas is forced to bubble slowly in the degassed solvent contained in the saturation chamber, PS to guarantee a complete saturation and the system is filled with the solvent-saturated gas to a total pressure close to 1 atm. When the mercury level in the manometer branches is equal, the system is isolated from the pre-saturator and allowed to equilibrate. It was found that the reproducibility of the measurements increases if the saturated gas is let to equilibrate for at least 10 hours. During this time, the equilibrium cell filled with the degassed solvent is closed to avoid solubilization of the gas into the solvent by diffusion.

The equilibrium cell, Ve, is based on the design of Carnicer et al. (1979) and was previously calibrated with mercury, by measuring the mercury levels in the cell capillaries and the corresponding weight of mercury. A relation between mercury levels and the cell volume is obtained being the cell volume approximately 7 cm^3.

The dissolution process is initiated by turning the liquid circulation on, forcing the solvent up the right capillary arm and to circulate through the left capillary arm forming a very thin film. As the gas dissolves, the system pressure is maintained at initial pressure by allowing the mercury from the reservoir to displace the gas in the system. After 15 minutes more then 95% of the gas is already dissolved. For the studied fluorinated compounds, the equilibrium is reached in about ½ h. The system is considered to have reached equilibrium when no further gas is dissolved. The displacement of the mercury level is measured with a cathetometer with a precision of ± 0.01 mm. Direct reading of the mercury levels of mercury and solvent levels in the equilibrium cell are the only measurements required to calculate the volume of gas dissolved in a given volume of solvent.

The entire apparatus is immersed in a Perspex isolated air bath capable of maintaining the temperature to within 0.1 K by means of a PID controller. The temperature is measured with a previously calibrated 25 Ω platinum resistance thermometer connected to a digital multimeter 34401A from Agilent for temperature values acquisition.

I.4.3. Data reduction

The Ostwald coefficient is a frequent measure of the solubility of a gas in a liquid. Of the several definitions of the Ostwald coefficient found in the literature (Battino, 1984), the most appropriate for the thermodynamically rigorous description of gas solubility is

$$L_{2,1}(T,P) = \left(\frac{C_2^{\,L}}{C_2^{\,V}} \right)_{equil} \tag{II.11}$$

Here, $C_2^{\,L}$ and $C_2^{\,V}$ are the concentrations of the solute (gas) in the liquid phase solution (indicated by a superscript *L*) and in the coexisting vapour phase solution (indicated by a superscript *V*), respectively at temperature *T* and pressure *P*. The link with the experimental accessible quantities is established through

$$L_{2,1}(T,P) = \left(\frac{V^V}{V^L} \right)_{equil} \tag{II.12}$$

where V^V is the volume of gas dissolved and V^L is the total volume of the liquid solution after equilibrium is reached, at a given temperature T and pressure P.

The molar fraction of component 2 (the gaseous solute) in the liquid solution can be directly related to the Ostwald coefficient by (Battino et al., 1977):

$$x_2 = \left[\frac{Z_{12}RT}{P_2 L_{2,1}(T,P) V^L(T,P)} + 1 \right]^{-1} \tag{II.13}$$

which for the accuracy of most of the experimental methods can be approximated to

$$x_2 = \frac{P_2 L_{2,1}(T,P) V^L(T,P)}{Z_{12}RT} \tag{II.14}$$

where P_2 is the partial pressure of the gas, Z_{12} the compressibility factor of the gaseous mixture and V^L, the molar volume of the liquid solution defined as

$$V^L = x_1 V_1^{*L} + x_2 V_2^{\infty L} \tag{II.15}$$

When dealing with low solubilities, $x_2 << 1$, which is the present case, V^L can be approximated to the molar volume of the pure solvent, V_1^{*L}.

For low to moderate pressures, the compressibility factor can be calculated as:

$$Z_{12} = 1 + \frac{P}{RT}(y_1 B_{11} + y_2 B_{22} + y_1 y_2 \delta_{12}) \quad \text{(II.16)}$$

where B_{11} and B_{22} are the second virial coefficients for the pure solvent and the pure solute respectively and $\delta_{12} = 2B_{12} - B_{11} - B_{22}$, where B_{12} is the solute-solvent cross second virial coefficient. The mole fractions in the vapor phase in equilibrium with the liquid solution, y_i, are calculated by an iterative process using the vapor-liquid equilibrium equation (Prausnitz et al., 1999):

$$y_1 = (1 - x_2)\left(\frac{P_1^{sat}}{P}\right)\left(\frac{\Phi_1^{sat}}{\Phi_1}\right)\exp\left[\frac{V_1^0 (P - P_1^{sat})}{RT}\right] \quad \text{(II.17)}$$

The second virial coefficient for the solute was taken from the compilation of Dymond and Smith (1980) and both B_{11} and B_{12} were estimated using the correlation of Tsonopoulos (Poling et al. 2001) without any adjustable parameters.

I.4.4. Experimental results and Discussion

To estimate the precision of the experimental apparatus, the solubility of oxygen in n-heptane was measured and compared with literature values in Table II.12. The result obtained at 298 K deviates 0.8%, 4.0% and 1.5% from the values reported by Hesse et al. (1996), Makranczy et al. (1976) and Thomsen and Gjaldbaek (1963) respectively. Our value agrees with the experimental data measured by these authors within the reported experimental error.

Table II.13 shows the experimental values obtained for the solubility of oxygen in the different perfluoroalkanes studied between 288 K and 313 K and pressures close to atmospheric.

Table II.12: Solubility of Oxygen in n-Heptane. Comparison Between Data Measured in This Work and Literature Data.

	$L_{2,1}$(T,p) (%)			
T (K)	This work	Hesse et al. (1996)	Makranczy et al. (1976)	Gjaldbaek et al. (1963)
298.15	0.335 ± 1	0.338 ± 0.5	0.322 ± 3	0.330 ± 1

Figures II.11 and II.12 intend to emphasize the temperature dependence of the different systems studied. The influence of the chain length and structure of the molecule, as shape and partial substitution of fluorine atoms, was studied .

The solute mole fraction is usually presented at a solute's partial pressure equal to 1 atm. From solute's mole fraction data reported in Table II.13, it is simple to calculate the corrected solute mole fraction since the Henry's law is applicable at the working conditions. In order to check the validity of the Henry's law for the systems under study, the solubility of oxygen in perfluoro-n-nonane was measured at several pressures different from atmospheric and at a fixed temperature of 298 K. Solubility data measured is given in Figure II.13. The linear relation obtained confirms the validity of the Henry's law for these systems.

The temperature dependence of the experimental values of the solubilities expressed in mole fraction x_2 (T, P), where P is equal to 1 atm was correlated using the following equation suggested by Benson and Krause (1976)

$$\ln x_2 = \sum_{i=0}^{1} A_i T^{-i} \tag{II.18}$$

The values obtained for the coefficients A_i for the different systems are given in Table II.14, together with the AAD of the experimental results defined as

$$AAD = N^{-1} \sum_{i=1}^{N} \left| \delta_i \right| \tag{II.19}$$

where N is the number of data points, whose individual percentage deviations are calculated as:

$$\delta_i = 100 \left[x_2(\exp) - x_2(calc) \right] / x_2(calc) \tag{II.20}$$

Table II.13. Experimental data for the solubility of oxygen in the studied perfluoroalkanes between 288 K and 313 K expressed as Ostwald's coefficients and solute's mole fraction in liquid an gaseous phases at equilibrium.

T (K)	P (bar)	$L_{2,1}$ (T,P)	x_2 x10^3	y_2
		C_6F_{14}		
287.40	1.007	0.580	3.98	0.82
291.39	1.006	0.530	3.45	0.78
298.65	1.025	0.485	2.86	0.70
301.73	1.025	0.448	2.47	0.66
306.65	1.027	0.395	1.92	0.58
		C_7F_{16}		
287.94	1.023	0.530	4.71	0.94
290.94	1.022	0.519	4.53	0.93
293.96	1.012	0.511	4.34	0.92
297.88	1.013	0.499	4.13	0.90
303.94	1.016	0.468	3.70	0.86
308.35	1.026	0.419	3.21	0.83
311.95	1.045	0.382	2.87	0.81
		C_8F_{18}		
290.03	1.015	0.510	5.14	0.98
292.02	1.020	0.512	5.15	0.97
297.08	1.012	0.503	4.92	0.96
299.12	1.019	0.490	4.79	0.96
299.86	1.004	0.487	4.67	0.96
305.74	1.019	0.473	4.49	0.94
309.95	1.017	0.457	4.24	0.93
314.25	1.017	0.462	4.18	0.91
		C_9F_{20}		
288.28	1.019	0.503	5.72	0.99
288.48	1.008	0.507	5.69	0.99
292.29	1.018	0.492	5.52	0.99
298.04	1.010	0.486	5.33	0.99
302.35	1.006	0.472	5.09	0.98
307.79	1.007	0.451	4.79	0.98
311.43	1.013	0.439	4.63	0.97

Table II.13. **(continued).**

T (K)	P (bar)	$L_{2,1}$ (T,P)	x_2 x10^3	y_2
		$C_{10}F_{18}$		
288.85	1.015	0.414	4.14	0.99
291.08	1.002	0.408	4.00	0.99
293.94	1.009	0.410	4.01	0.99
299.82	1.019	0.407	3.96	0.99
306.31	1.016	0.412	3.92	0.99
311.61	1.017	0.417	3.91	0.98
313.20	1.007	0.408	3.77	0.98
		1Br-C_8F_{17}		
289.58	1.020	0.463	5.02	0.99
292.71	1.017	0.466	5.00	0.99
297.37	1.015	0.453	4.79	0.99
302.63	1.021	0.449	4.71	0.99
304.80	1.010	0.450	4.64	0.99
308.09	1.020	0.446	4.60	0.99
312.57	1.032	0.435	4.49	0.98
		1H-C_8F_{17}		
289.15	1.014	0.462	4.54	0.99
294.50	1.012	0.459	4.43	0.98
299.17	1.012	0.451	4.29	0.98
304.47	1.018	0.446	4.19	0.97
308.55	1.017	0.444	4.10	0.96
312.48	1.016	0.440	3.99	0.95
		1H,8H-C_8F_{16}		
290.68	1.010	0.399	3.76	0.99
290.82	1.019	0.400	3.80	0.99
297.97	1.011	0.409	3.78	0.99
307.99	1.009	0.411	3.69	0.98

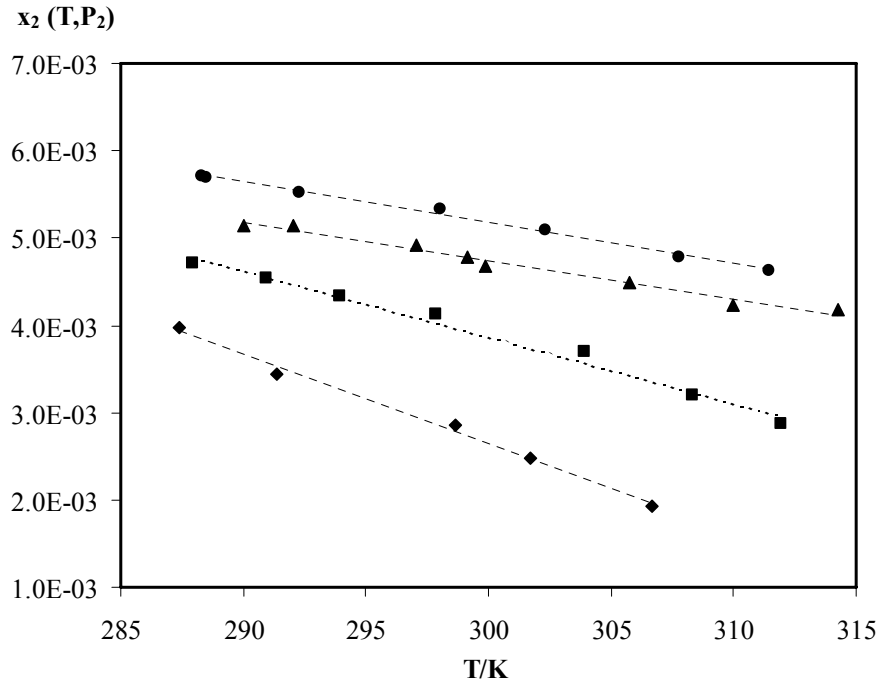

Figure II.11. Study of the effect of the chain on the solubility of oxygen in perfluoroalkanes. Oxygen's mole fraction as a function of the temperature in perfluoro-n-hexane (♦), perfluoro-n-heptane (■), perfluoro-n-octane (▲) and perfluoro-n-nonane (●) at solute's partial pressure.

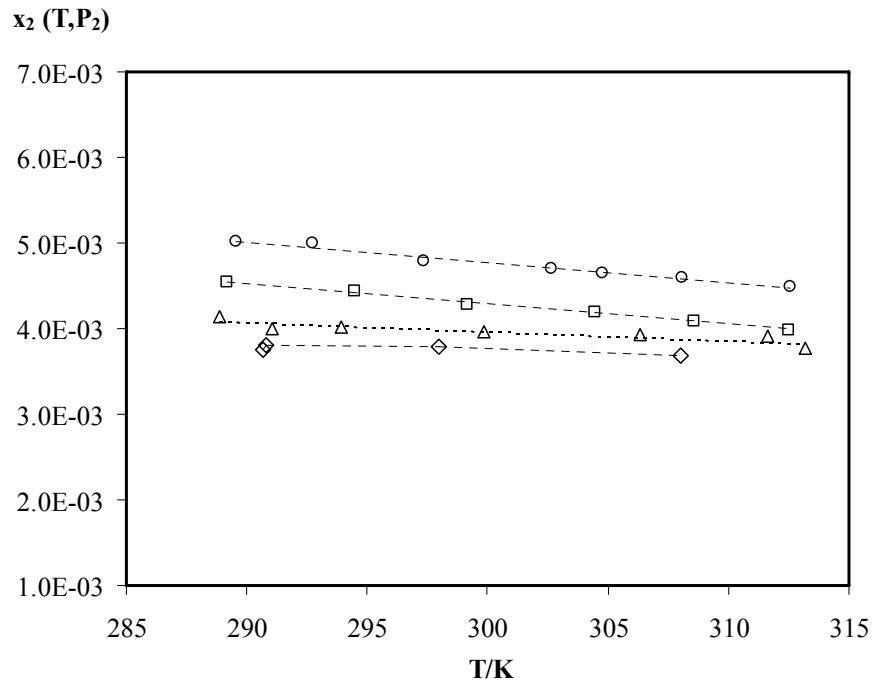

Figure II.12. Study of the effect of the structure on the solubility of oxygen in perfluoroalkanes. Oxygen's mole fraction as a function of the temperature in perfluorodecalin (Δ), 1Br-perfluoro-n-octane (○), 1H-perfluoro-n-octane (□) and 1H,8H-perfluoro-n-octane (◊)at solute's partial pressure.

Table II.14 Coefficients for Equation II.18 and Average Percentage Deviation, AAD, for the Correlation of the Experimental Data

Solvent	A_0	A_1	AAD
C_6F_{14}	-11.41	1751.91	1.77
C_7F_{16}	-11.59	1805.13	2.90
C_8F_{18}	-7.63	692.97	0.84
C_9F_{20}	-7.59	702.25	0.81
1Br - C_8F_{17}	-6.78	433.22	0.60
1H - C_8F_{17}	-6.67	373.49	0.22

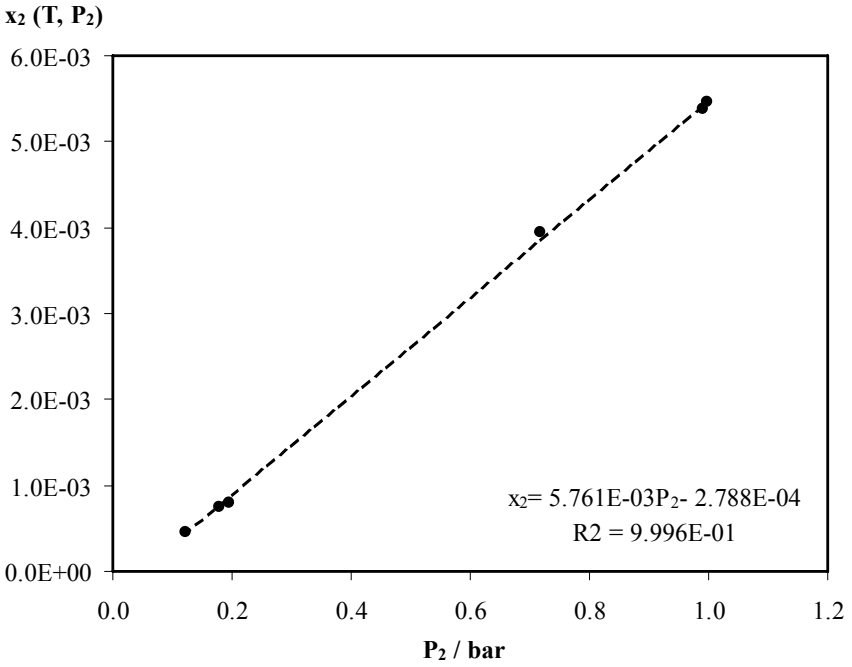

Figure II.13. Validation of the Henry's law for the systems under study. Oxygen's mole fraction in perfluoro-n-nonane at pressures different from atmospheric.

Comparison between data measured in this work and literature data is done in Figure II.14.

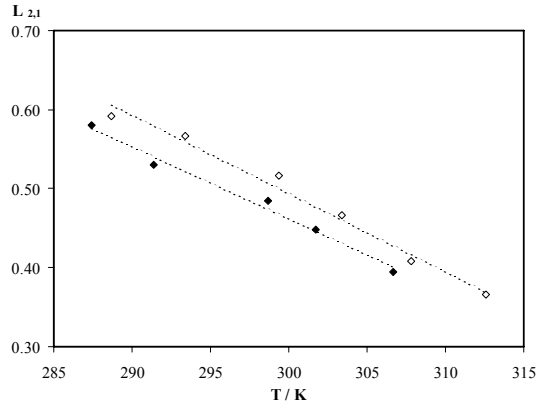

Fig II.14a. Comparison between Ostwald coefficient for perfluoro-n-hexane measured in this work (♦) and reported by (◊) Gomes et al. (2004)

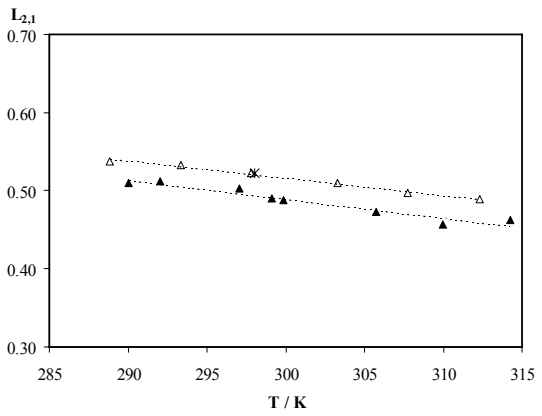

Fig II.14b. Comparison between Ostwald coefficient for perfluoro-n-octane measured in this work (▲) and reported by (Δ) Gomes et al. (2004) and (*) Wesseler et al. (1977)

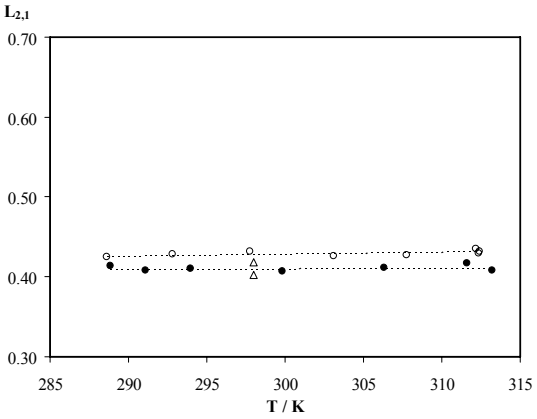

Fig II.14c. Comparison between Ostwald coefficient for perfluorodecalin measured in this work (●) and reported by (○) Gomes et al. (2004) and by (Δ) Wesseler et al. (1977)

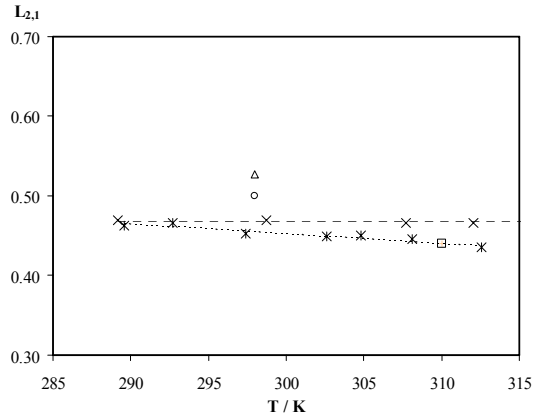

Fig II.14d. Comparison between Ostwald coefficient for 1Br-C_8F_{17} measured in this work (*) and reported by (x) Gomes et al. (2004), (Δ) Wesseler et al. (1977), (○) Riess (2001) and (□) Skurts et al. (1978)

No data was found for the solubility of oxygen in 1H-perfluoro-n-octane and 1H,8H-perfluoro-n-octane. It can be observed the perfluoro-n-hexane, perfluoro-n-octane and perfluorodecalin data measured in this work is systematically lower by 5%, than data measured by Gomes et al. (2004), in the temperature range studied. In the case of perfluoro-n-octane the single value reported by Wesseler et al. (1977) agree well with data measured by Gomes et al. (2004) but in the case of perfluorodecalin the values reported by Wesseler et al. (1977) are in agreement with the data measured in this work. For 1Br-perfluoro-n-octane, data measured in this work show a temperature dependence more

pronounced than data measured by Gomes et al. (2004). The value reported by Skarts et al. (1978) at 310.15 K agrees with the temperature dependence obtained in this work. The values reported by Wesseler et al. (1977) and Riess et al. (2001) at 298.15 K are 14 % and 9 % respectively higher than the values measured in this work at the same temperature. In the case of perfluoro-n-heptane and perfluoro-n-nonane, only one value was found for comparison, one reported by Gjaldbaek (1952) for perfluoro-n-heptane and the other reported by Wesseler at al. (1977) for perfluoro-n-nonane. The deviations are of 10% and 2 % respectively, higher than the values measured in this work at the same temperature. The higher deviation found in the case of perfluoro-n-heptane can be due to the low purity of the sample used in this work.

I.4.5. Derived properties

The dissolution of a gas into a liquid is associated with changes in thermodynamic functions namely standard Gibbs energy (ΔG_2^*), standard enthalpy (ΔH_2^*) and standard entropy (ΔS_2^*) of solvation that can be calculated from experimental solubility results. These functions represent the changes that occur in the solute neighborhood during dissolution process due to the transference of one solute molecule from the pure perfect gas state to an infinitely dilute state in the solvent, at a given temperature T and so they can correctly describe the average intermolecular interaction between the solute and the solvent Ben-Naim and Marcus (1984) and Ben-Naim (2001). The thermodynamic functions were calculated from the temperature dependence of the molar fraction according to the following equations

$$\Delta G_2^{\,*} = \Delta G^0 - RT \ln\left(\frac{RT}{V_1^{\,0}}\right) \tag{II.21}$$

$$\Delta H_2^{\,*} = \Delta H^0 - RT\left(T\alpha_1 - 1\right) \tag{II.22}$$

$$\Delta S_2^{\,*} = \Delta S^0 + R \ln\left(\frac{RT}{V_1^{\,0}}\right) - R\left(T\alpha_1 - 1\right) \tag{II.23}$$

where R is the gas constant, α_1 is the isobaric thermal expansibility of the solvent, calculated from density data, and ΔG^0, ΔH^0 and ΔS^0 are the thermodynamic functions associated with the hypothetical changes that happen in the solute neighborhood when the

molecules are transferred from the gas phase to a hypothetical solution where the mole fraction of solute is equal to one, which are calculated from the temperature dependence of the experimental solubility data measured according to the following equations (Ben-Naim, 1980 and Ben-Naim and Marcus, 1984),

$$\Delta G_2^{\,0} = -RT\left(\ln x_2\right)_p \tag{II.24}$$

$$\Delta H_2^{\,0} = -T^2\left(\frac{\partial(\Delta G^0/T)}{\partial T}\right)_p \tag{II.25}$$

$$\Delta S_2^{\,0} = -\left(\frac{\partial \Delta G^0}{\partial T}\right)_p \tag{II.26}$$

The values for the thermodynamic functions of dissolution of oxygen in the different compounds at 298.15 K are listed in Table II.15.

Table II.15. Thermodynamic properties of solvation for oxygen in different perfluoroalkanes at 298.15 K.

Solvent	ΔG_2^*	ΔH_2^*	ΔS_2^*
	kJ.mol^{-1}	kJ.mol^{-1}	J.mol^{-1}K^{-1}
C_6F_{14}	1.79	- 13.41	- 50.98
C_7F_{16}	1.81	- 9.66	- 38.47
C_8F_{18}	1.74	- 4.36	- 20.44
C_9F_{20}	1.80	- 4.40	- 20.81
1Br-C_8F_{17}	1.92	- 2. 06	- 13.36
1H-C_8F_{17}	1.94	- 1.64	- 12.00
1H,8H-C_8F_{16}	2.21	1.22	- 3.31
$C_{10}F_{18}$	2.17	0.05	- 7.09

It is interesting to notice that the Gibbs energy of solvation has similar values for all the systems studied. This is a consequence of the similar solubility of oxygen at 298.15 K for the different systems. It is also clear from the reported values that the enthalpy and the entropy of solution decrease significantly along the linear perfluoroalkanes series. Another interesting observation results from the comparison between the enthalpy of solvation of perfluoro-n-octane and the corresponding substituted 1Br-perfluoro-n-octane, 1H-perfluoro-n-octane and 1H,8H-perfluoro-n-octane. The enthalpy of solvation decreases from fully saturated perfluoroalkane to 1H,8H-perfluoro-n-octane where both extremities have a fluor atom substituted by an hydrogen atom. The enthalpies of solvation for the perfluoralkanes that have only one extremity substituted (by an atom of hydrogen or bromide) lay between the values obtained for perfluoro-n-octane and 1H,8H-perfluoro-n-octane. These results seem to indicate that the temperature dependence of the solubility data is related with the structure of the molecule, essentially with the degree of substitution of the terminal CF_3 group in the perfluorocarbon molecule and also that the interaction between oxygen and the CF_3 group is stronger than between oxygen and other end-groups.

Supporting this evidence is the fact that, the solubility of oxygen in perfluorodecalin, a cyclic compound without any CF_3 terminal group, is also temperature independent as is the case of the linear 1H,8H-perfluoro-n-octane. To assess the validity of any assumption about special solute-solvent interactions, it is necessary to analyse the different contributions to the overall solubility process namely cavity formation, mixing and interaction. This can be done by using the appropriate expressions from the scaled particle theory applied to solutions of gases in liquids considering a two step mechanism of the solution process (Pierotti, 1963)

$$\Delta G_2^{*} = G^{cav} + G^{\text{int}} \tag{II.27}$$

where G^{cav} and G^{int} are the partial molar Gibbs energy of cavity formation and interaction respectively. In this work, G^{cav} was calculated as suggested by Reiss et al. (1960) as a function of parameters of the solute and the solvent, namely the hard sphere diameter (HSD) and the density of the solvent. The HSD for oxygen was taken from the work of Wilhelm and Battino (1977) and is equal to 3.46 Å. For the solvents, the HSDs were calculated from enthalpy of vaporization and thermal expansivity data of the solvents, as suggested by Wilhelm and Battino (1971b), using the vapor pressure and density

measured. Table II.16 resumes the parameters for the different solvents studied along with the different enthalpic contributions.

The calculated enthalpies of cavity formation are very similar for the different solvents within the uncertainty of the calculation. The results presented in Table II.16 indicate that the differences observed in the enthalpies of solution reported in Table II.15 are mainly caused by differences in the enthalpies of interaction. The interaction energy between oxygen and perfluoro-n-octane is significantly higher than the interaction energy between oxygen and substituted perfluoroalkanes.

The study of the solubility of oxygen in linear fluorinated molecules presenting different degrees of substitution on the terminal CF_3 groups seems to indicate that the solvation of oxygen is carried by the end groups of the perfluorocarbons and the existence of interactions between the oxygen and the CF_3 group on the fluorinated molecules that is more than 2 kJ/mol higher than with other end groups.

Table II.16. Enthalpies of Cavity Formation, H^{cav} and Solute-Solvent Interaction, H^{int} for Oxygen in Different Fluorinated Compounds. Also Reported are the Solvent's Hard Sphere Diameter, σ and Molar Volume, V_1^0

Compound	σ Å	V_1^0 $cm^3.mol^{-1}$	H^{cav} $kJ.mol^{-1}$	H^{int} $kJ.mol^{-1}$
C_6F_{14}	6.62	201.69	9.53	- 22.94
C_7F_{16}	7.04	226.34	10.61	- 20.27
C_8F_{18}	7.38	248.24	10.64	- 14.99
C_9F_{20}	7.70	273.01	10.67	- 15.08
$CF_3 (CF_2)_6 CF_2Br$	7.67	260.58	11.12	- 13.37
$CF_3 (CF_2)_6 CF_2H$	7.38	240.06	11.43	-13.07
$CF_2H (CF_2)_6 CF_2H$	7.34	229.31	11.93	-10.71
$C_{10}F_{18}$	7.42	239.38	10.54	- 10.49

I.5. Solubility at high pressure

I.5.1. Bibliographic revision

Several authors published reviews on high-pressure phase equilibrium data, as is the case of Knapp et al. (1981) covering 1900–1980, Fornari et al. (1990) covering 1978–1987, Brunner and Dohrn (1995) covering 1988–1993 and Christov and Dohrn (2002) covering 1994-1999. The authors extensively discussed applications, advantages and disadvantages of different high-pressure methods. According to them, experimental methods for the investigation of high-pressure phase equilibria can be divided into two main classes, depending on how the composition is determined, the analytical methods (or direct sampling methods) and the synthetic methods (or indirect methods).

The analytical methods involve the determination of the compositions of the coexisting phases. This can be done by taking samples from each phase and analyzing them outside the equilibrium cell at normal pressure or by using physicochemical methods of analysis inside the equilibrium cell under pressure, e.g. spectroscopic methods (Marteau et al., 1996). Analytical methods can still be divided into static, recirculation and flow methods according to the procedure used to reach equilibrium (Nagahama, 1996). The method can be very accurate but especial care must be taken with the withdrawing of vapour and liquid phase samples since, removal of a large amount of sample from an autoclave causes a considerable pressure drop, which disturbs the phase equilibrium significantly. To avoid this pressure drop, several techniques have been implemented as using a variable-volume cell, or by withdrawing only a small sample using capillaries or special sampling valves inducing only a light pressure drop that does not affect the phase compositions significantly. Often sampling valves are directly coupled to analytical equipment, as gas chromatograph or a supercritical fluid chromatograph.

The synthetic methods consist in the preparation of a mixture of known composition followed by observation of the phase behaviour in an equilibrium cell. In this case no sampling is necessary. After known amounts of the components have been placed into an equilibrium cell, values of temperature and pressure are adjusted so that the mixture is homogeneous. Then the temperature or pressure is changed until the formation of a new phase is observed (Wendland et al., 1999). Each experiment yields one point of the P–T–x phase envelope. Synthetic methods can be used where analytical methods fail, as for example, when phase separation is difficult due to similar densities of the coexisting

phases, for instance near or even at critical points. Since no sampling is necessary, the experimental equipment can be rather inexpensive and the experimental procedure is usually easy and quick. For multicomponent systems, experiments with synthetic methods yield less information than with analytical methods. Therefore, synthetic methods are rarely used for ternary systems (Costa et al., 1996). Also, the precise detection of incipient phase formation especially for dew point is difficult and it causes inaccuracies in P and T. The detection of the equilibrium point can be done by visual observation of the resulting turbidity/meniscus that characterize the appearance of a new phase, in the case of non-isooptic systems, or by any other physical properties that can detect phase transitions as transmitted X-rays (Abedi et al. 1999), relative dielectric permittivity (Goodwin et al., 1997) or ultrasonic speed apparatus (Takagi et al., 1999). If the total volume of a variable-volume cell can be measured accurately, the appearance of a new phase can be obtained from PVT measurements taking advantage of the pronounced changes that appear on this properties that occurs at the phase boundary (Roy et al., 1997; Warowny, 1994).

Numerous binary and multicomponent systems have been studied using one of the high-pressure methods mentioned above. The choice of the best method depends essentially on the properties of the system and on the conditions to be studied. In spite of the amount of work done in this field, data relating solubility of carbon dioxide in fluorinated systems is almost inexistent in the open literature. In fact, data was found only for the CO_2/perfluoro-n-hexane system, which was studied by two authors. Table II.17 resumes the methods and experimental conditions used by the authors to perform their measurements.

Table II.17. Compilation of the references reporting experimental solubility data for CO_2/perfluorocabon systems

System	Method	T range (K)	P range (MPa)	Reference
CO_2/ C_6F_{14}	Analytical	314.65 and 353.25	2 - 10	Iezzi et al., 1989
CO_2/ C_6F_{14}	Synthetic	313	1 - 7	Lazzaroni et al., 2005

I.5.2. Apparatus and procedure

In this work, high pressure measurements for the CO_2/perfluoroalkane mixtures were carried out using a visual synthetic method. The experimental apparatus used in this work has been described in detail elsewhere and a good agreement with literature data was obtained for phase equilibria for the system methane/hexadecane (Pauly et al., 2005).

The experimental apparatus, shown in Figure II.15, is essentially made up of a variable volume high pressure cell.

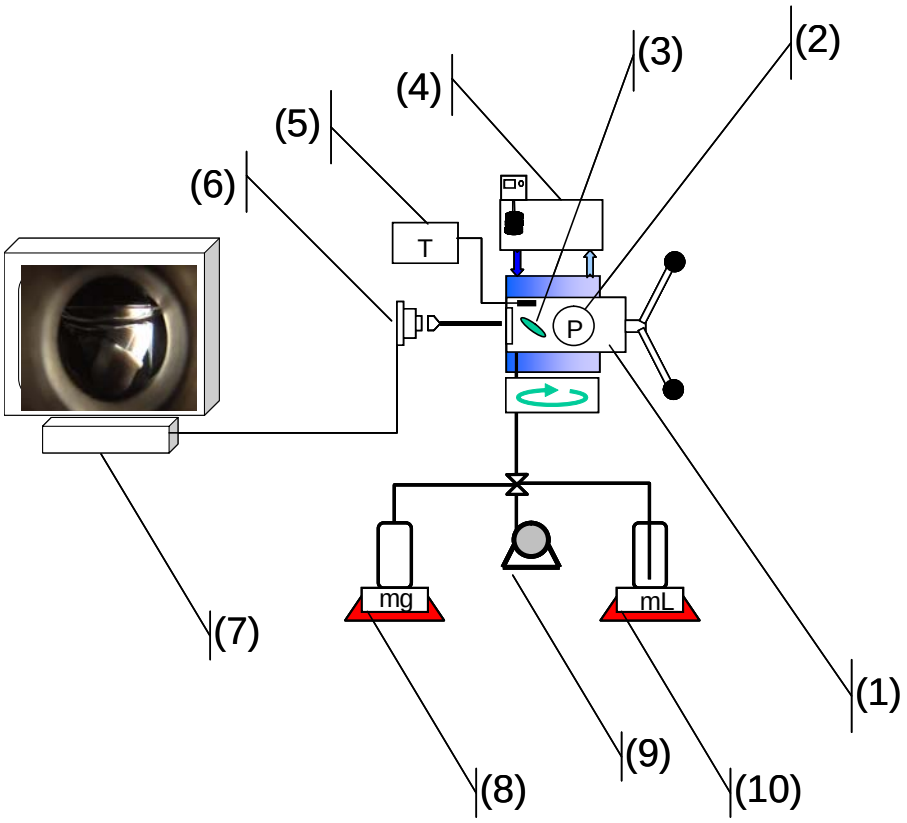

Figure II.15. Schematic diagram of the apparatus. (1) high-pressure variable-volume cell; (2) piezoresistive pressure transducers; (3) magnetic bar; (4) thermostat bath circulator; (5) thermometer connected to a platinium resistance; (6) endoscope plus a video camera; (7) screen; (8) perfluoroalkanes; (9) vacuum pump; (10) carbon dioxide

It consists of a horizontal hollow stainless steel cylinder closed at one end by a movable piston. A sapphire window that allows visual observation of the entire fluid in study closes the other end. A second sapphire window is fixed on the cylinder wall in order

to light the fluid with an optical fiber. This orthogonal positioning of light and observation limits the parasitic reflections and thus improves the observation in comparison to an axial lighting.

A video acquisition system made up of an endoscope plus a video camera is placed behind the sapphire windows in order to display on the screen of a computer what happens inside the measuring cell. A small magnetic bar is placed inside the cell to allow the homogenization of the mixture by means of an external magnetic stirrer. Due to the presence of this magnetic stirring bar as well as of the second window, the minimum internal volume is limited to 8 cm^3 whereas the maximum volume was fixed to 30 cm^3 to limit the size of the cell and thus to reduce thermal inertia and temperature gradients within the cell.

The temperature of the cell is kept constant by circulating a heat-carrier fluid thought three flow lines directly managed in the cell. This heat-carrier fluid is thermo-regulated with temperature stability of 0.01 K by means of a thermostat bath circulator (HAAKE). The temperature is measured with a high precision thermometer, Model PN 5207 with an accuracy of 0.01K connected to a calibrated platinum resistance inserted inside the cell close to the sample.

The pressure is measured by a piezoresistive silicon pressure transducer (Kulite) fixed directly inside the cell to reduce dead volumes. However, as this pressure transducer is placed inside the cell, it is subjected to changes in temperature and it needs to be calibrated. This calibration was done in the temperature range 273-507 K, by means of dead weight gauge (Bundenberg) with accuracy better than 0.02 %. The accuracy of the transducer in the experimental range studied is 0.2 MPa.

The binary mixtures are prepared directly in the measuring cell. The cell is first loaded with a known amount of liquid perfluoroalkane by vacuum extraction. The exact mass of liquid introduced is determined by weighting the cell during its introduction with a precision balance (Ohaus) with an accuracy of 0.1 mg. The carbon dioxide is then added under pressure. For this purpose, the gas is initially loaded at saturation pressure in an aluminium reservoir tank (Gerzat) fixed in the plate of high weight / high precision balance having a maximum weighting capacity of 2000 g with an accuracy of 1 mg (Sartorius) and connected to the measuring cell by means of a flexible high pressure capillary. The needed amount of gas is then transferred from the gas container to the measuring cell. The exact

mass of gas injected into the measuring cell is determined by weighing the reservoir tank during filling. After the mixture of known composition reaches the desired temperature at low pressure, the pressure is slowly increased at constant temperature until the system becomes homogeneous. During the experiment the mixture is continuously stirred at high frequency to keep the system in equilibrium during the compression. To avoid super-saturation effects the fluid phase boundary between two phase and single phase states is obtained by measuring the pressure of disappearance of the second fluid phase by visual observation. For each temperature the measurement is repeated 5 times. Reproducibility of the pressure disappearance measurements is within 0.02 MPa.

I.5.3. Experimental Results and Discussion

High pressure phase diagrams for the mixtures CO_2/perfluoro-n-octane, CO_2/perfluorodecalin, CO_2/perfluorobenzene, CO_2/perfluorotoluene and CO_2/perfluoromethylcyclohexane, at temperatures ranging from 293.15 to 353.15 K, were measured. Experimental results obtained for the five mixtures studied are reported in Table II.18. Figures II.16 *a* and *b* compare experimental data at the lowest and highest temperatures measured, respectively. It can be observed that the solubility of the CO_2 in different compounds is very similar, being the differences larger near the critical region. However, some differences should be noted: the solubility of CO_2 in perfluorodecalin is always smaller than in the linear perfluoroalkane (perfluoro-n-octane). The solubility of CO_2 in perfluoromethylcyclohexane is between that in perfluorodecalin and perfluoro-n-octane. At lower temperatures, the aromatic compounds present the highest CO_2 solubility and no significant difference can be observed between them. The temperature effect on the solubility is more pronounced for the aromatic perfluoroalkanes than for the saturated compounds. In order to address a possible chain size effect on the solubility of CO_2, data measured in this work for perfluoro-n-octane were compared with data measured for perfluoro-n-hexane by Iezzi et al. (1989) and Lazzaroni et al. (2005). As can be observed in Figure II.17, no significant difference was found between the two systems except near the critical point, where the CO_2/perfluoro-n-octane presents a slightly more extended two phase region at higher temperatures.

Table II.18. P(bar)-T(K)-x_{CO2} data for CO_2 – perfluoroalkane mixtures at different temperatures from 293.15 to 353.15 K

$CO_2 – C_8F_{18}$							
x_{CO2}	**293.15 K**	**303.15 K**	**313.15 K**	**323.15 K**	**333.15 K**	**343.15 K**	**353.15 K**
0.104	5.29	5.91	6.52	7.14	7.75	8.37	8.98
0.212	11.22	12.51	13.79	15.07	16.35	17.63	18.91
0.261	13.94	15.67	17.41	19.15	20.88	22.62	24.35
0.370	19.84	22.56	25.29	28.01	30.73	33.45	36.17
0.473	25.66	29.44	33.23	37.01	40.80	44.58	48.37
0.601	32.94	38.47	44.00	49.53	55.06	60.59	66.12
0.701	38.57	45.89	53.21	60.53	67.85	75.17	82.49
0.784	41.65	50.44	59.22	68.00	76.78	85.56	94.34
0.850	45.96	55.90	65.85	75.80	85.74	95.69	105.64
0.900	47.28	59.81	71.43	82.16	91.98	100.89	108.90
0.944	49.46	64.11	76.70	87.22	95.67	102.05	106.37
0.960	49.57	64.21	76.69	87.02	95.19		
$CO_2 – C_{10}F_{18}$							
x_{CO2}	**293.15 K**	**303.15 K**	**313.15 K**	**323.15 K**	**333.15 K**	**343.15 K**	**353.15 K**
0.098	7.26	8.00	8.74	9.48	10.22	10.96	11.70
0.262	16.99	19.07	21.16	23.25	25.33	27.42	29.50
0.349	22.22	25.24	28.27	31.29	34.31	37.33	40.35
0.473	29.03	33.85	38.66	43.48	48.30	53.12	57.94
0.570	34.64	41.12	47.60	54.08	60.56	67.04	73.52
0.674	40.39	48.84	57.29	65.73	74.18	82.62	91.07
0.775	45.01	55.48	65.95	76.41	86.88	97.34	107.81
0.850	48.79	60.65	72.51	84.37	96.23	108.10	119.96
0.900	51.08	63.92	76.76	89.60	102.44	115.28	128.13
0.946	53.22	67.98	81.69	94.34	105.94	116.48	125.97
0.850	44.92	56.30	67.68	79.06	90.45	101.83	113.21
0.900	48.35	61.74	74.26	85.94	96.76	106.73	115.84
0.950	52.49	66.57	79.05	89.92	99.18	106.84	112.88

Table II.18. (continued)

$CO_2 – C_6F_6$							
x_{CO2}	293.15 K	303.15 K	313.15 K	323.15 K	333.15 K	343.15 K	353.15 K
0.107	6.13	7.19	8.25	9.31	10.36	11.42	12.48
0.199	9.95	11.90	13.85	15.80	17.75	19.70	21.65
0.299	14.93	17.95	20.98	24.00	27.03	30.06	33.08
0.410	20.04	24.47	28.89	33.31	37.74	42.16	46.59
0.510	25.19	30.99	36.80	42.60	48.41	54.21	60.02
0.600	29.95	37.13	44.32	51.50	58.68	65.86	73.04
0.700	35.84	44.76	53.69	62.62	71.55	80.48	89.40
0.800	41.85	52.53	63.21	73.89	84.57	95.25	105.93
0.850	44.92	56.30	67.68	79.06	90.45	101.83	113.21
0.900	48.35	61.74	74.26	85.94	96.76	106.73	115.84
0.950	52.49	66.57	79.05	89.92	99.18	106.84	112.88
$CO_2 – C_7F_8$							
x_{CO2}	293.15 K	303.15 K	313.15 K	323.15 K	333.15 K	343.15 K	353.15 K
0.101	6.28	7.09	7.90	8.71	9.53	10.34	11.15
0.205	11.10	12.97	14.85	16.73	18.60	20.48	22.36
0.302	15.12	18.05	20.98	23.91	26.84	29.77	32.70
0.400	19.94	24.02	28.09	32.17	36.24	40.32	44.39
0.497	24.53	30.02	35.52	41.01	46.50	51.99	57.48
0.603	29.99	37.17	44.35	51.52	58.70	65.88	73.05
0.701	36.16	44.86	53.56	62.27	70.97	79.67	88.38
0.801	42.18	52.69	63.19	73.70	84.20	94.71	105.21
0.872	47.66	59.42	71.17	82.93	94.69	106.45	118.21
0.901	49.51	63.05	75.88	88.02	99.46	110.19	120.22
0.950	52.15	67.25	80.55	92.06	101.76	109.68	115.80
$CO_2 – C_7F_{14}$							
x_{CO2}	293.15 K	303.15 K	313.15 K	323.15 K	333.15 K	343.15 K	353.15 K
0.099	7.10	7.95	8.80	9.65	10.50	11.35	12.20
0.203	12.73	14.51	16.29	18.06	19.84	21.62	23.39
0.300	18.30	20.93	23.56	26.19	28.81	31.44	34.07
0.401	24.09	27.75	31.42	35.08	38.74	42.41	46.07
0.514	29.95	35.13	40.32	45.50	50.69	55.87	61.06
0.600	34.65	41.04	47.43	53.82	60.21	66.60	72.99
0.701	39.67	47.58	55.48	63.38	71.28	79.18	87.08
0.800	44.57	54.60	64.39	73.93	83.22	92.26	101.05
0.870	48.22	59.14	70.23	81.68	92.16	100.32	104.82
0.900	50.20	61.45	73.40	84.85	94.56	101.34	103.96
0.950	53.97	67.04	79.64	89.88	95.90	95.80	87.72

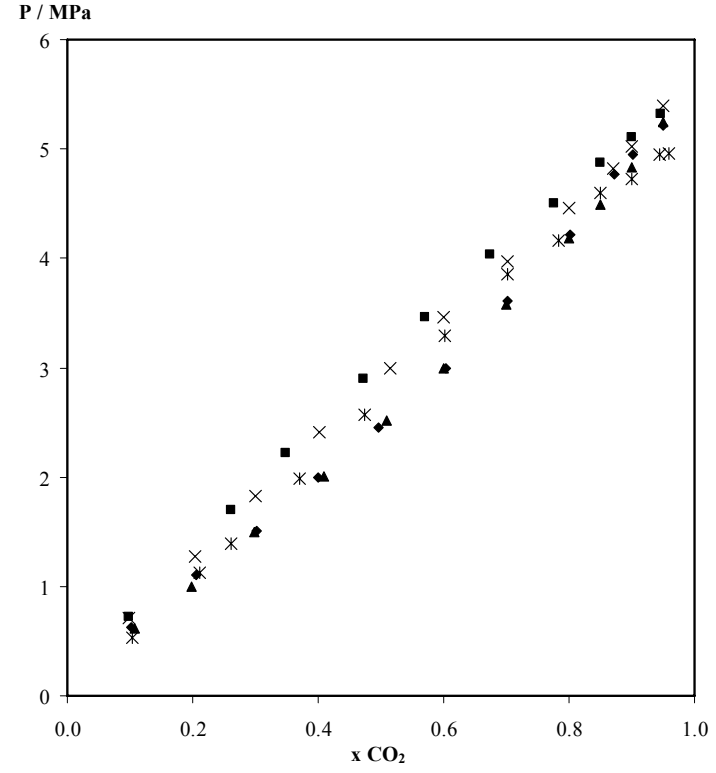

(a)

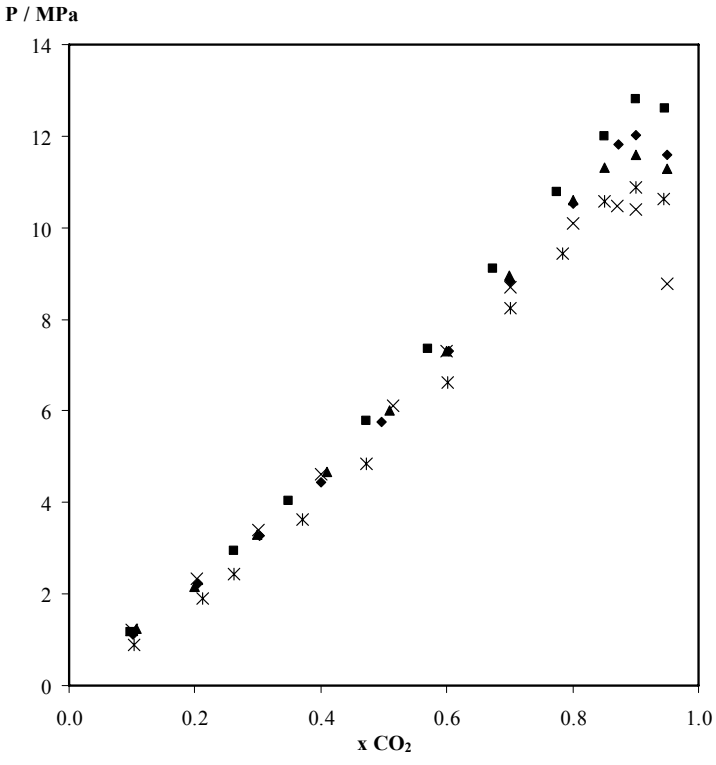

Figure II.16. Experimental measured solubility of CO_2 in perfluoroalkanes at 293.15K (a) and 353.15 K (b): Perfluoro-n-octane (*), Perfluorodecalin (■), Perfluorobenzene (▲), Perfluorotoluene (♦) and Perfluoromethylcyclohexane (x).

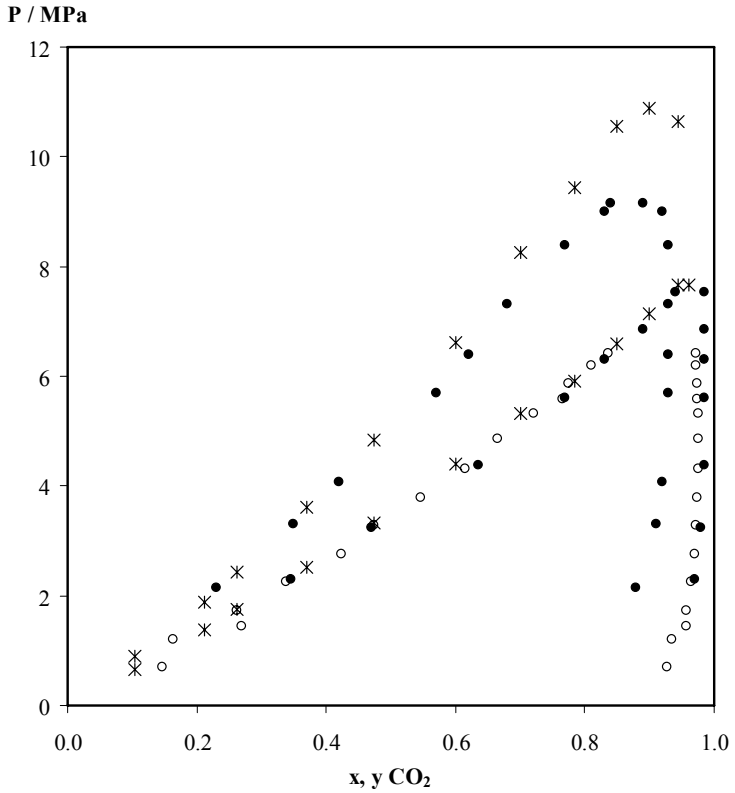

Figure II.17. Effect of the chain size on the solubility of CO_2 in perfluoralkane systems at 313 K and 353 K: data measured for CO_2/perfluoro-n-octane system in this work (*) and experimental data measured for CO_2/perfluoro-n-hexane system by (●) Iezzi et al. (1989) and (○) Lazzaroni et al. (2005). Note that data presented by Iezzi et al. (1989) for the lower temperature was actually measured at 314.65 K.

II.6. Liquid - Liquid Equilibrium

II.6.1. Bibliographic revision

The experimental methods for determining phase equilibria can be divided into two main categories: the synthetic and analytical methods. There are other less common methods and techniques to obtain liquid-liquid solubility data both directly or from derived properties that were compiled by Hefter (2003) and references there in. The choice between the different methods depends on many factors such as the stability of the components, the desired accuracy, the level of solubility, etc. For most of the studies concerning liquid-liquid equilibria the only variables are temperature and composition. System pressure generally has a negligible effect on the equilibria of most condensed phases up to about 100 atm, except near the critical solution temperature (Hefter, 2003).

The synthetic method involves the preparation, usually by mass, of a mixture of known composition, followed by measurement of its phase coalescence or separation temperature by some appropriate means. The advantages of the synthetic method are essentially the accuracy, the applicability and the simplicity. Providing the components are stable and not air sensitive or highly volatile, composition can be determined to high accuracy by mass measurements and the method can be applied to practically all liquid-liquid systems. The major disadvantage is that the method is not suitable to the determination of very low solubilities and is not easily automated. The main factors that control accurate measurements using this method are the phase change detection, the temperature control and the mixing of the sample. Phase changes for L-L mixtures can be detected by visual observation or by laser photometry. The advantages of the laser photometry over visual direct observation are clear if it is attended that mixtures can go from completely clear visually to fully opaque over a very narrow temperature range (0.02 K or less) and very quickly.

The analytical method requires that the liquid phases are equilibrated together, allowed to separate, sampled and then analyzed by some appropriated method (titration, spectrophotometry, chromatography, etc). Good temperature control is very important not only during equilibration but also during phase separation and sampling. Its speed, simplicity and lack of requirement for specialized apparatus are among the main advantages of this method. The method can be very time consuming once large

equilibration and phase separation periods are required in order to obtain accurate measurements. Also, care must be taken to guarantee that a complete separation of the phases was achieved before sampling.

The aim of this work is to contribute with new reliable experimental data for perfluoroalkane + alkane mixtures. A bibliographic revision on experimental data relating these systems is compiled in Table II.19. It resumes the methods and experimental conditions used to perform liquid-liquid solubility measurements for mixtures of linear, cyclic and aromatic alkanes and perfluoroalkanes that are liquid at ambient temperature.

Table II.19. Compilation of the References Reporting Experimental Liquid-Liquid Solubility Data for Perfluoroalkane + Alkane Systems

System	Method	T range (K)	P range (MPa)	Reference
$C_7F_{14} + C_6H_6$	Synthetic	308 - 359	0.1	Hildebrand and Cochran (1949)
$C_7F_{14} + C_7H_8$		316 - 362		
$C_7F_{16} + C_6H_6$	Synthetic	330 - 387	0.1	Hildebrand et al. (1950)
$C_7F_{16} + C_7H_{16}$		300 - 323		
$C_7F_{16} + C_8H_{18}$	Synthetic	300 - 341	0.1	Campbell and Hickman (1953)
$C_7F_{16} + C_6H_{14}$	Synthetic	283 - 302	0.1	Hickman (1955)
$C_6F_{14} + C_6H_{14}$	Synthetic	250 - 294	0.1	Bedford and Dunlap (1958)
$C_6F_{14} + C_6H_{14}$	Synthetic	290 - 295	0.1	Duce et al. (2002)
$C_6F_{14} + C_7H_{16}$		300 - 315		
$C_6F_{14} + C_8H_{18}$		286 - 325		

II.6.2. Apparatus and procedure

In this work, liquid-liquid equilibria (LLE) of binary mixtures of perfluoro-n-octane plus alkanes, n-C_nH_{2n+2} (n = 6 - 9), were measured, using the synthetic method, by turbidimetry at atmospheric pressure, and using a light scattering technique for measurements at pressures up to 1500 bar.

At atmospheric pressure, different samples of n-perfluorooctane + n-alkane were prepared by weighting and sealed in an ampoule with a magnetic stirrer. The pure compounds were kept into molecular sieves to avoid moisture contamination. The ampoules were sealed frozen in liquid nitrogen to avoid changes in the composition of the samples. The ampoules with mixtures at different compositions were then placed in a thermostatic bath where a calibrated Pt 100 temperature sensor with an uncertainty of

0.05K is immersed. The cloud points were determined by visual observation by heating the samples until a homogeneous phase is obtained followed by slow cooling of the mixtures until phase separation is observed.

The accurate detection of cloud points at higher pressures was performed with a He-Ne laser light scattering cell. The apparatus, as well as the methodology used for the determination of phase transitions, have been described in detail elsewhere (Sousa and Rebelo, 2000). The apparatus is easy, fast and safe to operate since both temperature and pressure are computer controlled and it is fully automated (including data acquisition and treatment).

The solution is contained in a high-pressure glass capillary (or sapphire capillary) and the phase transition can be induced either by changing the cell temperature (at constant pressure) or by changing pressure (at constant temperature), or by any other combination of these changes. The temperature accuracy is typically ± 0.01 K ($240 < T/K < 520$). The pressure accuracy is ± 0.01 MPa for pressures ranging from (0 to 7) MPa (glass cell) or 35 MPa (sapphire cell), although the final pressure accuracy of each cloud point determination is somewhat poorer.

During an experiment, the cell containing the solution of a known composition is immersed in the high precision oil (or water) bath at a given temperature and pressure, in the homogeneous one-phase region. The top cap of the capillary cell is fitted to an HPLC high-pressure valve, which allows the cell to be filled with solvent using syringes. Stirring is accomplished by using a magnetic stirrer, which is turned off during the data acquisition in order to avoid shear effects. By changing temperature and/or pressure the phase transition is induced. Light from a He-Ne LASER passes across the solution contained in the cell. Scattered and transmitted light intensities are converted into electrical signals by two photo-detectors. These signals are measured with a digital multimeter equipped with an automatic channel scanner. Pressure is generated by a high pressure screw injector, coupled to a stepper motor, and controlled by a control box and a personal computer. Pressure is measured by a digital manometer and by the multimeter. Temperature is measured with a platinum resistance thermometer linked to a $6^{1/2}$ digits multimeter. Both multimeters have IEEE-488 interfaces, which allow the computer data aquision.

Cloud-points are detected when there is a sudden increase in scattered light from the He-Ne LASER accompanied by a sudden decrease in transmitted light exiting the cell.

The intensity of scattered light (I_{sc}) and transmitted light (I_{tr}) are corrected for density fluctuations, reflections, and multiple scattering effects. The operational spinodal point will be taken at the interception point where 1/Isc,corr = 0. At this point, the intensity of scattered light has an infinite value. Since it is easy to apply and has good reproducibility, this extrapolation has been widely used.

II.6.3. Experimental Results and Discussion

Experimental data measured for the studied systems at atmospheric pressure and high pressure are presented in Table II.20 and II.21 respectively.

Table II.20. Experimental Liquid-Liquid Solubility Data for Perfluoro-n-octane (1) + Alkane (2) (C_6 - C_9) Mixtures at Atmospheric Pressure.

$C_8F_{18} + C_6H_{14}$		$C_8F_{18} + C_7H_{16}$		$C_8F_{18} + C_8H_{18}$		$C_8F_{18} + C_9H_{20}$	
T / K	x_1	T / K	x_1	T / K	x_1	T / K	x_1
293.98	0.0806	319.13	0.1024	334.24	0.0991	352.09	0.1116
306.36	0.1222	328.21	0.1772	345.48	0.1669	362.24	0.1650
308.95	0.1683	330.76	0.2611	349.16	0.2374	367.65	0.2526
310.83	0.2518	330.76	0.3185	350.52	0.3013	368.85	0.3505
310.81	0.2997	330.96	0.3818	350.44	0.4026	368.49	0.4342
310.71	0.3470	330.58	0.4967	349.70	0.4984	367.46	0.5395
310.65	0.3959	329.80	0.5437	346.09	0.5964	362.59	0.6391
309.61	0.4425	316.24	0.7048	336.01	0.7245	349.16	0.7639
308.49	0.4891			327.71	0.7640	322.99	0.8805
305.74	0.5440			299.71	0.8919		
303.05	0.6000						
296.93	0.6657						
293.89	0.6924						

Table II.21. Experimental Liquid-Liquid Solubility Data for Perfluoro-n-octane (1) + Alkane (2) (C_6 - C_9) Mixtures at Pressures P.

C_8F_{18} + C_6H_{14}					
x_1 = 0.2552		x_1 = 0.2678		x_1 = 0.2644	
T / K	P / MPa	T / K	P / MPa	T / K	P / MPa
311.58	1.48	311.13	0.85	311.72	1.43
312.08	2.18	311.80	1.74	312.52	2.45
312.59	2.88	311.41	1.23	313.29	3.40
313.31	3.78	310.89	0.53	314.02	4.42
314.12	4.95	313.24	3.60	314.81	5.45
310.98	0.71	312.42	2.57	322.99	16.70
310.53	0.13			332.97	31.00
				342.95	46.50
				353.00	62.80
				363.07	80.20
				373.16	98.00
				383.43	118.50
				394.15	143.00

C_8F_{18} + C_7H_{16}			
x_1 = 0.2552		x_1 = 0.2678	
T / K	P / MPa	T / K	P / MPa
331.90	1.52	330.88	0.14
333.29	3.20	331.33	0.60
333.78	3.83	331.92	1.37
332.48	2.24	332.82	2.41
		333.50	3.28
		334.49	4.46

C_8F_{18} + C_8H_{18}			
x_1 = 0.3608		x_1 = 0.7510	
T / K	P / MPa	T / K	P / MPa
349.80	0.15	332.302	4.02
350.18	0.60	331.999	3.55
350.93	1.48	331.619	3.04
351.80	2.49	331.124	2.54
352.64	3.46	330.628	1.87
353.44	4.42	332.604	4.26
		329.668	0.70
		329.308	0.29
		330.127	1.27

Table 2.20. (continued)

$C_8F_{18} + C_9H_{20}$	
$x_1 = 0.0828$	
T / K	**P / MPa**
344.34	0.16
344.68	0.84
345.34	1.85
345.78	2.50
346.46	3.48
347.12	4.41

It was observed that temperature versus composition diagrams for these mixtures are more symmetric when represented in terms of volume fraction than mole fraction, as can be observed in Figure II.18 *a* and *b*. Compositions in terms of volume fractions (□) are calculated using the relation

$$\phi = \frac{x}{x + K(1-x)} \tag{II.28}$$

where $K = \rho_1.M_2/\rho_2.M_1$, being ρ and M the densities and the molecular weights of components perfluoro-n-octane (1) and alkane (2).

The experimental data measured were correlated using relations derived from renormalization group (RG) theory, developed to describe systems near the critical point (Nagarajan et al., 1980). In the vicinity of the critical point, the corresponding thermodynamic functions are not analytical because of the flat slopes of the two branches of the coexistence curve in that region. The RG theory is used to express the composition for the critical point.

According to Sengers et al. (1976) the following relation is verified at the critical point

$$\Delta M = B(\tau)^{\beta} \tag{II.29}$$

where ΔM is the difference in order parameter between the coexisting phases. The order parameter is some quantity, mole fractions, volume fractions, densities, etc, chosen as a measure of the different between the two coexisting phases. In the non-asymptotic region Equation II.29 is modified by the presence of corrections to scaling (Wegner, 1972)

$$\Delta M = B_0 \tau^{\beta} \left[1 + B_1 \tau^{\Delta_1} + B_2 \tau^{2\Delta_1} + ...\right] \quad \text{(II.30)}$$

where β and Δ_1 are the correction exponents and $\tau = (T - T_c)/T_c$ is the reduced temperature and expresses the distance from the critical point. The diameter of the coexisting curve is given by the relationship (Koo and Green, 1977)

$$\frac{M_1^{\ I} + M_1^{\ II}}{2} = M_c \left[1 + A_1 \tau + A_2 \tau^{1-\alpha} + ...\right] \quad \text{(II.31)}$$

where α is a critical exponent and M_1^{I} and M_1^{II} represents the property chosen for order parameter of component 1 in phases I and II respectively. When Equations II.30 and II.31 are combined the result is the equation used in this work to correlate the experimental data measured

$$\phi - \phi_c = fA\left(\frac{T - T_c}{T_c}\right)^{\beta} \quad \text{(II.32)}$$

where $f = 1$ for $x > x_c$ and $f = -1$ for $x < x_c$. The volume fraction was chosen to be the order parameter. This relationship was used to correlate the mutual solubility for the experimental data measured for the entire temperature interval, including the critical region. The values for A and β to be used in Equation II.32 together with the calculated values for the critical temperature, mole fraction and volume fraction for each mixture are presented in Table II.21. The lines in Figure II.18 represent the correlated data.

Table II.21. Parameters to be Used in Equation II.29 Together With Critical Constants for the Studied Mixtures.

System	A	β	ϕ_c	x_c	T_c	T_c Literature
$C_8F_{18} + C_6H_{14}$	0.71426	0.25801	0.471	0.320	310.54	299 [a]
$C_8F_{18} + C_7H_{16}$	0.71572	0.25017	0.474	0.348	330.99	320 [a]
$C_8F_{18} + C_8H_{18}$	0.77238	0.27603	0.473	0.371	350.33	349 [b]
$C_8F_{18} + C_9H_{20}$	0.79521	0.28589	0.473	0.393	368.65	-

a - Edmonds (1972)

b - Bedford and Dunlap (1958)

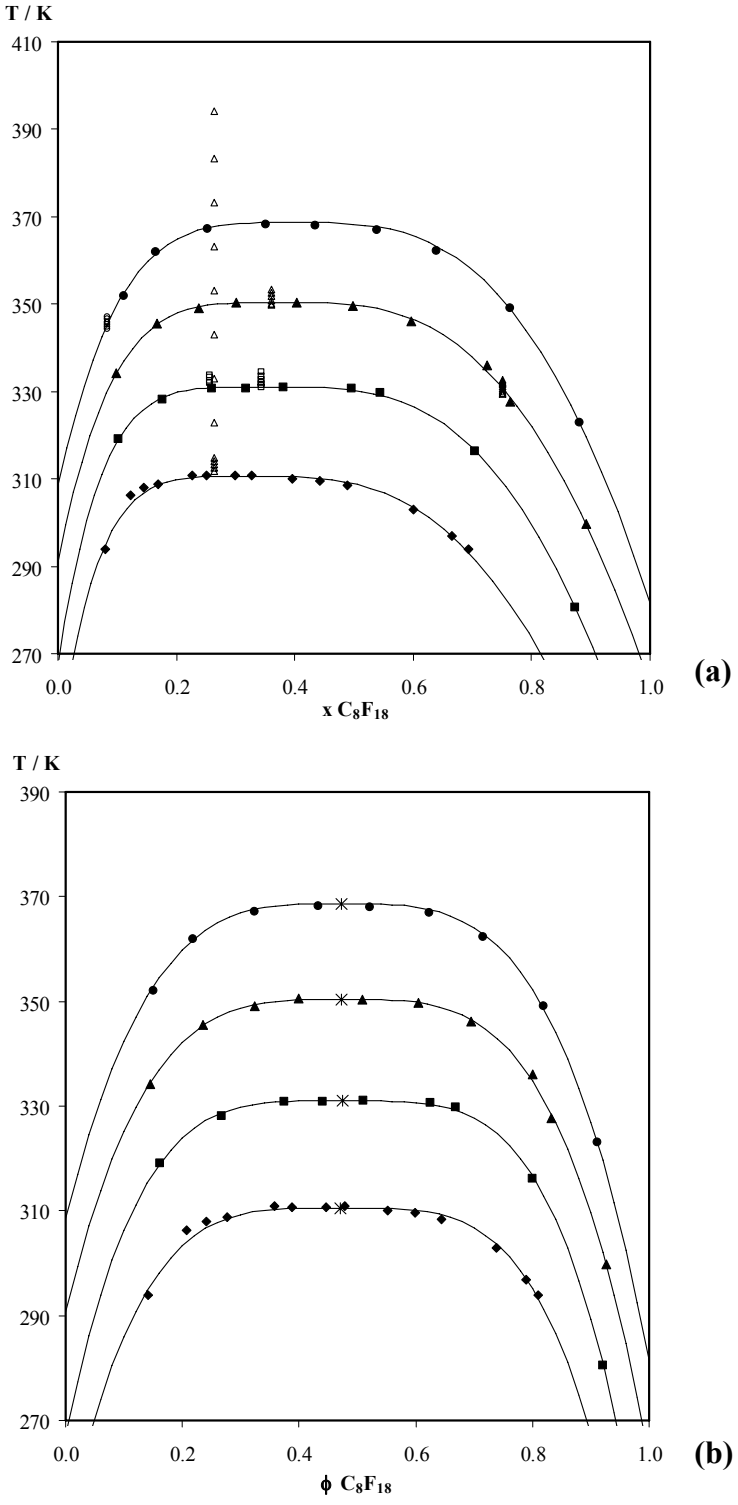

Figure II.18. Experimental and correlated coexisting curve of perfluoro-n-octane + alkanes (C_6 - C_9) in terms of mole fraction (a) and volume fraction (b). Symbols represent solubility in n-hexane (♦), n-heptane (■), n-octane (▲) and n-nonane (●). (*) Represents the critical point for each mixture. The non-filled symbols in Figure II.17 (a) represent the effect of the pressure on the liquid-liquid phase diagram.

References

Abedi, S.J.; Cai, H.-Y.; Seyfaie, S.; Shaw, J.M., *Simultaneous Phase Behaviour, Elemental Composition and Density Measurement Using X-ray Imaging,* Fluid Phase Equilibria (1999) 158–160: 775

Albert H. J.; Wood, R. H., *High-Precision Flow Densimeter for Fluids at Temperatures to 700 K and Pressures to 40 MPa*, Rev. Sci. Instrum. (1984) 55: 589

Ambrose D., *Reference Values of Vapour Pressure. The Vapour Pressure of Benzene and Hexafluorobenzene*, J. Chem. Thermodynamics (1981) 13: 1161

Ambrose, D.; Ewing, M. B.; Ghiasse, N. B.; Ochoa, J. C. Sanchez, J. Chem. Thermodynamics (1990) 22: 589

Ambrose, D.; Ellender, J. H. *The Vapour Pressure of Octafluorotoluene*, J. Chem. Thermodynamics (1981) 13: 901

Barton, A. F. M., *CRC Handbook of Solubility Parameters and Other Cohesion Parameters*, (1991) 2nd Edition, CRC Press

Battino, R.; Clever, H.L., *The Solubility of Gases in Liquids,* Chem. Rev. (1966) 66: 395

Battino, R.; Wilcock, R.; Wilhelm, E., *Low-Pressure Solubility of Gases in Liquid Water,* Chem. Rev. (1977) 77: 219

Battino, R., *The Ostwald Coefficient of Gas Solubility,* Fluid Phase Equilibria (1984) 15: 231

Bauer, N.; Lewin, S. Z., *Determination of Density*, in Weissberger A. ed. (1972)

Bedford, R. G.; Dunlap, R. D., *Solubilities and Volume Changes Attending Mixing for the System: Perfluoro-n-hexane-n-hexane*, J. Am. Chem. Soc. (1958) 80: 282

Ben Naim, A.; Baer, S. *Method for Measuring Solubilities of Slightly Soluble Gases in Liquids* Trans. Faraday Soc. (1963) 59: 2735

Ben Naim, A. *Hydrophobic Interactions*, Plenum Press, New York (1980)

Ben Naim, A. Marcus, Y. *Solvation Thermodynamics of Nonionic Solutes*, J. Chem. Phys. (1984) 81: 2016

Ben Naim, A. *On the Evolution of the Concept of Solvation Thermodynamics*, J. of Solution Chem. (2001) 30: 475

Benning, A. F.; Park, J.D., U. S. Patent 2, (1949) 490, 764

Benson, B.; Krause, D., *Empirical Laws for Dilute Aqueous Solutions of Nonpolar Gases*, J. Chem. Phys., (1976) 64: 689

Billet, T.; Morrison, T. J., J. Chem. Soc. (1948) 2033

Brunner, G.; Dohrn, R., *High-Pressure Fluid-Phase Equilibria: Experimental Methods and Systems Investigated (1988–1993),* Fluid Phase Equilib. (1995) 106: 213

Campbell, D. N.; Hickman, J. B., *Solubility Characteristics of Some Binary Liquid Mixtures*, J. Am. Chem. Soc. (1953) 75: 2879

Carnicer, J.; Gibanel, F.; Urieta, J.; Losa, C., Rev. Acad. Ciencias Zaragoza (1979) 34: 115

Chickos, J. S., *The Strain Energy of Cyclotetradecane is Small*, J. Org. Chem. (1992) 57 1897

Christov, M.; Dohrn, R., *High-Pressure Fluid Phase Equilibria. Experimental Methods and Systems Investigated (1994–1999),* Fluid Phase Equilibria 202 (2002) 153

Clever H. L., Battino R. in *Solutions and Solubilities*, Ed. M. R. J. Dack, J. Wiley and Sons, New York (1975) Chapter 7

Clever, H. L.; Battino, R., *The Experimental Determination of Solubilities*, Edited by G. T. Hefter and R. P.T. Tomkins, Wiley (2003) Chapter 2.1

Cook, M. W.; Hanson, D. N., *Accurate Measurements of Gas Solubiliy*, Rev. Sci. Instr., (1957) 28: 370

Costa, M.A.M.; Matos, H.A.S.; Nunes da Ponte, M.; Gomez de Azevedo, E.J.S., *Binary and Ternary Phase Behavior of α-Pinene, β-Pinene, and Supercritical Ethene,* J. Chem. Eng. Data (1996) 41: 1104

Counsell, J. F.; Green, J. H. S.; Hales, J. L.; Martin, J. F.; *Thermodynamic Properties of Fluorine Compounds.2. Physical and Thermodynamic Properties of Hexafluorobenzene*, Trans. Faraday Soc. (1965) 61: 212

Crowder, G. A.; Taylor, Z. L.; Reed, T. M.; Young, J. A., *Vapor Pressures and Triple Point Temperatures for Several Pure Fluorocarbons*, J. Chem. Eng. Data (1967) 12: 481

Dias A. M. A., Freire. M. G., Coutinho J. A. P., Marrucho I. M., *Solubility of Oxygen in Liquid Perfluorocarbons*, Fluid Phase Equilibria (2004) 222: 325

Douslin, D. R.; Osborn, A.; *Pressure Measurements in 0.01-30 Torr Range With an Inclined-Piston Gauge*, J. Sci. Instrum. (1965) 42: 369

Douslin, D. R.; Harrison, R. H.; Moore, R. T. *Pressure-Volume-Temperature Relations of Hexafluorobenzene,* J. Chem.Thermodynamics (1969) 1: 305

Duce, C.; Tinè, M. R.; Lepori, L.; Matteoli, E., *VLE and LLE of Perfluoroalkane + Alkane Mixtures*, Fluid Phase Equilibria (2002) 199: 197

Dunlap, R. D.; Murphy, C. J.; Bedford, R. G., *Some Physical Properties of Perfluoro-n-hexane,* J. Am. Soc. (1958) 80: 83

Dymond, J.; Smith, E., *The Virial Coefficients of Pure Gases and Mixtures*, Oxford University Press, Oxford (1980)

Edmonds B. (1972) *Chemistry*, University of Sheffield: Shefield

Ermakov, G.; Skripov, V. *Saturation line, critical parameters, and the maximum degree of superheating of perfluoro-paraffins* Russian Journal of Physical Chemistry (1967) 41: 39

Evans F. D.; Tiley, P. F. *Vapour Pressures and Critical Constants of Hexafluoro, Pentafluoo, Chloropentafluoro and Bromopentafluoro Benzene* J. Chem. Soc. B-Physical Organic (1966) 2: 134

Evans F. D., Battino R., *Solubility of Gases in Liquids. 3. Solubilities of Gases in Hexafluorobenzene and in Benzene*, J. Chem. Thermodynamics (1971) 3: 753

Findlay, T. J. V. *Vapor Pressures of Fluorobenzene from 5 Degrees C to 50 Degrees C*, J. Chem. Eng. Data (1969) 14: 229

Fogg P.G.T., Gerrard W., *Solubilities of Gases in Liquids*, John Wiley & Sons Lda, England (1991)

Fornari, R.; Alessi, P.; Kikic, I., *High Pressure Fluid Phase Equilibria: Experimental Methods and Systems Investigated (1978–1987),* Fluid Phase Equilib. (1990) 57: 1

Girard G., *Density* in Marsh K.N. ed., *Recommended Reference Materials for the Realization of Physicochemical Properties*, IUPAC, Blackwell, Oxford, Cap.2 (1987)

Gjaldbaek, J. C., *The Solubility of Hydrogen, Oxygen and Carbon Monoxide in Some Non-Polar Solvents*, Acta Chemica Scandinavica (1952) 6: 623

Glew, D.; Reeves, L. *Purification of perfluoro-n-heptane and perfluoromethylcyclohexane* J. Phys. Chem. (1956) 60: 615

Gomes, M. F. C.; Deschamps, J.; Menz, D. H. *Solubility of Dioxygen in Seven Fluorinated Liquids* J. of Fluorine Chem. (2004) 125: 1325

Good, W. D.; Douslin, D. R.; Scott, D. W.; George, A.; Lacina, J. L.; Dawson, J. P.; Waddington, G. *Thermochemistry and vapor pressure of Aliphatic Fluorocarbons. A*

Comparison of the C-F and C-H Thermochemical Bond Energies, J. Am. Chem. Soc., (1959) 63: 1133

Goodwin, A.R.H.; Moldover, M.R. *Phase Border and Density Determinations in the Critical Region of (carbon dioxide plus ethane) Determined from Dielectric Permittivity Measurements*, J. Chem. Thermodyn. (1997) 29: 1481

Greer, S. C.; Moldover, M.R.; Hocken R., *Differential Transformer as a Position Detector in a Magnetic Densimeter*, Rev. Sci. Instrum. (1974) 45: 1462

Hales, J. L. *Apparatus for Accurate Measurement of Liquid Densities Over an Extended Temperature Range*, J. Phys. E (1970) 3: 855

Hales, J. L.; Townsend, R. *Liquid Densities From 293 to 490 K of Eight Fluorinated Aromatic Compounds*, J. Chem. Thermodynamics (1974) 111-116

Hales, J. L.; Gundry, H. A., *An Apparatus for Accurate Measurement of Liquid and Vapor Densities on the Saturation Line, Up to the Critical-Temperature*, J. Phys. E: Sci. Instrum. (1983) 16: 91

Haszeldine, R.; Smith, F., *Organic Fluorides. Part VI. The Chemical and Physical Properties of Certain Fluorocarbons*, J. Chem. Soc. (1951) 603-608

Hefter, G. T. *Liquid-Liquid Solubilities in The Experimental Determination of Solubilities* Edited by Hefter, G. T. and Tomkins, R. P. T., John Wiley & Sons, Ltd (2003)

Hesse, P.; Battino, R.; Scharlin, P.; Wilhelm, E., *Solubility of Gases in Liquids. 20. Solubility of He, Ne, Ar, Kr, N2, O2, CH4, CF4, and SF6 in n-Alkanes n-ClH2l+2 (6 l 16) at 298.15 K*, J. Chem. Eng. Data, (1996) 41: 195

Hickman, J. B., *Solubility of Isomeric Hexanes in Perfluoroheptane*, J. Am. Chem. Soc. (1955) 77: 6154

Hildebrand, J. H.; Cochran, D. R. F., *Liquid-Liquid Solubility of Perfluoromethylcyclohexane with Benzene, Carbon Tetrachloride, Clorobenzene, Chloroform and Toluene*, J. Am. Chem. Soc. (1949) 71: 22

Hildebrand, J. H.; Fisher, B. B.; Benesi, H. A., *Solubility of Perfluoro-n-heptane with Benzene, Carbon Tetrachloride, Chloroform, n-Heptane and 2,2,4-Trimethylpentane*, J. Am. Chem. Soc. (1950) 72: 4348

Hildebrand J. H., Prausnitz, J. M., Scott, R. L., *Regular and Related Solutions*, Van Nostrand Reinhold, New York (1970) Chapter 8

Iezzi, A.; Bendale, P. ; Enick, R.; Turberg, M.; Brady, J., *Gel Formation in Carbon Dioxide – Semifluorinated Alkane Mixtures and Phase Equilibria of a Carbon Dioxide – Perfluorinated Alkane Mixture,* Fluid Phase Equilibria (1989) 52: 307

IUPAC *Recommended Reference Materials for the Realization of Physicochemical Properties*. Marsh, K. N.; editor. Blackwell (for IUPAC): Oxford (1987)
Kennan, R. P.; Pollack, G.L., *Solubility of Xenon in Perfluoroalkanes: Temperature Dependence and Therodynamics*, J. Chem. Phys, (1988) 89: 517

Koo, L.; Green, M. S. *Revised and Extended Scaling for Coexisting Densities of SF6* Phys. Rev. A (1977) 16: 2483

Kreglewski, A., *Determination of high-pressure liquid density for n-perfluorohexane and n-perfluorononane*, Bulletin de L'academie Polonaise des Sciences, (1962) vol.X: 629

Knapp, H.; Döring, R.; Oellrich, L.; Plöcker, U.; Prausnitz, J.M., *Vapor–Liquid Equilibria for Mixtures of Low-Boiling Substances*, DECHEMA Chem. Data Series VI (1981)

Lannung, A., *The Solubilities of Helium, Neon and Argon in Water and Some Organic Solvents*, J. Am. Chem. Soc. (1930) 52: 68

Lazzaroni, M. J.; Bush, D.; Brown, J. S.; Eckert, C. A., *High-Pressure Vapor-Liquid Equilbria of Some Carbon Dioxide+Organic Binary Systems*, J. Chem. Eng. Data (2005) 50: 60

Makranczy, J., *Solubility of Gases in Normal-Alkanes*, Hungarian Journal of Industrial Chemistry, (1976) 4: 269

Marteau, Ph.; Tobaly, P.; Ruffier-Meray, V.; Barreau, A., *In Situ Determination of High Pressure Phase Diagrams of Methane-Heavy Hydrocarbon Mixtures Using an Infrared Absorption Method,* Fluid Phase Equilib. (1996) 119: 213

Miguel, A. A. F.; Ferreira, A. G. M.; Fonseca, I. M. A, *Solubilities of Refrigerants in water*, Fluid Phase Equilibria (2000) 173: 97

Morrison, T. J.; Billett, F. *The Measurement of Gas Solubilities* J. Chem. Soc. (1948) 2033

Mousa, A. H. N. *Study of Vapor Pressure and Critical Properties of Perfluoro-n-hexane* J. Of Chemical and Engineering Data (1978) 23: 133

Nagahama, K. *VLE Measurements at Elevated Pressures for Process Development,* Fluid Phase Equilibria (1996) 116: 361

Nagarajan, N.; Kumar, A.; Gopal, E. S. R.; Greer, S. C. *Liquid-Liquid Critical Phenomena. The Coexistence Curve of n-heptane –acetic anhydride*, J. Phys. Chem. (1980) 84: 2883

Pádua, A. A. H., PhD Thesis (1994)

Patrick, C. R.; Prosser, G. S. *Vapour Pressures + Related Properties of Hexafluorobenzene* Transactions of the Faraday Society (1964) 60: 700

Pauly, J.; Daridon, J-Luc; Coutinho, J. A. P. *Fluid Phase Equilibria*, 2005 s*ubmited*

Pierotti, R. A. J., *Solubility of Gases in Liquids*, Phys. Chem. (1963) 67: 1840

Piñeiro, M. M.; Bessières, D.; Gacio, J. M.; Guirons, H. S.; Legido, J. L., *Determination of high-pressure liquid density for n-perfluorohexane and n-perfluorononane,* Fluid Phase Equilibria (2004) 220: 125

Poling, B.; Prauznitz, J.; O'Connell, J.*, The properties of Gases and Liquids*, McGraw-Hill, New York (2001) 5th edition

Prausnitz, J.; Lichtenthaler, R.; Azevedo, E., *Molecular Thermodynamics of Fluid-Phase Equilibria*, Prentice Hall, New Jersey (1999) 3rd Edition

Reiss, H.; Frisch, H. J.; Helfand, E.; Lebowitz, J. L., *Aspects of the Statistical Thermodynamics of Real Fluids*, J. Chem. Phys. (1960) 32: 119

Riess, J. C., *Oxygen Carriers ("Blood Substitutes")-Raison d'Etre, Chemistry, and Some Physiology*, Chem. Rev. (2001) 101: 2797

Roy, S.; Behar, E.; Ungerer, P., *Vapour-Liquid Equilibrium Data for Synthetic Hydrocarbon Mixtures. Application to Modelling of Migration from Source to Reservoir Rocks,* Fluid Phase Equilibria (1997) 135: 63

Sengers, J. M. H. L.; Greer, W. L; Sengers, J. V. *Scaled Equation of State Parameters for Gases in the Critical Region*, J. Phys. Chem. Ref. Data (1976) 5: 1

Serra, M. C. C.; Palavra, AM. F. *Solubility of 1-Butene in Water and in a Medium for Cultivation of a Bacterial Strain*, J. of Solution Chemistry (2003) 32: 527

Sousa, H. C.; Rebelo, L. P. N., *(Liquid + Liquid) Equilibria of (polystyrene + nitroethane). Molecular Weight, Pressure, and Isotope Effects*, J. Chem. Thermodynamics (2000) 32: 355

Skurts, C. M.; Reese, H. R., *The Solubility of Oxygen in Aqueous Fluorocarbon Emulsions* J. Fluorine Chem. (1978) 11: 637

Stiles, V.; Cady, G. *Physical Properties of Perfluoro-n-hexane and Perfluoro-2-methylpentane*, J. Am. Chem. Soc. (1952) 74: 3771

Takagi, T.; Sakura, T.; Tsuji, T.; Hongo, M., *Bubble Point Pressure for Binary Mixtures of Difluoromethane with Pentafluoroethane and 1,1,1,2-tetrafluoroethane,* Fluid Phase Equilibria (1999) 162: 171

Thomsen, E.; Gjaldbaek, J., *The Solubility of Hydrogen, Nitrogen, Oxygen and Ethane in Normal Hydrocarbons*, Acta Chemica Scandinavica, (1963) 17: 127

Vosmansky, J.; Dohnal, V., *Gas Solubility Measurements with an Apparatus of the Ben-Naim-Baer Type*, Fluid Phase Equilibria (1987) 33: 137

Warowny, W., *Volumetric and Phase Behavior of Acetonitrile at Temperatures from 363 to 463 K,* J. Chem. Eng. Data (1994) 39: 275
Wegner, F. J., *Corrections to Scaling Laws,* Phys. Rev. B (1972) 5: 4529

Wendland, M.; Hasse, H.; Maurer, G., *Experimental Pressure-Temperature Data on Three- and Four-Phase Equilibria of Fluid, Hydrate, and Ice Phases in the System Carbon Dioxide-Water,* J. Chem. Eng. Data (1999) 44: 901

Wesseler, E. P.; Iltis, R.; Clark, L. C. *The Solubility of Oxygen in Highly Fluorinated Liquids* J. of Fluorine Chem. (1977) 9: 137

Wilhelm, E.; Battino, R., *Solubility of Gases in Liquids. 1. Solubility of a Series of Fluorin-Containing Gases in Several Non-Polar Solvents*, J. Chem. Thermodynamics (1971a) 3: 379

Wilhelm, E.; Battino, R., *Estimation of Lennard-Jones (6,12) Pair Potential Parameters from Gas Solubility Data*, J. Chem. Phys. (1971b) 55: 4012

Wilhelm, E.; Battino, R.; Wilcock, R., *Low-Pressure Solubility of Gases in Liquid Water*, Chemical Reviews, (1977) 77: 219

III. Part

MODELING

III.1. Introduction

Most conventional engineering equations of state are variations of the van der Waals equation. They are based on the idea of a hard-sphere reference term to represent the repulsive interactions, and a mean-field term to account for the dispersion and any other long-range forces. Commonly used EoS (e.g. Peng-Robinson, Soave-Redlich-Kwong, modified Benedict-Webb-Rubin) involve improvements to either the treatment of the hard-sphere contribution or the mean-field terms. Such an approach is suitable for simple, non-polar, nearly spherical molecules such as hydrocarbons, simple inorganics as nitrogen and carbon monoxide, etc. For these compounds, the most important intermolecular forces are repulsion and dispersion, together with weak electrostatic forces due to dipoles, quadrupoles, etc. Nevertheless, many fluids, and particularly mixtures, do not fall within this simple classes as polar solvents, hydrogen-bonded fluids, polymers, electrolytes, liquid crystals, plasmas, and so on which are highly polar, associating and often non-spherical. Although it is possible, in practice, to use one of these classical equations for these systems, their limitations rapidly become evident. The correlation of data requires complex and unsound mixing rules and temperature dependent binary parameters, and the predictive capability of this approach is usually poor. The reason for this is that, for such fluids, important new intermolecular forces come into play such as Coulombic forces, strong polar forces, complexing forces, forces associated with chain flexibility, induction forces, etc. that are not taken into account explicitly. In such cases a more appropriate reference is one that incorporates both the chain length (molecular shape) and molecular association, since both effects have a dramatic effect on the fluid structure. Other interactions (e.g. dispersion, long-range dipolar forces, etc) can then be treated via a perturbation or approximate mean-field term.

The development of novel processes at extreme conditions (such as, for example, processes where one or more of the components are supercritical) and the design of new materials over the last two decades imposed the need for new models. At the same time, significant developments in the area of applied statistical mechanics resulted in a number of semi-empirical EoS, such as the lattice fluid theory (LFT), (Sanchez and Lacombe, 1976) the perturbed hard-chain theory (Donohue and Prausnitz, 1978), and their modifications. These EoS are more complex than cubic EoS but significantly more accurate for various complex fluids, such as hydrogen bonding fluids, supercritical fluids,

and polymers. Furthermore, the tremendous increase of computing power at reasonable prices made these new complex models attractive for process simulation calculations.

Statistical mechanics is a reliable tool for calculating the structure and thermodynamics of a fluid given its intermolecular potential function. However, for most systems of interest, this solution requires the use of one or more approximations, which determine the accuracy of the theory. Two methods can be used for the modeling of complex homogeneous fluids, namely, integral-equation theories and perturbation theories. Both have been successful in solving the thermodynamic properties of some moderately complex fluids (nonspherical molecules, polar and polarizable fluids) (Hansen and McDonald, 1986; Gray and Gubbins, 1984). The possibility of molecular association can be introduced into integral-equation theories by considering a strong, spherically symmetric attraction, such as would be observed in the case of ionic systems. Although initial attempts failed to reproduce the low density limit for associating fluids, this difficulty has since been overcome. In perturbation approaches, one considers a reference fluid with well-known properties (e.g., a homomorphic, nonassociating fluid) and obtains the properties due to association through a perturbation expansion. This however, is not straightforward, as the association forces involved are strong and highly directional and the typical expansions used for weakly attractive fluids fail to converge (Muller and Gubbins, 2000).

In a series of four papers, Wertheim developed a statistical thermodynamic theory for fluids with a repulsive core and one or more highly directional short range attractive sites, known as TPT (Wertheim, 1984, 1986 and 1987). In TPT, the Helmholtz free energy, A, is calculated from a graphical summation of interactions between different species. Based on the first-order TPT, usually referred as TPT-1, Chapman, Gubbins, and co-workers developed an EoS for spherical and chain molecules with one or more hydrogen-bonding sites (Jackson et al., 1988 and Chapman et al., 1988). The essence of their approach was the use of Wertheim's theory to describe a reference fluid which includes both the molecular shape and molecular association, instead of the much simpler hard-sphere model employed in most engineering equations of state. The effect of weaker intermolecular forces, like dispersion and induction, were included through a mean-field perturbation term. They called this approach the Statistical Associating Fluid Theory (SAFT).

The pioneering work of Wertheim in the mid-1980s resulted in a family of engineering EoS developed in the 1990s that includes SAFT (Jackson et al., 1988 and Chapman et al., 1988), polar-SAFT (Walsh et al., 1992) SAFT-HS (Green and Jackson, 1992), simplified SAFT (Fu and Sandler, 1995) SAFT-LJ (Muller and Gubbins, 1995a; Kraska and Gubbins, 1996) copolymer SAFT (Banaszak et al., 1996), soft-SAFT (Blas and Vega, 1997, 1998a, 1998b; Pàmies and Vega, 2001), SAFT-VR (Gil-Villegas et al., 1997) SAFT1 (Adidharma and Radosz, 1998), SAFT-BACK (Pfohl and Brunner, 1998), crossover SAFT (Kiselev and Ely, 1999a, 1999b and 2000), PC-SAFT (Gross and Sadowski, 2001), crossover soft-SAFT (Llovell et al., 2004) and SAFT-VRX (McCabe and Kiselev, 2004). The different versions differ mainly on the intermolecular potential chosen to describe the reference fluid. The original SAFT EoS uses a perturbation expansion with a hard-sphere fluid as a reference and a dispersion term as a perturbation. The hard-sphere Helmholtz free energy is calculated through the expression of Carnahan and Starling and the dispersion term through correlations of molecular simulation data for the LJ fluid, which are functions of the reduced temperature and density (Jackson et al., 1988 and Chapman et al., 1988). Other intermolecular potentials, such as the square-well (Banaszak et al., 1993 and Tavares et al, 1997) and the Yukawa potential (Davies et al. 1999) have been used as the model for the segment interactions. Jackson *et al.* proposed a generalized potential function with an attractive part of variable range in the so-called SAFT-VR approach (Gil-Villegas et al., 1997). The availability of an analytical EoS for the LJ fluid (Johnson et al., 1993 and Kolafa and Nezbeda, 1994) led to other versions of the SAFT equation (Muller and Gubbins, 1995a; Kraska and Gubbins, 1996), like the soft-SAFT EoS that will be described in the next section. Two excellent reviews on the development, applications and different versions of SAFT-type equations were provided by Müller and Gubbins (2001) and also by Economou (2002).

Due to its robustness, versatility and elegance the SAFT model and its different versions have received an impressive acceptance in academia and in industry for phase equilibrium calculations of VLE of hydrocarbons, alcohols, fluorohydrocarbons, LLE for hydrocarbons, alcohols, solvating mixture, fluid phase equilibria of aqueous mixtures, phase equilibria of reservoir fluids, phase behaviour and solubility of polymer and copoymer solutions, supercritical extraction, among others (Muller and Gubbins, 2000). The theory is now finding application to a range of complex fluid problems, including

polymers and their mixtures, surfactants and micellar systems, liquid crystals, liquid immiscible mixtures, water and electrolytes, and fluids in which intramolecular bonding is important.

It is important to notice that in order to obtain an equation that is simple to use, the TPT-1 theory assumes some approximations that can limit the level of accuracy obtained when the theory is applied. The first-order theory gives a good approximation for the configurational properties of linear chains (Muller and Gubbins, 1993), even up to the infinite-length limit. However, TPT-1 does not make a distinction with regard to bond angles within a molecule. This means that the first-order theory implies conformality between branched and linear isomers of the same number of segments. For instance, the theory assumes that a *n*-alkane has the same reduced EoS as a *neo*-alkane (Pàmies, 2003). One can overcome this situation by using the second-order or higher levels of the theory, which accounts for the simultaneous bonding of more then two molecules. However, each level of approximation requires the corresponding structural information for the fluid, which, most of the times is not available (Muller and Gubbins, 1993).

Another important aspect is that for attractive flexible chains, the Wertheim formalism does not take into account the intramolecular attraction, and therefore, the predicted low-density limit is unrealistic (Johnson et al., 1994). No coil-up of the chains is accounted for at low temperatures, and phase diagrams of these fluids are inaccurate; at higher densities, intramolecular effects are effectively counterbalanced by intermolecular interactions, and these considerations are less important. Applications to ring structures also require particular modifications to the theory (Filipe et al., 1997). New approaches to overcome this problem are being proposed as is the case of the PC-SAFT model from Gross and Sadowski (Gross and Sadowski, 2001) who used a hard-chain reference with a Barker-Henderson-type perturbation (Barker and Henderson, 1967a and 1967b) to account for the attraction of these chains (as opposed to adding the perturbation on the segment level).

III.2. Soft-SAFT Model

A SAFT equation based on a reference LJ potential was presented in 1997 by Blas and Vega and it was named soft-SAFT EoS. By the time this thesis started, the soft-SAFT EoS had already been applied to successfully describe the VLE of the pure n-alkanes, n-alkenes, 1-alkanols series and binary and ternary mixtures of alkanes (Blas and Vega, 1998a and 1998b), and the solubility of gases as hydrogen (Florusse et al. 2003) and carbon dioxide in alkanes and alkanols (Pàmies and Vega, in preparation). The good results obtained for the different applications motivated the use of the equation to study the thermodynamic properties of pure perfluoroalkanes and their mixtures with gases and alkanes.

The soft-SAFT EOS is a modification of the original SAFT equation, also based on Wertheim's TPT-1. The main differences between the original SAFT and the soft-SAFT equations are that

(a) the latter uses the LJ potential for the reference fluid, which accounts in a single term for dispersive and repulsive forces, while the original equation uses a perturbation scheme based on a hard-sphere fluid (reference) + dispersion contribution (perturbation term)

(b) the original SAFT uses the radial distribution function (or pair correlation function) of hard spheres in the chain and association terms, while in soft-SAFT both terms depend on the radial distribution function of a LJ fluid of nonbonded spheres

(c) in contrast to the hard-sphere potential, the use of a soft potential allows the association sites to be fully embedded inside the reference core. This allows some overlapping between the segments that contain the two association sites involved in a bond, which is a more realistic situation.

The use of a soft potential as opposed to a hard (repulsive) potential as a reference simplifies the overall perturbation approach, since both the repulsive and dispersive contributions are taken into account simultaneously. The accuracy of the soft-SAFT EoS was tested against Monte Carlo simulations for homonuclear and heteronuclear associating and nonassociating LJ mixtures of chain molecules (Blas and Vega, 1997) giving excellent results. The modified version of SAFT proposed by Ghonasgi and Chapman (1994) and the EoS for LJ chains of Johnson *et al.* (1994) also use a LJ potential and radial distribution

function. Additionally, the LJ-SAFT equation of Kraska and Gubbins (1996) considers dipole-dipole interactions.

In the soft-SAFT model, molecules are represented as united atoms or sites: to each site correspond parameter values to represent a specific atom or group of atoms in the molecule of interest. The site-site interaction potentials are the microscopic molecular analogue of the group contribution engineering models. In contrast to macroscopic models, the molecular structure is well-defined at the micoscopic level. The model attempts to conjugate simplicity, in order to make calculations possible, and enough complexity to quantitatively predict the behaviour of interest. Homonuclear chain molecules are modeled as *m* Lennard-Jones segments of equal diameter σ, and the same dispersive energy ε, bonded tangentially to form a chain. Intermolecular and intramolecular dispersive energies are taken into account through the Lennard-Jones potential

$$\phi = 4\sum_i \sum_j \varepsilon_{ij} \left[\left(\frac{\sigma_{ij}}{r} \right)^{12} - \left(\frac{\sigma_{ij}}{r} \right)^{6} \right] \tag{III.1}$$

This model accounts for three important attributes of chain molecular architecture, that are, the segment connectivity, to represent topological constraints and internal flexibility, the excluded volume effects, and the attraction between different segments. Although the model is simple compared to more realistic models, it conserves the relevant features of the real system. For associating molecules with specific interactions, additional parameters are needed. Following Muller et al. (1994, 1995b), the associating sites are modeled as square-well sites placed at a distance *b* from the center of the Lennard-Jones core. The depth of the energy well is ε_{HB}, and the σ_{HB} is the diameter of the site:

$$\phi^{HB} = \begin{cases} -\varepsilon^{HB} & if\ r_{AB} \le \sigma^{HB} \\ o & otherwise \end{cases} \tag{III.2}$$

where r_{AB} is the square-well site-site distance. Two molecules are considered bonded when r_{AB} is smaller than σ^{HB}.

A schematic representation of the soft-SAFT concept is pictured in Figure III.1 a, b and c.

The equation of state is written in terms of the Helmholtz free energy. The different microscopic contributions that control the macroscopic properties of the fluid are explicitly considered when building the theory. The residual Helmholtz free energy for an n-component mixture of associating chain molecules can be expressed as a sum of three terms: a reference term, A^{ref}, including the repulsive and the attractive energies, a chain

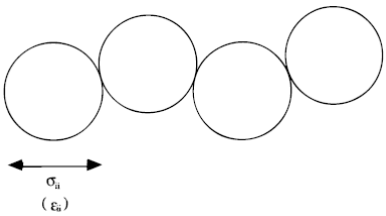

Figure III.1a. Two-dimensional view of a homonuclear nonassociating Lennard-Jones chain with equal segment sizes and dispersive energies (Blas and Vega, 1998a).

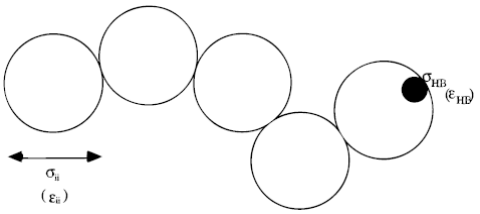

Figure III.1b. Two-dimensional view of the homonuclear associating chain. The large circles represent the Lennard-Jones cores and the small circle is an associating site (Blas and Vega, 1998a)

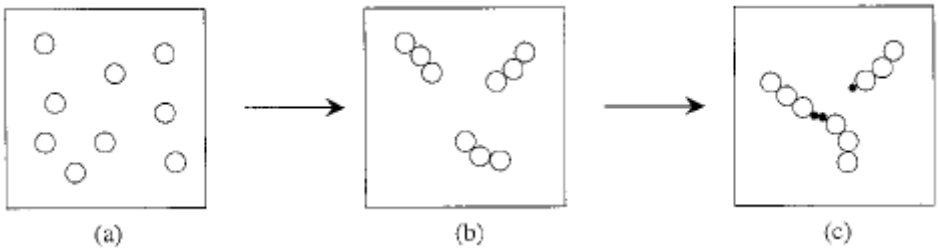

Figure III.1c. Perturbation scheme for the formation of a molecule within the SAFT formalism. (a) An initial system of reference particles is combined to form linear chains (b). To these chain molecules, association sites are added, which allow them to bond among themselves (c), (Muller and Gubbins, 2001)

term, A^{chain}, and a perturbation term, A^{assoc}, which explicitly takes into account the contribution due to the association,

$$A^{res} = A - A^{ideal} = A^{ref}\left(m\rho, T, \sigma, \varepsilon\right) + A^{chain}\left(\rho, T, x_i, \sigma_i, \varepsilon_i, m_i\right) + \\ + A^{assoc}\left(\rho, T, x_i, \sigma_i, \varepsilon_i, \varepsilon^{\alpha_i\beta_j}, k^{\alpha_i\beta_j}\right) + ... \qquad \text{(III.3)}$$

where ρ is the (chain) molecular density, T the absolute temperature, and x_i the composition of species i in the mixture. Molecular parameters are m, the number of spherical segments forming a chain molecule, and the diameter σ and dispersive energy ε

of the segments. The strength of the association bond between site α on specie i and site β on specie j depends on the energy $\varepsilon^{\alpha i \beta j}$ and volume of association $k^{\alpha i \beta j}$. The dots indicate that other terms can be added in a perturbation manner. A brief description of each of the terms follows:

Ideal term

The form of A^{ideal} for the case of a multicomponent system is

$$A^{ideal} = RT\sum_{i=1}^{n}\left(x_i \ln \rho_m{}^{(i)}\Lambda_i{}^3\right) - 1 \tag{III.4}$$

The sum is over all species i of the mixture, $x_i = N_m{}^{(i)}/N_m$ is the molar fraction, $\rho_m{}^{(i)} = N_m{}^{(i)}/V$ the molecular density, $N_m{}^{(i)}$ the number of molecules, Λ_i the thermal de Broglie wavelength, and V the volume of the system. ρ_m, the total number of chains divided by the volume, can be related to the total monomeric density by

$$\rho = \left(\sum_{i=1}^{n} m_i x_i\right)\rho_m = \sum_{i=1}^{n} m_i \rho^{(i)} \tag{III.5}$$

being $\rho^{(i)} = x_i\rho_m$ the monomeric density of species i and m_i its chain length.

Lennard-Jones Reference Term

The reference term accounts for the repulsive and attractive interactions of the segments forming the chains giving the Helmholtz free energy of a mixture of spherical Lennard-Jones. In this work the Lennard-Jones EOS proposed by Johnson et al. (1993), which is a modified Benedict-Webb-Rubin EOS was used to describe the reference fluid.

$$A^{ref} = \varepsilon\left(\sum_{p=1}^{8}\frac{a_p}{p}\left(\rho N_A\sigma^3\right)^p + \sum_{p=1}^{6} b_p G_p\right) \tag{III.6}$$

where N_A is the Advogadro number and parameters a_p, b_p and G_p were fitted to molecular simulation data of the LJ fluid over a broad range of temperatures and densities (Johnson et al., 1993).

Chain Term

Originally Wertheim derived in an analytical way the energetic contribution (and thus the form of the corresponding EoS) that came about from the association of spherical particles. One of the successes of the theory came from the fact that, in the limit of infinitely strong bonding on an infinitely small association site placed at the edge of a given molecule, one can, in fact, account for polymerization of the monomers. The resulting equations are both reasonably simple and accurate.

Multisegmented chain molecules are formed by imposing strong, covalent-like bonds on the equisized segments, each of which has one or two bonding sites. To form a chain of *m* segment diameters in length, a fluid is created made up of m species of LJ spheres. Numbering the species 1, 2, 3,…,*m* it is specified that spheres of type 1 bond only to spheres of type 2, and spheres of type 2 bond only to spheres of type 1 and 3, …, and spheres of type *m* bond only to spheres of type *m*-1. Also it is required that a stoichiometric ratio of spheres is present. As a result, all the spheres will be forced to bond as specified and thus to create a chain.

The Helmholtz free energy due to the formation of chains from m_i spherical monomers is

$$A^{chain} = RT\sum_{i=1}^{n} x_i (1-m_i)\ln g_{LJ}{}^{(ii)}(\sigma_{ii}) \qquad \text{(III.7)}$$

where R is the ideal gas constant. The pair radial distribution function $g_{LJ}^{(ii)}(\sigma_{ii})$ of the reference fluid for the interaction of two segments in a mixture of segments, evaluated at the segment contact σ, provides structural information to the theory at the first-order level. As explained before, this means that the model assumes conformality between branched and linear isomers of the same number of segments and also any information is considered about the attractive chain self-interaction beyond the formation of bonds.

Association Term

Associating fluids are able to form clusters of associated molecules. The fraction of clusters of a given size can be estimated by using general statistical arguments (Flory, 1953).

The Helmholtz energy change due to association is calculated from

$$A^{assoc} = RT\sum_i x_i \left[\sum_\alpha \left(\ln X_i^{\ \alpha} - \frac{X_i^{\ \alpha}}{2} \right) + \frac{M_i}{2} \right] \tag{III.8}$$

where M_i is the number of association sites on each molecule of specie *i*, $\Sigma\alpha$ represents a sum over all associating sites (on molecules of specie *i*) and X_i^{α} is the fraction of nonbonded sites α of molecules *i*, defined as

$$X_i^{\alpha} = \frac{1}{1 + N_A \rho \sum_j x_j \sum_\beta X_j^{\beta} \Delta^{\alpha_i \beta_j}} \tag{III.9}$$

All the non-zero site-site interactions should be defined previously in order to solve the equation. $\Delta^{\alpha_i \beta_j}$ involves an unweighted integral over all the orientations and an integration over all separations of molecules 1 and 2, defined as

$$\Delta^{\alpha_i \beta_j} = \int g_{LJ}^{ij}(12) f^{\alpha_i \beta_j}(12) d(12) \tag{III.10}$$

with $g_{LJ}^{ij}(12)$ the pair distribution function of the reference fluid, $f^{\alpha i \beta j}(12) = \exp(\varepsilon_{AB}^{\ HB}/k_B T) - 1$ is the Mayer function of the association potential, and d(12) denotes an unweighted average over all orientations and an integration over all separations of molecules 1 and 2. The integration of Equation III.10 is not straightforward, since the pair distribution function is not readily available. An assumption is made that, for the purposes of the integration, the reference fluid pair correlation function is equivalent to that of the segment as part of a chain. This is a reasonable approximation if the bonding site is thought to be diametrically opposed to the backbone of the chain (Blas and Vega, 1998a). As mentioned before, further refinement of this approximation requires higher-order theories. The pair distribution function of the Lennard-Jones chain fluid was then replaced by the pair distribution function of the Lennard-Jones segment fluid, evaluated at the same temperature and segment density. In order to accurately calculate the integral, the expression from Muller and Gubbins (1995a) for a particular position of the association site inside the Lennard-Jones sphere has been used. Different association schemes can be assumed including cross-association. For more detail on the equations to use in each case see reference (Pàmies, 2003).

The model is easily extended to mixtures. In fact, only the reference term needs to be extended to mixtures since the chain and association terms depend explicitly on composition and thus they are already applicable to mixtures. Mixtures consist in chains with different number of segments, which in turn can be of different size and/or dispersive energy and because of that, averaged parameters that simulate an "averaged" fluid that has the same thermodynamic properties as the mixture are needed. This is done by means of mixing rules. Several options exist (Economou and Tsonopoulos, 1997) but the van der Waals' one fluid theory is the most used. It is a well-established conformal solution theory that defines parameters of a hypothetical pure fluid having the same residual properties as the mixture of interest. Van der Waals' mixing rules are in good agreement with molecular simulation data for spheres of similar size (Rowlinson and Swinton, 1982). The corresponding expressions for the size and energy parameters of the conformal fluid are:

$$\sigma^3 = \frac{\sum_i \sum_j x_i x_j m_i m_j \sigma_{ij}^3}{\left(\sum_i x_i m_i\right)^2} \tag{III.11}$$

$$\varepsilon\sigma^3 = \frac{\sum_i \sum_j x_i x_j m_i m_j \varepsilon_{ij} \sigma_{ij}^3}{\left(\sum_i x_i m_i\right)^2} \tag{III.12}$$

The expressions III.11 and III.12 involve the mole fraction x_i and the chain length m_i of each of the components of the mixture of chains, denoted by the indices i and j, and the unlike ($j \neq i$) interaction parameters σ_{ij} and ε_{ij}, which are determined by means of combination rules. The Lorentz-Berthelot combining rules are commonly used and were also employed in this work

$$\sigma_{ij} = \eta_{ij} \frac{\sigma_{ii} + \sigma_{ij}}{2} \tag{III.13}$$

$$\varepsilon_{ij} = \xi_{ij} \sqrt{\varepsilon_{ii} \varepsilon_{jj}} \tag{III.14}$$

where the factors η_{ij} and ξ_{ij} modify the arithmetic and geometric averages, respectively, between components *i* and *j*. Both parameters are usually set to one for mixtures of segments of similar size and energy. In this case, Equations III.13 and III.14 reduce to the simple Lorentz-Berthelot rules. Further information about the appropriateness of several combination rules can be found in reference (Diaz et al., 1982).

III.2.1 The Quadrupole Moment

To account for electrostatic contribution for the thermodynamic properties of a given system where at least one of the components has a quadrupole moment, a polar term, A^{polar}, may be included into Equation III.3. The leading multipole term for fluids of linear symmetrical molecules, like carbon dioxide, nitrogen, benzene, etc., is the quadrupole-quadrupole potential (Gubbins and Two, 1978). An expansion of the Helmholtz free energy in terms of the perturbed quadrupole-quadrupole potential with the Padé approximation was proposed by Stell et al. (1974):

$$A^{qq} = A_2^{qq}\left(\frac{1}{1-\frac{A_{3A}^{qq}+A_{3B}^{qq}}{A_2^{qq}}}\right) \tag{III.15}$$

Expressions for A_2 and A_3, the second and third-order perturbation terms, are calculated according to the segment approach presented by Jog et al. (2001) which is a modification of the molecular approach previously derived by Two and Gubbins (Two and Gubbins, 1975; Two, 1976) for an arbitrary intermolecular reference potential. The expressions for A_2 and A_3 were derived in the works of Gubbins and Two (1978) and Jog et al. (2001) and are presented here for completeness:

$$A_2{}^{qq} = -\frac{14\pi N_m \rho}{5k_B T}\sum_i\sum_j x_i x_j m_i m_j x_{p_i} x_{p_j}\frac{Q_i{}^2 Q_j{}^2}{\sigma_{ij}{}^7} I_{2,ij} \tag{III.16}$$

$$A_{3A}{}^{qq} = -\frac{144\pi N_m \rho}{245(k_B T)^2}\sum_i\sum_j x_i x_j m_i m_j x_{pi} x_{pj}\frac{Q_i{}^3 Q_j{}^3}{\sigma_{ij}{}^{12}} I_{2,ij} \tag{III.17}$$

$$A_{3B}{}^{qq} = \frac{32\pi^3}{2{,}025}\left(2{,}002\pi\right)^{1/2}\frac{N\rho^2}{\left(k_BT\right)^2}\sum_i\sum_j\sum_k x_i x_j x_k m_i m_j m_k x_{pi} x_{pj} x_{pk}\frac{Q_i^2 Q_j^2 Q_k^2}{\sigma_{ij}^3\sigma_{ik}^3\sigma_{jk}^3} I_{3,ijk} \qquad \text{(III.18)}$$

The integrals I are calculated using molecular dynamic results for a pure Lennard-Jones fluid, and the resulting values were fitted to simple functions of reduced density and temperature as reported by Gubbins and Two (1978).

As can be observed from Equations III.16 to III.18, when the quadrupole moment is explicitly taken into account, two more parameters have to be considered in the model, the quadrupolar moment Q (C.m^2) and $x_{p,}$ defined as the fraction of segments in the chain that contain the quadrupole as will be discussed latter in session III.4.3.

III.2.2. The Crossover Approach

As any other equation of state, soft-SAFT is unable to correctly describe the scaling of thermodynamic properties as the critical point is approached giving systematically higher predictions near this point. The mean-field equations of state provide a reasonable description of fluid equilibrium properties far away from the critical point. However, near the critical point, due to density and/or concentration fluctuations caused by long-range correlation between molecules, the thermodynamic properties of a fluid show singularities and therefore, classical analytical equations fail. Attempts to deal with this problem include the rescaling of molecular parameters so that the experimental critical point of the pure compound is matched (Blas and Vega, 1998b; McCabe and Jackson, 1999 and Pàmies and Vega, 2002). The simple rescaling of molecular parameters improves predictions of the critical behaviour of several mixtures, but a new set of different molecular parameters for each family of components is required for the near-critical region. This approach can be viewed as a practical one but it does not correctly solve the problem since the fluctuations inherent to the critical region are still ignored in this case.

Renormalization-group methods (RG) have been very successful in describing the properties of systems near their critical point (Wilson, 1971; Wilson and Fischer, 1972). However, for engineering applications, the ideal situation would be a model that could correctly describe, using the same set of parameters and equation, the thermodynamics of the system far and close to the critical point.

There are different approaches in which the long-wavelength density fluctuations can be taken into account in the near-critical region, searching for a global equation for real

fluids (Anisimov and Senger, 2000). A brief overview over the three most developed/used approaches follows:

1. Crossover approach based on a Landau expansion: Based on the universality of critical properties and with the help of renormalization group theory, Chen et al. (1990a and 1990b) developed a phenomenological crossover theory for fluids. Near the critical point, the free energy, written as a Landau expansion, contains two contributions: one comes from the analytic background and the other comes from the singularity due to molecular long-range correlations. Apart from some system-dependent coefficients, the singular part of the free energy is a universal scaling function of the rescaled temperature and the order parameter. Here rescaled temperature means the temperature modified by a crossover function. A typical order parameter is the fluid's number density. The crossover-Landau method successfully represents experimental data for pure fluids (Agayan et al., 2001) but requires many adjustable parameters. With the help of crossover theory, Kiselev (1998) and Kiselev and Ely (1999a) formally separated the Helmholtz free energy, calculated from a classical equation-of-state, into two parts similar to those in the crossover-Landau method; and then applied the crossover functions to the critical part of the free energy. Kiselev's theory takes advantage of a well-developed classical equation-of-state where equilibrium properties far from the critical point are well described, and correctly reproduces the critical scaling behaviour near the critical point, using Chen et al.'s (1990a and 1990b) scaling function. However, because the crossover theory is essentially phenomenological, Kiselev's method also requires many adjustable parameters to fit experimental data.

2. Crossover approach based on a first-principle hierarchical reference theory: the first-principle theory begins by constructing the Hamiltonian in a partition function and does not use any adjustable parameters beyond those required in the two-body potential function (e.g. Lennard–Jones). The first-principle hierarchical reference theory (HRT) of fluids (Parola and Reatto, 1985, 1991 and 1995) uses the RG idea that the long-range correlation is incorporated by integration over partial degrees of freedom. In HRT, a cut-off-dependent free energy is defined and the long-range correlations are gradually *"turned on"* by changing the cut-off wave vector from infinity to zero. Because HRT starts from an exact formal expansion for the free energy, there is no need to fit any parameters. Although

HRT is a promising theory, its mathematical structure is too complex for typical engineering applications.

3. Crossover approach based on a phase-space cell approximation: Based on Wilson's phase-space cell approximation (Wilson, 1971), White and co-workers derived a recursion procedure for pure fluids (White, 1993 and White and Zhang, 1993). White's global RG theory consists of a set of recursion relations where the contribution of longer and longer wavelength density fluctuations up to the correlation length is successively taken into account in the free energy density. In this way, properties approach the asymptotic behaviour in the critical region, and they exhibit a crossover between the classical and the universal scaling behaviour in the near-critical region. Lue and Prausnitz, (1998) extended the accuracy and range of White's equations through an improved Hamiltonian. The theory was applied to square-well fluids and results compared to simulation and experimental results, using the square-well model. The approach was then used by Jiang and Prausnitz (1999 and 2000) to describe the pure *n*-alkanes family and some of their mixtures. Jiang and Prausnitz were the first who applied the theory to chain molecules, modelled as square well chains. An advantage of this method versus Kiselev's is that it is an easy-computing numerical method based on recursive equations, and the two additional parameters can be transferred within the same series. The main disadvantage is its numerical character, versus the analytical nature of Kiselev's method. However, the resolution of the involved recursive equations is very fast in computers available nowadays. Compared to HRT, it has a simpler mathematical structure that can be applied to a classical equation-of-state. Thus, White's theory is useful for engineering application as shown previously (Jiang and Prausnitz, 1999).

Unfortunately, RG theory cannot easily be generalized to mixtures except for a nearly pure system with a trace impurity (Wilson, 1975). Fisher and others have proposed that a theory for critical phenomena of mixtures can be based on the assumption that a universal property of a mixture near its critical point is isomorphic to that of a one-component system, provided that certain appropriately chosen thermodynamic variables are kept constant (Fischer, 1968; Anisimov et al., 1971). Under this assumption, RG theory for a one-component system can be applied directly to mixtures. The results of some RG theories based on the isomorphism approximation are in good agreement with experimental data (Parola and Reatto, 1995; Jin and Sengers, 1993; Hager and Sengers,

2002). However, isomorphism between a one-component system and a mixture requires choosing chemical potentials as independent variables rather than the much more convenient mole fractions. For engineering application, this requirement makes computation difficult because all practical equations of state use mole fractions, not chemical potentials, as independent variables. Nevertheless, as shown by Kiselev and Friend (1999), choosing mole fractions as independent variables provides a good approximation to the original isomorphism assumption, although some scaling behaviour is not correctly represented. This formalism has been recently extended to mixtures by Cai and Prausnitz (2004) and Sun et al. (2005).

The procedure followed in this work is the one based on Wilson's RG theory following the implementation of White's global RG method as done by Prausnitz and co-workers (Lue and Prausnitz, 1998; Jiang and Prausnitz, 1999 and 2000; Cai and Prausnitz, 2000). The interaction potential is divided into a reference contribution, due mainly to the repulsive interactions, and a perturbative contribution, due mainly to the attractive interactions. The RG theory is only applied to the attractive part, since it is considered that the other term contributes mainly with density fluctuations of very short wavelengths. The effect of the density fluctuations due to the attractive part of the potential is then divided into short-wavelength and long-wavelength contributions, with the assumption that contributions from fluctuations of wavelengths less than a certain cut-off length L can be accurately evaluated by a mean-field theory. The effect of short-wavelength contributions can be calculated using the soft-SAFT equation, or any other mean-field theory (Llovell et al., 2004).

The contribution of the long-wavelength density fluctuations is taken into account through the phase-space cell approximation (Wilson, 1971; Wilson and Fischer, 1972). In a recursive manner, the Helmholtz free energy per volume of a system at density ρ can be described as (White, 1999 and 2000)

$$a_n(\rho) = a_{n-1}(\rho) + da_n(\rho) \tag{III.19}$$

$$a_0(\rho) = a^{soft-SAFT}(classical) \tag{III.20}$$

where a is the Helmholtz free energy density and da_n the term where long-wavelength fluctuations are accounted for in the following way:

$$da_n(\rho) = -K_n \ln \frac{\Omega_n{}^s(\rho)}{\Omega_n{}^l(\rho)}, \qquad 0 \le \rho \le \frac{\rho_{\max}}{2} \tag{III.21}$$

$$da_n(\rho) = 0, \qquad \frac{\rho_{\max}}{2} \le \rho \le \rho_{\max} \tag{III.22}$$

where ρ_{max} is the maximum possible molecular density and it depends on the selected model. In this work it was defined as

$$\rho_{\max} = \frac{1}{mN_A\sigma^3} \tag{III.23}$$

When the density is greater than half the maximum density, the long-wavelength fluctuations are not relevant compared to the mean-field value, since the critical region is still far away. Ω^s and Ω^l represent the density fluctuations for the short-range and long-range attraction, respectively, and K_n is a coefficient,

$$K_n = \frac{k_B T}{2^{3n} L^3} \tag{III.24}$$

where T is the temperature and L the cut-off length.

$$\Omega_n^\beta(\rho) = \int_0^\rho \exp\left[\frac{-G_n^\beta(\rho,x)}{K_n}\right] dx \tag{III.25}$$

$$G_n^\beta(\rho,x) = \frac{\bar{a}_n^\beta(\rho+x) + \bar{a}_n^\beta(\rho+x) - 2\bar{a}_n^\beta(\rho)}{2} \tag{III.26}$$

The superindex β refers to both long (l) and short (s) range attraction, respectively, and G^β is a function that depends on the evaluation of the function $\bar{a}$, calculated as

$$\bar{a}_n^l(\rho) = a_{n-1}(\rho) + \alpha(m\rho)^2 \tag{III.27}$$

$$\bar{a}_n^s(\rho) = a_{n-1}(\rho) + \alpha(m\rho)^2 \frac{\phi w^2}{2^{2n+1} L^2} \tag{III.28}$$

where m is the LJ segment parameter, ϕ an adjustable parameter, α is the interaction volume with units of energy volume, and w refers to the range of the attractive potential. For the LJ fluid, α and w are given by

$$\alpha = \frac{16\pi\varepsilon\sigma^3}{9} \tag{III.29}$$

$$w^2 = \frac{9\sigma^2}{7} \tag{III.30}$$

The integral in Equation III.25 is evaluated numerically, by the trapezoid rule. The density step has been set to obtain good accuracy, without compromising the speed of the calculations. A density step ρ/500 gives accurate results for the critical region, but if one is specifically interested in the critical point, ρ/1000 is strongly recommended (Lovell et al., 2004).

To resume, the soft-SAFT is a general equation of state, with a Lennard-Jones system as the reference fluid, applicable to spherical and chain molecules, associating and non-associating molecules, polar and non-polar molecules, pure fluids and mixtures. The model is adapted according to the system to study. Chemical, thermal and mechanical stability are satisfied by imposing the equality of chemical potentials of each component in the coexisting phases at a fixed temperature and pressure. The fugacity method is used to perform the equilibrium calculations. To calculate phase equilibria, the equality of pressure and chemical potential in both phases is required. The total pressure of the system and the chemical potentials of each component in both phases are derived from the Helmoltz free energy. For the solution of the system of nonlinear algebraic equations that arise from the fugacity method, a modification of the Powell's hybrid method (Powell, 1970) is used. When optimizing parameters, because there are more restrictions than unknowns, one has to face a nonlinear optimization problem. It is solved in soft-SAFT by a Levenberg-Marquardt nonlinear least squares algorithm (More, 1977), which is one of the most widely employed nonlinear curve fitting methods.

III.3. Application to Pure Compounds

III.3.1. soft-SAFT without crossover

Values for the molecular parameters of pure compounds are usually adjusted by minimizing deviations from the theory with respect to VLE experimental data. Nevertheless, whenever possible, it is important to use physical information in order to minimize the number of parameters to be optimised. In this way, xenon was, as in other works (Filipe et al., 2000), modelled as a single sphere. In the case of radon, experimental VLE data was difficult to find. Vapor pressure data was available at NIST Chemistry WebBook but only one value for the liquid density at 211 K was found (Herreman, 1980). This value was used as a reference to calculate radon liquid densities for a broader temperature range following the methods described in Poling et al. (2001). For fluorocarbons, experimental studies indicate that C-C bond lengths for crystalline poly(tetrafluoroethylene) and polyethylene are equivalent (Cui et al., 1998) and so, the values of the *m* parameter for *n*-perfluoalkanes were set equal to those optimised for the *n*-alkanes in a previous work (Pàmies and Vega, 2001). Also, the values of σ for perfluoroalkanes are greater than in the corresponding alkanes as would be expected once CF_3 and CF_2 groups are bigger than the corresponding CH_2 and CH_3 for alkanes. In the case of the substituted perfluorooctanes, the *m* parameter was set equal to the saturated perfluoro-n-octane once the size of the molecules should be essentially the same.

The remaining molecular parameters of the nonassociating model for the pure compounds were calculated by fitting vapour pressures and saturated liquid densities to experimental data away from the critical region, and they are listed in Table III.1. They were adjusted using, whenever available, experimental data up to about Tr = T/Tc = 0,8. The references of the experimental vapour pressure and density data used for the optimisation of the parameters are also presented in the table.

Very limited experimental data are available in the literature for the complete vapour pressure curve or saturated liquid density of most of the fluorinated compounds studied here and in some cases there are obvious inconsistencies between the available sources as discussed before in Part II. It is believed that an improvement in the accuracy of the soft-SAFT results could be obtained if reliable data were available for the entire phase diagram as in the case of the alkanes.

Table III.1. Optimised Molecular Parameters for the Pure Components and References from where Experimental Vapour Pressure and Density Data Were Taken.

Compound	m	σ (Å)	ε/k_B (K)	Reference
		Gases		
O_2	1.168	3.198	111.5	NIST Chemistry WebBook
Xe	1.000	3.953	226.6	NIST Chemistry WebBook
Rn	1.460	3.606	233.6	NIST Chemistry WebBook
CO_2	2.681	2.534	153.4	NIST Chemistry WebBook
		Linear saturated perfluoroalkanes		
CF_4	1	4.217	190.1	Smith and Srivastava (1986)
C_2F_6	1.392	4.342	204.5	Smith and Srivastava (1986)
C_3F_8	1.776	4.399	214.7	Smith and Srivastava (1986)
C_4F_{10}	2.134	4.433	223.0	Brown and Mears (1958)
C_5F_{12}	2.497	4.449	230.2	Barber and Cady (1956) Burguer and Cady (1951)
C_6F_{14}	2.832	4.479	236.6	This work; Dunlap et al. (1958); Crowder et al. (1967) and Mousa (1978)
C_7F_{16}	3.169	4.512	242.7	Oliver et al. (1951) ; Steele et al. (1997); Oliver and Grisard (1951); Milton and Oliver (1952)
C_8F_{18}	3.522	4.521	245.1	This work Kreglewski (1962)
C_9F_{20}	3.901	4.526	246.8	This work Piñeiro et al. (2004)
		Cyclic and substituted fluoroalkanes		
$C_{10}F_{18}$	2.696	4.999	310.1	This work
C_7F_{14}	3.463	4.150	228.6	Glew and Reeves (1956) Good et al. (1959)
C_6F_6	3.148	3.647	253.6	This work; Ambrose (1981); Hales and Townsend (1974)
C_7F_8	3.538	3.764	253.0	This work; Ambrose and Ellender (1981); Hales and Townsend (1974)
1Br-C_8F_{17}	3.522	4.652	268.9	This work
1H-C_8F_{17}	3.522	4.492	253.6	This work
1H,8H-C_8F_{16}	3.522	4.456	267.8	This work

From the optimised parameters of the linear perfluoroalkanes from C_1 to C_9, a simple relationship of the molecular parameters with the carbon number, *CN*, was obtained:

$$m = 0.3580 + 0.679\ CN \quad \text{(III.31)}$$

$$m\sigma^3 = 35.49 + 42.38\ CN \quad \text{(III.32)}$$

$$m\varepsilon/k_B = 96.60 + 91.64\ CN \quad \text{(III.33)}$$

Units of σ and ε/k_B are Å and K, respectively. Parameters from these relationships deviate from the fitted parameters with an absolute averaged deviation (AAD) lower than 1%. One of the advantages of molecular theories compared to macroscopic models is that the former need fewer meaningful parameters. To provide additional evidence of this, optimised size and energy parameters are plotted in Figure III.2 with respect the carbon number *CN* for the linear perfluoroalkane chain. Because the model is homonuclear and the effect of the extreme CF_3 groups weakens as the chain length increases, the LJ parameters should tend to an asymptotic value, as seen in Figure III.2. Furthermore, molecular simulation united-atom model (Cui et al., 1998; Hariharan and Harris, 1996) in which the LJ potential for the nonbonded interactions is used (without Coulombic interactions), employ optimised values for the size parameter in the range $\sigma_{CF2} = \sigma_{CF3} = 4.65 \pm 0.05$ Å. These simulations give quantitative predictions for equilibrium properties of chains from *n*-perfluoropentane to *n*-perfluorohexadecane. The corresponding value from our model (equivalent to a chain of infinite number of carbons), straightforwardly calculated from Equations III.31-III.33, is 4.63 Å. The similarity among the parameters of different theories acts in favour of the physical meaning of them.

Figures III.3-III.7 present equilibrium liquid densities and vapour pressures for the gases, linear perfluoroalkanes and cyclic and substituted fluoroalkanes under study. Results obtained with the soft-SAFT EoS were compared with the ones given by the original form of the Peng-Robinson EoS (Peng and Robinson, 1976). Full lines represent the soft-SAFT correlation using the parameters given in Table III.1 while dashed lines represent the results given by the Peng-Robinson EoS. Since no critical data were found for perfluorodecalin nor substituted fluoroalkanes, only the correlation from the soft-SAFT EoS is presented in these cases.

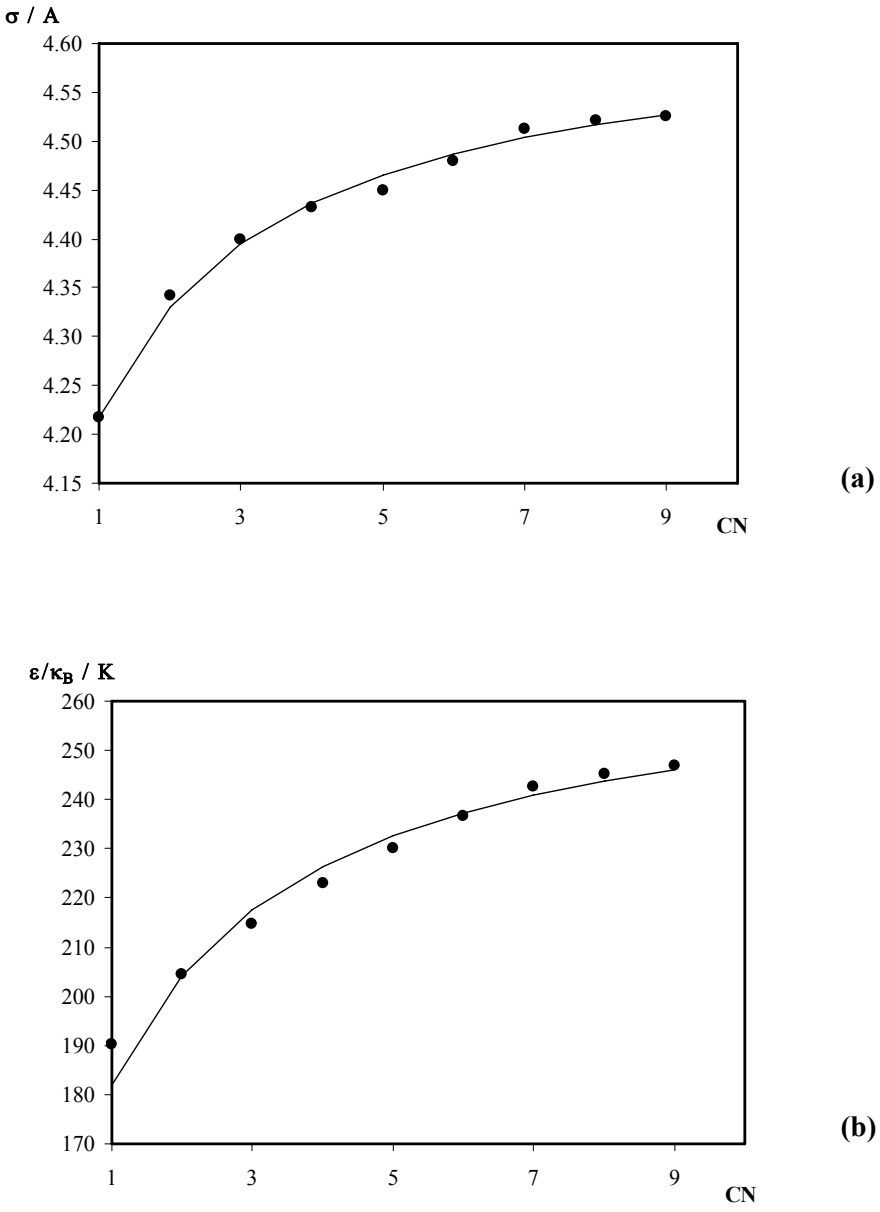

Figure III.2. Molecular parameters for linear perfluoroalkanes: (a) segment diameter; (b) dispersive energy. Lines correspond to the values from the relationships of Equations III.31-III.33.

Table III.2 compares for the same temperature range the absolute average deviation (AAD) obtained when soft-SAFT and the Peng-Robinson equations of state are used to correlate experimental density and vapour pressure data for highly fluorinated compounds and also for the gases under study. Generally it can be said that soft-SAFT correlates experimental vapor pressure and density data better than the Peng-Robinson EoS for all the compounds studied (gases and liquids) except for the lower molecular weight perfluoroalkanes where soft-SAFT gives higher deviations in vapor pressure.

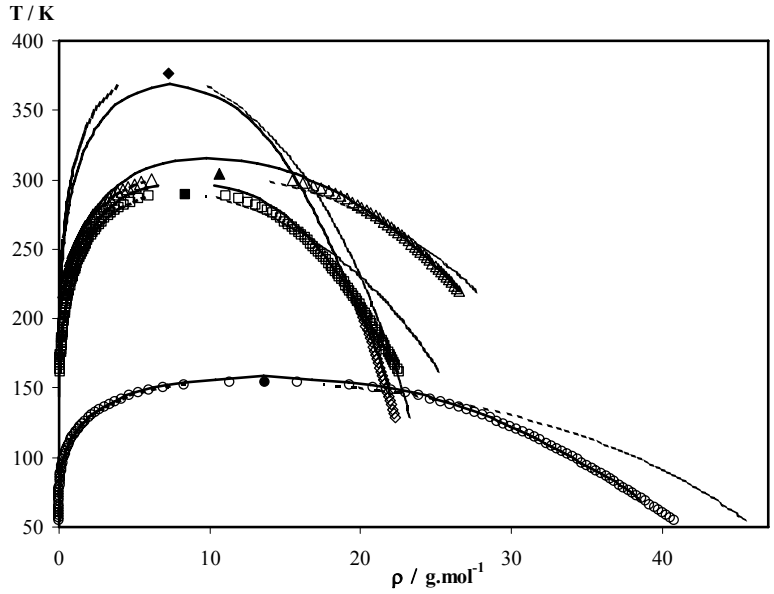

Figure III.3. Coexisting densities of pure oxygen (○), xenon (□), carbon dioxide (Δ) and radon (◊). Filled symbols represent the critical point. Symbols are experimental data from the NIST chemistry Webbook, lines correspond to the soft-SAFT model with optimised parameters and dashed lines to the Peng-Robinson EoS.

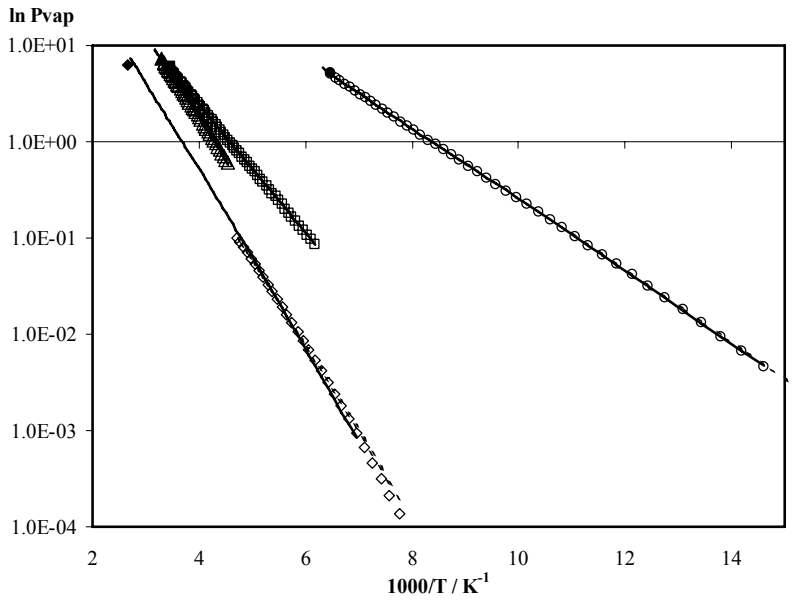

Figure III.4. Vapor pressures of pure oxygen (○), xenon (□), carbon dioxide (Δ) and radon (◊). Legend as in III.3.

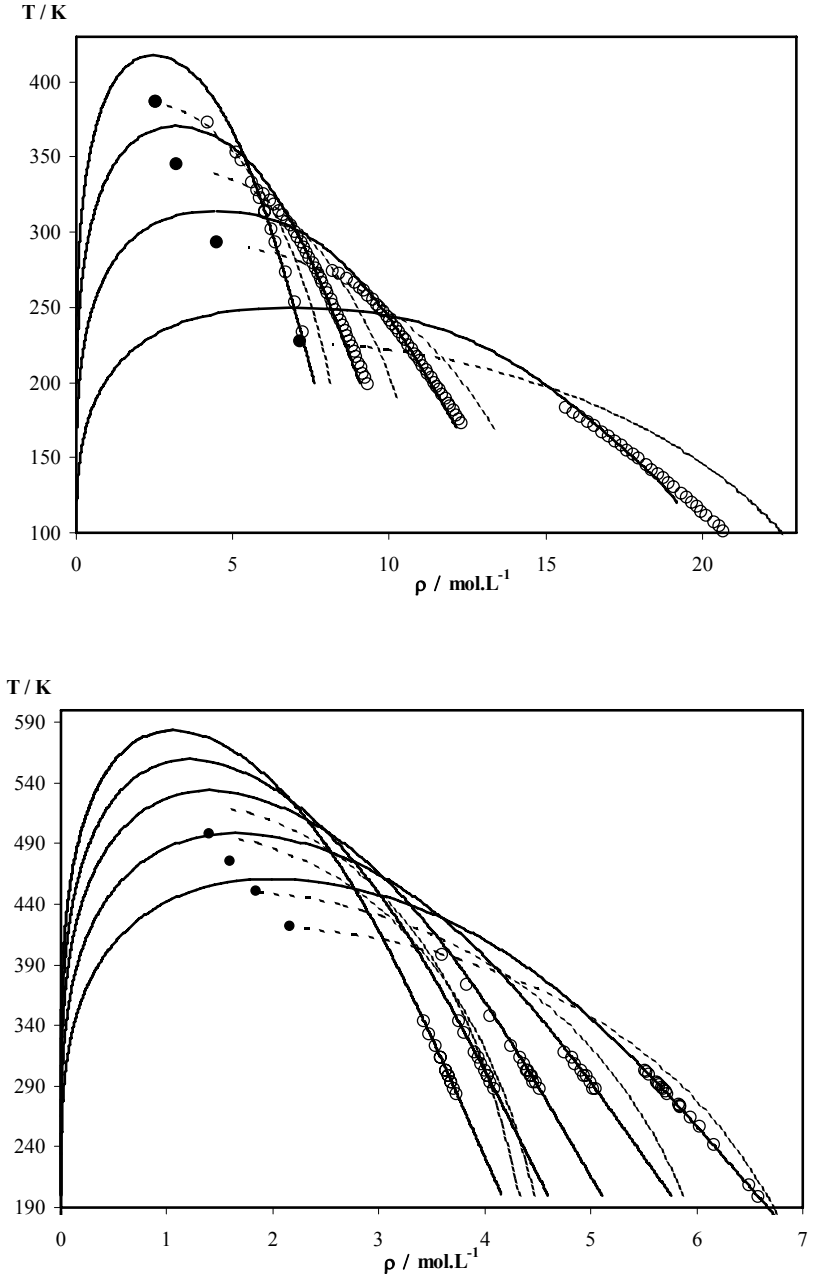

Figure III.5. Liquid densities of linear perfluoroalkanes from C_1 to C_4 (a) and C_5 to C_9 (b). Symbols represent experimental data referred in Table III.1. Legend as in Figure III.1.

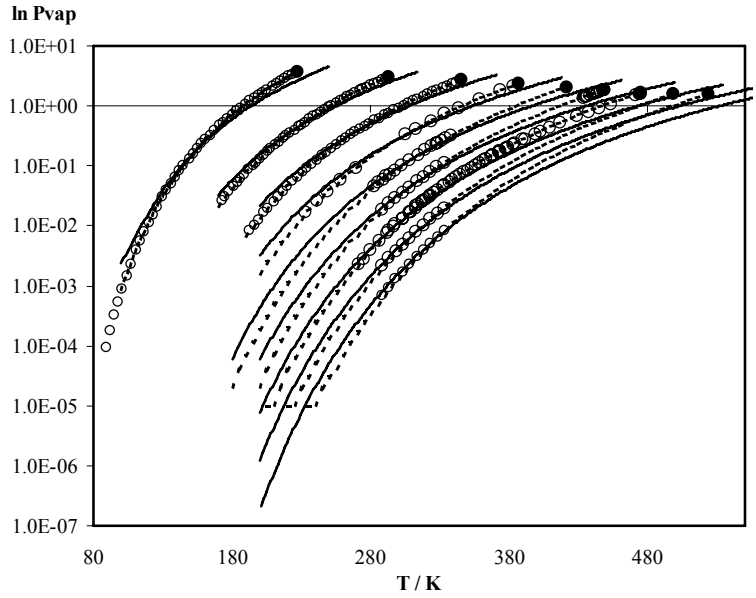

Figure III.6. Vapor pressures of linear perfluoro-n-alkanes from C_1 to C_9. Legend as in Figure III.5.

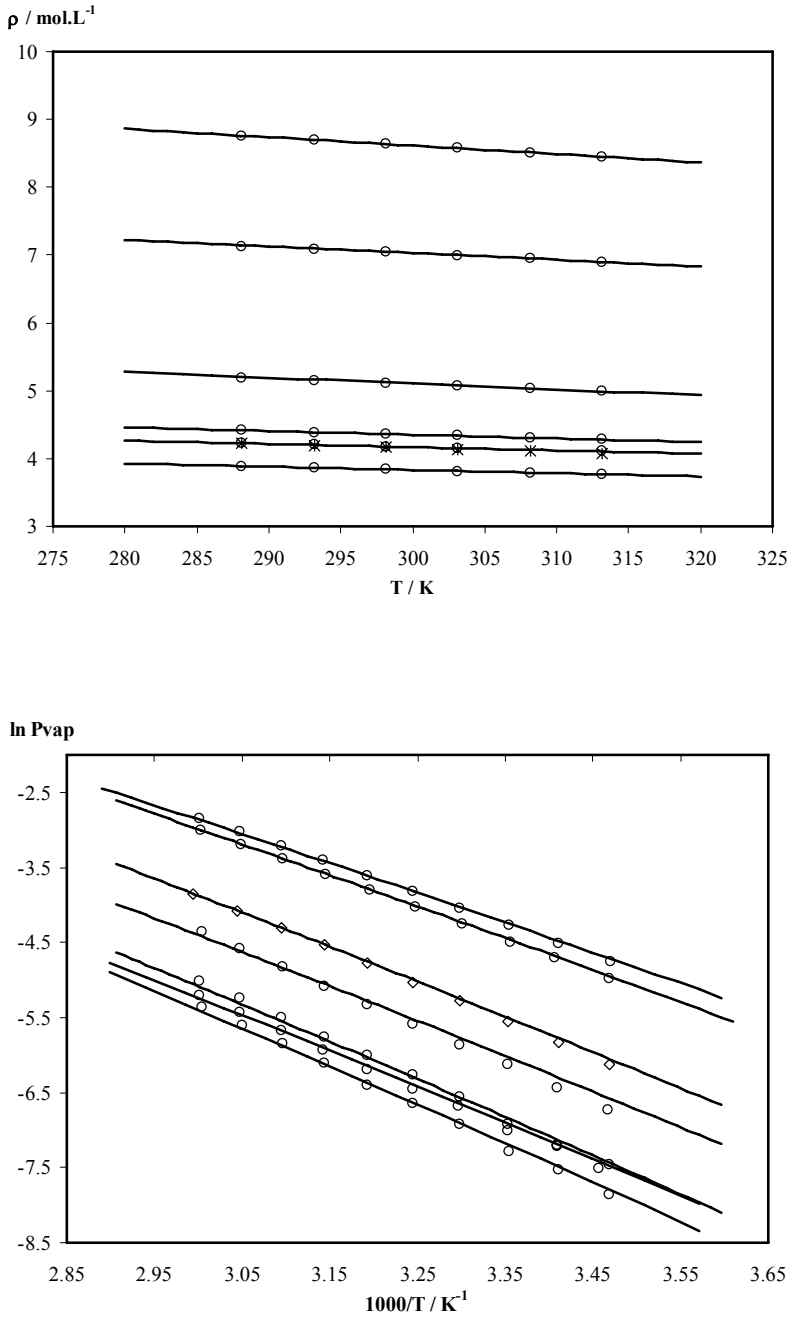

Figure III.7. Liquid densities (a) and vapor pressures (b) of substituted, cyclic and aromatic fluoroalkanes. Legend as in Figure III.5.

Table III.2. Absolute Average Deviation obtained for the Correlation of Vapour Pressure and Density Data of Gases and Highly Fluorinated Compounds with the soft-SAFT and the Peng-Robinson EoS

Compound	% AAD				T range
	Liquid Density		Vapor Pressure		
	PR	SAFT	PR	SAFT	
O_2	10.13	0.35	1.50	0.95	68 - 142
Xe	7.86	0.64	0.93	0.79	162 - 270
Rn	4.67	0.47	2.95	8.52	144 - 210
CO_2	2.97	0.25	0.46	0.44	220 - 290
CF_4	9.50	1.06	1.32	14.31	120 - 185
C_2F_6	6.11	0.89	0.31	14.99	170 - 260
C_3F_8	7.81	1.39	1.68	18.59	200 - 305
C_4F_{10}	6.13	0.77	2.05	14.41	230 - 330
C_5F_{12}	3.11	0.15	5.56	5.72	280 - 340
C_6F_{14}	5.45	0.23	6.20	6.75	280 - 340
C_7F_{16}	3.66	0.25	2.41	5.19	280 - 340
C_8F_{18}	2.57	0.09	4.41	3.66	280 - 340
C_9F_{20}	10.71	0.09	11.68	7.60	285 - 345
$C_{10}F_{18}$	--	0.05	--	3.80	288 - 313
C_7F_{14}	5.35	0.16	14.15	1.73	Pvap: 290 - 335 ρ: 290 - 315
C_6F_6	3.26	0.19	1.23	3.61	290 - 460
C_7F_8	5.53	0.52	2.46	3.11	Pvap: 290 - 400 ρ: 290 - 500
1Br-C_8F_{17}	--	0.01	--	4.0	288 - 313
1H-C_8F_{17}	--	0.04	--	5.0	288 - 313
1H,8H-C_8F_{16}	--	0.03	--	5.0	288 - 313

III.3.2. soft-SAFT with crossover

The inclusion of the crossover treatment requires the adjust of two additional parameters, the cut-off length *L,* related to the maximum wavelength fluctuations that are accounted for in the uncorrected free energy, and ϕ the average gradient of the wavelength function (White 1999 and 2000). In this work the procedure used by Llovell et al. (2004) to apply the soft-SAFT crossover to linear alkanes was followed which implies to treat both *L* and ϕ as adjustable parameters. The authors tested the accuracy of the soft-SAFT crossover equation by comparison with molecular simulations of LJ chains and did several studies about the influence of both values ϕ and *L* in predicting the phase envelope when compared to simulation data. The model was then applied to experimental systems of chainlike molecules, the *n*-alkane series, providing a set of transferable parameters equally accurate far from and close to the critical region.

As before, *n*-perfluoroalkanes are described as homonuclear chainlike molecules, modeled as *m* Lennard-Jones segments of equal diameter σ, and the same dispersive energy ε, bonded tangentially to form the chain. According to the crossover model, these three molecular parameters plus the crossover parameters ϕ and *L*, are enough to describe all thermodynamic properties. To minimize the number of adjusted parameters, the parameter *L* was fixed equal to the one previously adjusted for the n-alkane series (Llovell et al., 2004). A new set of parameters, able to describe simultaneously the vapor-liquid equilibria diagram away and close to the critical region, in contrast to previous correlations accurate for only far from the critical point, was obtained. The correlation comes from optimised parameters for the eight first members of the alkanes series, obtained by fitting experimental saturated liquid densities and vapor pressures, as done before when the model without crossover was applied. The new proposed correlations are given by

$$m = 0.689 + 0.352\ \mathrm{CN} \tag{III.31}$$

$$m\sigma^3 = 43.05 + 34.65\ \mathrm{CN} \tag{III.32}$$

$$m\varepsilon/k_B = 98.29 + 92.55\ \mathrm{CN} \tag{III.33}$$

$$m\phi = 1.08 + 3.33\ \mathrm{CN} \tag{III.34}$$

$$mL = 0.11 + 0.12\ \mathrm{CN} \tag{III.35}$$

The correlation coefficients for each of the linear relations is higher than 0.995 in all cases. In the case of the n-alkanes series, Llovell et al. (2004) obtained good results using a fixed *m* equal to the one adjusted with the original soft-SAFT model. However, in the case of the n-perfluoroalkane series the *m* parameter was also slightly modified together with σ and ε. The experimental critical temperature, pressure and density and those predicted from the original soft-SAFT and soft-SAFT with crossover for the first eight members of the *n*-alkanes series are presented in Table III.3. Experimental data was taken from the works of (Smith and Srivastava, 1986) and Vandana et al. (1994). While soft-SAFT overestimates the critical temperature and pressure, as expected, soft-SAFT with crossover is able to predict both critical properties with high accuracy. However, as already observed by other authors using a similar approach, the critical density is slightly overestimated.

Table III.3. Critical Constants for Linear (C_1-C_9) and Aromatic Perfluoroalkanes. Comparison Between Experimental Data and Predictions Given by the soft-SAFT EoS With and Without Crossover.

Compound	Tc (K)			Pc (MPa)			Dc (mol/L)		
	Exp	soft SAFT	soft SAFT + CV	Exp	soft SAFT	soft SAFT + CV	Exp	soft SAFT	soft SAFT + CV
CF_4	227.6	249.60	227.70	3.74	4.55	3.70	7.17	6.86	8.76
C_2F_6	293.0	314.00	292.85	3.04	3.72	3.01	4.49	4.44	5.61
C_3F_8	345.1	370.11	345.17	2.67	3.26	2.60	3.34	3.18	4.04
C_4F_{10}	386.5	417.51	386.37	2.31	2.93	2.21	2.65	2.46	3.09
C_5F_{12}	421.4	460.67	421.93	2.04	2.67	1.96	2.16	1.99	2.5
C_6F_{14}	450.6	498.43	448.78	1.88	2.43	1.81	1.84	1.65	2.2
C_7F_{16}	475.3	533.27	474.79	1.62	2.23	1.53	1.60	1.40	1.88
C_8F_{18}	498.2	559.70	498.40	1.55	2.05	1.37	1.39	1.21	0.97
C_9F_{20}*	524.0	583.31	517.52	1.56	1.88	1.27	--	1.06	1.47
C_6F_6	516.7	555.84	516.22	3.23	4.44	3.03	2.98	2.67	3.36
C_7F_8	534.5	578.67	534.60	2.71	3.64	2.60	2.34	2.08	2.70

* Critical values extrapolated from the correlations obtained for the linear perfluoroalkane series from C_1 to C_8.

Using the correlations from III.31 to III.35, the parameters for perfluoro-n-nonane were calculated and the critical properties for this compound were estimated and are also given in Table III.3. Agreement between experimental and predicted values is fairly good especially knowing that, as stated by Vandana et al. (1994), the experimental critical properties for perfluoro-n-nonane might be slightly over predicted.

Figure III.8 shows the coexistence curve for the eight first members of the *n*-perfluoroalkane series comparing experimental data and soft-SAFT predictions when the crossover treatment is included. Agreement is excellent in all cases, correcting the behaviour in the critical region due to the incorporation of density fluctuations into the equation. Figure III.9 shows vapor pressures for the same members of the series. Again, excellent agreement is obtained in all cases.

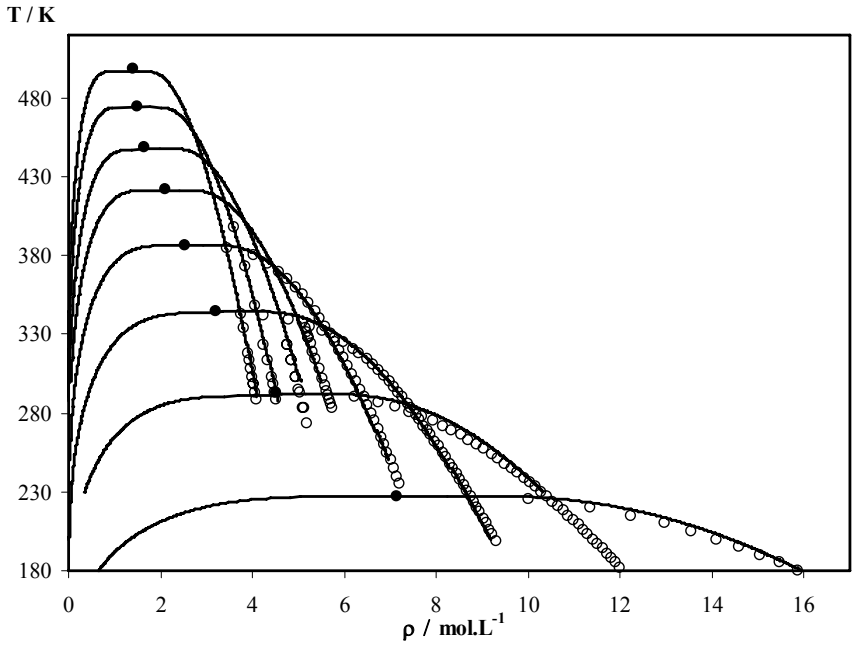

Figure III.8. Temperature-density diagram for the light members of the *n*-perfluoroalkane series, from C_1 to C_8. Symbols represent the experimental data and solid lines the results obtained with the soft-SAFT with crossover.

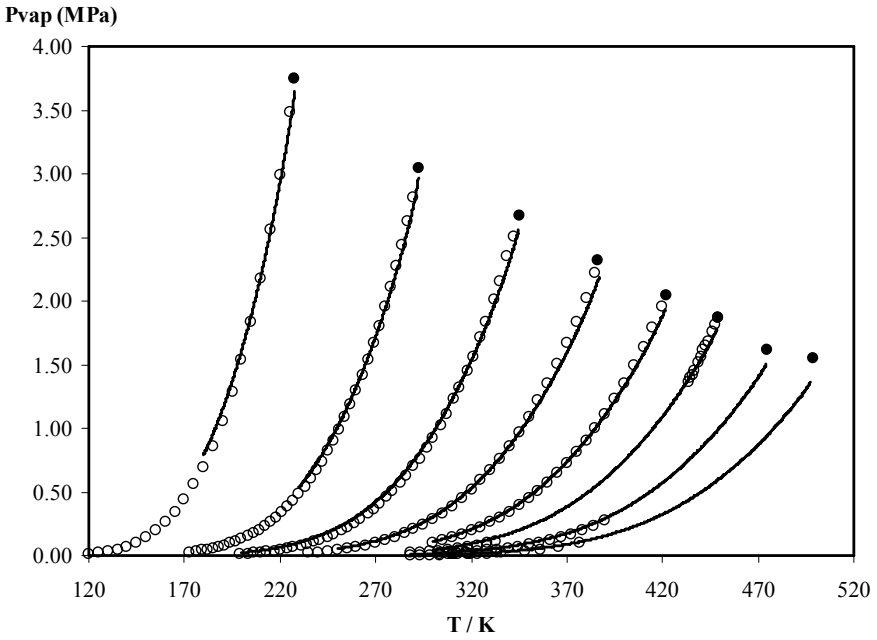

Figure III.9. Temperature-Vapor pressure diagram for the light members of the *n*-perfluoroalkane series, from C_1 to C_8. Symbols represent the experimental data and solid lines the results obtained with the soft-SAFT with crossover.

III.4. Application to Mixtures

III.4.1. Solubility of Oxygen in Perfluoroalkanes at Atmospheric Pressure

Attempts to estimate the solubility of oxygen in fluorinated compounds can be found in the literature, as is the case of the group aditivity method developed by Lawson et al. (1978) and the Regular Solution Theory (Gjaldbaek, 1952 and Hildebrand et al., 1970). Those methods provide estimates of the solubility typically to within 10 per cent but were applied only at one temperature (298.15 K). Until now, the inexistence of experimental data over a sufficiently large temperature range to observe tendencies slowed the test and development of models to describe these systems. More recently, molecular simulation using all-atom force fields was applied to describe the solubility of oxygen in fluorinated systems. Among others the solubility of oxygen in perfluoro-n-hexane and 1Br-perfluoro-n-octane was studied (Dias et al., 2003 and Deschamps et al., 2004). However, this study was focused on the comparison between the solubility of oxygen in different solvents (fluorinated and non-fluorinated) to help to elucidate and confirm theories related with the solubilization process and test if molecular simulation would be a reliable method to predict those differences. Discrepancies around 20% were obtained between simulated and experimental data because the authors used Lorentz-Berthelot combining rules without any adjusted binary parameter. Although they state that the inclusion of those binary interaction parameters could improve the results, the fact is that, to date, no effort was dedicated to the study of the temperature dependence of the solubility of oxygen in fluorinated systems.

In this work, the first attempts tried in order to correctly describe the solubility of oxygen in linear saturated perfluoroalkanes over the temperature range studied were done using the PR-EoS and the Regular Solution Theory:

1. The Peng-Robinson EoS

The original PR-EoS (Peng and Robinson, 1976) given by Equation III.36 was used:

$$P = \frac{RT}{V-b} - \frac{a(T)}{V(V+b)+b(V-b)} \qquad \text{(III.36)}$$

The mixture parameters *a* and *b* are calculated from the parameters of the pure components a_{ii} and b_{ii} using the one fluid van der Waals mixing rules

$$a = \sum_i \sum_j z_i z_j a_{ij} \tag{III.37}$$

$$b = \sum_i z_i b_i \tag{III.38}$$

where z_i is the phase mole fraction of component *i*. The combining rule used for *a* is

$$a_{ij} = \left(1 - k_{ij}\right)\left(a_{ii} a_{jj}\right)^{1/2} \tag{III.39}$$

The k_{ij} is an adjustable parameter for each binary mixture. The k_{ij}´s fitted to the experimental solubility data obtained in this work for O_2/*n*-perfluoroalkanes, show strong temperature dependence mainly for perfluoro-n-hexane and perfluoro-n-heptane where a quadratic equation of the type

$$k_{ij} = A + \frac{B}{T} + \frac{C}{T^2} \tag{III.40}$$

had to be used in order to correctly describe the experimental data (Coutinho et al., 1994).The coefficients A, B and C for the systems studied in this work are given in Table III.4.

Table III.4. Coefficients for Equation III.40 and Average Binary Interaction Parameters, for all the Temperatures. AAD is the Corresponding Average Absolute Errors for Binary Oxygen-Perfluoroalkane Mixtures When an Averaged $\overline{k_{ij}}$ is Used

System	A	B	C	$\overline{k_{ij}}$	AAD %
$O_2 - C_6F_{14}$	3.66×10^1	-2.08×10^4	2.94×10^6	0.122	12.35
$O_2 - C_7F_{16}$	2.20×10^1	-1.26×10^4	1.80×10^6	0.091	10.07
$O_2 - C_8F_{18}$	0.658	-196.42	--	0.004	2.64
$O_2 - C_9F_{20}$	0.481	-165.10	--	-0.073	2.95

Figure III.10 compares experimental results with the predictions given by the PR-EOS using the average binary interaction parameter k_{ij} given in Table III.4. It can be observed that a temperature independent k_{ij} cannot describe the oxygen solubility in perfluoroalkanes. The average absolute deviation given in Table III.4 decreases from the O_2-C_6F_{14} to the O_2-C_9F_{20} systems because the temperature dependence of the solubility decreases along the perfluorocarbon series. The Peng-Robinson EoS, with one adjusted interaction binary parameter, has limited predictive capability providing only a qualitative description of the temperature dependence of the oxygen solubility in linear saturated perfluoroalkanes.

2. Regular Solution Theory

According to the definition of Hildebrand and Scott (1970) a regular solution is one involving no entropy and no volume change when a small amount of one of its components is transferred to it. Considering this assumption, the following equation can be deduced in order to describe the solubility of a non-polar gas in a non-polar solvent:

$$-\log x_2 = -\log x^i{}_2 + \frac{0.4343\overline{V}_2}{RT}\left(\delta_1 - \delta_2\right)^2 \qquad \text{(III.41)}$$

where x_2 is the mole fraction gas solubility, $x^i{}_2$ is the ideal gas solubility, $\overline{V}_2$ is the partial molar volume of the gas in the solution and δ_1 and δ_2 are the solubility parameters for the solvent and the solute, respectively.

When the entropic contribution is significant, the Regular Solution Theory alone cannot describe correctly the solubility of a solute in a solvent. The entropic contribution can be accounted for, if the Flory-Huggins combinatorial term is introduced:

$$-\log x_2 = -\log x^i{}_2 + \log\frac{\overline{V}_2}{V_1} + 0.4343\left(1 - \frac{\overline{V}_2}{V_1}\right) + \frac{0.4343\overline{V}_2}{RT}\left(\delta_1 - \delta_2\right)^2 \qquad \text{(III.42)}$$

where V_1 is the molar volume of the solvent.

Equation III.42 requires three parameters for the solute ($x^i{}_2, \overline{V}_2, \delta_2$) and two parameters for the solvent (V_1 and δ_1). All these parameters are temperature dependent, but

the assumptions made by the Regular Solution Theory imply that the term $\overline{V}_2(\delta_1 - \delta_2)$ must be temperature independent (Prausnitz and Shair, 1961). Accordingly, any convenient temperature may be used to specify $\overline{V}_2$ and δ_2, if the same temperature is used for δ_1 and V_1. In this work, the chosen temperature was 298 K. The ideal gas solubility however, must be treated as a function of temperature. The ideal gas solubility is calculated from:

$$-\log x^{i}_{2} = \frac{\Delta H_2^{vap}}{4.575}\left(\frac{1}{Tb} - \frac{1}{T}\right) \qquad \text{(III.43)}$$

as suggested by Gjaldbaek (1952) where ΔH_2^{vap} is the solute's enthalpy of vaporization at its boiling point T_b.

The partial molar volume of the gas, $\overline{V}_2$, and the solubility parameter of the solute, δ_2, were obtained from Prauznitz and Shair (Prausnitz and Shair, 1961) and are equal to 33.0 $cm^3.mol^{-1}$ and 16.7 $(J.cm^{-3})^{1/2}$ respectively.

The ideal gas solubility is calculated from Equation III.43 using oxygen's enthalpy of vaporization, ΔH_2^{vap}, equal to 6785.1 $J.mol^{-1}$ at its boiling point Tb, 90.188 K (DIPPR, 1998). The solvent's parameters are the molar volume, V_1^0 and the solubility parameter of the solvent, δ_1 taken from this work at 298 K (see Part II).

A comparison between the experimental data and the predictions obtained by the Regular Solution Theory is presented in Figure III.10. Again, the proposed model cannot correctly describe the temperature dependence of the solubility data.

It was expected that a more fundamental equation as the soft-SAFT EoS could be able to capture the correct temperature dependence of the experimental results. Having the molecular parameters for the pure oxygen and perfluoroalkanes, the soft-SAFT model was applied to correlate the experimental solubility data measured. Both solute and solvents were modelled as non-associating species and no association was considered between solute and solvent. The results however showed that, as obtained before with the Peng-Robinson EoS and the Regular Solution Theory for linear perfluoroalkanes, the soft-SAFT model predicts much weaker temperature dependence regardless of the values of the binary interaction parameters used (Figure III.11a). On the other hand, in the case of perfluorodecalin for which the solubility of oxygen is almost temperature independent, the model correctly describes the experimental data measured (Figure III.11b).

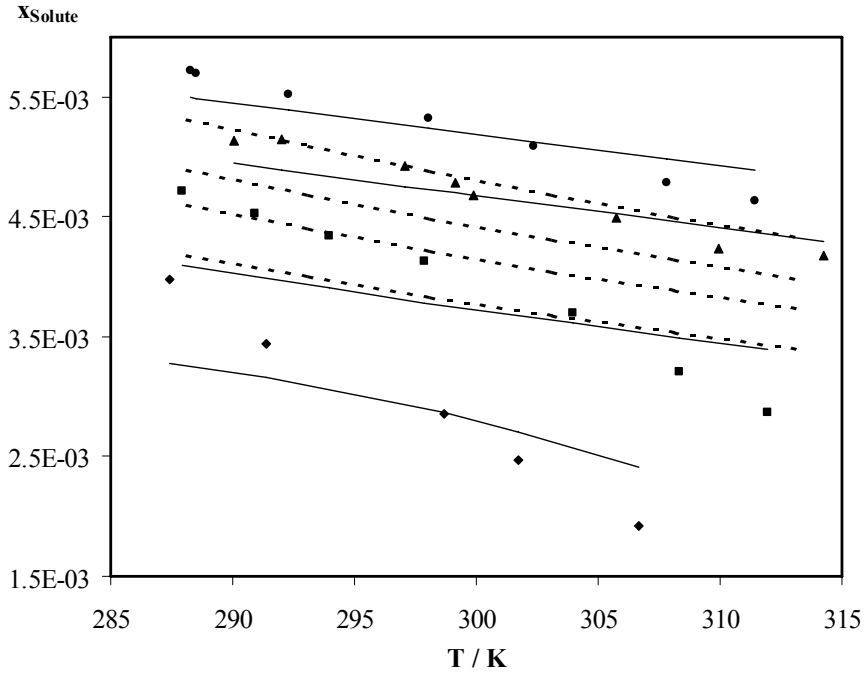

Figure III.10. Correlation of oxygen solubility data in linear perfluoroalkanes. Symbols represent experimental data: (♦) perfluoro-n-hexane, (■) perfluoro-n-heptane, (▲) perfluoro-n-octane and (●) perfluoro-n-nonane. Lines represent correlation with Peng-Robinson EoS using a medium k_{ij} (full lines) and Regular Solution Theory (dashed lines)

These results indicate that additional interactions may exist in this mixture, which are not being considered by the previous models. It was already discussed in Part II that, according to the experimental data measured for the solubility of oxygen in linear fluorinated molecules presenting different degrees of substitution on the terminal CF_3 groups, the solvation of oxygen seems to be carried out by the end groups of the perfluorocarbons and the existence of strong interactions between the oxygen and the CF_3 group on the fluorinated molecules. A literature research on the subject revealed that *ab initio* calculations of the interaction potentials for the complex CF_4-O_2 provided evidence for an interaction between the oxygen and the positive carbon nucleus in CF_4, with the formation of a very strong complex (Mack and Oberhammer, 1987). Unfortunately no further work was done for other higher fluorinated molecules to conclude if this favourable interaction could also exist between the oxygen molecule and the terminals CF_3 groups. Also, through ^{19}F NMR techniques it was demonstrated that the terminal trifluoromethyl groups have the greatest sensitivity to oxygen when compared with the CF_2 groups of molecules as 1Br-perfluoro-n-octane, perfluorotripropylamine and perfluorotributylamine (Shukla et al., 1995). It was then proposed to add the free energy of cross-association

between oxygen and perfluoroalkane molecules to the total energy of the system to test the existence of the preferential interaction between oxygen and the terminal CF_3 groups.

One of the main advantages of using an equation as the SAFT EoS is that one can taylor the equation to the system under study by introducing or removing terms to the original equation. To model the interaction between solute and solvent, both molecular oxygen and perfluoroalkanes were modelled as associating molecules with two association sites on each. In the case of oxygen, sites represent the two lone pairs of electrons and, in the case of perfluoroalkanes, the two ends of the molecule where the carbon atoms are more exposed (less screened by the fluorine atoms). The magnitude of the site-site interaction between oxygen and perfluoroalkane molecules in the SAFT model depends on the two cross-association parameters, ε/κ_B = 2000 K and k = 8000 Å^3, which were set constant for all mixtures.

In the case of the substituted perfluoroalkanes, 1Br-perfluoro-n-octane and 1H-perfluoro-n-octane were modelled considering that they have only one association site corresponding to the saturated CF_3 group while 1H,8H-perfluoro-n-octane was modelled considering that it does not have any association site. The same energy and volume parameters were used to describe the association site when it exists. Binary size, η, and energy, ξ interaction parameters fitted to experimental data for each mixture, are listed in Table III.5.

Figure III.11 shows the results obtained for the different systems studied when this model is considered. Figure *a* compares the results obtained from the soft-SAFT model with and without cross-association for the linear perfluoroalkanes series. Figure *b* presents the results obtained for the different substituted systems assuming the existence or not of preferential interactions between the oxygen and the CF_3 groups on the solvent´s molecules. In both cases agreement with experimental data is very good and the proposed model can correctly describe the different temperature dependences presented by the different systems.

Table III.5. Adjusted Binary Parameters for the Solubility of Oxygen in Fluorinated Compounds and AADs of the Calculations by the Soft-SAFT EOS with Respect to Experimental Data

Solvent	η	ξ	Nº of association sites	AAD (%)
C_6F_{14}	1.12	0.32	2	4
C_7F_{16}	1.38	0.83	2	3
C_8F_{18}	1.85	1.16	2	2
C_9F_{20}	1.92	1.20	2	2
$C_{10}F_{18}$	1.17	1.02	0	1
1Br-C_8F_{17}	1.56	1.21	1	1
1H-C_8F_{17}	1.56	1.17	1	1
1H,8H-C_8F_{16}	1.26	1.11	0	1

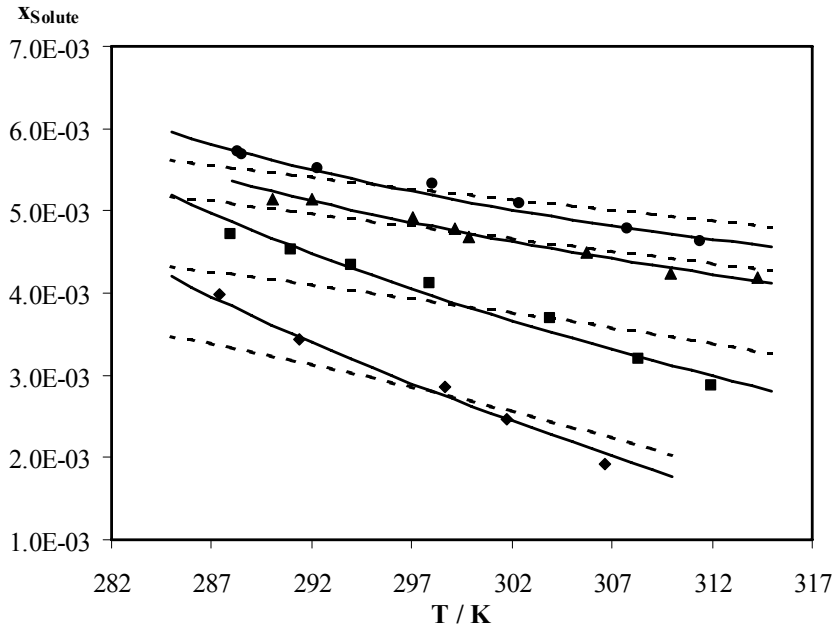

Figure III.11a. Correlation of oxygen solubility data in linear perfluoroalkanes at the solute's partial pressure. Symbols represent experimental data: (♦) perfluoro-n-hexane, (■) perfluoro-n-heptane, (▲) perfluoro-n-octane and (●) perfluoro-n-nonane. Full and dashed lines represent the correlation using the soft-SAFT EoS with and without cross-association, respectively.

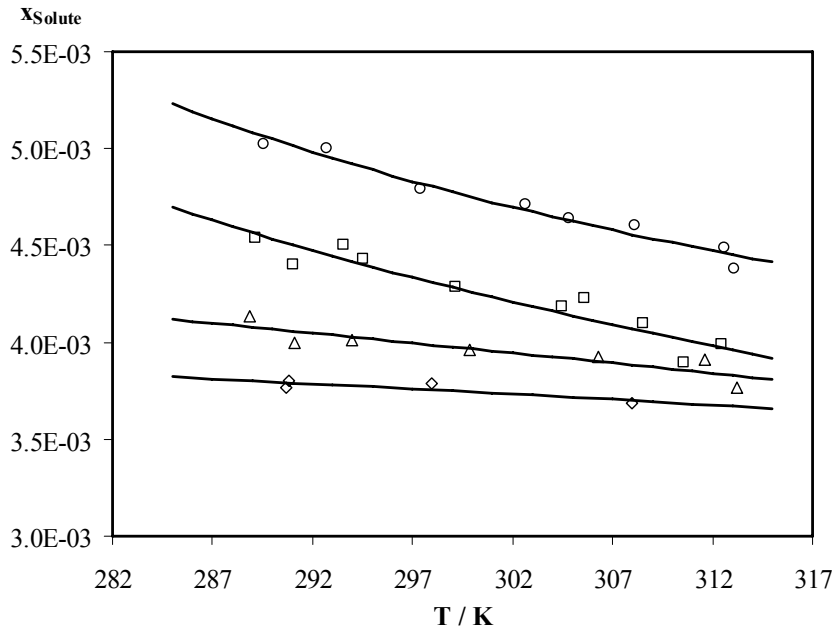

Figure III.11b. Correlation of oxygen solubility data in substituted fluoroalkanes and perfluorodecalin. Symbols represent experimental data: (○) 1Br-perfluoro-n-octane, (□) 1H-perfluoro-n-octane, (Δ) perfluorodecalin and (◊) 1H,8H-perfluoro-n-octane. Full lines represent the correlation using the soft-SAFT EoS with and without cross-association depending on the number of CF_3 groups present in the molecule.

III.4.2. Solubility of Rare Gases in Perfluoroalkanes at Atmospheric Pressure

It was shown that to correctly describe experimental data relating the solubility of oxygen in perfluoroalkanes, a special interaction between the oxygen molecule and the fluorinated molecules had to be considered in some cases. It would be interesting to test the model for the same solvents but with a solute where no interaction could be possible, as is the case of rare gases, in order to confirm that the inaccuracy of the soft-SAFT model without cross-association in describing some O_2/perfluoroalkanes systems is due to an abnormal behaviour of these mixtures instead of a failure of the model.

Data for the solubility of xenon and radon in perfluoroalkanes were measured by Kennan and Pollack (1988) and Lewis et al. (1987), respectively. In the case of the solubility of xenon, besides the practical applications that xenon's solubility can find in nuclear medicine and for studies of general anesthesia and nuclear reactor safety, the authors also wanted to study the solubility of an inert solute in perfluoroalkanes to compare with previous results they obtained for the solubility in the corresponding alkanes and take conclusions about the solubilization process in both cases. In the case of radon, the authors where looking for a good solvent to help in the removal of radon from the ventilation streams in uranium mines to meet radiation exposure limits. They suggested that conventional packed bed scrubbers could be used if an appropriate nonaqueous solvent could be identified. The characteristics of such a solvent include high radon solubility, low vapor pressure at operating temperature, nonflammable and non-toxic, chemically unreactive and with low viscosity. As perfluorinated compounds present almost all the right properties required for the wanted solvent, they decided to study the solubility of radon in several perfluoroalkanes.

In both works solubility data were presented in terms of Ostwald coefficient and solute molar fraction at a partial pressure of the gas equal to 1 atm. The equilibrium molar fractions of the liquid and gaseous phase where calculated according to the procedure for data reduction presented previously on Part II.

Previous studies have been done on the modelling of the solubility data of xenon in perfluoroalkanes, particularly perfluoro-n-hexane (Bonifácio et al., 2002). The authors used both molecular simulation and the SAFT-VR EoS to describe experimental data. They observed that in both cases a binary interaction parameter had to be introduced in order to reproduce the experimental results. They were expecting this behaviour since in a

previous work, dealing with the phase diagram of xenon in lighter alkanes (C_1 to C_4) and perfluoroalkanes (C_1 to C_2), also using the SAFT-VR, they showed that while the behaviour of xenon correlated strongly with that of the n-alkanes (the experimental phase diagrams and excess volumes could be described accurately using simple Lorentz-Berthelot combining rules to determine the cross interaction parameters), for xenon in n-perfluoroalkanes the existing experimental data could only be reproduced by introducing a binary interaction parameter (Filipe et al., 2000 and McCabe et al., 2001). The energetic binary interaction parameter used by the authors was the same that they used in an earlier study of alkane + perfluoroalkanes binary mixtures (McCabe et al., 2001), equal to 0.92. They stated that although this was not the best value and a slight improvement would be possible if the parameter were fitted to the specific system, they preferred to use the parameters in a transferable way giving importance to the predictive capability of the equation instead of look for the accuracy of the results given by the model.

In this work a similar study were carried out using the soft-SAFT EoS to describe solubility data for xenon and radon in perfluoroalkanes. Both solutes and solvents were modelled as non associating molecules and any kind of interaction was admitted between them. As in the work of Filipe et al. (2000) only the energetic parameter had to be included to correctly describe experimental data. It was adjusted for each mixture and is listed in Table III.6.

Table III.6. Adjusted Binary Parameters for the Solubility of Xenon and Radon in Fluorinated Compounds and AADs of the Calculations by the Soft-SAFT EOS with Respect to Experimental Data

Solvent	η	ξ	AAD (%)
	Xenon		
C_6F_{14}	1	0.870	3
C_7F_{16}	1	0.860	2
C_8F_{18}	1	0.860	1
	Radon		
C_6F_{14}	1	0.825	7
C_8F_{18}	1	0.825	4

The results obtained for the correlation of the experimental data with the soft-SAFT model are presented in Figures III.12.

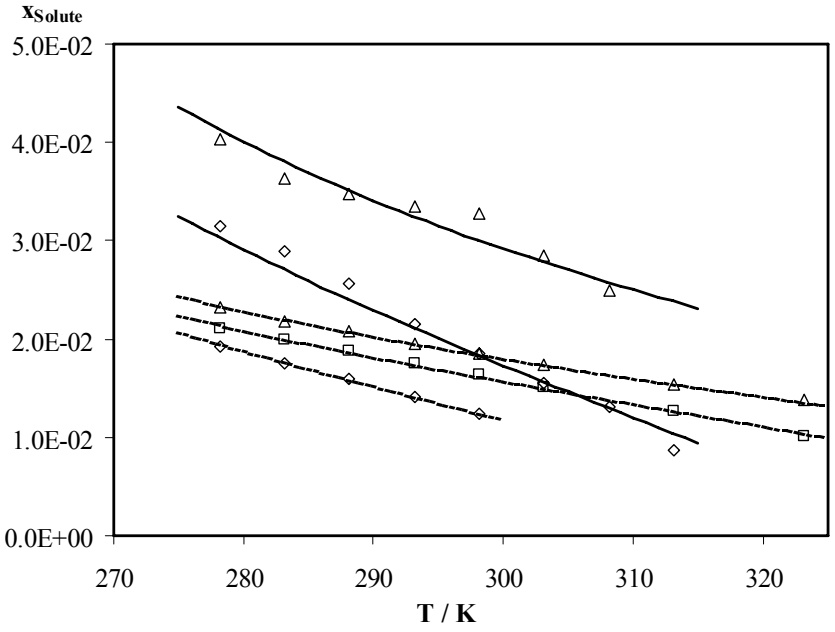

Figure III.12. Solubility of xenon and radon in linear perfluoroalkanes. Symbols represent experimental data for perfluoro-n-hexane (◊), perfluoro-n-heptane (□), and perfluoro-n-octane (Δ). Lines correspond to the results from the soft-SAFT EOS: full lines are the results for the solubility of radon and dashed lines for the solubility of xenon.

In the case of the solubility of xenon, the same energetic parameter is used for perfluoro-n-heptane and perfluoro-n-octane and a slightly different parameter had to be used to perfluoro-n-hexane to obtain a quantitative description. In the case of the solubility of radon, the same parameters are used for both systems. The deviations in this case are higher but this is not due to the binary interaction parameters used since others were tested and similar deviations were obtained. It is believed that the larger errors had to due with the less accurate adjustment of the molecular parameters for pure radon for the motives referred before. However, it can be observed that in both cases the soft-SAFT model without any association can correctly describe the experimental solubility data. The temperature dependences for these systems are even higher than in the case of the oxygen in perfluoroalkanes and the model can correctly describe it using only one adjusted parameter.

These results confirm that the model is able to correlate solubility data for systems that do not interact, corroborating the idea that oxygen has a special behaviour when mixed with fluorinated compounds.

III.4.3. Solubility of Carbon Dioxide in Perfluoroalkanes at High Pressure

This section addresses the modelling of the phase diagrams measured for the system CO_2/perfluoroalkanes (perfluoro-n-octane, perfluorodecalin, perfluorobenzene, pefluorotoluene and perfluoromethylcylohexane).

Several authors employing different techniques and methods have worked on these systems with results leading to different conclusions. To explain the higher solubility of CO_2 in perfluoroalkanes when compared with the corresponding alkanes, some authors suggested a specific solute-solvent interaction between the fluoroalkanes and the CO_2. Cece et al. (1996) justified by *ab initio* calculations the enhanced binding in the CO_2-C_2F_6 due to the electrostatic interaction between the positively charged carbon atom of CO_2 and the negatively charged fluorine atoms in the perfluoroalkane. Also through *ab initio* calculations, Raveendran and Wallen (2002) studied the effect of stepwise fluorination on the CO_2-philicity. The authors concluded that CO_2-perfluoralkane and CO_2-alkane interactions have a different nature, although energetically comparable. The perfluoroalkanes interact with CO_2 through its carbon atom, while alkanes interact through the oxygen atoms. These findings agree with the experimental results of Dardin et al. (1998) who, using high-pressure ^{1}H and ^{19}F NMR, identified specific solute-solvent interactions, which were qualitatively explained in terms of the surface accessibility of fluorine atoms in the various CF_2CF_3 units in perfluoroalkanes.

Contrary to the previous studies, Diep et al. (1998) using higher levels of theory than those employed in the study by Cece et al. (1996) did not find any particular attraction between CO_2 and perfluoroalkanes, relative to the corresponding alkanes. Furthermore, the authors reported binding energies of CO_2-alkanes ranging from -0.79 to -1.17 kcal/mol, which are slightly higher than those in the CO_2-perfluoroalkanes species. The same conclusions were achieved by Yee et al. (1992) through infrared spectroscopy, founding no evidence of special attractive interactions between CO_2 and perfluoroethane. Yonker and Palmer (2001) studied high-pressure ^{1}H and ^{19}F NMR spectra of the neat fluorinated methanes and their CO_2 mixtures and concluded that there are no distinct or specific interactions between the fluorinated methanes and CO_2.

Molecular simulations have also been performed for some carbon dioxide/alkane and carbon dioxide/perfluoro-n-alkane mixtures. Cui et al. (1999) carried out a molecular simulation study of the vapor-liquid equilibria of n-hexane-CO_2 and perfluoro-n-hexane-

CO_2 binary mixtures using the Gibbs ensemble Monte Carlo method. The authors did not introduce any binary interaction parameters in their study and so their results are, in the authors' own words, essentially qualitative. However, the fact that simple interaction-site models correctly predicted the increase of the miscibility for perfluoroalkane-CO_2 compared with the alkane-CO_2 mixture indicates that geometric packing and dispersion interactions have a major role on the miscibility in the two mixtures.

Recently, Gomes and Pádua (2003) obtained conformational and structural properties of perfluoralkanes and alkanes applying the molecular dynamics method using flexible, all-atom force fields containing electrostatic charges. The authors concluded that it is easier to form a cavity in perfluoroalkanes than in alkanes. This fact can justify the higher solubility of gases in perfluoroalkanes but can not justify the higher solubility of a bigger molecule, such as CO_2, when compared to other smaller gases, a fact that the authors explain as resulting from differences in solute-solvent interactions. The same study refers that electrostatic terms play a minor role in the interactions between CO_2 and both alkanes and perfluoroalkanes, and that stronger interactions of carbon dioxide with non-polar solvents should be attributed to dispersion forces and not to any particular affinity of CO_2 for perfluorinated liquids. In a recent work, Zhang and Siepmann (2005) presented phase diagrams for selected n-alkanes, n-perfluoroalkanes and carbon dioxide ternary mixtures, as a function of pressure, from Monte Carlo simulations. They used two binary interaction parameters for the alkane-perfluoroalkane mixtures, fitted to a particular mixture, and used them in a transferable manner for the rest of the mixtures involving the two compounds. Carbon dioxide was modelled considering the polar charges in an explicit manner, and no binary interaction parameters were used for the carbon dioxide binary mixtures. The agreement with the available data for the binary phase diagrams is fair, and hence a qualitative agreement with the ternary mixtures is expected. An interesting part of this work is the use of molecular simulations to study the structure and microheterogeneity of the mixtures through the analysis of the radial distribution functions.

Colina et al. (2004) studied the phase behavior of mixtures containing carbon dioxide, *n*-alkanes and *n*-perfluoroalkanes using the SAFT-VR. In their work the quadrupole was not treated explicitly but in an effective way via the square-well potential of depth ε_{11} and adjustable range $\lambda_{11.}$ They used two binary parameters for the mixtures, fitted to the CO_2/n-tridecane mixture. These binary parameters were used to predict the

behavior of CO_2/n-alkane and CO_2/n-perfluoroalkane mixtures, obtaining good agreement for the CO_2/n-alkane mixtures but only a fair agreement for the CO_2/perfluorohexane mixture (the only experimental CO_2/perfluoroalkane mixture available). Better results would probably be obtained if the binary parameters were fitted to the perfluoroalkane mixture specifically. No electrostatic interactions were explicitly included.

These studies are continued in this work, with the advantage that now, more experimental data is available to help to elucidate the questions that are still under discussion. Two main conclusions are expected to be achieved with this work namely, the influence of the structure on the solubility of carbon dioxide in perfluoroalkanes, which was already addressed in Part II, and the influence of electrostatic contributions to the global properties of systems containing at least one component with a quadrupole moment. This last point will be discussed in this section and for that purpose, a polar term was added to the original soft-SAFT EoS (Equation III.3) to account for electrostatic contributions as explained in Section III.3.2.

When the quadrupole moment is explicitly taken into account, two more parameters have to be considered, the quadrupolar moment Q and $x_{p,}$ defined as the fraction of segments in the chain that contain the quadrupole. Three of the compounds studied in this work have a quadrupole moment: carbon dioxide, perfluorobenzene and perfluorotoluene. Experimental values for the quadrupole moment in carbon dioxide (Vrabec et al., 2001) and perfluorobenzene (Vrbancich and Ritchie, 1980) are available in the literature. No reference was found regarding the quadrupole in perfluorotoluene but, knowing that the quadrupole moment for benzene is similar to that of toluene (Casas et al., 2003) and that of perfluorobenzene although with a symmetric sign (Vrbancich and Ritchie, 1980), it is legitimate to admit that the quadrupole in perfluorotoluene will be similar to that in perfluorobenzene and with the same sign. Regarding the molecular parameter $x_{p,}$ it was fixed to 1/3 for carbon dioxide and 1/6 for perfluorobenzene and perfluorotoluene mimicking the molecules as three and six segments with a quadrupole in one of them. Therefore, with x_p and Q fixed, only the usual m, σ and ε parameters need to be adjusted for the molecule presenting a quadrupole moment. They were readjusted in the usual way by fitting vapor pressure and saturated liquid densities to experimental. The parameters for carbon dioxide, perfluorobenzene and perfluorotoluene with and without the quadrupole moment included are presented in Table III.7. Also in the table is given the absolute

average deviation (AAD) between experimental liquid coexisting densities and vapor pressures of carbon dioxide, perfluorobenzene and perfluorotoluene given by the soft-SAFT EoS, with and without the inclusion of the quadrupole moment on the molecule. In both cases, vapour pressures and liquid densities are fitted to experimental data with an AAD inferior to 3 % and 0.5 % respectively. For perfluoro-n-octane and perfluoromethylcyclohexane the parameters that will be used are in Table III.1.

Table III.7. soft-SAFT molecular parameters for CO_2 and perfluoroalkanes with and without quadrupole

Component	m	σ (Å)	ε/k_B (K)	Q ($C.m^2$)	AAD (%) Pvap	AAD (%) Density
CO_2	2.681	2.534	153.4	--	0.25	0.44
CO_2	1.571	3.184	160.2	4.4×10^{-40}	0.50	0.90
C_6F_6	3.148	3.647	253.6	--	3.61	0.19
C_6F_6	3.253	3.602	245.5	5.0×10^{-40}	2.39	0.30
C_7F_8	3.538	3.764	253.0	--	3.11	0.52
C_7F_8	3.636	3.723	246.5	5.0×10^{-40}	2.63	0.40

Figures III.13, III.14 and III.15 show a comparison between the experimental data for the systems CO_2/perfluorobenzene, CO_2/perfluorotoluene and CO_2/perfluoro-n-octane with predictions from the soft-SAFT equation with and without the quadrupole term, at three different temperatures, 293.15, 323.15 and 353.15 K. Symbols correspond to the experimental data; dashed lines show calculations with soft-SAFT without the quadrupole, while the full lines represent calculations with the polar term. No binary parameters were fitted in these cases and so the lines are full predictions from the pure component parameters. It can be observed that the quadrupole has a significant influence on the description of the phase behaviour of the mixtures involving aromatic compounds. Polar soft-SAFT is able not only to provide an overall better agreement, but it also captures the changes in the curvature as a function of temperature. As before, the results given by the soft-SAFT EoS are compared with the ones given by the Peng-Robinson EoS represented in the figures by the lighter full lines. In the case of the CO_2/aromatic compounds, especially for the CO_2/perfluorobenzene mixture, the results given by the Peng-Robinson EoS are much better than could be expected when using such a simple equation.

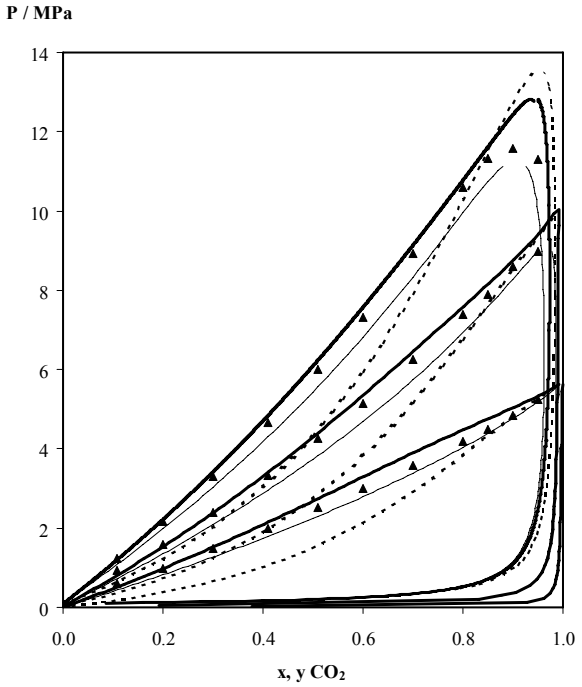

Figure III.13. Predictions of VLE of CO_2/perfluobenzene system at 293.15, 323.15 and 353.15 K. Symbols represent experimental data measured in this work. Solid dark lines correspond to the soft-SAFT model including the polar term and dashed lines to the original soft-SAFT model. In both cases the size and the energy binary interaction parameters are set to one. The lighter solid lines are predictions given by the Peng Robinson EoS with k_{ij}=0.

Results obtained for perfluorodecalin and perfluoromethylcyclohexane are similar to the ones obtained for perfluoro-n-octane, meaning that the introduction of the quadrupole effect in CO_2 does not seem to noticeably influence the description of the phase equilibria for non aromatic perfluorocompounds.

In a previous work, it was observed that binary parameters are needed for obtaining quantitative predictions if the lengths of the two molecules involved in the mixtures are different and/or their shape deviates from spherical (Kontogeorgis et al., 1996). Using other EoS the authors showed that for athermal mixtures the use of a size binary parameter could provide a better and more meaningful description of data and reduce the magnitude of the energy binary parameter in systems were energetic interactions are important. Thus, a good description of the phase diagrams of CO_2/non-aromatic-perfluoroalkanes requires the use of two interaction parameters, as previously observed for oxygen/perfluoroalkanes mixtures.

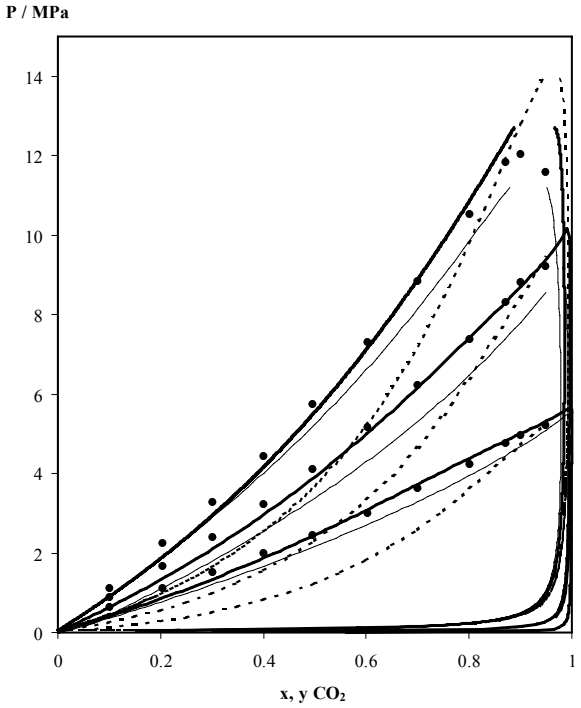

Figure III.14. Predictions of the vapor-liquid equilibrium of CO_2/perfluorotoluene system at 293.15K, 323.15K and 353.15K. Legend as in Figure III.13.

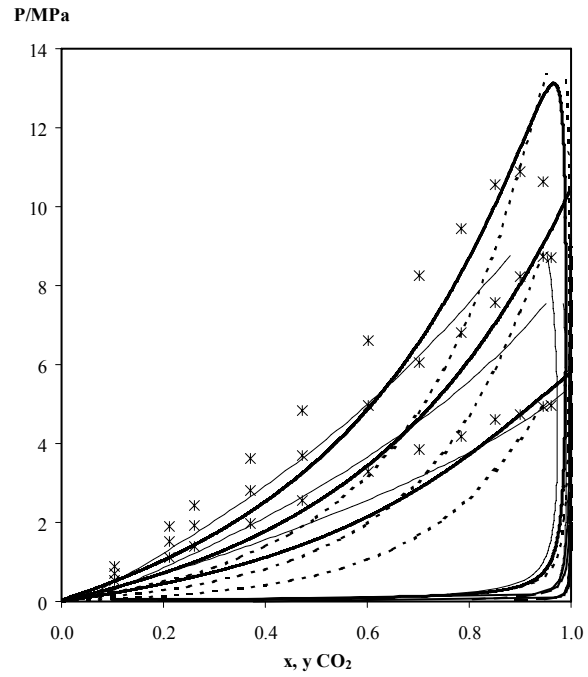

Figure III.15. Predictions of the vapor-liquid equilibrium of CO_2/perfluoro-n-octane system at 293.15K, 323.15K and 353.15K. Legend as in Figure III.13.

The P-x curves for the mixtures CO_2/perfluoro-n-octane, CO_2/perfluorodecalin, and CO_2/perfluoromethylcylohexane were found to be sensitive to the energy binary parameter, $\xi_{ij,}$ but relatively insensitive to binary size parameter, $\eta_{ij,.}$ Hence, the procedure followed was to fix the binary size parameter and adjust only the energy parameter to experimental data at 323.15 K for each mixture and use it in a predictive manner for the other temperatures. In this way, the size and energy binary parameters were transferred within the same mixture at different conditions. Additionally, the size parameter was also transferred for different compounds.

Table III.8 compares the binary parameters adjusted when the quadrupole moment is considered explicitly and in an effective way. When the polar term is included, the binary energy and size parameters are consistently closer to unity than when the non-polar soft-SAFT EoS is used. This is expected, since the polar equation explicitly considers the quadrupole, with an extra parameter, in this case the binary parameters account only for the unlike van der Waals interactions. On the contrary, when the quadrupole is not included, the binary parameters effectively account for it, showing larger deviations from unity, particularly the energy parameter. Also presented in Table III.8 are the k_{ij} parameters adjusted for each mixture to be used in the Peng-Robinson EoS. The k_{ij} parameter was adjusted at the same intermediate temperature of 323.15 K and then used to predict the phase diagrams at different temperatures following the procedure used to adjust the binary parameters for the soft-SAFT EoS.

Table III.8. Optimised size and energy binary interaction parameters for the soft-SAFT EoS and kij parameter for the Peng-Robinson EoS.

	Soft-SAFT EoS				**Peng-Robinson EoS**
	With polar term		**Without polar term**		
System	η_{ij}	ξ_{ij}	η_{ij}	ξ_{ij}	k_{ij}
$CO_2 - C_8F_{18}$	1.04	0.890	1.06	0.790	0.070
$CO_2 - C_{10}F_{18}$	1.04	0.836	1.06	0.732	0.124
$CO_2 - C_7F_{14}$	1.04	0.902	1.06	0.806	0.112

Figures III.16, III.17 and III.18 present P-x diagrams where experimental data for the binary mixtures CO_2/perfluoro-n-octane, CO_2/perfluoromethylcyclohexane and CO_2/perfluorodecalin respectively are compared against the soft-SAFT calculations. It can be observed that the agreement between the experimental data and the description provided by the soft-SAFT model with and without the polar term are both excellent for the three mixtures, at all conditions studied.

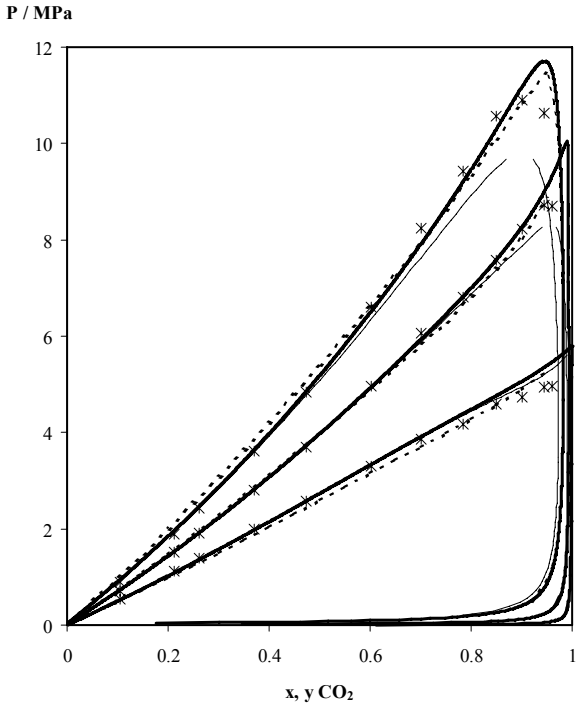

Figure III.16. Vapor-liquid equilibrium of CO_2/perfluoro-n-octane system at 293.15K, 323.15K and 353.15K. Symbols represent experimental data measured in this work. Solid lines corresponds to the soft-SAFT model including the polar term and black dashed lines to the original soft-SAFT model at optimised size and the energy binary interaction parameters from Table III.8. The lighter solid lines are predictions given by the Peng Robinson EoS with k_{ij} also from Table III.8.

Obviously that a more realistic molecular model as is the soft-SAFT EoS can predict the experimental data more accurately, capturing the different curvatures presented by the phase diagrams. However, globally the results obtained with the Peng-Robinson EoS are surprisingly good except in the case of the CO_2/perfluorodecalin system, where the equation predicts a LLE region at 293.15 K that was not observed experimentally. These results confirm the idea that the empirical success of the Peng-Robinson equation of state is unique; there is no other simple equation of state of the van der Waals form that has

shown such wide and reliable applicability to the calculation of vapor-liquid equilibria (VLE) for systems containing light hydrocarbons, permanent gases, carbon dioxide, and as shown here, perfluoroalkanes.

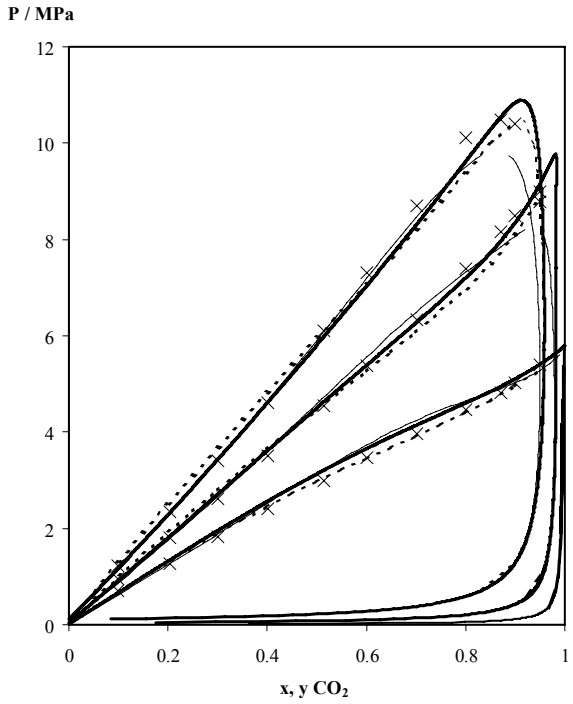

Figure III.17. Vapor-liquid equilibrium of CO_2/perfluoromethylcyclohexane system at 293.15K, 323.15K and 353.15K. Legend as in Figure III.16.

As a further test of the reliability of the parameters provided here for the soft-SAFT EoS, the performance of the soft-SAFT equation was checked, without and with the quadrupolar term for the mixture CO_2/perfluoro-n-hexane, for which there is available data in the literature (Iezzi et al, 1989). Figure III.19 shows predictions of the original and the polar soft-SAFT equation for this mixture. Figure III.19a depicts pure predictions from the two versions of the equation. Figure III.19b presents calculations from both versions of soft-SAFT with the size binary parameters taken from Table III.8, and binary size energy parameters equal to 0.807 and 0.916, respectively. The energy parameters were fitted at 314.65K and used in a transferred manner for the higher temperature, 353.25K. Regarding the pure predictions (Figure III.19a) it is interesting to see the effect the addition of the quadrupole has in accurately describing the behaviour of the mixture as compared to the original equation. The simulation results obtained by Cui et al. (1998) and also by Zhang and Siepmann (2005) from Monte Carlo simulations for this mixture lye between

calculations from the original soft-SAFT equation and those provided from the polar soft-SAFT equation, being polar soft-SAFT superior than the simulations in this case. Note that in these simulations explicit charges were considered for the CO_2 molecule.

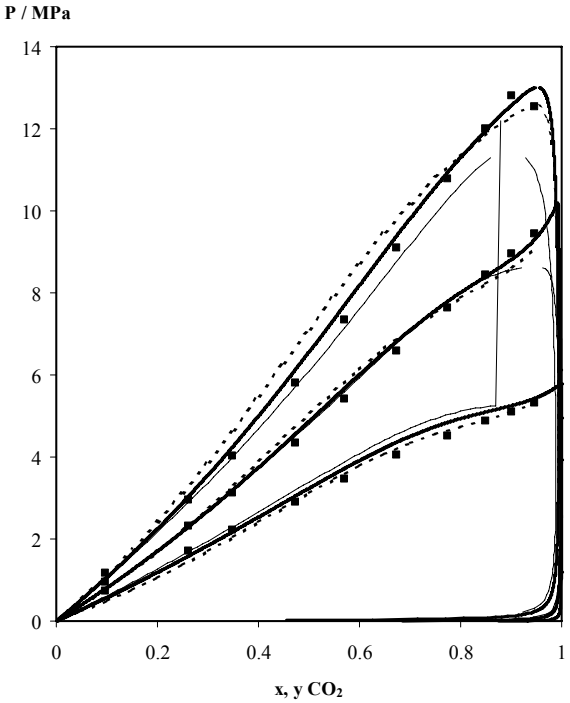

Figure III.18. Vapor-liquid equilibrium of CO_2/perfluorodecalin system at 293.15K, 323.15K and 353.15K. Legend as in Figure III.16

Excellent agreement is observed when both versions of the equation are used with binary parameters (Figure III.19b), as expected from the rest of the results shown here.

A similar study was carried for CO_2/alkane mixtures. The alkanes studied are the corresponding alkanes for the perfluoroalkanes studied in this work. Table III. 9 reports the references from where the VLE data for these mixtures was taken as well as the temperature range studied in each case and the intermediate temperature used in this work to adjust the binary interaction parameters. The main objective of this comparison is to observe the influence of fluorination on the solubility of carbon dioxide and to compare the influence of the electrostatic contributions for these mixtures, using as tool the soft-SAFT EoS. Experimentally, for all the systems studied in this work, the solubility of carbon dioxide is always higher in the fluorinated molecules. This effect is maximum for the CO_2/perfluorodecalin vs CO_2/decalin systems. At the thermodynamic conditions presented the CO_2/decalin system presents a LL region for carbon dioxide mole fractions higher than

0.5. No LL region was observed for the CO_2/perfluorodecalin system at the thermodynamic conditions studied.

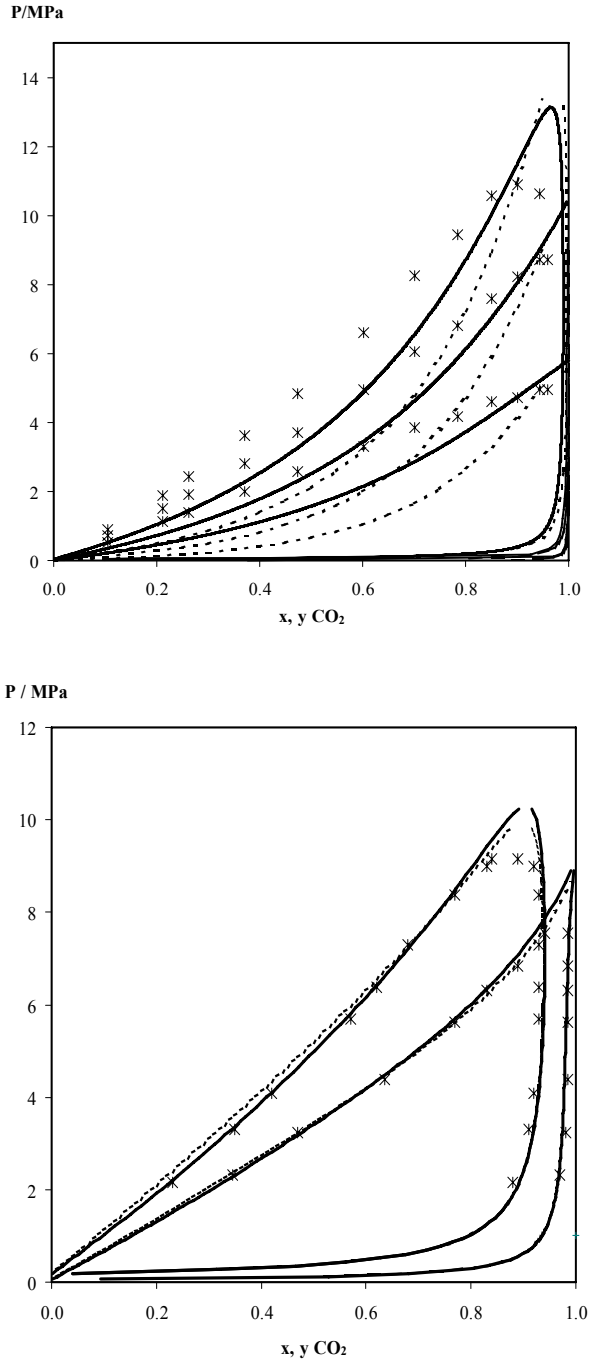

Figure III.19. Vapor-liquid equilibrium of CO_2/perfluoro-n-hexane system at 314.65, 353.25 K. Symbols represent experimental data measured by Iezzi et al. (1989) **(a)** Predictions given by the soft-SAFT model **(b)** soft-SAFT calculations with binary interaction parameters. Legend as in Figure III.16.

Table III.9. References for VLE experimental data for CO_2/alkane mixtures

Mixture	Reference	T range (K)	P range (bar)	T used to adjust η and ζ
$CO_2 - C_8H_{18}$	Weng and Lee (1992)	313-348	1.4-11.4	328
$CO_2 - C_{10}H_{18}$	Tiffin et al. (1978) Anderson et al. (1986)	273-348 323-423	1.0-7.1 1.5-10.7	323
$CO_2 - C_7H_{14}$	Ng and Robinson (1979) Nasrifar et al. (2003)	311-477 270-350	0.3-14.9 0.4-11.0	311
$CO_2 - C_6H_6$	Ohgaki and Katayama (1976) Gupta et al. (1982) Kim et al. (1986)	298-313 313-393 313-393	0.9-7.8 0.1-13 0.5-6.5	313
$CO_2 - C_7H_8$	Ng and Robinson (1978) Fink and Hershey (1990) Chang et al. (1995)	311-477 308-353 290-310	0.3-15.3 0.5-12.4 1.1-7.5	323

The first step was to adjust the molecular parameters for the pure solvents. For n-octane the molecular parameters m, σ and ε had already been adjusted in a previous work (Pàmies and Vega, 1998). The parameters for decalin, methylcyclohexane, benzene and toluene where adjusted using experimental density and vapour pressure data taken from DIPPR, 1998. A quadrupole moment was included in both benzene and toluene and it was equal to the one previously presented for perfluorobenzene and perfluorotoluene. The adjusted parameters are presented in Table III.10.

Table III.10. soft-SAFT Molecular Parameters for Decalin, Methylcyclohexane, Benzene and Toluene With and Without Quadrupole

Component	**m**	**σ (Å)**	**ε/k_B (K)**	**Q ($C.m^2$)**	**T range**
$C_{10}H_{18}$	2.404	4.578	384.7	--	230-600
C_7H_{14}	2.546	4.104	296.1	--	200-500
C_6H_6	2.364	3.727	300.1	--	273-373
C_6H_6	2.333	3.754	299.3	-5.0×10^{-40}	273-500
C_7H_8	2.753	3.889	294.8	--	180-600
C_7H_8	2.692	3.925	296.5	-5.0×10^{-40}	273-500

Relating the solubility of carbon dioxide in benzene and toluene, the first approach was to calculate the phase diagrams without using any adjusted binary parameters as done

before for the fluorinated compounds. Figures III.20 and III.21 present the results obtained for the CO_2/benzene and CO_2/toluene mixtures.

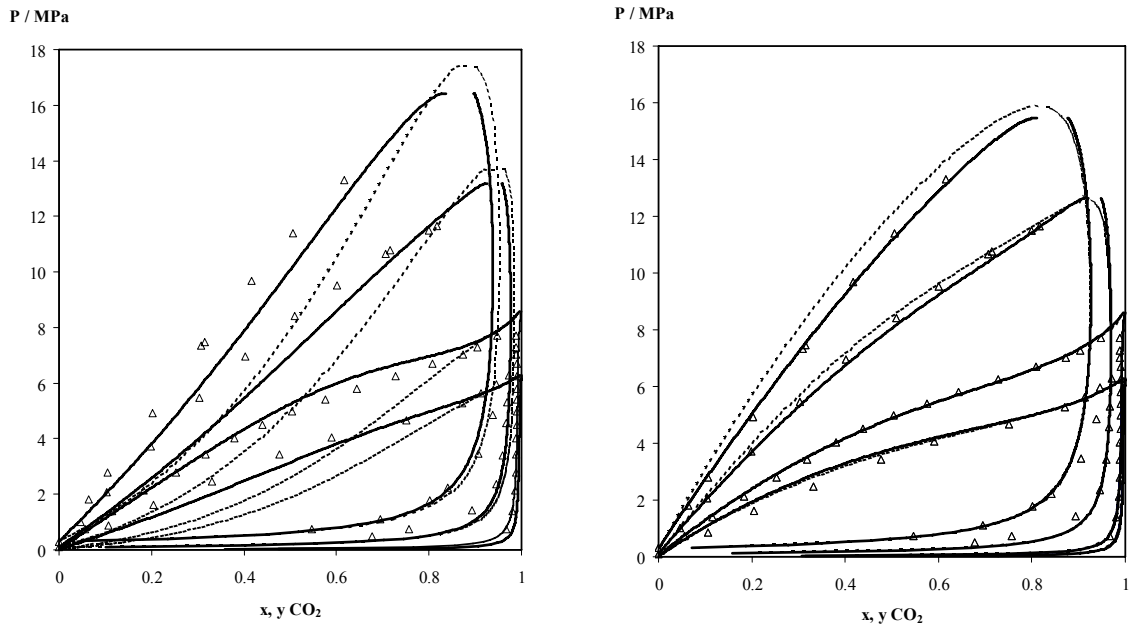

Figure III.20. Predictions of the vapor-liquid equilibrium of CO_2/benzene system at 298, 313 and 353 and 393 K. Symbols represent experimental data. Solid lines correspond to the soft-SAFT model including the polar term and dashed lines to the original soft-SAFT model. (a) Size and the energy binary interaction parameters are set to one; (b) Size and the energy binary interaction parameters adjusted at 313 K.

The full and dashed lines in Figure III.20a represent the predictions given by the soft-SAFT EoS with and without the quadrupole moment respectively, setting the binary interaction parameters equal to one. For the CO_2/benzene mixture it is observed that the inclusion of the quadrupole moment has again an important influence on the description of the experimental results but is not enough to describe quantitatively the experimental data. In the case of CO_2/toluene mixture, the results in Figure III.21 show a similar behaviour as observed for the CO_2/benzene system. Contrary to the CO_2/aromatic perfluoroalkanes, in the case of the aromatic alkanes binary parameters have also to be adjusted to experimental data. Results obtained when this is done are presented in Figures III.20b and III.21b. These results agree with the ones obtained by Pfohl and Brunner (1998) who also had to consider to binary interaction parameters to describe the CO_2/toluene mixture when using an extended SAFT EoS were the solvents are modelled by the BACK EoS.

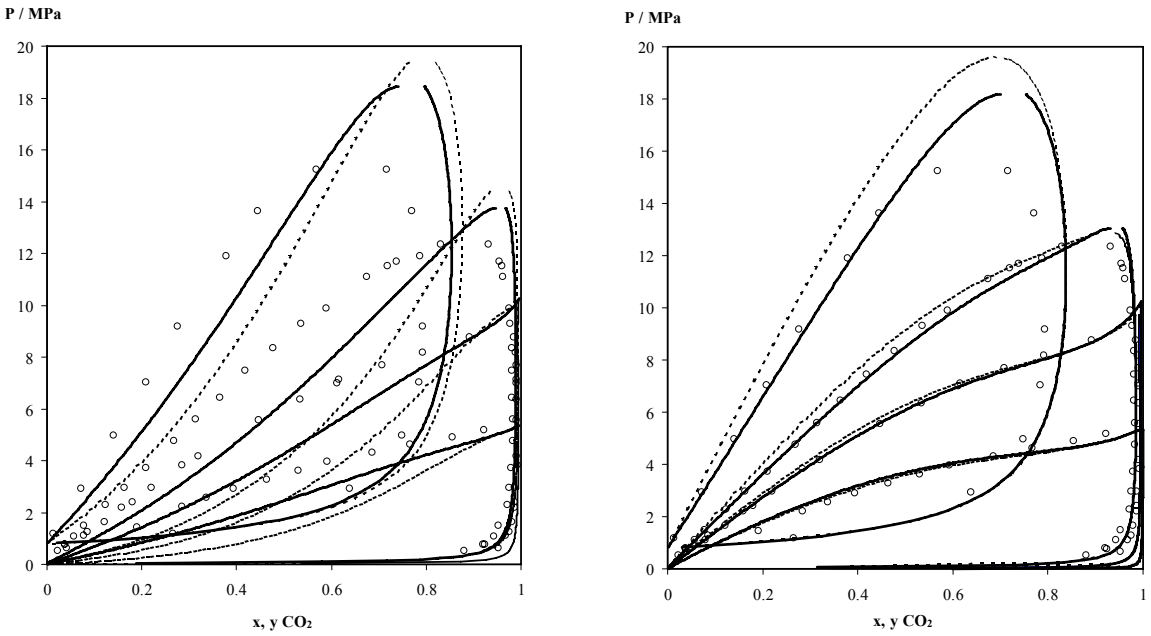

Figure III.21. Predictions of the vapor-liquid equilibrium of CO_2/toluene system at 290.8, 323.17, 353.18 and 477.04 K. Legend as in Figure III.20. Binary parameters were adjusted at 323 K.

Figures III.22 and III.23 present the results obtained for the CO_2/n-octane and CO_2/methylcyclohexane mixture, which are very similar to the ones obtained before for the CO_2/perfluoroalkanes corresponding mixture. Besides the inclusion of the quadrupole moment, the binary parameters have also to be adjusted to experimental data in order to obtain quantitative agreement. When this is done, both versions of the soft-SAFT EoS give excellent results at moderate temperatures but in the case of the CO_2/toluene and CO_2/methylcyclohexane mixtures it can be observed that for higher temperatures the polar version gives better predictions that the original version of the soft-SAFT model. This happens because as mentioned before, when the polar contribution is included in equations of state in an effective manner, i.e. through the van der Waals attraction term, one may obtain artificial interaction energies parameters with poor prediction capacity. Better results are obtained when the quadrupole interaction is explicitly considered as in the polar soft-SAFT version.

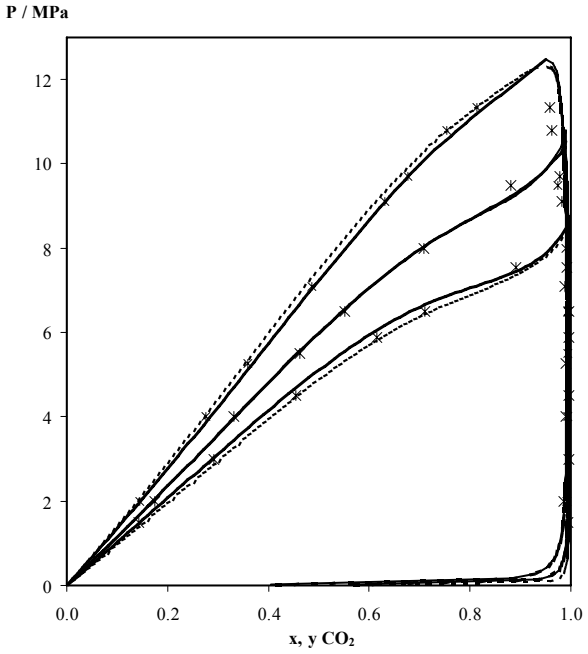

Figure III.22. Predictions of the vapor-liquid equilibrium of CO_2/n-octane system at 313.15, 328.15 and 348.15 K. Legend as in Figure III.21. Binary parameters were adjusted at 328 K.

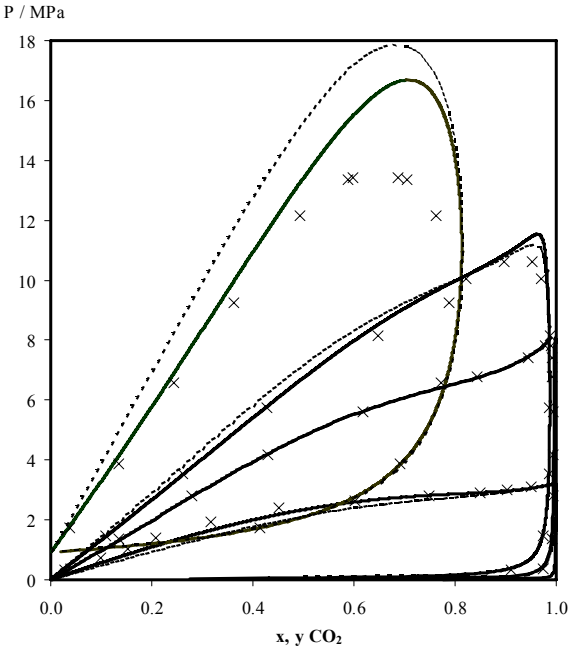

Figure III.23. Predictions of the vapor-liquid equilibrium of CO_2/methylcyclohexane system at 270, 311, 338.9 and 477 K. Legend as in Figure III.22. Binary parameters were adjusted at 311 K.

Finally, Figure III.24 presents the results obtained for the CO_2/decalin mixture. This mixture presents a region of liquid-liquid equilibria as reported by Tiffin et al. (1978). The upper critical solution temperature (UCST), identified by the star in the figure, occurs at 316.45 K. Both versions overestimate the liquid-liquid region by predicting a LLE at a temperature above the UCST. However, it can be observed that the polar soft-SAFT gives better predictions at lower and higher temperatures than the original soft-SAFT EoS.

Table III.11 compares the adjusted binary parameters when the quadrupole moment is considered explicitly and in an effective way. As observed before, when the polar term is included, the binary energy and size parameters are consistently closer to unity than when the non-polar soft-SAFT EoS is used for the same reasons mentioned above. Also, the CO_2/alkane mixtures were found to be more sensitive to the size binary parameter and although slightly differences are found between them, it was decided not to fix the parameter in order to obtain a quantitative description of the experimental data.

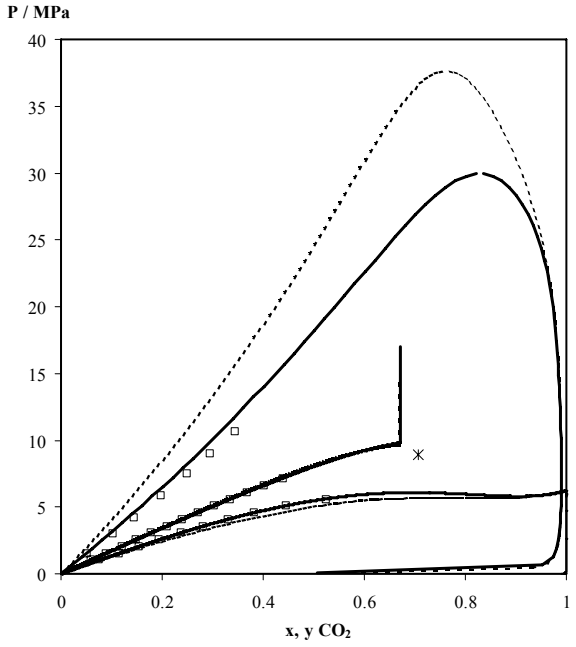

Figure III.24. Predictions of the vapor-liquid equilibrium of CO_2/decalin system at 298, 348 and 423 K. Legend as in Figure III.23. Binary parameters were adjusted at 323 K. The star indicates the upper critical solution temperature of this mixture.

Table III.11. Optimised size and energy binary interaction parameters for the CO_2/alkane mixtures.

	With polar term		Without polar term	
System	η_{ij}	ξ_{ij}	η_{ij}	ξ_{ij}
$CO_2 - C_8H_{18}$	1.02	0.930	1.04	0.823
$CO_2 - C_{10}H_{18}$	1.03	0.883	1.06	0.757
$CO_2 - C_7H_{14}$	1.01	0.945	1.03	0.819
$CO_2 - C_6H_6$	1.02	0.957	1.03	0.869
$CO_2 - C_7H_8$	1.02	0.928	1.04	0.834

It was demonstrated that the soft-SAFT EoS is able to correctly correlate and predict the phase diagrams of CO_2/perfluoroalkanes and CO_2/alkane mixtures including linear, cyclic and aromatic compounds. The objective of the comparison between CO_2/perfluoroalkane vs CO_2/alkane mixtures was to study the influence of the quadrupole moment on these mixtures. From the results obtained it seems that, within the soft-SAFT context, the quadrupole moment has an important effect only when describing the CO_2/aromatic perfluoroalkanes mixtures.

III.4.4. VLE and LLE of Alkane and Perfluoroalkane Mixtures

A significant amount of experimental data is available for perfluoroalkane + alkane systems but, even so, the thermodynamic behaviour of these systems is not completely understood. Althought both alkanes and perfluoroalkanes are nonpolar species and thus it would be expected that their mixtures behave almost ideally, in fact they display large positive deviations from ideality (Hildebrand and Scott, 1950).

The first attempts to account for this anomalous behaviour appeared in the early 50s just after the publication of the experimental data for symmetric perfluoralkane + alkane mixtures (Hildebrand et al., 1950; Simons and Dunlap, 1950 and Simons and Mausteller, 1952) showing substantial regions of liquid-liquid immiscibility. To that date it was believed that such mixtures would be completely miscible in all proportions and that the regular solution theory would also describe these mixtures, at least in a qualitatively way.

In 1958 Scott (Scott, 1958) reviewed the various explanations proposed and concluded that none of the suggestions accounted fully for the anomalous behaviour of all systems investigated. Among the various explanations were the interpenetration between neighboring C-H groups giving an abnormally strong hydrocarbon-hydrocarbon interaction energy leading to the failure of the geometric combining rule proposed by Simons and Dunlap (1950), an empirical shift in the solubility parameter, δ, for hydrocarbons in order to fit the data proposed by Hildebrand (1950), corrections to the regular solution theory to include the effect of volume changes, that occur on mixing proposed by Simons and Dunlap (1950) and modification of regular solution theory to take into account size and ionization potential differences between the two components proposed by Reed (1955). The author concluded that none of these explanations could account for the behaviour of all of the anomalous systems.

In the early 70s Dantzler and Knobler (1971) measured the second virial coefficients of *n*-alkanes, perfluoro-*n*-alkanes, and their mixtures and concluded that the anomalous behavior of alkane + perfluoroalkane systems was due to the failure of the geometric mean rule to describe the unusually weak hydrocarbon-fluorocarbon attractive interaction. They discussed possible reasons for such a weak unlike interaction between the two components: noncentral forces, large ionization potential differences, and large size differences, concluding that the observed deviation from the geometric-mean prediction was most likely due to the latter. This explanation had previously been suggested by Dyke

et al. (1959) from studies of the gas-liquid critical line and Rowlinson (1969) based on a review of the data available. The results indicate that the interactions between perfluoroalkanes and alkanes were about 10% weaker than the geometric mean of the like-molecule interactions.

Similar conclusions were taken by Mousa et al. (1972) when they tried to apply the theory of conformal solutions to calculate the critical properties of several perfluoralkane + alkane mixtures. The authors observed that accurate results were obtained only when an unlike parameter equal to 0.92 was used to calculate the mixed interaction constant. Archer et al. (1996) reported the first attempt to account for the liquid-liquid thermodynamics of alkane + perfluoroalkanes mixtures using the bonded hard-sphere theory (BHS), a theory that has its roots in the theory of Wertheim (1984), as the soft-SAFT EoS, and incorporate in its development the same structural idea. The authors used the BHS theory to account for repulsive interactions and van der Waals one fluid theory to describe attractive interactions and they found this approach accurate enough to describe properly the critical properties of alkanes, perfluoroalkanes and their mixtures. The authors observed that to correctly describe the UCST of the alkane + perfluoroalkanes mixtures, the correction parameter ξ in the geometric-mean rule for the van der Waals cross-term must be equal to 0.909 for all the mixtures studied. The difference was generally no more than 7% from the experimental value. It must be remembered that only one mixture (butane + perfluorobutane) was used to obtain the interaction parameters. The UCSTs of the other mixtures were obtained from these values. The only exception was the methane + perfluoromethane mixture for which different parameters for the pure compounds had to be adjusted. However the ξ parameter used for this mixture was the same than for all the others symmetric and unsymmetrical mixtures studied.

New interest on the subject came out recently with the work of McCabe et al. (1998) and Colina et al. (2004) which modelled the mixing thermodynamics of liquid alkane + perfluoroalkanes mixtures using the statistical associating fluid SAFT-VR approach. Interestingly, these authors found that to reproduce the observed mixing behaviour within the SAFT-VR model, the interaction energies between perfluoroalkane and alkane interaction sites had to be reduced by ± 8% relative to the geometric mean prediction, a result quite similar to that found by Knobler and co-workers (Dantzler and Knobler, 1971). McCabe et al. (1998) studied the high-pressure phase behavior of a

number of perfluro-n-alkane (C_1-C_4) + n-alkane (C_1-C_7) binary mixtures, and suggested a value $\xi = 0.9234$. Latter, Colina et al. (2004) slightly modified this value to $\xi = 0.929$ in order to provide a better fit to the upper critical solution temperature (UCST) of the C_6F_{14} + C_6H_{14} system. The unlike parameter was than used in a transferable way to predict liquid-liquid envelope and the vapor–liquid phase behavior of some of the mixtures measured by Duce et al. (2002). As presented, the model could describe quite well the UCST of the mixtures but predicted narrower phase envelopes than the experimental. Also, the P-x-y diagram were over predicted when compared with experimental data as a result of the over prediction in the pure component vapor pressures due to rescaling the parameters to the critical point which makes that the predictions they provide for sub critical properties are fairly less accurate.

Song et al. (2003) examined the use of typical all atom Lennard-Jones 12-6 plus Coulomb potential functions for simulating the interactions between perfluorinated molecules and alkanes together with the Lorentz-Berthelot combining rules usually used with such potentials. This model had already been applied to accurately account for many of the liquid-phase properties of pure perfluoroalkanes (Watkins and Jorgensen, 2001) and alkanes (Jorgensen et al., 1996) and the authors believed that departures from the geometric mean rule mentioned above resulted from inadequate treatment of molecular geometries or possibly charge distributions in the models employed in these earlier studies. However, they noticed that the special character of perfluoroalkane + alkane interactions was definitely not captured if standard combining rules are used. The authors compared their calculations with experimental data for second virial coefficients, gas–liquid solubilities and enthalpies of liquid mixing and observed that a reduction of ± 10% in the interactions between unlike pairs of molecules is required, which is the same reduction required when simple single-site representations of molecules are used. The authors tried, in alternative, two-parameter combining rules as well as more sophisticated approaches to calculate the cross interaction parameters but the results were not conclusive. Ultimately, the underlying physical origins of the unusual mixing behaviour remained unclear.

The experimental VLE and LLE data measured by Duce et al. (2002) and the LLE data measured in this work were used to study perfluoroalkanes + alkane systems with the soft-SAFT EoS. Results obtained with the model are compared with the results mentioned before obtained with different models and lower molecular weight mixtures.

Binary perfluoroalkane + alkane mixtures belong to the type II phase behavior in the classification of Konynenburg and Scott (1990), characterized by a continuous vapor-liquid critical line and the presence of liquid-liquid phase separation, when the difference in chain length between the two components is not very large (symmetric or close to symmetric systems). Because of the nonideal interactions in these mixtures, the unlike energy parameter was treated as adjustable, and it was set at the optimum value ξ = 0.9146 for the correct prediction of the experimental azeotrope of the perfluoro-n-hexane + n-hexane mixture at 298.15 K. The unlike size parameter was not adjusted (η = 1), because it was verified that the simple Lorentz combination rule provided satisfactory results. It is important to notice that the value of the unlike energy parameter agrees well with the values found by other authors using different models to describe these systems. In a transferable manner, the same optimized energy parameter value was used to predict the rest of the mixtures at different thermodynamic conditions.

Composition diagrams of binary mixtures of perfluoro-n-hexane + *n*-alkane from (C_5 - C_8) and of *n*-hexane + *n*-perfluoroalkane from (C_5 - C_8) modeled in this work are presented in Figures III.25 and III.26, respectively. Figure III.27 and III.28 depicts P-x-y diagrams of the systems shown in Figure III.25 and III.26. Very good agreement is obtained between soft-SAFT predictions and experimental data in all cases, considering that the average uncertainty of the experimental compositions is 4%. In all cases the azeotropic point is correctly predicted and deviations from experimental data are lower than 5%, except in the case of the perfluoro-n-hexane + octane mixture. According to the authors (Duce et al., 2002), at 313.15 K the mixture was not completely miscible in the entire studied composition range and for perfluorohexane mole fractions between 0.189 and 0.709 they obtained demixed mixtures indicating that they were very close to a liquid-liquid region as predicted in fact by the soft-SAFT EoS (Figure III.25b). The UCST calculated by the authors for this mixture is 324 K.

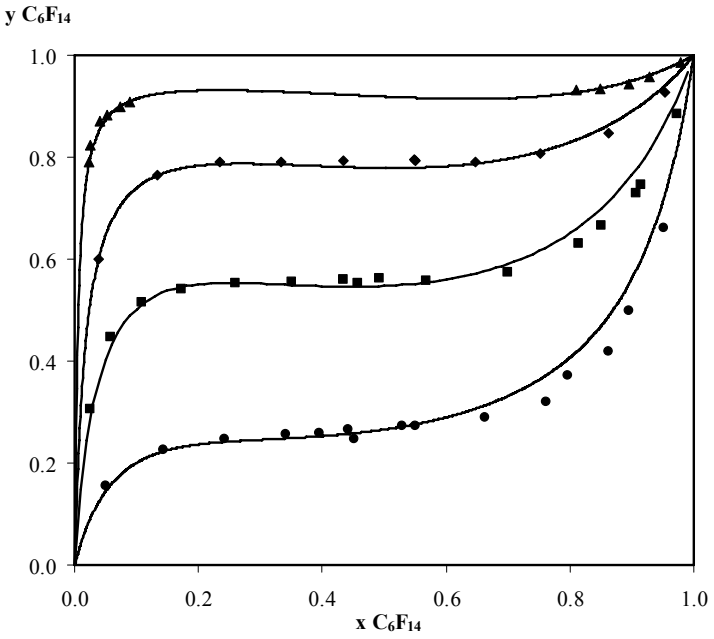

Figure III.25. Vapor-phase mole fraction versus the liquid mole fraction for *n*-perfluorohexane + *n*-alkane mixtures: *n* = 5 at 293.65 K (circles), *n* = 6 at 298.15 K (squares), *n* = 7 at 317.65 K (diamonds), and *n* = 8 at 313.15 K (triangles). Symbols represent experimental data (Duce et al., 2002) and lines correspond to the predictions from the soft-SAFT EoS.

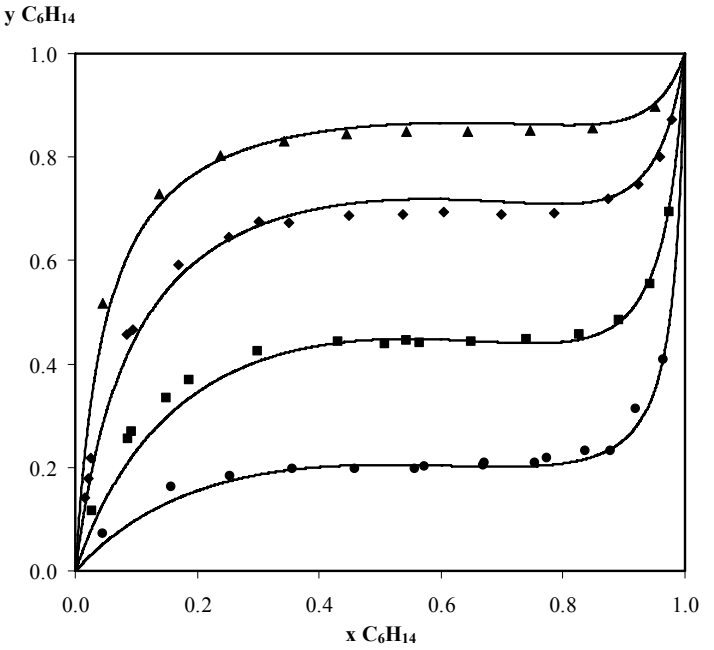

Figure III.26. Vapor-phase mole fraction versus the liquid mole fraction for *n*-hexane + *n*-perfluoroalkane mixtures: *n* = 5 at 293.15 K (circles), *n* = 6 at 298.15 K (squares), *n* = 7 at 303.15 K (diamonds), and *n* = 8 at 313.15 K (triangles). Symbols represent experimental data (Duce et al., 2002) and lines correspond to the predictions from the soft-SAFT EOS.

The same parameters were used to predict the P-x diagrams for alkane + perfluoroalkanes symmetric mixtures with low molecular weight components as CF_4 + CH_4 and C_4F_{10} + C_4H_{10} (Thorpe and Scott, 1956). Figures III.29 and III.30 show the predictions given by the soft-SAFT EoS compared with experimental data found in the literature. Although in these cases higher deviations were obtained, with an average over prediction of about 10%, the results are acceptable since only one binary parameter adjusted for a mixture at very different thermodynamic conditions from the ones observed for these mixtures. Also, the molecular parameters for the pure components of these mixtures already presented a significant discrepancy from the pure experimental data as discussed before.

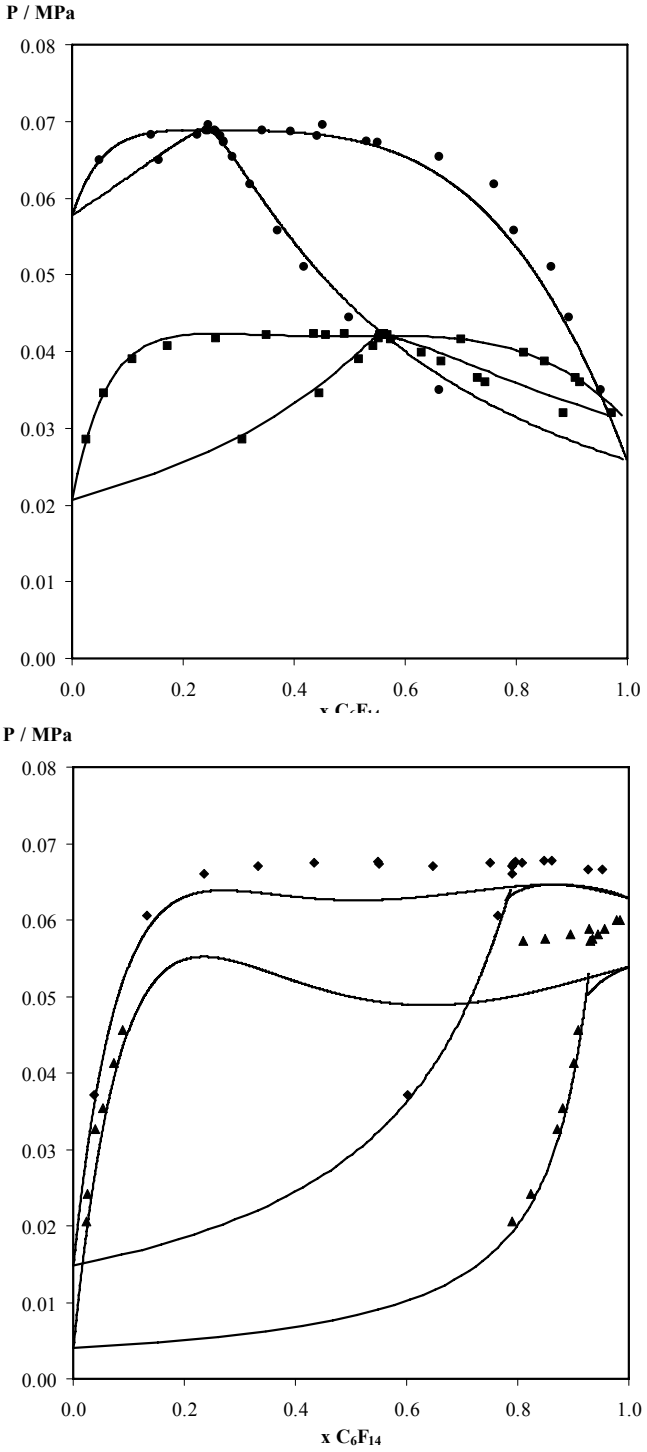

Figure III.27. P-x diagrams for C_6F_{14} + C_nH_{2n+2} mixtures. (a) n = 5 at 293.65 K (circles), n = 6 at 298.15 K (squares) and (b) n = 7 at 317.65 K (diamonds), and n = 8 at 313.15 K (triangles). Symbols represent experimental data (Duce et al., 2002) and lines correspond to the predictions from the soft-SAFT EoS

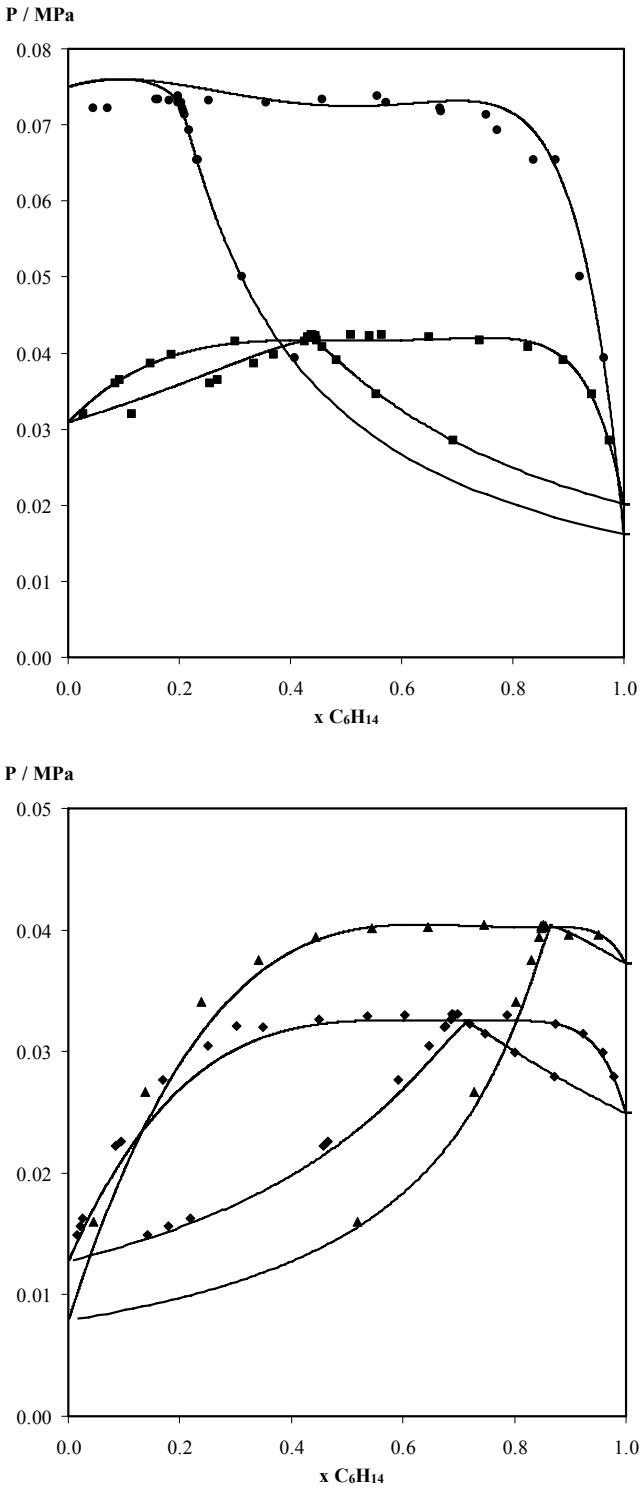

Figure III.28. P-x diagrams for C_6H_{14} + C_nF_{2n+2} mixtures. (a) n = 5 at 293.65 K (circles), n = 6 at 298.15 K (squares) and (b) n = 7 at 317.65 K (diamonds), and n = 8 at 313.15 K (triangles). Symbols represent experimental data (Duce et al., 2002) and lines correspond to the predictions from the soft-SAFT EoS.

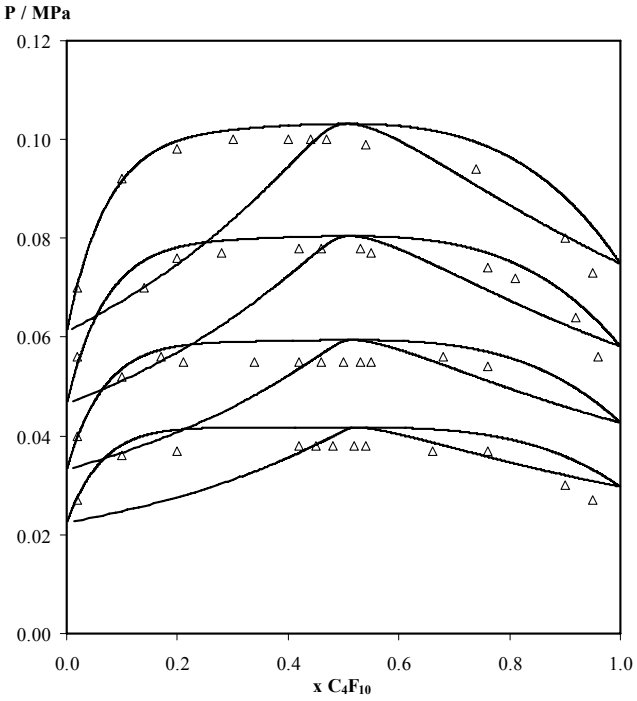

Figure III.29. P-x diagrams at 259.95 K, 253.62 K, 246.35 K and 238.45 K for C_4F_{10} + C_4H_{10} mixture compared with soft-SAFT predictions. The triangles describe the experimental data (Thorpe and Scott, 1956) and the solid curves the theoretical predictions.

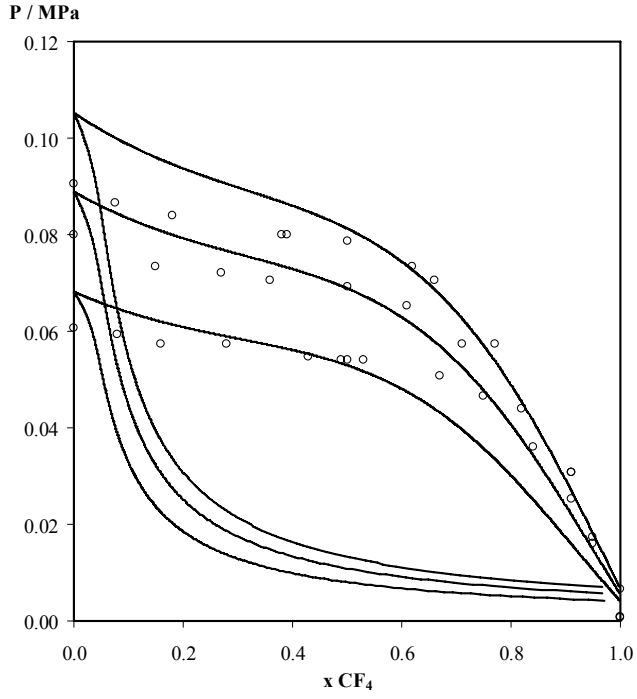

Figure III.30. P-x diagrams at 110.5 K, 108.5 K and 105.5 K for CF_4 + CH_4 mixture compared with soft-SAFT predictions. The circles describe the experimental data (Thorpe and Scott, 1956) and the solid curves the theoretical predictions.

As a further verification of the transferability of the parameters, the same value for the binary energy parameters used in the former VLE predictions was used to predict LLE data for perfluro-n-hexane + alkanes (C_6 - C_8), measured by Duce et al. (2002) and for perfluoro-n-octane + alkanes (C_6 - C_9) measured in this work. Comparison between experimental and theoretical predictions is done in Figures III.31 and III.32 for perfluoro-n-hexane + alkanes and perfluoro-n-octane + alkanes respectively.

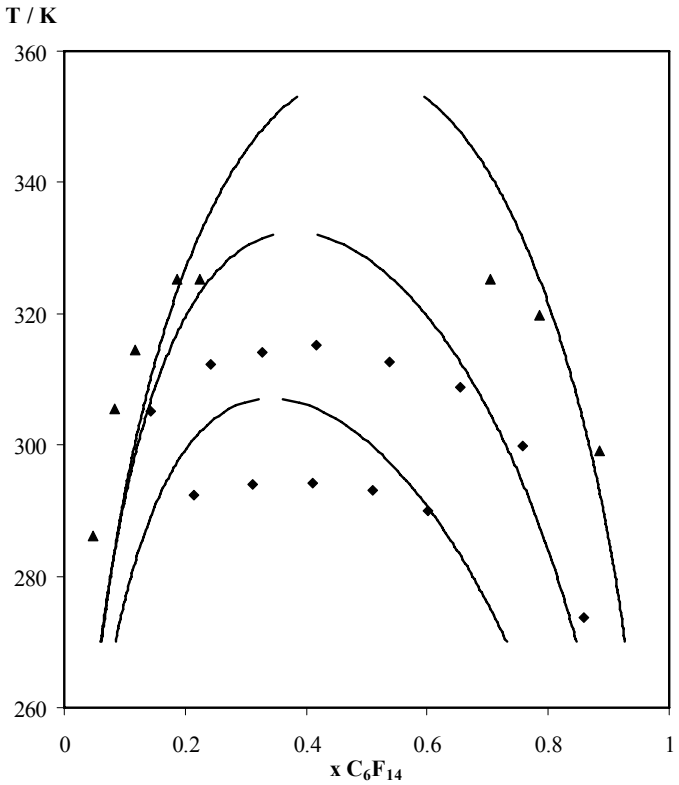

Figure III.31. LLE of C_6F_{14} + C_nH_{2n+2} mixtures at 0.1 MPa: n = 6 (diamonds), n = 7 (squares) and n = 8 (triangles). Symbols represent experimental data (Duce et al., 2002). Solid lines correspond to the predictions from the soft-SAFT EoS.

Since crossover-soft-SAFT equation is not ready, yet, for LLE, because the isomorphism assumption used to develop it does not apply to this type of phase equilibria, over predictions of the UCST were found. However, although most of the experimental points are located in the critical region, it is observed that in both cases the shape of the curve is correct and the quantitative prediction of the low-temperature region is acceptable. To correctly describe the entire phase diagram, a crossover approach has to be considered, as mentioned before. In fact, Hof et al. (2001) applied to the NRTL equation the crossover

approach based on the method developed by Kiselev (1998), and obtained excellent results describing LLE data for nitroethane and nitrobenzene + alkanes. As recently mentioned by Cai and Prausnitz (2004) this method can only be applied to VLE and not to LLE because a different order parameter is required. Studies are being carried in order to implement a crossover approach in the soft-SAFT EoS that can describe both VLE and LLE of mixtures.

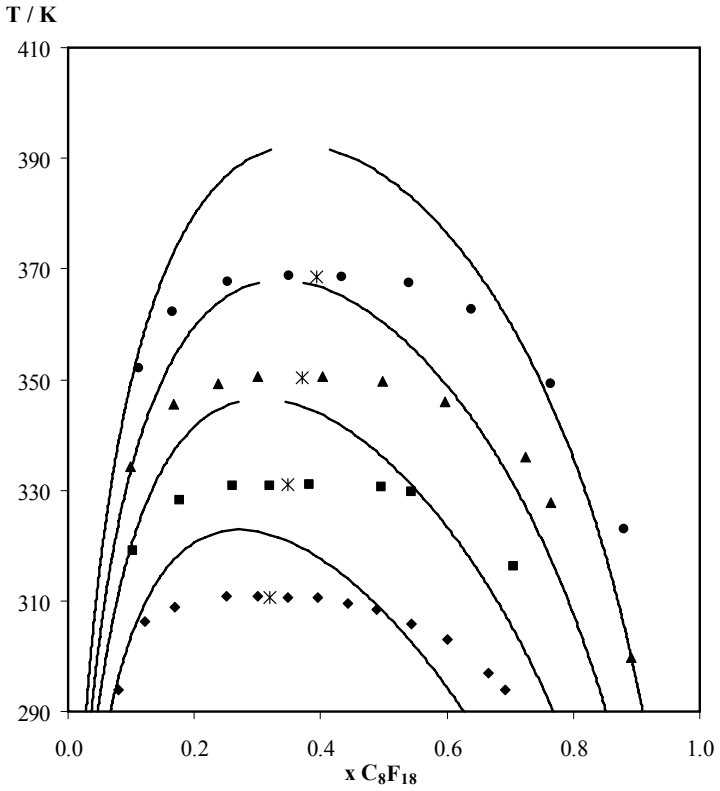

Figure III.32. LLE of C_8F_{18} + C_nH_{2n+2} mixtures at 0.1 MPa: *n* = 6 (diamonds), *n* = 7 (squares), *n* = 8 (triangles) and n = 9 (circles). Symbols represent experimental data (Duce et al., 2002). Solid lines correspond to the predictions from the soft-SAFT EoS. Stars represent the upper critical solution temperature for each mixture.

References

Adidharma, H.; Radosz, M., *Prototype of an Engineering Equation of State for Heterosegmented Polymers,* Ind. Eng. Chem. Res. (1998) 37: 4453

Agayan, V.; Anisimov, M.; Sengers, *Crossover Parametric Equation of State for Ising-like Systems*, J. Phys. Rev. E (2001) 64: 026125

Ambrose D., *Reference Values of Vapour Pressure. The Vapour Pressure of Benzene and Hexafluorobenzene,* J. Chem. Thermodynamics (1981) 13: 1161

Ambrose, D.; Ellender, J.H., *The Vapour Pressure of Octafluorotoluene*, J. Chem. Thermodynamics (1981) 13: 901

Anderson, J. M.; Barrick, M. W.; Robinson, R. L., *Solubility of Carbon Dioxide in Cyclohexane and trans-Decalin at Pressures to 10.7 MPa and Temperatures from 323 to 423 K,* J. Chem. Eng. Data (1986) 31: 172

Anisimov, M.; Voronel, A.; Gorodetskii, E., *Isomorphism of Critical Phenomena*, Soviet Phys. JETP (1971) 33: 605

Anisimov, M. A.; Senger, J. V., *Equations of State for Fluids and Fluid Mixtures, Critical, Chapter 11 Critical Region*, Editors, J. V. Senger, R. F. Kayser, C. J. Peters, and H. J. White, Jr., Elsevier, Amsterdam (2000)

Archer, A. L.; Amos, M. D.; Jackson, G.; McLure, I. A. *The Theoretical Prediction of the Critical Points of Alkanes, Perfluoroalkanes, and Their Mixtures Using Bonded Hard-Sphere (BHS) Theory* Int. J.Thermophys. (1996) 17: 201

Banaszak, M.; Chiew, Y. C.; Radosz, M., *Thermodynamic Perturbation Theory. Sticky Chains and Square-Well Chains,* Phys. Rev. E (1993) 48: 3760

Banaszak, M.; Chen, C. K.; Radosz, M. *Copolymer SAFT Equation of State. Thermodynamic Perturbation Theory Extended to Heterobonded Chains* Macromolecules (1996) 29: 6481

Barber, E. J.; Cady, G. H. *Vapor Pressures of Perfluoropentanes* J. Phys. Chem. (1956) 60: 504

Barker, J. A.; Henderson, D. *Perturbation Theory and Equation of State for Fluids. I. The Square-Well Potential,* J. Chem.Phys. (1967a) 47: 2856

Barker, J. A.; Henderson, D. *Perturbation Theory and Equation of State for Fluids. II. A Successful Theory of Liquids,* J. Chem. Phys. (1967b) 47: 4714

Blas, F. J.; Vega, L. F., *Thermodynamic Behaviour of Homonuclear and Heteronuclear Lennard-Jones Chains With Association Sites from Simulation and Theory,* Molecular Physics (1997) 92: 135

Blas, F. J.; Vega, L. F., *Prediction of Binary and Ternary Diagrams Using the Statistical Associating Fluid Theory (SAFT) Equation of State,* Ind. Eng. Chem. Res. (1998a) 37: 660

Blas, F. J.; Vega, L. F., *Critical Behavior and Partial Miscibility Phenomena in Binary Mixtures of Hydrocarbons by the Statistical Associating Fluid Theory*, J. Chem. Phys. (1998b) 109: 7405

Blas, F. J.; Vega, L. F., *Thermodynamic Properties and Phase Equilibria of Branched Chain Fluids Using First- and Second-Order Wertheim's Thermodynamic Perturbation Theory,* J. Chem. Phys. (2001) 115: 3906

Bonifácio, R. P.; Filipe, E. J. M.; McCabe, C.; Gomes, M. F. C.; Pádua, A H. A., *Predicting the Solubility of Xenon in n-hexane and n-perfluorohexane: a Simulation and Theoretical Study,* Molecular Physics (2002) 100: 2547

Brown, J. A.; Mears, W. H., *Physical Properties of n-Perfluorobutane*, J. Phys. Chem. (1958) 62: 960

Burger, L. L.; Cady, C. H., *Physical Properties of Perfluoropentanes,* J. Am. Chem. Soc. (1951) 73: 4243

Cai, J.; Prausnitz, J. M., *Thermodynamics for Fluid Mixtures Near to and Far From the Vapor–Liquid Critical Point*, Fluid Phase Equilibria (2004) 219: 205

Casas, S. P.; Trujillo, J. H.; Costas, M., *Experimental and Theoretical Study of Aromatic-Aromatic Interactions. Association Enthalpies and Central and Distributed Multipole Electric Moments Analysis,* J. Phys. Chem. B (2003) 107: 4167

Chang, C. J.; Chen, C. Y.; Lin, H. C., *Solubilities of Carbon Dioxide and Nitrous Oxide in Cyclohexanone, Toluene and N,N-Dimethylformamide at Elevated Pressures*, J. Chem. Eng. Data (1995) 40: 850

Cece, A.; Jureller, S. H.; Kerschner, J. L., *Molecular Modeling Approach for Contrasting the Interaction of Ethane and Hexafluoroethane with Carbon Dioxide*, J. Phys. Chem. (1996) 100: 7435

Chapman, W. G.; Jackson, G.; Gubbins, K. E., *Phase Equilibria of Associating Fluids. Chain Molecules with Multiple Bonding Sites,* Mol. Phys. (1988) 65: 1057

Chen, Z.; Abbaci, A.; Tang, S.; Sengers, *Global Thermodynamic Behavior of Fluids in the Critical Region*, J. Phys. Rev. A (1990a) 42: 4470

Chen, Z.; Albright, P.; Sengers, *Crossover From Singular Critical to Regular Classical Thermodynamic Behavior of Fluids,* Phys. Rev. A (1990b) 41: 3161

Chen, C.; Banaszak, M.; Radosz, M., *Statistical Associating Fluid Theory Equation of State with Lennard-Jones Reference Applied to Pure and Binary n-Alkane Systems,* J. Phys. Chem. B (1998) 102: 2427

Colina, C. M.; Galindo, A.; Blas, F. J.; Gubbins, K. E., *Phase Behavior of Carbon Dioxide Mixtures With n-alkanes and n-perfluoroalkanes*, Fluid Phase Equilibria (2004) 222: 77

Coutinho, J.; Kontogeorgis, M.; Stenby, E., *Binary Interaction Parameters for Nonpolar Systems With Cubic Equations of State: a Theoretical Approach 1. CO2/Hydrocarbons Using SRK Equation of State*, Fluid Phase Equilibria (1994) 102: 31

Crowder, G. A.; Taylor, Z. L.; Reed, T. M.; Young, J. A., *Vapor Pressures and Triple Point Temperatures for Several Pure Fluorocarbons,* J. Chem. Eng. Data (1967) 12: 481

Cui, S. T.; Siepmann, J. I.; Cochran, H. D.; Cummings, P. T., *Intermolecular Potentials and Vapor-Liquid Phase Equilibria of Perfluorinated Alkanes*, Fluid Phase Equilibria (1998) 146: 51

Cui, S. T.; Cochran, H. D.; Cummings, P. T., *Vapor-Liquid Phase Coexistence of Alkane-Carbon Dioxide and Perfluoroalkane-Carbon Dioxide Mixtures,* J. Phys. Chem. B (1999) 103: 4485

Dantzler Siebert, E. M.; Knobler, C. M. *Interaction virial coefficients in hydrocarbon-fluorocarbon mixtures* J. Phys. Chem. (1971) 75: 3863

Dardin, A.; DeSimone, J. M.; Samulski, E. T., *Fluorocarbons Dissolved in Supercritical Carbon Dioxide. NMR Evidence for Specific Solute-Solvent Interactions,* J. Phys. Chem. B (1998) 102: 1775

Davies, L. A.; Gil-Villegas, A.; Jackson, G., *An Analytical Equation of State for Chain Molecules Formed from Yukawa Segments,* J. Chem. Phys. (1999) 111: 8659

Deschamps, J.; Gomes, M. F. C.; Padua, A. A. H. *Solubility of Oxygen, Carbon Dioxide and Water in Semifluorinated Alkanes and in Perfluorooctylbromide by Molecular Simulation,* Journal of Fluorine Chemistry (2004) 125: 409

Dias, A. M. A.; Bonifácio, R. P.; Marrucho, I. M.; Pádua A. A. H.; Gomes, M. F. C., *Solubility of Oxygen in n-hexane and in n-perfluorohexane. Experimental Determination and Prediction by Molecular Simulation*, Phys. Chem. Chem. Phys. (2003) 5: 543

Díaz Peña, M.; Pando, C.; Renuncio, J. A. R., *Combination Rules for Intermolecular Potential Parameters. I. Rules Based on Approximations for the Long-Range Dispersion Energy,* J. Chem. Phys. (1982) 76: 325

Diep, P.; Jordan, K. J.; Johnson, J. K.; Beckman, E. J., *CO_2-Fluorocarbon and CO_2-Hydrocarbon Interactions from First-Principles Calculations,* J. Phys. Chem. A (1998) 102: 2231

DIPPR, Thermophysical Properties Database, 1998

Dyke. D. E. L.; Rowlinson, J. S.; Thacker, R. *The Physical Properties of Some Fluorine Compounds and Their Solutions 4. Solutions in Hydrocarbons* Transactions of the Faraday Soc. (1959) 55: 903

Donohue, M. D.; Prausnitz, J. M., *Perturbed Hard Chain Theory for Fluid Mixtures: Thermodynamic Properties for Mixtures in Natural Gas and Petroleum Technology,* AIChE J. (1978) 24: 849

Duce, C.; Tinè, M. R.; Lepori, L.; Matteoli, E., *VLE and LLE of Perfluoroalkane + alkane mixtures*, Fluid Phase Equilibria (2002) 199: 197

Dunlap, R. D.; Murphy, C. J.; Bedford, R. G. *Some Physical Properties of Perfluoro-n-hexane*, J. Am. Soc. (1958) 80: 83

Economou, I. G.; Tsonopoulos, C., *Associating Models and Mixing Rules in Equations of State for Water/Hydrocarbon Mixtures,* Chem. Eng. Sci. (1997) 52: 511

Economou, I. G., *Statistical Associating Fluid Theory: A Successful Model for the Calculation of Thermodynamic and Phase Equilibrium Properties of Complex Fluid Mixtures*, Ind. Eng. Chem. Res. (2002) 41: 953

Filipe, E. J. M.; Pereira, L. A. M.; Dias, L. M. B.; Calado, J. C. G.; Sear, R. P.; Jackson, G., *Shape Effects in Molecular Liquids: Phase Equilibria of Binary Mixtures Involving Cyclic Molecules*, J. Phys. Chem. B (1997) 101: 11243

Filipe, E. J. M., Gomes de Azevedo, E. J. S., Martins, L. F. G., Soares, V. A. M., Calado, J. C. G., McCabe, C., and Jackson, G., *Thermodynamics of Liquid Mixtures of Xenon with Alkanes: (Xenon + n-Butane) and (Xenon + Isobutane),* J. Phys. Chem. B (2000) 104:1322

Fink, S. D.; Hershey, H. C. *Modeling the Vapor-Liquid Equilibria of 1,1,1-Trichloroethane + Carbon Dioxide and Toluene + Carbon Dioxide at 308, 323 and 353 K* Ind. Eng. Chem. Res. (1990) 29: 295

Fisher, M., *Renormalization of Critical Exponents by Hidden Variables*, Phys. Rev. (1968) 176: 257

Florusse L. J; Pamies, J. C.; Vega, L. F. Peters, C. J.; Meijer, H., *Solubility of Hydrogen in Heavy n-alkanes: Experiments and SAFT Modelling,* AIChE J. (2003) 49: 3260

Flory, P. J. *Principles of Polymer Chemistry*. Cornell University Press, Ithaca, NY, 1953

Fu, Y.-H.; Sandler, S. I. *A Simplified SAFT Equation of State for Associating Compounds and Mixtures.* Ind. Eng. Chem. Res. (1995) 34: 1897

Ghonasgi, D.; Chapman, W. G. *Prediction of the Properties of Model Polymer-Solutions and Blends,* AIChE J. (1994) 40: 878

Gil-Villegas, A.; Galindo, A.; Whitehead, P. J.; Mills, S. J.; Jackson, G.; Burgess, A. N., *Statistical Associating Fluid Theory for Chain Molecules with Attractive Potentials of Variable Range,* J. Chem. Phys. (1997) 106: 4168

Gjaldbaek, J., *The Solubility of Hydrogen, Oxygen and Carbon Monoxide in Some Non-Polar Solvents,* Acta Chemica Scandinavica (1952) 6: 623

Glew, D. N.; Reeves, L. W., *Purification of Perfluoro-heptane and Perfluoromethylcyclohexane,* J. Phys. Chem. (1956) 60: 615
Gomes, M. F. C.; Padua, A. H., *Interactions of Carbon Dioxide with Liquid Fluorocarbons,* J. Phys. Chem. B (2003) 107: 14020

Good, W.D.; Douslin, D.R.; Scott, D.W.; George, A.; Lacina, J.L.; Dawson, J.P.; Waddington, G., *Thermochemistry and Vapor Pressure of Aliphatic Fluorocarbons. A Comparison of the C-F and C-H Thermochemical Bond Energies*, J. Phys. Chem. (1959) 63: 1133

Gray, C. G.; Gubbins, K. E., *Theory of Molecular Fluids,* Clarendon Press: Oxford, U.K., Vol. 1 (1984)

Green, D. G.; Jackson, G., *Theory of Phase Equilibria for Model Aqueous Solutions of Chain Molecules: Water + Alkane Mixtures,* J. Chem. Soc., Faraday Trans. (1992) 88: 1395

Gross, J.; Sadowski, G., *Perturbed-Chain SAFT: An Equation of State Based on a Perturbation Theory for Chain Molecules,* Ind. Eng. Chem. Res. (2001) 40: 1244

Gubbins, K. E.; Two, C. H., *Thermodynamics of Polyatomic Fluid Mixtures - I Theory*, Chem. Eng, Sci. (1978) 33: 863

Hager, J.; Anisimov, M.; Sengers, J.; Gorodetskii, E., *Scaling of Demixing Curves and Crossover From Critical to Tricritical Behavior in Polymer Solutions*, J. Chem. Phys. (2002) 117: 5940

Hales, J. L.; Townsend, R. *Liquid Densities From 293 to 490 K of Eight Fluorinated Aromatic Compounds*, J. Chem. Thermodynamics (1974) 111-116

Hansen, J. P.; McDonald, I. R. *Theory of Simple Liquids*, 2nd ed.; Academic Press: London (1986)

Hariharan, A.; Harris, J. G., *Structure and Thermodynamics of the Liquid-Vapour Interface of Fluorocarbons and Semifluorinated Alkane Diblocks – A Molecular-Dynamics Study*, J. Chem. Phys. (1994) 101: 4156

Herreman W. *Calculation of the Density of Liquid Radon* Cryogenics (1980) 20: 133
Hildebrand, J. H.; Scott, R. L. *Solubility of Nonelectrolytes,* 3rd ed.; Reinhold Publishing Corp.: New York, 1950

Hildebrand, J. H.; Fisher, B. B.; Benesi, H. A., *Solubility of Perfluoro-n-heptane with Benzene, Carbon Tetrachloride, Chloroform, n-Heptane and 2,2,4-Trimethylpentane*, J. Am. Chem. Soc. (1950) 72: 4348

Hildebrand, J.; Prausnitz, J.; Scott, R. *Regular and Related Solutions - The solubility of Gases*, Liquids and solids, New York, Van Nostrand Reinhold (1970)

Hof, A.; Japas, M. L.; Peters, C. *Description of Liquid-Liquid Equilibria Including the Critical Region With the Crossover-NRTL Model* Fluid Phase Equilibria (2001) 192: 27

Iezzi, A.; Bendale, P.; Enick, R.; Turberg, M.; Brady, J., *'Gel' Formation in Carbon Dioxide-Semifluorinated Alkane Mixtures and Phase Equilibria of a Carbon Dioxide-Perfluorinated Alkane Mixture,* Fluid Phase Equilibria (1989) 52: 307

Jackson, G.; Chapman, W. G.; Gubbins, K. E., *Phase Equilibria of Associating Fluids. Spherical Molecules with Multiple Bonding Sites,* Mol. Phys. (1988) *65*: 1

Jiang, J.; Prausnitz, J. M. J., *Equation of State for Thermodynamic Properties of Chain Fluids Near-To and Far-From the Vapor–Liquid Critical Region*, Chem. Phys. (1999) 111: 5964

Jiang, J.; Prausnitz, J. M., *Phase Equilibria for Chain-Fluid Mixtures Near To and Far From the Critical Region*, AIChE J. (2000) 46: 2525

Jin, G.; Tang, S.; Sengers, *Global Thermodynamic Behavior of Fluid Mixtures in the Critical Region*, J. Phys. Rev. E (1993) 47: 388

Jog, P. K.; Sauer, J. B.; Chapman, W. G., *Application of Dipolar Chain Theory to the Phase Behavior of Polar Fluids and Mixtures*, Ind. Eng. Chem. Res. (2001) 40: 4641

Johnson, J. K.; Zollweg, J. A.; Gubbins, K. E., *The Lennard-Jones Equation of State Revisited,* Mol. Phys. (1993) 78: 591

Johnson, J. K.; Muller, E. A.; Gubbins, K. E., *Equation of State for Lennard-Jones Chains* J. Phys. Chem. (1994) 98: 6413

Jorgensen, W. L.; Maxwell, D. S.; Tirado-Rives, J. *Development and Testing of the OPLS All-Atom Force Field on Conformational Energetics and Properties of Organic Liquids* J. Am. Chem. Soc. (1996) 118: 11225

Kennan, R. P.; Pollack, G. L. *Solubility of Xenon in Perfluoroalkanes: Temperature Dependence and Thermodynamics* J. Chem. Phys. (1988) 89: 517

Kim, CH; Vimalchand, P.; Donohue, M. D., *Vapor-Liquid Equilibria for Binary Mixtures of Carbon Dioxide with Benzene, Toluene and p-Xylene*, Fluid Phase Equilibria (1986) 31: 299

Kiselev, S., *Cubic Crossover Equation of State,* Fluid Phase Equilibria (1998) 147: 7

Kiselev, S. B.; Ely, J. F., *Crossover SAFT Equation of State: Application to Normal Alkanes,* Ind. Eng. Chem. Res. (1999a) 38: 4993

Kiselev, S.; Friend, D., *Cubic Crossover Equation of State for Mixtures*, Fluid Phase Equilibria (1999b) 162: 51

Kiselev, S. B.; Ely, J. F. *Simplified Crossover SAFT Equation of State for Pure Fluids and Fluid Mixtures,* Fluid Phase Equilibria (2000) 174: 93

Kolafa, J.; Nezbeda, I., *The Lennard-Jones Fluid - an Accurate Analytic and Theoretically-Based Equation of State,* Fluid Phase Equilibria (1994) 100: 1

Kontogeorgis, G. M.; Voutsas, E. C.; Yakoumis, I. V.; Tassios, D. P., *An Equation of State for Associating Fluids,* Ind. Eng. Chem. Res. (1996) 35: 4310

Konynenburg, P. H.; Scott, R. L. *Critical Lines and Phase Equilibria in Binary van Der Waals Mixtures* Philosophical Transactions of the Royal Society of London. Series A, Mathematical and Physical Sciences (1980) 298: 495

Kraska, T.; Gubbins, K. E. Phase Equilibria *Calculations With a Modified SAFT Equation of State. 1. Pure Alkanes, Alkanols, and Water* Ind. Eng. Chem. Res. (1996) 35: 4727

Kreglewski, A., *Vapour Pressures and Molar Volumes of Liquid Perfluoro-n-Octane Trifluoroacetic Acid and its Anhydride*, Bulletin de L'academie Polonaise des Sciences, (1962) vol.X: 629

Lawson, D. D.; Moacanin, J.; Sherer, K. V.; Terranova, T. F.; Ingham, J. D. *Methods for Estimation of Vapor-Pressures and Oxygen Solubilities of Fluorochemicals for Possible Aplication in Artificial Blood Formulations* J. Flurine Chem. (1978) 12: 221

Lewis, C.; Hopke, P. K.; Stukel, J. J. *Solubility of Radon in Selected Perfluorocarbon Compounds and Water* Ind. Eng. Chem. Es. (1987) 26: 356

Lovell, F.; Pàmies, J. C.; Vega, L. F. *Thermodynamic Properties of Lennard-Jones Chain Molecules: Renormalization-Group Corrections to a Modified Statistical Associated Fluid Theory* J. Chem. Phys. (2004) 121

Lue, L.; Prausnitz, J. M., *Thermodynamics of Fluid Mixtures Near To and Far From the Critical Region*, AIChE J. (1998) 44: 1455

Mack H. G., Oberhammer H. J., *An ab initio Approach to the Interaction of CF_4 and CH_4 with O_2, CO_2, N_2, and CO. The Nature of the Interaction Force in Perfluorochemical Artificial Blood*, Chem. Phys. (1987) 87: 2158

McCabe C.; Galindo A.; Gil-Villegas A.; Jackson G. *Predicting the high-pressure phase equilibria of binary mixtures of perfluoro-n-alkanes plus n-alkanes using the SAFT-VR approach* J.l of Phys. Chem. B (1998) 102 (41): 8060

McCabe, C.; Jackson, *SAFT-VR Modelling of the Phase Equilibrium of Long-Chain n-alkanes*, Phys. Chem. Chem. Phys. (1999) 1: 2057

McCabe, C.; Dias, L. M. B.; Jackson, G.; Filipe, E. J. M., *On the Liquid Mixtures of Xenon, Alkanes and Perfluorinated Compounds*, Phys. Chem. Chem. Phys. (2001) 3: 2852

McCabe, C.; Kiselev, S. B., *A Crossover SAFT-VR Equation of State for Pure Fluids: Preliminary Results for Light Hydrocarbons,* Fluid Phase Equilibria (2004) 219: 3

McCarty, R. D. *Correlations for the Thermophysical Properties of Xenon*, National Institute of Standards and Technology, Boulder, CO (1989)

Milton, H. T.; Oliver, G. D., *High Vapor Pressure of n-Hexadecafluoroheptane,* J. Am. Chem. Soc. (1952) 74: 3951

More, J. J. *The Levenberg-Marquardt Algorithm: Implementation and Theory. Numerical Analysis*; Watson, G. A. (editor); Springer-Verlag, New York (1977)

Mousa, A E. H. N.; Kreglews, A.; Kay, W. B. *Critical Constants of Binary Mixtures of Certain Perfluoro-Compounds with Alkanes* J. Chem. Thermodynamics (1972) 4: 301

Mousa, A. E. H. N. *Study of Vapor pressure and Critical Properties of Perfluoro-n-hexane,* J. Chem. Eng. Data (1978) 23: 133

Muller, E. A.; Gubbins, K. E. *Simulation of Hard Triatomic and Tetratomic Molecules. A Test of Associating Fluid Theories,* Mol. Phys. (1993) 80: 957

Muller, E. A.; Vega, L. F. Vega, Gubbins, K. E. *Theory and Simulation of Associating Fluids: Lennard-Jones Chains with Association Sites,* Mol. Phys. (1994) 83: 1209

Muller, E. A.; Gubbins, K. E. *An Equation of State for Water from a Simplified Intermolecular Potential,* Ind. Eng. Chem. Res. (1995a) 34: 3662

Muller, E. A.; Vega, L. F., Gubbins, K. E. *Molecular Simulation and Theory of Associating Chains Molecules,* Int. J. Thermophys. (1995b) 16: 705

Muller, E. A.; Gubbins, K. E., *Associating Fluids and Fluid Mixtures* Chapter 12 in *Equations of State for Fluids and Fluid Mixtures*, J. V. Sengers, R. F. Kayser, C. J. Peters, H. J. White Jr. Editors, Elsevier, Amsterdam (2000)

Muller, E. A.; Gubbins, K. E., *Molecular-Based Equations of State for Associating Fluids: A Review of SAFT and Related Approaches,* Ind. Eng. Chem. Res. (2001) 40: 2193

Nasrifar, Kh.; Heuvel, M. M. M.; Peters, C. J.; Ayatollahi, Sh.; Moshfeghian, M. *Measurements and Modeling of Bubble Points in Binary Carbon Dioxide Systems With Tetrahydropyran and Methylcycloexane* Fluid Phase Equilibria (2003) 204: 1

Ng, H. J.; Robinson, D. B. *The equilibrium Phase Properties of Selected Naphthenic Binary Systems: Carbon Dioxide - Methylcyclohexane, Hydrogen Sulfide – Methylcyclohexane* Fluid Phase Equilibria (1979) 2: 283

Ohgaki, K.; Katayama, T., *Isothermal Vapor-Liquid Equilibrium Data for Binary Systems Containing Carbon Dioxide at High Pressures: Methanol-Carbon Dioxide, n-Hexane-Carbon Dioxide, and Benzene-Carbon Dioxide Systems,* J. of Chem. Eng. Data (1976) 21: 53

Oliver, G.; Blumkin, S.; Cunningham, *Some Physical Properties of Hexadecafluoroheptane*, J. Am. Chem. Soc. (1951) 73: 5722

Oliver, G.; Grisard, J., *Some Thermodynamic Properties of Hexadecafluoroheptane,* J. Am. Chem. Soc. (1951) 73: 1688

Pàmies, J. C.; Vega, L. F., *Vapor-Liquid Equilibria and Critical Behavior of Heavy n-Alkanes Using Transferable Parameters from the Soft-SAFT Equation of State,* Ind. Eng. Chem. Res. (2001) 40: 2532

Pàmies, J. C.; Vega, L. F., *Critical Properties of Homopolymer Fluids Studied by a Lennard-Jones Statistical Associating Fluid Theory*, Mol. Phys. (2002) 100: 2519

Pàmies, J. C., PhD Thesis, University Rovira e Virgilli, 2003

Pàmies, J. C.; Vega, L. F., *Fluid Phase Behavior of Carbon Dioxide Mixtures with Alkanes and Alkanols from the soft-SAFT Equation of State*, In preparation

Parola, A.; Reatto, L., *Hierarchical Reference Theory of Fluids and the Critical Point*, Phys. Rev. A (1985) 31: 3309

Parola, A.; Reatto, L., *Microscopic Approach to Critical Phenomena in Binary Fluids*, Phys. Rev. A (1991) 44: 6600

Parola, A.; Reatto, L., *Liquid State Theories and Critical Phenomena*, Adv. Phys. (1995) 44: 211

Peng, D. Y.; Robinson, D. B., *A New Two-Constant Equation of State,* Ind. Eng. Chem. Fundam. (1976) 15: 59

Pfohl, O.; Brunner, G., *Use of BACK to Modify SAFT in Order to Enable Density and Phase Equilibrium Calculations Connected to Gas-Extraction Processes,* Ind. Eng. Chem. Res. (1998) 37: 2966

Piñeiro, M. M.; Bessières, D.; Gacio, J. M.; Guirons, H. S.; Legido, J. L., *Determination of High-Pressure Liquid Ddensity for n-perfluorohexane and n-perfluorononane,* Fluid Phase Equilibria, (2004) 220: 125

Poling, B.; Prauznitz, J.; O'Connell, J., *The properties of Gases and Liqui*ds, McGraw-Hill, New York (2001) 5th edition

Powell, M. J. D., *A Fortran Subroutine for Solving Systems of Nonlinear Algebraic Equations. Numerical Methods for Nonlinear Algebraic Equations*; Rabinowitz, P. (editor); Gordon & Breach, New York (1970)

Prausnitz, J.; Shair, F. A.I.Ch.E. J. (1961) 7: 682

Raveendran, P.; Wallen, S. L., *Cooperative C-H···O Hydrogen Bonding in CO_2-Lewis Base Complexes: Implications for Solvation in Supercritical CO_2*, J. Am. Chem. Soc. (2002) 124: 12590

Reed, T. M. *The Theoretical Energies of Mixing for Fluorocarbon-Hydrocarbon Mixtures* J. Phys. Chem. (1955) 59: 425

Rowlinson, J. S. *Liquids and Liquid Mixtures,* 2nd ed.; Butterworth Scientific: London, 1969

Rowlinson, J. S.; Swinton, F. L. *Liquid and Liquid Mixtures*. Butterworth Scientific, London (1982)

Sanchez, I. C.; Lacombe, R. H., *An Elementary Molecular Theory of Classical Fluids. Pure Fluids,* J. Phys. Chem. (1976) 80: 2352

Scott, R. L. *The Anomalous Behavior of Fluorocarbon Solutions* J. Phys. Chem. (1958) 62: 136

Shukla H., Mason R., Woessner D., Antich P., *A Comparison of Three Commercial Perfluorocarbon Emulsions as High-Field 19F NMR Probes of Oxygen Tension and Temperature,* J. Mag. Res. Series B (1995) 106: 131

Simons, J. H.; Dunlap, R. D. *The Properties of n-Pentforane and Its Mixtures with n-Pentane* J. Chem. Phys. (1950) 18: 335

Simons, J. H.; Mausteller, J. W. *The Properties of Normal-Butforane and Its Mixtures with Normal-Butane* J. Chem. Phys. (1952) 20: 1516

Smith, B.; Srivastava, R., *Thermodynamic Data for Pure Compounds*, Elsevier, London (1986)

Song, W.; Rossky, P. J.; Maroncelli, M. *Modeling Alkane-Perfluoroalkane Interactions Using All-atom Potentials: Failure of the Usual Combining Rules* J. Chem. Chem. Phys. (2003) 119: 1945

Steele, W. V.; Chirico, R. D.; Knipmeyer, S. E.; Nguyen, A., *Vapor Pressure, Heat Capacity, and Density along the Saturation Line, Measurements for Cyclohexanol, 2-Cyclohexen-1-one, 1,2-Dichloropropane, 1,4-Di-tert-butylbenzene, (±)-2-Ethylhexanoic*

Acid, 2-(Methylamino)ethanol, Perfluoro-n-heptane, and Sulfolane, J. Chem. Eng. Data (1997) 42: 1021

Stell, G.; Rasaiah, J. C.; Narang, H., *Thermodynamic Perturbation-Theory for Simple Polar Fluids*, Mol. Phys. (1974) 27: 1393

Sun, L.; Zhao, H.; Kiselev, S. B.; McCabe, C., *Predicting Mixture Phase Equilibria and Critical Behavior Using the SAFT-VRX Approach,* J. Phys. Chem. B (2005) 109: 9047

Tavares, F. W.; Chang, J.; Sandler, S. I., *A Completely Analytic Equation of State for the Square-Well Chain Fluid of Variable Well Width,* Fluid Phase Equilib. (1997) 140: 129

Tiffin, D. L.; DeVera, A. L.; Luks, K. D.; Kohn, J. P., *Phase-Equilibria Behavior of the Binary Systems Carbon Dioxiden- Butylbenzene and Carbon Dioxide-trans-Decalin,* J. of Chem. and Eng. Data (1978) 23: 1978

Thorpe, N.; Scott, R. L. J. Phys. Chem. (1956) 6: 670

Two, C. H.; Gubbins, K. E.; Gray, C. G., *Excess Thermodynamic Properties for Liquid-Mixtures of Non-Spherical Molecules*, Mol. Phys. (1975) 29: 713

Two, C. H., PhD Dissertation, University of Florida (1976)

Vandana, V.; Rosenthal, D. J.; Teja, A S., *The Critical Properties of Perfluoro-n-alkanes,* Fluid Phase Equilibria (1994) 99: 209

Vrabec, J.; Stoll, J.; Hasse, H., *A Set of Molecular Models for Symmetric Quadrupolar Fluids,* J. Phys. Chem. B (2001) 105: 12126

Vrbancich, J.; Ritchie, G. L. D., *Quadrupole Moments of Benzene, Hexafluorobenzene and other Non-dipolar Aromatic Molecules,* J. Chem. Soc. Faraday II (1980) 76: 648

Walsh, J. M.; Guedes, H. J. R.; Gubbins, K. E., *Physical Theory for Fluids of Small Associating Molecules,* J. Phys. Chem. (1992) 96: 10995

Watkins, E. K.; Jorgensen, W. L. *Perfluoroalkanes: Conformational Analysis and Liquid-State Properties from ab Initio and Monte Carlo Calculations* J. Phys. Chem. A (2001) 105: 4118

Weng, W. L.; Lee, M. J., *Vapor-Liquid Equilibrium of the Octane/Carbon Dioxide, Octane/Ethane, and Octane/Ethylene Systems*, J. Chem. Eng. Data (1992) 37: 213

Wertheim, M. S., *Fluids with Highly Directional Attractive Forces. I. Statistical Thermodynamics,* J. Stat. Phys. (1984) 35: 19

Wertheim, M. S., *Fluids with Highly Directional Attractive Forces. II. Thermodynamic Perturbation Theory and Integral Equations,* J. Stat. Phys. (1984) 35: 35

Wertheim, M. S., *Fluids with Highly Directional Attractive Forces. III. Multiple Attraction Sites,* J. Stat. Phys. (1986) 42 : 459

Wertheim, M. S. *Thermodynamic Perturbation Theory of Polymerisation*, J. Chem. Phys. (1987) 87: 7323

White, J. A., *Contribution of Fluctuations to Thermal Properties of Fluids with Attractive Forces of Limited Range: Theory Compared with PT and Cv Data for Argon*, Fluid Phase Equilib. (1992) 75: 53

White, J.; Zhang, S., *Renormalization Group Theory for Fluids*, J. Chem. Phys. (1993) 99: 2012

White, J. A., *Lennard-Jones as a Model for Argon and Test of Extended Renormalization Group Calculations*, J. Chem. Phys. (1999) 111: 9352

White, J. A., *Global Renormalization Calculations Compared with Simulations for Lennard-Jones Fluid*, J. Chem. Phys. (2000) 112: 3236

Wilson, K. G., *Renormalization Group and Critical Phenomena. I. Renormalization Group and the Kadanoff Scaling Picture,* Phys. Rev. B (1971) 4: 3174

Wilson, K. G.; Fischer, M. E., *Critical Exponents in 3.99 Dimensions*, Phys. Rev. Lett. (1972) 28: 240

Wilson, K. G., *The Renormalization Group: Critical Phenomena and the Kondo Problem*, Rev. Mod. Phys. (1975) 47: 773

Yee, G. G.; Fulton, J. L.; Smith, R. D., *Fourier Ttransform Infrared Spectroscopy of Molecular Interactions of Heptafluoro-1-butanol or 1-butanol in Supercritical Carbon Dioxide and Supercritical Ethane*, J. Phys. Chem. (1992) 96: 6172

Yonker, C. R.; Palmer, B. J., *Investigation of CO_2/Fluorine Interactions through the Intermolecular Effects on the ^{1}H and ^{19}F Shielding of CH_3F and CHF_3 at Various Temperatures and Pressures*, J. Phys. Chem. A (2001) 105: 308

Zhang, L.; Siepmann, J. I., *Pressure Dependence of the Vapor-Liquid-Liquid Phase Behavior in Ternary Mixtures Consisting of n-Alkanes, n-Perfluoroalkanes, and Carbon Dioxide*, J. Phys. Chem. B (2005) 109: 2911

Publication List

Dias, A. M. A.; Bonifácio, R. P.; Marrucho, I. M.; Pádua, A. A H.; Gomes, M. F. C. *Solubility of Oxygen in n-hexane and in n-perfluorohexane. Experimental determination and prediction by molecular simulation*, Phys. Chem. Chem. Phys. (2003) 5: 543

Dias, A. M. A; Freire, M. G.; Coutinho, J. A. P.; Marrucho, I. M. *Solubility of Oxygen in Liquid Perfluorocarbons*, Fluid Phase Equilibria (2004) 222-223: 325

Dias, A. M. A; Pàmies, J. C.; Coutinho, J. A. P.; Marrucho, I. M.; Vega, L. F. *SAFT Modeling of the Solubility of Gases in Perfluoroalkanes*, J. of Phys. Chem. B (2004) 108: 1450

Dias, A. M. A; Coutinho, J. A. P.; Piñeiro M.; Gomes, M. F. C.; Marrucho, I. M. *Thermodynamic Properties of Perfluoro-n-octane*, Fluid Phase Equilibria (2004) 225: 39

Freire, M. G.; Dias, A. M. A.; Coelho, M. A. Z.; Coutinho, J. A. P.; Marrucho, I. M. *Ageing Mechanisms of Perfluorocarbon Emulsions using Image Analysis*, J. of Colloid and Interface Science (2004) 286: 224

Freire, M. G.; Dias, A. M. A.; Coelho, M. A. Z; Coutinho, J. A. P.; Marrucho, I. M. *Enzymatic Method for Determining Oxygen Solubility in Perfluorocarbon Emulsions*, Fluid Phase Equilibria (2004) 231: 109

Dias, A. M. A.; Gonçalves, C. M.; Caço, A. I.; Santos, L. M. N. B. F.; Piñeiro, M. M.; Vega, L. F.; Coutinho, J. A. P.; Marrucho, I. M. *Densities and Vapor Pressures of Highly Fluorinated Compounds*, J. of Chem. Eng. Data (2005) 50: 1328

Dias, A. M. A.; Gonçalves, C. M. B.; Legido, JJJ. L.; Coutinho, J. A. P.; Marrucho, I. M. *Solubility of Oxygen in Substituted Perfluorocarbon,* Aceite em Fluid Phase Equilibria (2005)

Dias, A. M. A; Pàmies, J. C.; Vega, L. F.; Coutinho, J. A. P.; Marrucho, I. M. Modelling the Solubility of Gases in Saturated and Substituted Perfluoroalkanes Aceite em Polish Journal of Chemistry (2005)

Dias, A. M. A.; Pamies, J.; Carrier, H.; Daridon, JL; Vega, L. F.; Coutinho, J. A. P.; Marrucho, I. M. *Vapor – Liquid Equilibrium of Carbon Dioxide – Perfluoroalkane Mixtures: experimental data and SAFT modeling*, Submetido a IECR (2005)

Melo, M. J. P.; Dias, A. M. A.; Blesic, M.; Rebelo, L. P. N.; Vega, L. F.; Coutinho, J. A. P.; Marrucho, I. M., *Liquid-Liquid Equilibrium of (Perfluoroalkane + Alkane) Binary Mixtures*, Submetido a IECR (2005)